CROP PEST CONTROL AND POLLINATION

EDITED BY: Fang Ouyang, Wei Li, Xingyuan Men and Wen Xie
PUBLISHED IN: Frontiers in Sustainable Food Systems

frontiers Research Topics

ISSN 1664-8714
ISBN 978-2-83250-677-6
DOI 10.3389/978-2-83250-677-6

About Frontiers

Frontiers is more than just an open-access publisher of scholarly articles: it is a pioneering approach to the world of academia, radically improving the way scholarly research is managed. The grand vision of Frontiers is a world where all people have an equal opportunity to seek, share and generate knowledge. Frontiers provides immediate and permanent online open access to all its publications, but this alone is not enough to realize our grand goals.

Frontiers Journal Series

The Frontiers Journal Series is a multi-tier and interdisciplinary set of open-access, online journals, promising a paradigm shift from the current review, selection and dissemination processes in academic publishing. All Frontiers journals are driven by researchers for researchers; therefore, they constitute a service to the scholarly community. At the same time, the Frontiers Journal Series operates on a revolutionary invention, the tiered publishing system, initially addressing specific communities of scholars, and gradually climbing up to broader public understanding, thus serving the interests of the lay society, too.

Dedication to Quality

Each Frontiers article is a landmark of the highest quality, thanks to genuinely collaborative interactions between authors and review editors, who include some of the world's best academicians. Research must be certified by peers before entering a stream of knowledge that may eventually reach the public - and shape society; therefore, Frontiers only applies the most rigorous and unbiased reviews.
Frontiers revolutionizes research publishing by freely delivering the most outstanding research, evaluated with no bias from both the academic and social point of view. By applying the most advanced information technologies, Frontiers is catapulting scholarly publishing into a new generation.

What are Frontiers Research Topics?

Frontiers Research Topics are very popular trademarks of the Frontiers Journals Series: they are collections of at least ten articles, all centered on a particular subject. With their unique mix of varied contributions from Original Research to Review Articles, Frontiers Research Topics unify the most influential researchers, the latest key findings and historical advances in a hot research area! Find out more on how to host your own Frontiers Research Topic or contribute to one as an author by contacting the Frontiers Editorial Office: frontiersin.org/about/contact

CROP PEST CONTROL AND POLLINATION

Topic Editors:
Fang Ouyang, Institute of Zoology, Chinese Academy of Sciences (CAS), China
Wei Li, Hunan Agricultural University, China
Xingyuan Men, Institute of plant protection, Shandong Academy of Agricultural Sciences, China
Wen Xie, Insititute of Vegetables and Flowers, Chinese Academy of Agricultural Sciences, China

Citation: Ouyang, F., Li, W., Men, X., Xie, W., eds. (2022). Crop Pest Control and Pollination. Lausanne: Frontiers Media SA. doi: 10.3389/978-2-83250-677-6

Table of Contents

frontiers | Frontiers in Sustainable Food Systems

TYPE Editorial
PUBLISHED 19 October 2022
DOI 10.3389/fsufs.2022.1028134

OPEN ACCESS

EDITED AND REVIEWED BY
Stacy Michelle Philpott,
University of California, Santa Cruz,
United States

*CORRESPONDENCE
Fang Ouyang
ouyangf@ioz.ac.cn
Wei Li
liwei350551@163.com

SPECIALTY SECTION
This article was submitted to Agroecology and Ecosystem Services, a section of the journal Frontiers in Sustainable Food Systems

RECEIVED 25 August 2022
ACCEPTED 03 October 2022
PUBLISHED 19 October 2022

CITATION
Ouyang F, Li W, Xie W and Men X (2022) Editorial: Crop pest control and pollination.
Front. Sustain. Food Syst. 6:1028134.
doi: 10.3389/fsufs.2022.1028134

Editorial: Crop pest control and pollination

Fang Ouyang[1]*, Wei Li[2]*, Wen Xie[3] and Xingyuan Men[4]

[1]State Key Laboratory of Integrated Management of Pest and Rodents, Institute of Zoology, Chinese Academy of Sciences, Beijing, China, [2]College of Plant Protection, Hunan Agricultural University, Changsha, China, [3]Institute of Vegetables and Flowers, Chinese Academy of Agricultural Science, Beijing, China, [4]Institute of Plant Protection, Shandong Academy of Agricultural Sciences, Jinan, China

KEYWORDS

crop production, pest control, agricultural landscapes, ecological regulation and control, plant defense

Editorial on the Research Topic
Crop pest control and pollination

Crop production meets the basic need of human nutrition. Crop production in increasingly intensive, large-scale and simplified agricultural landscapes often face or suffer from various threats, such as pest damage (caused by insect pests, pathogenic microbes, nematode, weeds, rodents, and so on) or a shortage of pollinators. Crop pests can cause serious loss during crop production and food storage, however, effective pest management benefits to reduce crop loss and pesticide abuse. Moreover, most vegetable and fruit tree crops require insect pollination to ensure high yields and quality. Research on strategies and techniques of pest management and their potential impact on pest control and pollination in agricultural landscapes is of great significance to sustainable crop production (Gurr et al., 2017).

Over the past decades, pest control largely relied on pesticides which can control crop pests and decrease crop losses in the short term (Tilman et al., 2001; Ringland and George, 2011). However, pesticide abuse causes a series of problems in the long run, for example, the risk of development of pesticide resistance by crop pest, as well as pesticides residues in soil, water, and agricultural products (Van Meter et al., 2016). Long-term, improper, and excessive use of pesticides during crop production ultimately harms biodiversity and human health (Larsen et al., 2017). New strategies and techniques for environmentally-friendly pest control should be developed in order to support natural enemy and pollinator diversity while also supporting food production and bolstering food security, food safety and biodiversity protection.

There are ways in which crop pests are regulated from "top down" regulation of pests from natural enemies and biodiversity and from "bottom up" regulation of pests from plant defense mechanisms. Ecological regulation and control of pests in agricultural landscapes are always important frontier areas in science and technology for prevention and management of crop diseases and insect pests (Ouyang et al., 2020). Plant defenses are instinctive adaptations that decrease the damage and mortality caused by pests such as herbivores and pathogens (Coley and Barone, 2001). Omics

is applied more and more widespread to illustrate signaling pathways, mechanism and candidate targets of plant immunity system. For instance, transcriptome analysis is an effective strategy to find out which signaling pathway(s) is related to some plant disease resistance, and screen the functional genes related to disease resistance. In addition, clone plant lesion mimic genes which display spontaneous cell death and activated plant disease resistance can also provide gene resource for crops breeding for pest control. Understanding how human activities, agricultural landscape structure and plant defenses influence crop diseases and insect pests and their natural enemies is important for prevention and management of pests (Thies and Tscharntke, 1999; Faulkner, 2016). Likewise, understanding how biodiversity influences ecosystem function and plant defenses can elucidate pest control mechanisms (Duffy et al., 2010).

In this Research Topic, we present nine articles that discuss specific aspects of ecological regulation and control of pests and defenses mechanisms in plant. Three of the articles (Dong et al.; Tripathi et al.; Suprapta) discuss the impacts of habitat management and natural enemies on crop pests. Four articles (Xie, Jiang, Huang, et al., Zhang et al.; Gao et al.; Tang et al.) focus on genome and transcriptome technologies for pest control. The last two articles (Wang et al.; Shen et al.) focus on lesion-specific mutants and the ways in which plant defense can regulate pests. The first article, Dong et al. reported ecological effects of flower and grass strips for increase of natural enemies in apple orchards in Beijing, China Beijing, China. Sowing plants strips that provide food resources (pollen, nectar and alternative prey) in orchards is a potential practice of habitat management for promoting biological control. The second article, Tripathi et al. assessed the impacts of climate-smart agriculture (CSA) on crop yield and biodiversity in the East Usambara Mountains, Tanzania. The study compared the impacts of climate-smart agriculture (CSA) with other agricultural management practices on invertebrate pest and natural enemy diversity, and the associated effects on crop damage and crop yield. The findings illustrate that the CSA practices in the area, terracing and trenching with live and compost mulches, could promote crop production, pest suppression and agricultural income. The third article, by Suprapta reported the biological control of anthracnose disease on chili pepper using a beneficial microorganism formulation containing *Paenibacillus polymyxa* c1. Anthracnose disease on chili pepper has been known to seriously disturb the plant growth and obviously decrease the yield. The disease is caused by *Colletotrichum* spp. In Bali, Indonesia, six species of *Colletotrichum* have been identified: *Colletotrichum scovillei*, *C. acutatum*, *C. nymphaeae*, *C. gloeosporioides*, *C. truncatum*, and *C. fructicola*. The results revealed that the formulation of the beneficial microorganism *P. polymyxa* C1 effectively restraint the anthracnose disease on chili pepper, particularly on chili pepper cultivar Cabe Besar, and thus can be proposed as field testing to confirm its stability under field conditions.

Genome and transcriptome analysis technology is an effective systems-biology method for the investigation of pest and host plant. The two articles in this Research Topic by Xie, Jiang, Chen, et al., Zhang et al. reported the transcriptome profile of the pest *Myllocerinus aurolineatus* Voss in Tea Plants and soybean treated with *Pseudomonas syringae* phytotoxin Coronatine (COR), respectively. According to the reports, the global transcriptome profile of pest and host plant provides a valuable genomic resource and clues for further study the interaction between pest and plant, therefore, transcriptome sequencing promotes the development of new pest management strategies. The article by Gao et al. reported that RNA sequencing analysis of *Metopolophium dirhodum* (Walker) (Hemiptera: Aphididae) reveals the mechanism underlying insecticide resistance. The study identified a total of 5,265 differentially expressed genes (DEGs). And, the transcriptome data generated in this study can be used for functional gene characterization such as aphid development, metabolism, environmental adaptation, and insecticide resistance. The article by Tang et al. reported that genome identification and expression analysis of GRAS family related to development, hormone and pathogen stress in *Brachypodium distachyon* which is a new model system for functional genomics like plant-pathogen interactions in grasses. This study used bioinformatics method to search and found 63 GRAS family genes in *B. distachyon*. These results will provide data source for further study of GRAS gene function in *B. distachyon*.

Furthermore, the another two articles by Wang et al. and Shen et al. reported that the lesion-mimic mutants are useful materials to dissect mechanisms controlling programmed cell death (PCD) and defense response in plants, and the lesion mimic genes are applicable gene resource for pest control. Two lesion mimic rice genes both located on chromosome 12 were mapped/cloned and reported in this Research Topic back to back (Wang et al.; Shen et al.). Interestingly, although both these two lesion mimic genes negatively regulate cell death and antioxidation metabolism, these two genes act opposite effect on disease resistance, which one is negative regulator of plant immunity and the other one is positive regulator (Wang et al.; Shen et al.). These findings further uncover the mechanism of lesion mimic genes regulating plant disease resistance and cell death, and provide valuable gene resource for rice resistance breeding.

Based on these findings in this Research Topic, habitat management could be used to promote the pest control with natural enemies, and plant defense could also be beneficial to suppress the occurrence and damage of pests. New strategies and techniques, which include "top down" regulation of pests from natural enemies and biodiversity and "bottom up" regulation of pests from plant defense, could be incorporated into integrated pest management in increasingly intensive, large-scale and simplified agricultural landscapes.

Author contributions

All authors listed have made a substantial, direct, and intellectual contribution to the work and approved it for publication.

Funding

This research is supported by the National Key Research and Development Program of China (No. 2022YFF1301801) and the Natural Science Foundation of Hunan Province, China (No. 2021JJ30010).

Acknowledgments

All authors of the Research Topic on Crop pest control regulated from natural enemies and plant defense for providing study cases to the Editorial.

Conflict of interest

The authors declare that the research was conducted in the absence of any commercial or financial relationships that could be construed as a potential conflict of interest.

Publisher's note

References

Coley, P. A. and Barone, J. A. (2001). *Encyclopedia of Biodiversity (Second Edition).*

Duffy, J. E., Cardinale, B. J., France, K. E., Mcintyre, P. B., Elisa, T., and Loreau, M. (2010). The functional role of biodiversity in ecosystems: incorporating trophic complexity. *Ecol. Lett.* 10, 522–538. doi: 10.1111/j.1461-0248.2007.01037.x

Faulkner, C. (2016). Defense mechanisms in plants. *Encycloped. Immunobiol.* 1, 389–396. doi: 10.1016/B978-0-12-374279-7.12001-6

Gurr, G. M., Wratten, S. D., Landis, D. A., and You, M. S. (2017). Habitat management to suppress pest populations: progress and prospects. *Ann. Rev. Entomol.* 62, 91–109. doi: 10.1146/annurev-ento-031616-035050

Larsen, A.E., Gaines, S.D., and Deschênes, O. (2017). Agricultural pesticide use and adverse birth outcomes in the San Joaquin Valley of California. *Nat. Commun.* 8, 302. doi: 10.1038/s41467-017-00349-2

Ouyang, F., Men, X., and Ge, F. (2020). "Landscape-level drivers of biocontrol and a case study from local to regional scale in China," in *Integrative Biological Control: Ecostacking for Enhanced Ecosystem Services,* eds Gao, Y., Hokkanen, H. M. T., Menzler-Hokkanen, I. (Cham: Springer International Publishing), pp. 145–164.

Ringland, J., and George, P. (2011). Analysis of sustainable pest control using a pesticide and a screened refuge. *Evol. Applicat.* 4, 459–470. doi: 10.1111/j.1752-4571.2010.00160.x

Thies, C., and Tscharntke, T. (1999). Landscape structure and biological control in agroecosystems. *Science* 285, 893–895. doi: 10.1126/science.285.5429.893

Tilman, D., Fargione, J., Wolff, B, D'Antonio, C., Dobson, A., Howarth, R., Schindler, D., et al. (2001). Forecasting agriculturally driven global environmental change. *Science*. 13, 281–284. doi: 10.1126/science.1057544

Van Meter, R.J., Glinski, D.A., Henderson, W.M., and Purucker, S.T. (2016). Soil organic matter content effects on dermal pesticide bioconcentration in American toads (Bufo Americanus). *Environ. Toxicol. Chem.* 35, 2734–2741. doi: 10.1002/etc.3439

frontiers in Sustainable Food Systems

ORIGINAL RESEARCH
published: 28 January 2021
doi: 10.3389/fsufs.2021.637382

Detection of Southern Rice Black-Streaked Dwarf Virus Using Western Blotting With P6

Xin Xie[1†], *Junmei Jiang*[1†], *Maoxi Huang*[2,3], *Meiqing Chen*[1], *Zhiguang Qu*[1] *and Xiangyang Li*[2,3*]

[1] *Key Laboratory of Agricultural Microbiology, College of Agriculture, Guizhou University, Guiyang, China,* [2] *State Key Laboratory Breeding Base of Green Pesticide and Agricultural Bioengineering, Ministry of Education, Guizhou University, Guiyang, China,* [3] *Key Laboratory of Green Pesticide and Agricultural Bioengineering, Ministry of Education, Guizhou University, Guiyang, China*

The southern rice black-streaked dwarf virus (SRBSDV) is a severe threat to the yield and quality of rice products worldwide. Traditional detection methods for diagnosing SRBSDV infection show several false positives and thus provide inaccurate findings. However, Western blotting (WB) can precisely solve this problem. In this study, P6—a viral RNA-silencing suppressor—was expressed and purified *in vitro*. Two polyclonal P6 antibodies were obtained and quantified by enzyme-linked immunosorbent assay and WB. Subsequently, WB was performed using the P6 antibodies to identify SRBSDV antigens derived from the suspected rice samples collected from nine districts in Guizhou, China. The assay results showed that Libo, Pingtang, Huishui, Dushan, and Anshun districts had experienced an SRBSDV outbreak. The virus content in the sampled rice tissues was quantified by WB. Our results revealed that SRBSDV mainly accumulated in rice stems rather than rice leaves. Thus, the findings of our study show that the SRBSDV P6 antibody can be used in WB for detecting and monitoring SRBSDV infection in infected rice plants.

Keywords: SRBSDV, P6, antibody production, virus detection, western blot

OPEN ACCESS

Edited by:
Wei Li,
Chinese Academy of Agricultural Sciences, China

Reviewed by:
Xiaoting Zhang,
Henan Agricultural University, China
Xiaofeng Su,
Biotechnology Research Institute (CAAS), China

***Correspondence:**
Xiangyang Li
xyli1@gzu.edu.cn

[†] *These authors have contributed equally to this work*

Specialty section:
This article was submitted to Agroecology and Ecosystem Services, a section of the journal Frontiers in Sustainable Food Systems

Received: *03 December 2020*
Accepted: *07 January 2021*
Published: *28 January 2021*

Citation:
Xie X, Jiang J, Huang M, Chen M, Qu Z and Li X (2021) Detection of Southern Rice Black-Streaked Dwarf Virus Using Western Blotting With P6. Front. Sustain. Food Syst. 5:637382. doi: 10.3389/fsufs.2021.637382

INTRODUCTION

Southern rice black-streaked dwarf virus (SRBSDV) is a severe threat to both the yield and quality of rice products worldwide (Wang et al., 2019). In 2010, ∼2.97 million acres of agricultural land in China was affected by SRBSDV infection (Wu et al., 2017).

Similar to rice black-streaked dwarf virus (RBSDV), SRBSDV is an icosahedral virus with a diameter of 70–75 nm. The SRBSDV genome comprises ten segments (S1–S10) in the decreasing order of molecular weight. Ten SRBSDV segments encode five putative structural proteins (P2, P3, P4, P8, and P10) and eight putative nonstructural proteins (P1, P5-1, P5-2, P6, P7-1, P7-2, P9-1, and P9-2) (Mao et al., 2013; Wang et al., 2013; Li et al., 2017; Yu et al., 2017). Among these proteins, P6 is a viral RNA-silencing suppressor that may affect its interaction with other viral proteins such as P7-1 and P9-1 (Wang et al., 2011; Jia et al., 2012; Wu et al., 2013). Thus, P7-1 and P9-1 were used as targets for detecting SRBSDV infection (Wang et al., 2015; Ran et al., 2018).

Several methods have been used to detect SRBSDV infection such as polymerase chain reaction (PCR) with SRBSDV using S7-1, S9-1, and S10 genes (Wang et al., 2015); immunoassays with SRBSDV P9-1 (Wang et al., 2015); dot enzyme-linked immunosorbent assay (dot-ELISA) with

SRBSDV P7-1, P9-1, and P10 (Chen et al., 2012; Wang et al., 2012; Uehara-Ichiki et al., 2013); yeast two-hybrid screening assay with P9-1 (Wang et al., 2015); and proteomics with SRBSDV proteins (Wang et al., 2017; Yang et al., 2017; Yu et al., 2017). Dot-ELISA is a simple and rapid method, but it shows an increased number of false positives. However, Western blotting (WB) can precisely solve this problem. In *Spodoptera frugiperda* cells induced by SRBSDV infection, P6 is recruited in the whole viroplasm matrix by directly interacting with P9-1 and P5 (Li et al., 2013, 2015a). To date, no study has reported the detection of SRBSDV with P6 using WB.

In the present study, P6 was expressed and regarded as a potential target of antiviral compound because of the importance of P6 in the whole viroplasm matrix (Wang et al., 2015). In our research, P6 was initially expressed and purified *in vitro*. Two polyclonal P6 antibodies were obtained and measured using ELISA. Subsequently, a WB approach was developed for identifying SRBSDV antigens derived from SRBSDV-infected rice samples collected from nine districts in Guizhou, China. The primary aim of the present study was to use WB to diagnose suspected SRBSDV infection in rice plants. To the best of our knowledge, this is the first study to diagnose SRBSDV infection in rice using WB with P6.

MATERIALS AND METHODS

Plant Materials

Suspected SRBSDV-infected rice samples with typical dwarf symptoms were collected from Tianzhu, Meitan, Dejiang, Puan, Libo, Pingtang, Huishui, Dushan, and Anshun districts in Guizhou, China (**Figure 1**). The samples were kept in liquid nitrogen and subsequently stored at −80°C.

Gene Cloning and Plasmid Construction

SRBSDV RNA was extracted from SRBSDV-inoculated rice leaves using the TRIzol reagent method (TaKaRa, Japan), and the cDNA of P6 was obtained through cDNA synthesis. *P6* gene was amplified using forward and reverse primers (5′-CGGGATCCA TGTCTACCAACCTCACGAACATA-3′) and (5′-GCTCTAGAT TACTCTGAAATAAGTTGCCACAA-3′), with a *BamH* I and *Xho* I at both ends, respectively. The target gene and the pCold-SUMO vector (Novagen, USA) were digested, purified through

FIGURE 1 | Investigation and collection of SRBSDV in Guizhou Province. Rice samples from Tianzhu, Meitan, Dejiang, Puan, Libo, Pingtang, Huishui, Dushan, and Anshun 9 districts of Guizhou were selected in this assay.

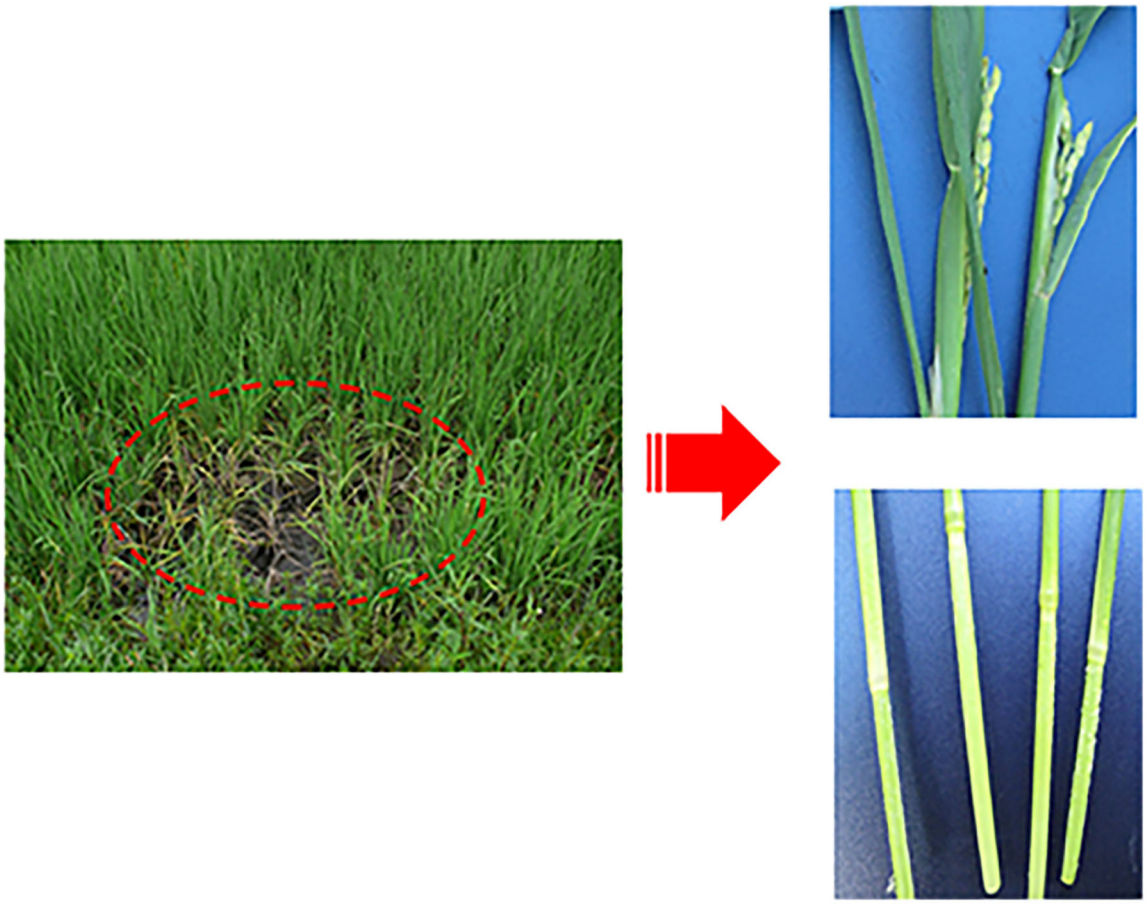

FIGURE 2 | Symptoms of rice infected with SRBSDV. Dashed oval represents rice infected by SRBSDV in the field. The right figures are enlarged symptoms of infected rice leaves **(Upper)** and stems **(Lower)** by SRBSDV.

electrophoresis, and ligated with T4 ligase. The ligation products were transformed into DH5α competent cells. Colonies were identified by PCR. Positive clones were sequenced and identified by restriction enzyme digestion.

P6 Protein Expression and Purification

The recombinant SRBSDV P6 plasmid was transformed into the *Escherichia coli* strain BL21 (DE3). The cells were harvested at 4 h after inoculation and after isopropyl-β-d-thiogalactopyranoside (IPTG) induction at 25°C. Subsequently, the cells were resuspended in a lysis buffer (50 mM Tris pH 7.5, 100 mM NaCl, 1 mM EDTA, 1% Triton X-100, 1 mg/mL lysozyme, and bacterial protease inhibitor cocktail) and sonicated for 2 min on ice. The lysates were incubated on ice for 30 min.

Protein purification was performed according to the protocols reported previously (Ran et al., 2018). The extracted cell lysates were incubated with equilibrated agarose beads (GE Healthcare, IL, USA) for at least 2 h at 4°C. Centrifugation was performed at 2,000 × g for 2 min to remove the supernatant. Thereafter, the beads were washed 5 times with a wash buffer [1×phosphate-buffered saline (PBS), 0.5% Triton X-100, and 1 mM EDTA]. The purified protein was eluted in a freshly prepared elution buffer (10 mM reduced glutathione, and 50 mM Tris pH 8.8).

Rabbit Immunization

Immunization and blood sample collection were performed at a biotechnology company (Youke, China). In this assay, two rabbits were injected with the suspended antigen in Freund's Adjuvant solution (Sigma, USA). On day 1, each rabbit was subcutaneously injected with 2 mL antigen solution (1 mL antigen with 1 mL Freund's Complete Adjuvant solution). The rabbits were administered three booster doses on days 15, 29, and 43 after immunization with 2 mL antigen solution (1 mL antigen with 1 mL Freund's Incomplete Adjuvant solution) as per the protocol in the first immunization. Pre- and post-immunization blood samples were collected, and 55 mL of each post-immunization blood sample was purified using protein A (Millipore, MA, USA).

Antibody Titer Detection

The titers of the purified antibody were tested by ELISA. Antigens were diluted to 1 μg/mL with citrate-buffered saline buffer (15 mM Na_2CO_3, 35 mM $NaHCO_3$, pH 9.6) and blocked

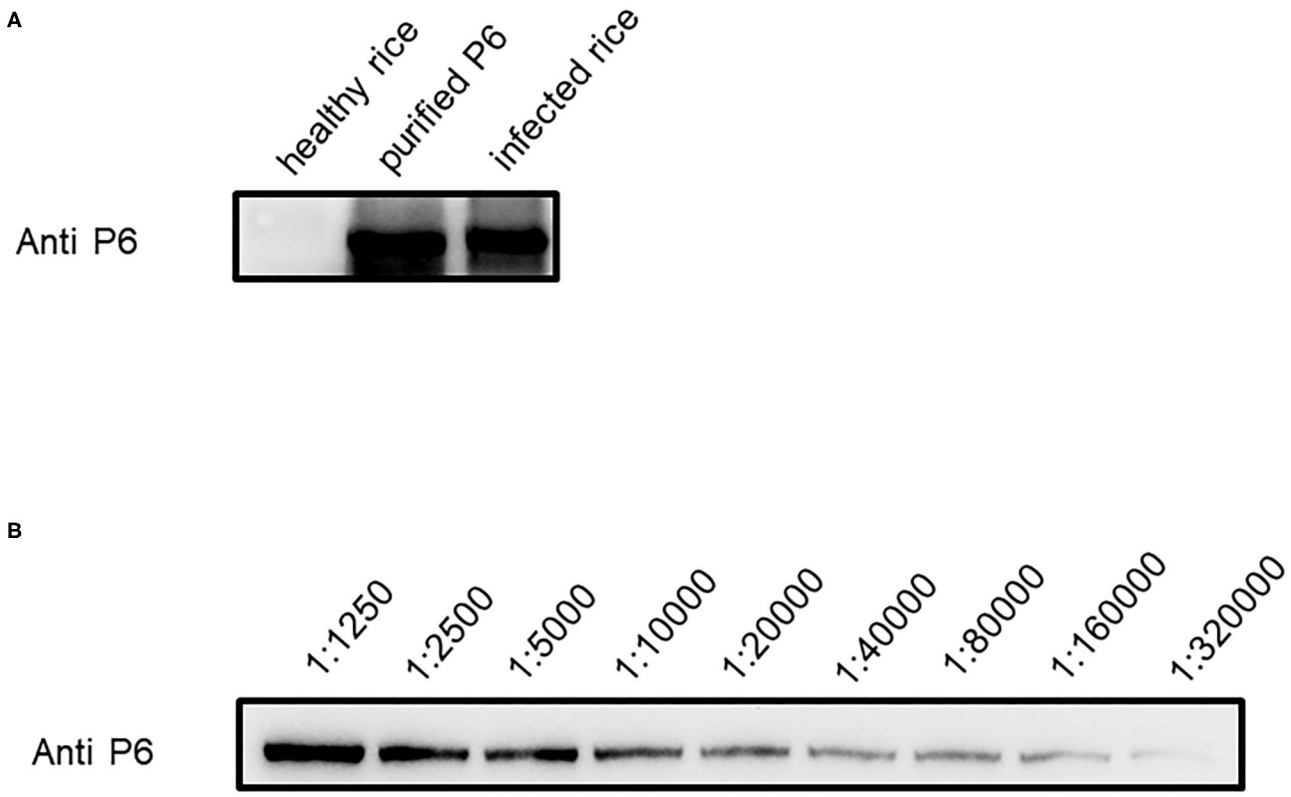

FIGURE 3 | Efficiency of P6 antibody in detecting SRBSDV. **(A)** SRBSDV detection of P6 antibody in healthy rice, protein antigen, and infected rice. **(B)** SRBSDV detection sensitivity of P6 antibody. Antigen diluted in series times such as 1:1250, 1:2500, 1:5000, 1:10000, 1:20000, 1:40000, 1:80000, and 1:160000 was used to test for P6 antibody detection limitation.

with 5% non-fat milk in PBS. Incubation was performed with the first and second antibodies. Then, the results of ELISA were detected using a spectrophotometer at A450 nm after the addition of the 3,3′,5,5′-tetramethylbenzidine reaction buffer (CWBio, China). For the titer test, antigens were diluted in a series ratio as follows: 1:1250, 1:2500, 1:5000, 1:10000, 1:20000, 1:40000, 1:80000, 1:160000, 1:320000, 1:640000, and 1:1280000. A healthy rabbit was used as the control.

Protein Extraction and Western Blotting Analysis

Rice leaves and stems were collected and ground in liquid nitrogen and were then resuspended in a protein lysis buffer (50 mM Tris PH 7.5, 6 M urea, 150 mM NaCl, 0.1% NP40, and 1 mM PMSF). The lysates were vortexed for 30 s and placed on ice for 30 min. Following lysis, the protein mixture was centrifuged at 20,000 × g for 20 min at 4°C to eliminate insoluble materials. The extracted protein was boiled with the sodium dodecyl sulfate (SDS)-loading buffer (250 mM Tris PH 6.8, 10% SDS, 0.5% bromophenol blue, and 50% glycerol) for 5 min and cooled on ice.

WB was conducted via the following steps. The extracted protein was loaded and run on SDS-polyacrylamide gel electrophoresis (SDS-PAGE) gel for protein electrophoresis. The protein in the gel was transferred onto a PVDF membrane for antibody detection (the PVDF membrane was soaked for 30 s in methanol before use). The PVDF membrane was blocked for 2 h at room temperature in 5% non-fat milk in PBS Tween-20 (PBST: PBS with 0.5% Tween-20). The first and second antibodies were incubated for 2 and 1 h, respectively, at room temperature in 5% non-fat milk in PBST. Signals were detected by adding the horseradish peroxidase substrate (Millipore, cat. WBKLS0100, USA).

RESULTS

SRBSDV and Symptoms in Rice

Our group collected 50 rice samples with suspected SRBSDV infection from nine districts in Guizhou, China, from June to September 2017 and 2018. All the samples were collected from Tianzhu, Meitan, Dejiang, Puan, Libo, Pingtang, Huishui, Dushan, and Anshun districts in Guizhou, China (**Figure 1**). Most of the samples had at least one of the typical symptoms of SRBSDV infection such as serious dwarfing, wrinkled leaves, and tumor-like protrusion symptoms on their stems (**Figure 2**).

P6 Cloning, Expression and Purification

The results of 1% agarose gel electrophoresis showed that 2,382 bp of the P6 fragment was cut in pCold-SUMO-P6 by *BamH* I

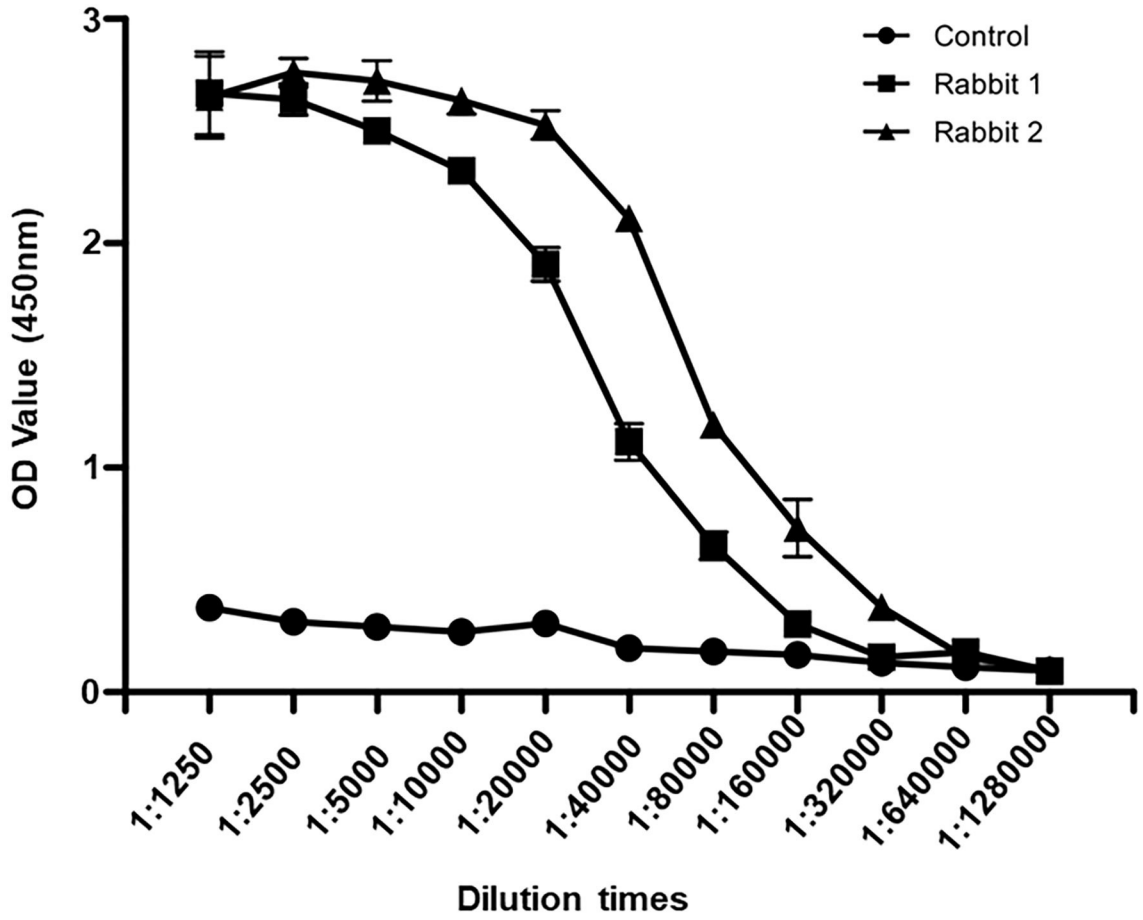

FIGURE 4 | Antibody titer detection by ELISA. Sera from rabbit one, rabbit two, and healthy rabbit were diluted to 1:1250, 1:2500, 1:5000, 1:10000, 1:20000, 1:40000, 1:80000, 1:160000, 1:320000, 1:640000, and 1:1280000. The values of OD450 were recorded.

and *Xho* I, and the target gene segment was matched with the reported length of the P6 gene (**Supplementary Table 1**). P6 was overexpressed at 101 kDa (with a SUMO tag about 11 kDa) when the final concentration was increased to 0.7 mM IPTG and when the solution was left for 16 h at 25°C. These His-tagged fusion proteins were purified in an Ni-NTA column (GE Healthcare). More than 90% of P6 was eluted from the beads with 100–300 mM imidazole in 50 mM Tris-HCl and 100 mM NaCl buffer at pH 7.5, as revealed by the results of 8% SDS-PAGE analysis (**Supplementary Table 2**). These purified P6 at 101 kDa were then concentrated to ∼1 mg/mL in 20 mM Tris-HCl and 100 mM NaCl at pH 7.5 for further analysis.

Rabbit Immunization and Antibody Induction

To detect SRBSDV, we produced SRBSDV antibodies in rabbits (rabbits 1 and 2). Two rabbits were injected with the purified P6. At 40 days after immunization, rabbit serum was collected and purified to obtain the P6 antibody. To verify the capability of this antibody, the purified P6 and rice leaves infected by SRBSDV were used as antigens. Our results showed that the P6 antibody displays specificity in detecting SRBSDV using WB (∼101 kDa) (**Figure 3A**). Subsequently, the titer of the P6 antibody was tested by ELISA. As shown in **Figure 4**, the titers of the P6 antibody from rabbit one and rabbit two were about 1:80000 and 1:160000, respectively. Thus, the antibody generated from rabbit two was used for further assays. The antibody from rabbit two was further confirmed by WB (**Figure 3B**). The P6 antibody could detect SRBSDV, although the antigen was diluted 320,000 times (**Figure 3B**).

Detection of SRBSDV in Guizhou Province

To shed light on the dynamics of the occurrence of SRBSDV in Guizhou, China, we collected rice samples showing SRBSDV infection symptoms (**Figure 2**) in rice-growing areas such as Dejiang, Meitan, Tianzhu, Anshun, Puan, Huishui, Pingtang, Dushan, and Libo (**Figure 1**). Samples from three different locations of the same district were harvested and stocked in liquid nitrogen immediately. Their proteins were extracted and detected using the P6 antibody for identifying SRBSDV. As shown in **Figure 5**, the rice samples from Anshun, Huishui, Pingtang, Dushan, and Libo, which are the southern districts, showed

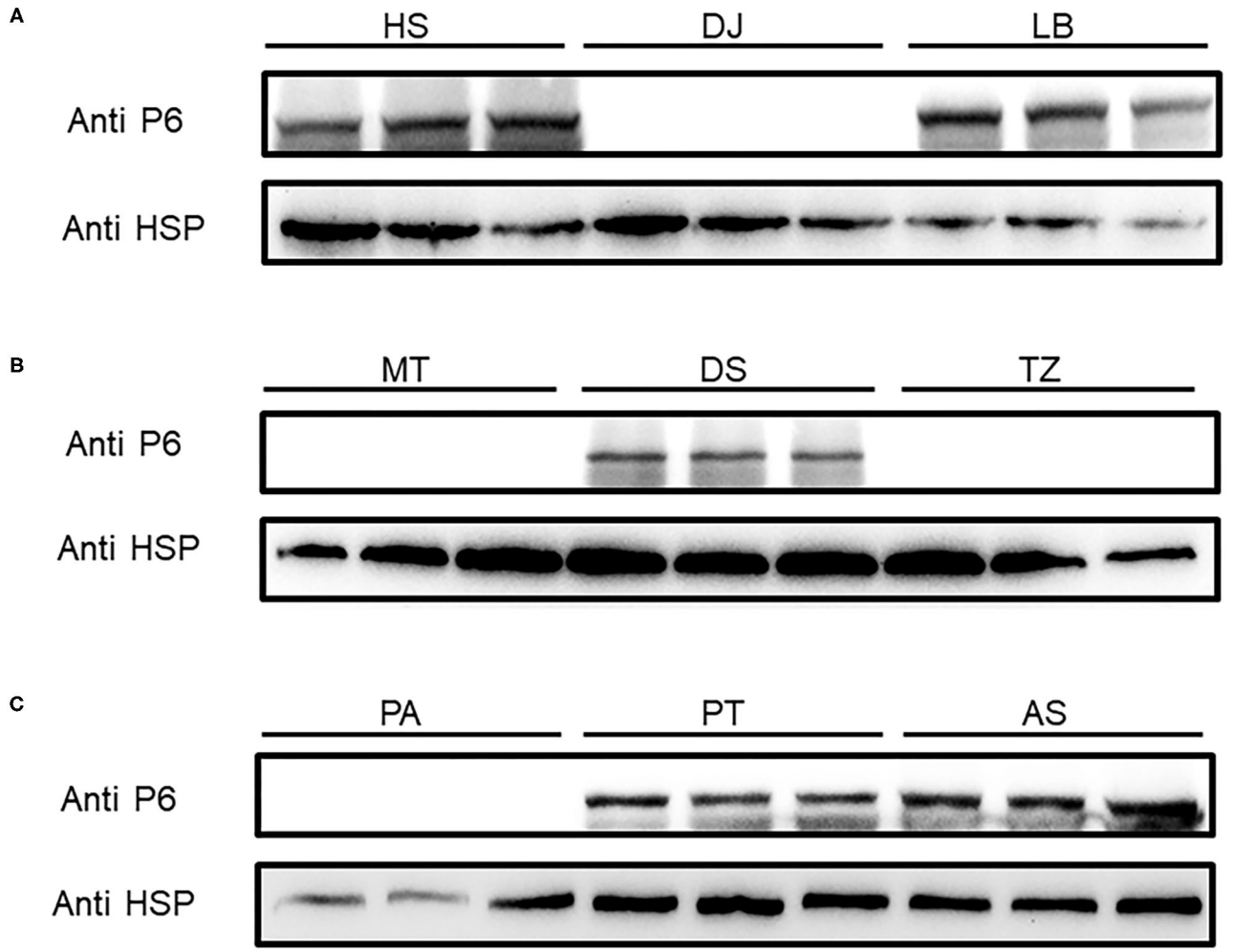

FIGURE 5 | SRBSDV detection in nine districts of Guizhou province. Rice samples from Huishui (HS), Dejiang (DJ), Libo (LB) **(A)**, Meitan (MT), Dushan (DS), Tianzhu (TZ) **(B)**, and Puan (PA), Pingtang (PT), and Anshun (AS) **(C)** were investigated by Western blot. P6 antibody was used to detect SRBSDV, and rice protein HSP90 was used as the internal control.

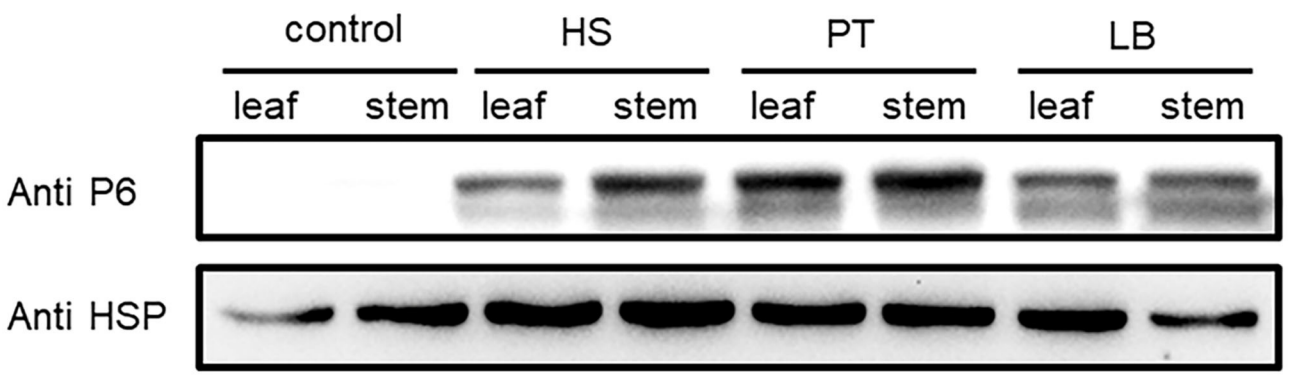

FIGURE 6 | Comparison of SRBSDV content in rice tissues. Rice leaves and stems from Huishui (HS), Pingtang (PT), and Libo (LB) were used to evaluate SRBSDV content. Healthy rice was used as a negative control, and rice internal control HSP90 was used as the internal control.

the P6 band, indicating that the rice plants in these areas were infected by SRBSDV. However, we did not detect the P6 band in the samples from the northern and western districts such as Dejiang, Meitan, Tianzhu, and Puan, thereby indicating that no SRBSDV existed in these districts. These findings implied that SRBSDV in Guizhou may have spread from the south to north of China.

Quantitative Comparison of SRBSDV Content in Rice Tissues

The virus content could vary across the plant tissues (Rettcher et al., 2015; Morán et al., 2018). To determine the SRBSDV content in rice leaves and stems that showed different symptoms when infected with SRBSDV (as illustrated in **Figure 2**), we quantified the SRBSDV content in rice leaves and stems using the P6 antibody. SRBSDV was detected in the rice leaves and stems from Huishui, Pingtang, and Libo districts. As shown in **Figure 6**, the SRBSDV content in rice stems was much higher than that in rice leaves. These findings indicate that SRBSDV is mainly accumulated in rice stems and then transmitted to rice leaves.

DISCUSSION

Rice plants infected by SRBSDV have caused a significant economic loss mainly in China and other Asian countries in recent years (Alonso et al., 2019). Moreover, rice plants infected by SRBSDV show a long latent period and are difficult to detect at an early stage, but they result in serious destruction at the later stage. Therefore, a reliable early monitoring and detection method will be useful for managing this infection and evaluating its risk (Zhang et al., 2008; Zhou et al., 2008; Hoang et al., 2011). To date, several methods have been used for detecting plant viruses, such as reverse transcription (RT) loop-mediated isothermal amplification, RT–PCR, and RT–qPCR; however, these methods provide false positive results, thereby causing inaccurate determination (López et al., 2006; Londoño et al., 2016; Malandraki et al., 2017; Treder et al., 2018). WB is a stable, reliable, and highly sensitive method that has been widely used for determining protein interaction and identification, quantifying protein expression, and detecting pathogen and virus movement (Samuilova et al., 2013; Huo et al., 2018; Wu et al., 2018). In our study, we established a WB assay to detect and quantify SRBSDV in infected rice plants. Using P6—a non-structural protein in SRBSDV—as the target, we could effectively detect SRBSDV in a rice paddy field and quantify the concentration of SRBSDV in different rice tissues, indicating that this assay is a salutary method for SRBSDV monitoring and forecasting as well as controlling and managing SRBSDV infection in the early stage.

Monoclonal antibodies have been produced and applied for detecting several plant virus infections (Tian et al., 2014; Li et al., 2015b; Zhang et al., 2018), but compared with polyclonal antibodies, monoclonal antibodies are much more expensive; they have a longer production period and are at more risk for failure. In this study, we aimed to detect SRBSDV infection in rice plants using polyclonal antibodies. First, the solubility of P6 was determined and then P6 was purified in *E. coli*. Second, two polyclonal P6 antibodies were obtained and quantified using WB. Then, a WB assay was developed for identifying SRBSDV infection in Guizhou, China. Finally, our results had shown for the first time that WB could be used to identify SRBSDV infected using the SRBSDV P6 antigen.

DATA AVAILABILITY STATEMENT

The datasets presented in this study can be found in online repositories. The names of the repository/repositories and accession number(s) can be found in the article/**Supplementary Material**.

AUTHOR CONTRIBUTIONS

XX and XL: conceptualization and funding acquisition. JJ and ZQ: methodology. JJ: validation and data curation. MH: formal analysis. MC: investigation. XL: resources, writing—review and editing, supervision, and project administration. XX: writing—original draft preparation. All authors contributed to the article and approved the submitted version.

FUNDING

This research was funded by the National Natural Science Foundation of China (Nos. 31801691, 31960546, and 32060614), the Science and Technology Foundation of Guizhou Province ([2019]2408), the Advanced Programs of Guizhou Province for the Returned Overseas Scholars ([2018]02), the Ph.D. Funding of Guizhou University, (No. 201754) and the Project of Guizhou Province [No. (2018)5781], Program of Introducing Talents of Discipline to Universities of China (111 Program, D20023).

SUPPLEMENTARY MATERIAL

The Supplementary Material for this article can be found online at: https://www.frontiersin.org/articles/10.3389/fsufs.2021.637382/full#supplementary-material

REFERENCES

Alonso, P., Gladieux, P., Moubset, O., Shih, P., Mournet, P., Frouin, J., et al. (2019). Emergence of southern rice black-streaked dwarf virus in the centuries-old Chinese Yuanyang agrosyst of rice landraces. *Viruses* 11:985. doi: 10.3390/v11110985

Chen, Z., Liu, J., Zeng, M., Wang, Z., Yu, D., Yin, C., et al. (2012). Dot immunobinding assay method with chlorophyll removal for the detection of southern rice black-streaked dwarf virus. *Molecules* 17, 6886–6900. doi: 10.3390/molecules17066886

Hoang, A. T., Zhang, H. M., Yang, J., Chen, J. P., Hébrard, E., Zhou, G. H., et al. (2011). Identification, characterization, and distribution of southern rice black-streaked dwarf virus in Vietnam. *Plant Dis.* 95, 1063–1069. doi: 10.1094/PDIS-07-10-0535

Huo, Y., Yu, Y., Chen, L., Li, Q., Zhang, M., Song, Z., et al. (2018). Insect tissue-specific vitellogenin facilitates transmission of plant

virus. *PLoS Pathog*. 14:e1006909. doi: 10.1371/journal.ppat.1006909

Jia, D., Chen, H., Zheng, A., Chen, Q., Liu, Q., Xie, L., et al. (2012). Development of an insect vector cell culture and RNA interference system to investigate the functional role of fijivirus replication protein. *J. Virol*. 86, 5800–5807. doi: 10.1128/JVI.07121-11

Li, J., Xue, J., Zhang, H., Yang, J., Lv, M., Xie, L., et al. (2013). Interactions between the P6 and P5-1 proteins of southern rice black-streaked dwarf fijivirus in yeast and plant cells. *Arch. Virol.* 158, 1649–1659. doi: 10.1007/s00705-013-1660-4

Li, J., Xue, J., Zhang, H., Yang, J., Xie, L., and Chen, J. (2015a). Characterization of homologous and heterologous interactions between viroplasm proteins P6 and P9-1 of the fijivirus southern rice black-streaked dwarf virus. *Arch. Virol*. 160, 453–457. doi: 10.1007/s00705-014-2268-z

Li, N., Chen, Z., Liu, Y., Liu, Y., Zhou, X., and Wu, J. (2015b). Development of monoclonal antibodies and serological assays specific for Barley yellow dwarf virus GAV strain. *Virol. J*. 12:136. doi: 10.1186/s12985-015-0367-4

Li, S., Zhang, T., Zhu, Y., and Zhou, G. (2017). Co-infection of two reoviruses increases both viruses accumulation in rice by up-regulating of viroplasm components and movement proteins bilaterally and RNA silencing suppressor unilaterally. *Virol. J*. 14:150. doi: 10.1186/s12985-017-0819-0

Londoño, M. A., Harmon, C. L., and Polston, J. E. (2016). Evaluation of recombinase polymerase amplification for detection of begomoviruses by plant diagnostic clinics. *Virol. J*. 13:48. doi: 10.1186/s12985-016-0504-8

López, R., Asensio, C., Guzman, M. M., and Boonham, N. (2006). Development of real-time and conventional RT-PCR assays for the detection of potato yellow vein virus (PYVV). *J. Virol. Methods*. 136, 24–29. doi: 10.1016/j.jviromet.2006.03.026

Malandraki, I., Beris, D., Isaioglou, I., Olmos, A., Varveri, C., and Vassilakos, N. (2017). Simultaneous detection of three pome fruit tree viruses by one-step multiplex quantitative RT-PCR. *PLoS ONE* 12:e0180877. doi: 10.1371/journal.pone.0180877

Mao, Q., Zheng, S., Han, Q., Chen, H., Ma, Y., Jia, D., et al. (2013). New Model for the Genesis and maturation of viroplasms induced by fijiviruses in insect vector cells. *J. Virol*. 87, 6819–6828. doi: 10.1128/JVI.00409-13

Morán, F., Olmos, A., Lotos, L., Predajna, L., Katis, N., Glasa, M., et al. (2018). A novel specific duplex real-time RT-PCR method for absolute quantitation of *Grapevine Pinot gris virus* in plant material and single mites. *PLoS ONE* 13:e0197237. doi: 10.1371/journal.pone.0197237

Ran, L., Ding, Y., Luo, L., Gan, X., Li, X., Chen, Y., et al. (2018). Binding constants of Southern rice black-streaked dwarf virus coat protein with ferulic acid derivatives. *Data Brief*. 17, 321–324. doi: 10.1016/j.dib.2018.01.031

Rettcher, S., Jungk, F., Kühn, C., Krause, H. J., Nölke, G., Commandeur, U., et al. (2015). Simple and portable magnetic immunoassay for rapid detection and sensitive quantification of plant viruses. *Appl. Environ. Microbiol*. 81, 3039–3048. doi: 10.1128/AEM.03667-14

Samuilova, O., Santala, J., and Valkonen, J. P. (2013). Tyrosine phosphorylation of the triple gene block protein 3 regulates cell-to-cell movement and protein interactions of potato mop-top virus. *J. Virol*. 87, 4313–4321. doi: 10.1128/JVI.03388-12

Tian, Y. P., Hepojoki, J., Ranki, H., Lankinen, H., and Valkonen, J. P. (2014). Analysis of potato virus Y coat protein epitopes recognized by three commercial monoclonal antibodies. *PLoS ONE* 9:e115766. doi: 10.1371/journal.pone.0115766

Treder, K., Chołuj, J., Zacharzewska, B., Babujee, L., Mielczarek, M., Burzyński, A., and Rakotondrafara, A. M. (2018). Optimization of a magnetic capture RT-LAMP assay for fast and real-time detection of potato virus Y and differentiation of N and O serotypes. *Arch. Virol.* 163, 447–458. doi: 10.1007/s00705-017-3635-3

Uehara-Ichiki, T., Shiba, T., Matsukura, K., Ueno, T., Hirae, M., and Sasaya, T. (2013). Detection and diagnosis of rice-infecting viruses. *Front. Microbiol*. 4:289. doi: 10.3389/fmicb.2013.00289

Wang, D., Xie, X., Gao, D., Chen, K., Chen, Z., Jin, L., et al. (2019). Dufulin intervenes the viroplasmic proteins as the mechanism of action against southern rice black-streaked dwarf virus. *J. Agric. Food Chem*. 67, 11380–11387. doi: 10.1021/acs.jafc.9b05793

Wang, Q., Tao, T., Han, Y., Chen, X., Fan, Z., Li, D., et al. (2013). Nonstructural protein P7-2 encoded by rice black-streaked dwarf virus interacts with SKP1, a core subunit of SCF ubiquitin ligase. *Virol. J*. 10:325. doi: 10.1186/1743-422X-10-325

Wang, Q., Tao, T., Zhang, Y., Wu, W., Li, D., Yu, J., et al. (2011). Rice black-streaked dwarf virus P6 self-interacts to form punctate, viroplasm-like structures in the cytoplasm and recruits viroplasm-associated protein P9-1. *Virol. J*. 8:24. doi: 10.1186/1743-422X-8-24

Wang, Z., Li, X., Wang, W., Zhang, W., Yu, L., Hu, D., et al. (2015). Interaction research on the antiviral molecule dufulin targeting on southern rice black streaked dwarf virus p9-1 nonstructural protein. *Viruses* 7, 1454–1473. doi: 10.3390/v7031454

Wang, Z., Yu, D., Li, X., Zeng, M., Chen, Z., Bi, L., et al. (2012). The development and application of a Dot-ELISA assay for diagnosis of southern rice black-streaked dwarf disease in the field. *Viruses* 4, 167–183. doi: 10.3390/v4010167

Wang, Z., Yu, L., Jin, L., Wang, W., Zhao, Q., Ran, L., et al. (2017). Evaluation of rice resistance to southern rice black-streaked dwarf virus and rice ragged stunt virus through combined field tests, quantitative real-time PCR, and proteome analysis. *Viruses* 9:37. doi: 10.3390/v9020037

Wu, G., Cui, X., Chen, H., Renaud, J. B., Yu, K., Chen, X., et al. (2018). Dynamin-like proteins of endocytosis in plants are coopted by potyviruses to enhance virus infection. *J. Virol*. 92, e01320–e01318. doi: 10.1128/JVI.01320-18

Wu, J., Li, J., Mao, X., Wang, W., Cheng, Z., Zhou, Y., et al. (2013). Viroplasm protein P9-1 of rice black-streaked dwarf virus preferentially binds to single-stranded RNA in its octamer form, and the central interior structure formed by this octamer constitutes the major RNA binding site. *J. Virol*. 87, 12885–12899. doi: 10.1128/JVI.02264-13

Wu, Y., Zhang, G., Chen, X., Li, X., Xiong, K., Cao, S., et al. (2017). The influence of *Sogatella furcifera* (Hemiptera: Delphacidae) migratory events on the southern rice black-streaked dwarf virus epidemics. *J. Econ. Entomol*. 110, 854–864. doi: 10.1093/jee/tox062

Yang, A., Yu, L., Chen, Z., Zhang, S., Shi, J., Zhao, X., et al. (2017). Label-free quantitative proteomic analysis of chitosan oligosaccharide-treated rice infected with southern rice black-streaked dwarf virus. *Viruses* 9:115. doi: 10.3390/v9050115

Yu, L., Shi, J., Cao, L., Zhang, G., Wang, W., Hu, D., et al. (2017). A novel method for transmitting southern rice black-streaked dwarf virus to rice without insect vector. *Virol. J*. 14:155. doi: 10.1186/s12985-017-0815-4

Zhang, H. M., Yang, J., Chen, J. P., and Adams, M. J. (2008). A black-streaked dwarf disease on rice in China is caused by a novel fijivirus. *Arch. Virol*. 153, 1893–1898. doi: 10.1007/s00705-008-0209-4

Zhang, M., Chen, R., Zhou, X., and Wu, J. (2018). Monoclonal antibody-based serological detection methods for wheat dwarf virus. *Virol. Sin*. 33, 173–180. doi: 10.1007/s12250-018-0024-3

Zhou, G., Wen, J., Cai, D., Li, P., Xu, D., and Zhang, S. (2008). Southern rice black-streaked dwarf virus: a new proposed fijivirus species in the family Reoviridae. *Chin. Sci. Bull*. 53, 3677–3685. doi: 10.1007/s11434-008-0467-2

Conflict of Interest: The authors declare that the research was conducted in the absence of any commercial or financial relationships that could be construed as a potential conflict of interest.

frontiers in Sustainable Food Systems

ORIGINAL RESEARCH
published: 01 March 2021
doi: 10.3389/fsufs.2021.631990

De novo Transcriptome Assembly of *Myllocerinus aurolineatus* Voss in Tea Plants

Xin Xie[1†], *Junmei Jiang*[1†], *Meiqing Chen*[1], *Maoxi Huang*[2], *Linhong Jin*[2] *and Xiangyang Li*[2*]

[1] Key Laboratory of Agricultural Microbiology, College of Agriculture, Guizhou University, Guiyang, China, [2] State Key Laboratory Breeding Base of Green Pesticide and Agricultural Bioengineering, Key Laboratory of Green Pesticide and Agricultural Bioengineering, Ministry of Education, Guizhou University, Guiyang, China

Myllocerinus aurolineatus Voss is a species of the insecta class in the arthropod. In this study, we first observed and identified *M. aurolineatus* Voss in tea plants in Guizhou, China, where it caused severe quantity and quality losses in tea plants. Knowledge on *M. aurolineatus* Voss genome is inadequate, especially for biological or functional research. We performed the first transcriptome sequencing by using the Illumina Hiseq^{TM} technique on *M. aurolineatus* Voss. Over 55.9 million high-quality paired-end reads were generated and assembled into 69,439 unigenes using the Trinity short read software, resulting in a cluster of 1,207 bp of the N50 length. A total of 69,439 genes were predicted by BLAST to known proteins in the NCBI database and were distributed into Gene Ontology (20,190), eukaryotic complete genomes (12,488), and the Kyoto Encyclopedia of Genes and Genomes (3,170). We also identified 96,790 single-nucleotide polymorphisms and 13,121 simple sequence repeats in these unigenes. Our transcriptome data provide a useful resource for future functional studies of *M. aurolineatus* Voss for dispersal control in tea plants.

Keywords: *Myllocerinus aurolineatus* Voss, transcriptome, pest, tea (*Camellia sinensis*), identification of pests

OPEN ACCESS

Edited by:
Wei Li,
Institute of Plant Protection (CAAS), China

Reviewed by:
Xueqing Geng,
Shanghai Jiao Tong University, China
Qun En Liu,
China National Rice Research Institute (CAAS), China
Zhiqiang Li,
Institute of Plant Protection (CAAS), China

***Correspondence:**
Xiangyang Li
xyli1@gzu.edu.cn

*These authors have contributed equally to this work

Specialty section:
This article was submitted to Agroecology and Ecosystem Services, a section of the journal Frontiers in Sustainable Food Systems

Received: *21 November 2020*
Accepted: *25 January 2021*
Published: *01 March 2021*

Citation:
Xie X, Jiang J, Chen M, Huang M, Jin L and Li X (2021) De novo Transcriptome Assembly of Myllocerinus aurolineatus Voss in Tea Plants. Front. Sustain. Food Syst. 5:631990. doi: 10.3389/fsufs.2021.631990

INTRODUCTION

Tea plant *Camellia sinensis* is a major economic crop in China and accounts for half of the total plantation area worldwide (Li et al., 2017). Many nutritional ingredients are produced in tea shoots, which are used as raw materials for commercial tea processing (Comblain et al., 2016). However, various tea plant pests jeopardize the quantity and quality of tea, such as the tea leaf beetle, one of the most serious pests affecting tea plants in China, Vietnam, Indonesia, Japan, and other tea-producing countries in Asia (Sun et al., 2010; Yang et al., 2013; Roy and Muraleedharan, 2014). Here, we reported a leaf beetle, *Myllocerinus aurolineatus* Voss in tea plant in Guizhou province, China. *M. aurolineatus* was first reported in China in 1991, where the species emerged in tea plants (Zhang, 1991).

M. aurolineatus is an exceptionally destructive and productive pest that shows strong tolerance and adaptability against environment challenges, including those with pesticide treatment, extreme temperatures, and volatile compound attractions (Sun et al., 2010, 2017). In Meitan district, Guizhou, *M. aurolineatus* pupates from March to April, then larvae become adult and begin to mate from June to July. Finally, the outbreak of this pest will be from July to August. Pesticide resistance, the diapause process, and other biological flexibilities are moderated by series molecular mechanisms (Casida, 2017; Jugulam and Gill, 2018; Zhang et al., 2018). However, lack of bona

fide reference regarding gene annotation and genomic information restricts our research on the molecular mechanism of these physiological processes for exploring new management approaches for this species. To date, only 157 nucleotide sequences including 51 expressed sequences (EST) have been deposited in GenBank for this beetle. In addition, only few genetic markers have been reported for *M. aurolineatus* (Ma et al., 2014; Mukhopadhyay et al., 2016).

De novo transcriptome assemblies constitute a valid technology to study reference-free genomes in non-model organisms and provided abundant sequence and gene expression information for further functional research (Gayral et al., 2013; Smith-Unna et al., 2016). With the development of sequencing technologies, such as Illumina and 454 Life Sciences, genomic information in model and non-model organisms have been broadly uncovered along with numerous genes involved in biotic and abiotic stresses, pesticide resistance, developmental pathways, diapause transitions, and hormone regulations by homology blast with related organisms (Ekblom and Galindo, 2011; Tarrant et al., 2016).

In this study, Illumina Hiseq™ technique was used for *de novo* transcriptome assembly and analysis of *M. aurolineatus*, a new reported tea plant pest. Sequences were performed with a BLAST search to the known proteins of the NCBI database and the CDS fragments were predicted. Gene Ontology (GO), euKaryotic Ortholog Groups (KOG), and the Kyoto Encyclopedia of Genes and Genomes (KEGG) were annotated. Furthermore, we used these data to generate simple sequence repeat (SSR), and single-nucleotide polymorphism (SNP) markers, which will be potential resources for trait mapping. We believe that the transcriptome assembly of *M. aurolineatus* obtained in our study represents crucial resources for research into molecular pathway, gene function, metabolic regulation associated with pesticide resistance, and biocontrol areas.

MATERIALS AND METHODS

M. aurolineatus Collection

In August, the mature *M. aurolineatus* were captured from the top leaves of the 20-year tea plant in Meitan District, Guizhou,

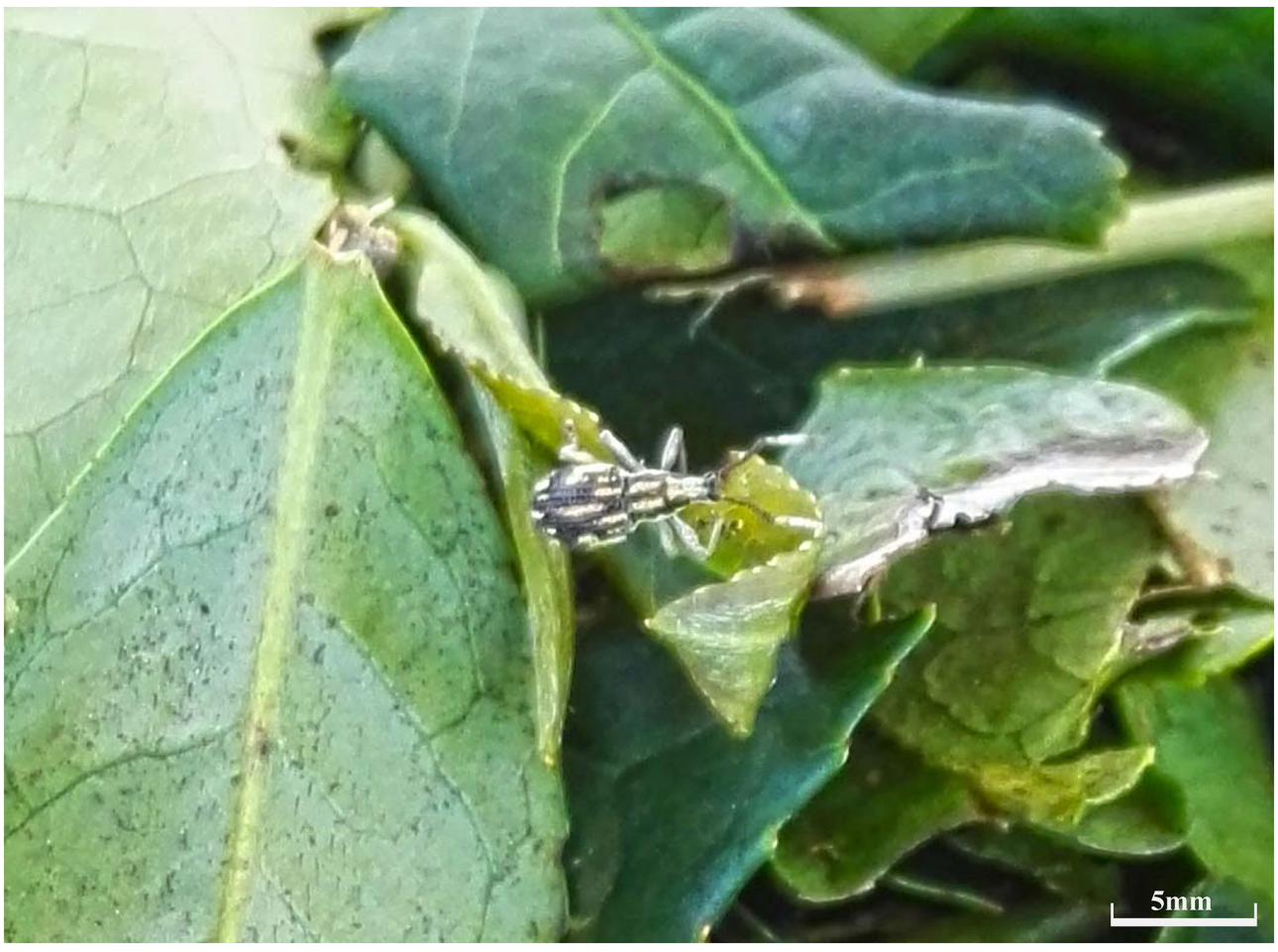

FIGURE 1 | The morphological characteristics of the adult *M. aurolineatus* on tea leaves.

TABLE 1 | Summary of the *M. aurolineatus* transcriptome.

Details	Raw data number	Clean data number
Total Reads Count (#)	55,915,882	52,794,150
Total Bases Count (bp)	8,387,382,300	7,746,012,937
Average Read Length (bp)	150.0	146.72
Q10 Bases Count (bp)	8,387,296,556	7,745,994,501
Q10 Bases Ratio (%)	100.00%	100.00%
Q20 Bases Count (bp)	8,078,659,930	7,608,560,972
Q20 Bases Ratio (%)	96.32%	98.23%
Q30 Bases Count (bp)	7,651,532,640	7,271,169,235
Q30 Bases Ratio (%)	91.23%	93.87%
N Bases Count (bp)	85,744	18,436
N Bases Ratio (%)	0.00%	0.00%
GC Bases Count (bp)	3349,606,239	3,098,514,104
GC Bases Ratio (%)	39.94%	40.00%

China. Three beetles were kept in liquid nitrogen as a group and subsequently used for transcriptome sequencing.

Nucleic Acid Isolation

Total RNA was extracted using the Trizol kit (Sangon, China) according to the manufacturer's protocol, and treated with RNase-free DNase I to remove genomic DNA contamination. RNA integrity was evaluated with a 1.0% agarose gel. Thereafter, RNA quality and quantity were assessed using a Nanodrop (Thermo, USA) and an Agilent 2100 Bioanalyzer (Agilent Technologies, USA). The high-quality RNA samples were subsequently submitted for library preparation and sequencing.

Library Preparation and Sequencing

A total of 2 μg of RNA sample was used as input material for the RNA sample preparations. Sequencing libraries were generated using VAHTSTM mRNA-seq V2 Library Prep Kit for Illumina® following the manufacturer's protocols. First-strand cDNA was synthesized using random hexamer primer and M-MuLV Reverse Transcriptase. Second-strand cDNA synthesis was subsequently performed using DNA polymerase I and RNase H. Remaining overhangs were converted into blunt ends via exonuclease/polymerase activities. To select cDNA fragments of preferentially 150–200 bp in length, the library fragments were purified with AMPure XP system (Beckman Coulter, Beverly, USA). Then, 3 μl of USER Enzyme (NEB, USA) was utilized with size-selected, adaptor-ligated cDNA at 37°C for 15 min followed by 5 min at 95°C in PCR cycler. Finally, PCR products were purified (AMPure XP system) and the library quality was assessed on the Agilent Bioanalyzer 2100 system. The libraries were then quantified and pooled. Paired-end sequencing of the library was performed on the HiSeq XTen sequencers (Illumina, USA).

Data Assessment and Quality Control

FastQC (version 0.11.2) was used for evaluating the quality of sequenced data. Raw reads were filtered by Trimmomatic (version 0.36) according to five steps: (1) removing adaptor sequence; (2) removing low quality bases from reads $3'$ to $5'$ ($Q < 20$); (3) removing low-quality bases from reads $5'$ to $3'$ ($Q < 20$); (4) using a sliding window method to remove the base value <20 of reads tail (window size is 5 bp); (5) removing reads with reads length <35 nt and its pairing reads. The remaining clean data were used for further analysis.

Transcriptome Assembly and Gene Annotation

The remaining clean reads were *de novo* assembled into transcripts using Trinity short read software (version 2.0.6) (parameter: min_kmer_cov 2). Transcripts with a minimum length of 200 bp were clustered to minimize redundancy. For each cluster (representing the transcriptional complexity for the same gene), the longest sequence was preserved and designated as a unigene. Unigenes were blasted against the NCBI non-redundant protein database, SwissProt, TrEMBL, Conserved Domain Database (CDD), Protein family (Pfam), and KOG databases (*E*-value $< 1e^{-5}$). According to the priority order of the best aligned results, the Unigene ORF (open reading frame) was determined using the ORF-predictor server. At the same time, TransDecoder (version 3.0.1) was used to predict the CDS sequences of the un-aligned Unigenes. GO functional annotation information was obtained according to transcript annotation results of SwissProt and TrEMBL. KEGG Automatic Annotation Server (version 2.1) was used for the KEGG annotation.

RESULTS AND DISCUSSION

M. aurolineatus Identification

M. aurolineatus were captured in the tea plant in Meitan District, Guizhou, China, and the morphological character was described as follows: body, gray black; head with two longitudinal lines yellow pale, with metallic shimmer in dorsal view; antennae geniculate, with scapus straight and thin, expanded in apical three flagella; pronotum with four longitudinal lines yellow pale; elytra with several yellow pale long patches, with black traverse patches in the center in dorsal view (**Figure 1**).

Illumina Sequencing and *De novo* Assembly

We used the Illumina Hiseq™ platform to sequence the constructed cDNA library of *M. aurolineatus* and obtained 55,915,882 raw reads. To acquire clean reads, 3,121,732 of the low-quality reads and adapter sequences were trimmed by using FastQC software, thus generating 52,794,150 clean reads from the *M. aurolineatus* transcriptomes. The Q20 and Q30 percentages (sequencing error rate < 0.1%) of *M. aurolineatus* were 98.23 and 93.87%, respectively (**Table 1**). The average read length was 146.72 bp, and the percentage of GC content was 40.00% (**Table 1**). Subsequently, 69,439 unigenes were assembled from the high-quality reads with an average length of 669.28 bp and an N50 of 1,207 bp and N90 of 253 bp. Unigenes with a length of more than 500 and 1,000 bp were 22,395 and 11,856 (**Table 2**). The length and GC content frequency distributions of all unigenes are shown in **Table 2** and **Figure 2**.

TABLE 2 | Transcriptome assembly results.

Type	Number	> =500 bp	> =1,000 bp	N50	N90	Max length	Min length	Total length	Average length
Transcript	113,670	42,599	24,929	1,563	270	19,627	201	89,903,658	790.92
Unigene	69,439	22,395	11,856	1,207	253	19,627	201	46,474,325	669.28

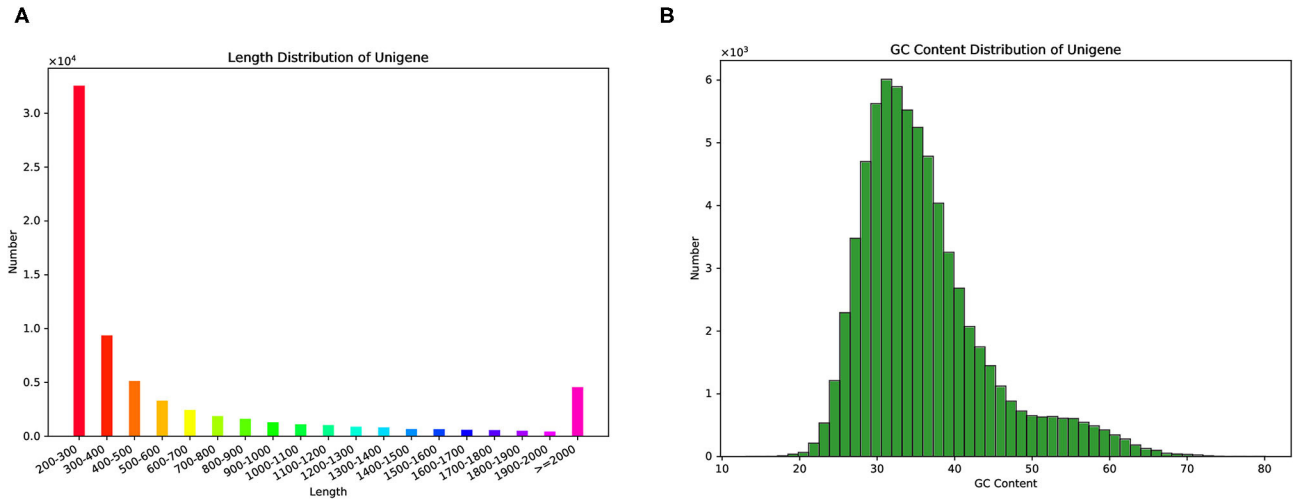

FIGURE 2 | The length and GC content frequency distributions of all unigenes. **(A)** The length distributions; **(B)** GC content frequency distributions.

TABLE 3 | Percentage of annotated genes.

Database	Number of genes	Percentage (%)
Annotated in CDD	13,494	19.43
Annotated in KOG	12,488	17.98
Annotated in NR	23,491	33.83
Annotated in NT	6,576	9.47
Annotated in PFAM	10,254	14.77
Annotated in Swissprot	17,040	24.54
Annotated in TrEMBL	23,422	33.73
Annotated in GO	20,190	29.08
Annotated in KEGG	3,170	4.57
Annotated in at least one database	26,351	37.95
Annotated in all database	1,011	1.46
Total genes	69,439	100

Annotation of Predicted Proteins

To annotate the proteins, we employed the BLASTx program for blasting against NT (NCBI nucleotide sequences), NR (NCBI non-redundant protein sequences), COG (Clusters of Orthologous Groups of proteins), KOG (euKaryotic Ortholog Groups), Swiss-Prot (a manually annotated and reviewed protein sequence database), TrEMBL, Pfam, CDD, GO, and KEGG databases. Of the *M. aurolineatus* transcripts, 69,439 unigenes were annotated in the above databases, including 23,491 unigenes (33.83%) in the NR database and 17,040 unigenes (24.54%) in the SwissProt database. Moreover, 26,351 unigenes (37.95%) were annotated in at least one database (**Table 3**). These results were similar to other Arthropoda species, such as 10,218 unigenes were identified in *Dendroctonus ponderosae* (Regniere and Bentz, 2007), 4,251 in *Tribolium castaneum* (Li et al., 2008), 1,207 in *Papilio xuthus* (Zhang and Zhang, 2017), and 353 in *Acyrthosiphon pisum* (Bishnoi and Singla, 2017). A total of 43.56% annotated unigenes were matched from *D. ponderosae* according to the proportion on the distribution of best-matched species, followed by 18.12, 5.15, 1.51, and 1.27% sequences that matched sequences from *T. castaneum*, *P. xuthus*, *A. pisum*, and *Oryctes borbonicus*, respectively. The remaining 30.39% of sequences were matched from other species (**Figure 3**).

GO, KOG, and KEGG Classifications of Unigenes

Cluster groups of the unigenes were calculated against GO, KOG, and the KEGG databases using BLASTx search with a cutoff E value of 10^{-5}. A total of 29.08% unigenes (20,190) were annotated in these three databases (**Table 3**).

As an international standardized gene functional classification system, GO determines the functional description of genes and their products (Tarrant et al., 2016). Three independent classifications, namely, "biological process," "cellular component," and "molecular function," are included in this process. As shown in **Figure 4** and **Supplementary Table 1**, 20,190 (29.08%) unigenes were assigned to the main GO classifications, including 71 sub-classifications. Within the

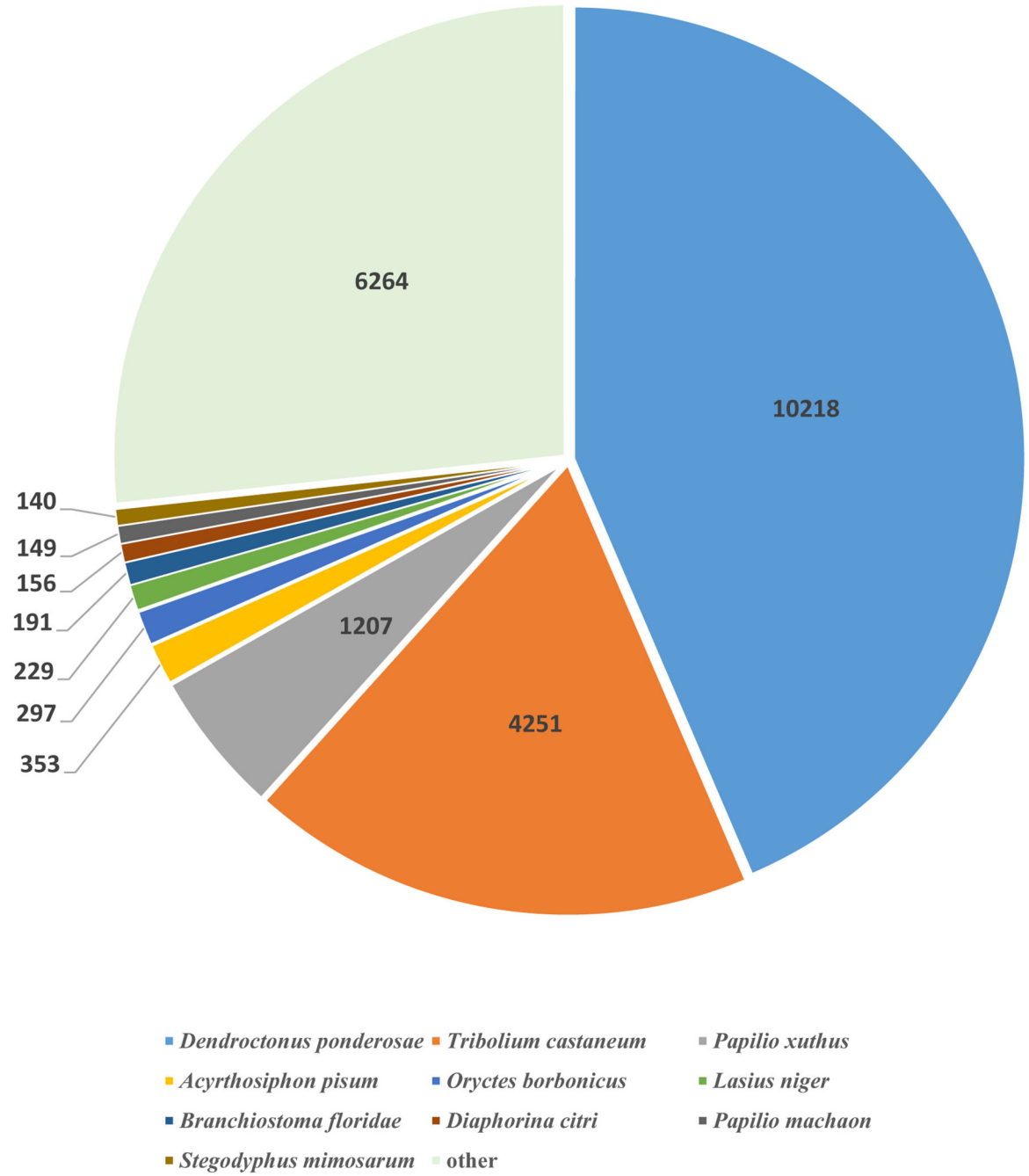

FIGURE 3 | Species distribution of top BLASTx results. The pie chart shows the species distribution of unigenes top BLASTx results against the NR protein database with a cutoff E value $<1e^{-3}$.

molecular function group, binding (GO:0005488) and catalytic activity (GO:0003824) processes were the main proportions with 12,042 and 9,471 unigenes, respectively. In the biological process, cellular (GO:0009987) and metabolic processes (GO:0008152) were the largest two groups including 13,156 and 10,939 unigenes, respectively. Cell (GO:0005623, 13,874 unigenes) and cell part (GO:0044464, 13,837 unigenes) represented the majority of processes in the cellular component category.

KOG annotation is widely used to cluster the protein functions in many species (Moon et al., 2008; Kuzniar et al., 2009). In our study, a total of 12,488 unigenes were clustered into 26 functional categories (**Figure 5**). Among the 26 KOG

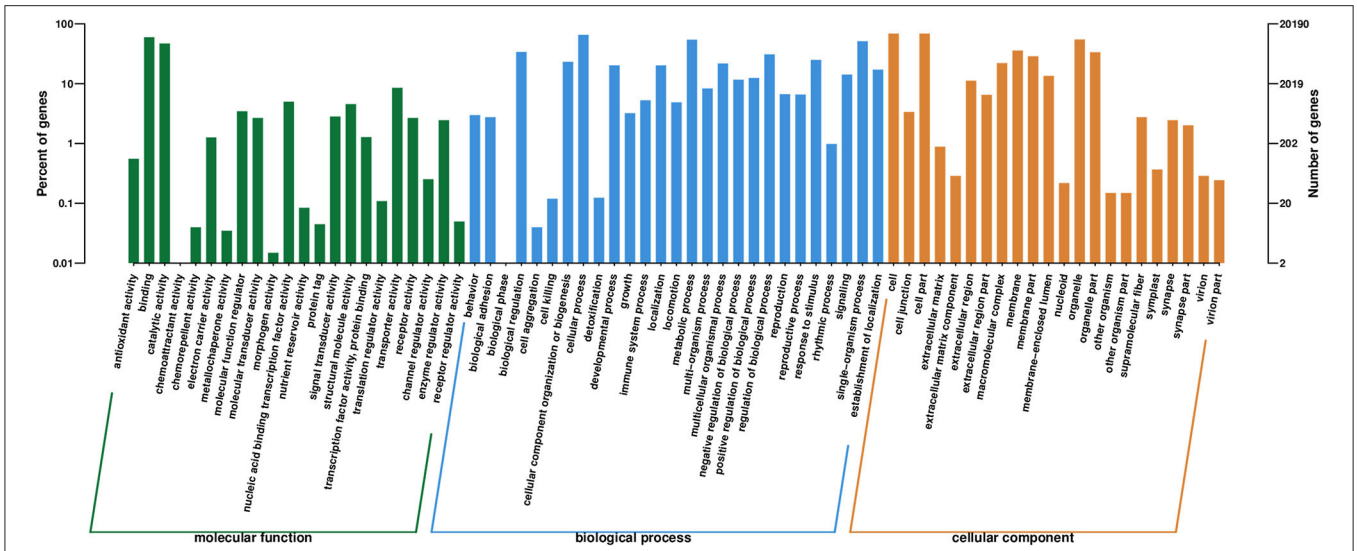

FIGURE 4 | Gene Ontology (GO) categories of the unigenes. Distribution of the GO categories assigned to the *M. aurolineatus* transcriptome. Unique transcripts (unigenes) were annotated in three categories: cellular components, molecular functions, and biological process.

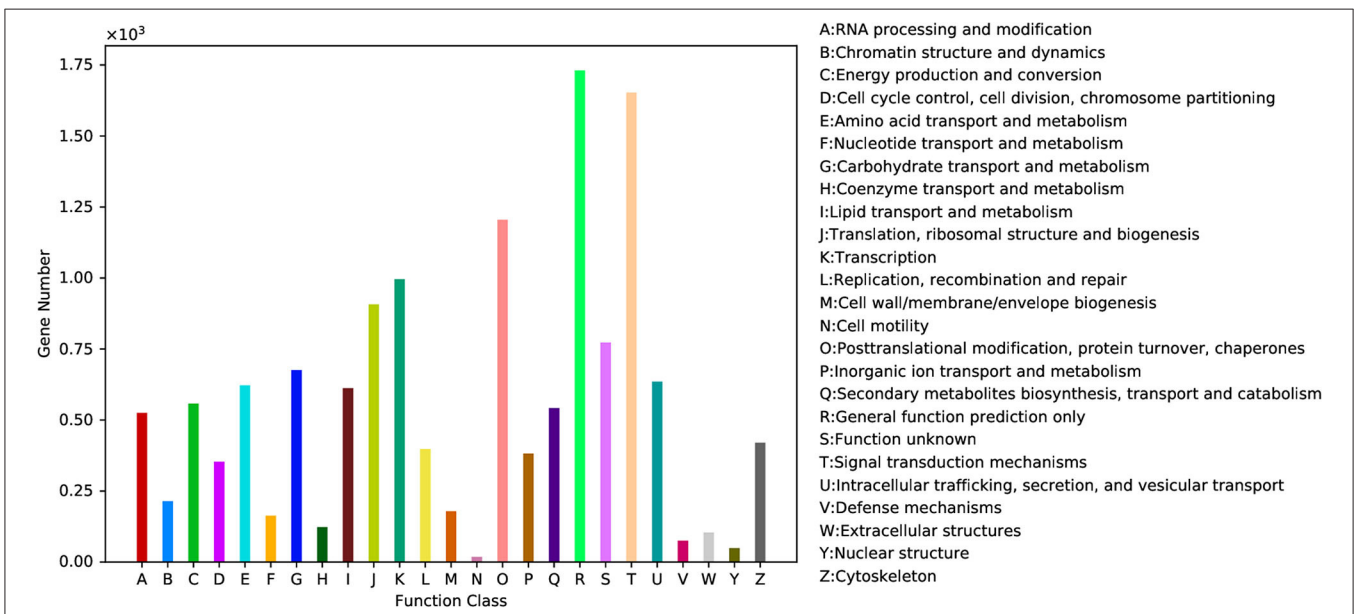

FIGURE 5 | Cluster of KOG classification of the unigenes.

categories, the cluster for "General function prediction only" (1,731, 13.86%) was the largest group, followed by "Signal transduction mechanisms" (1,653, 13.24%), "Post-translational modification, protein turnover, chaperones" (1,205, 9.65%), and "Transcription" (996, 7.98%). Only few unigenes were assigned under the "Nuclear structure," "Cell motility," and "Defense mechanisms" groups (**Figure 5** and **Supplementary Table 2**).

To further identify the predicted proteins' biological pathways, the KEGG pathway database was employed to annotate the unigenes by analyzing the gene functions systematically and integrating the chemical and genomic information (Du et al., 2016; Kanehisa et al., 2016). In our results, 3,170 unigenes were assigned and annotated to 279 different biological pathways (**Supplementary Table 3**). "Signal transduction" (667 unigenes) was the most enriched pathway, followed by "Translation" (415 unigenes), "Transport and catabolism" (364 unigenes), and "Folding sorting and degradation" (329 unigenes) (**Figure 6**).

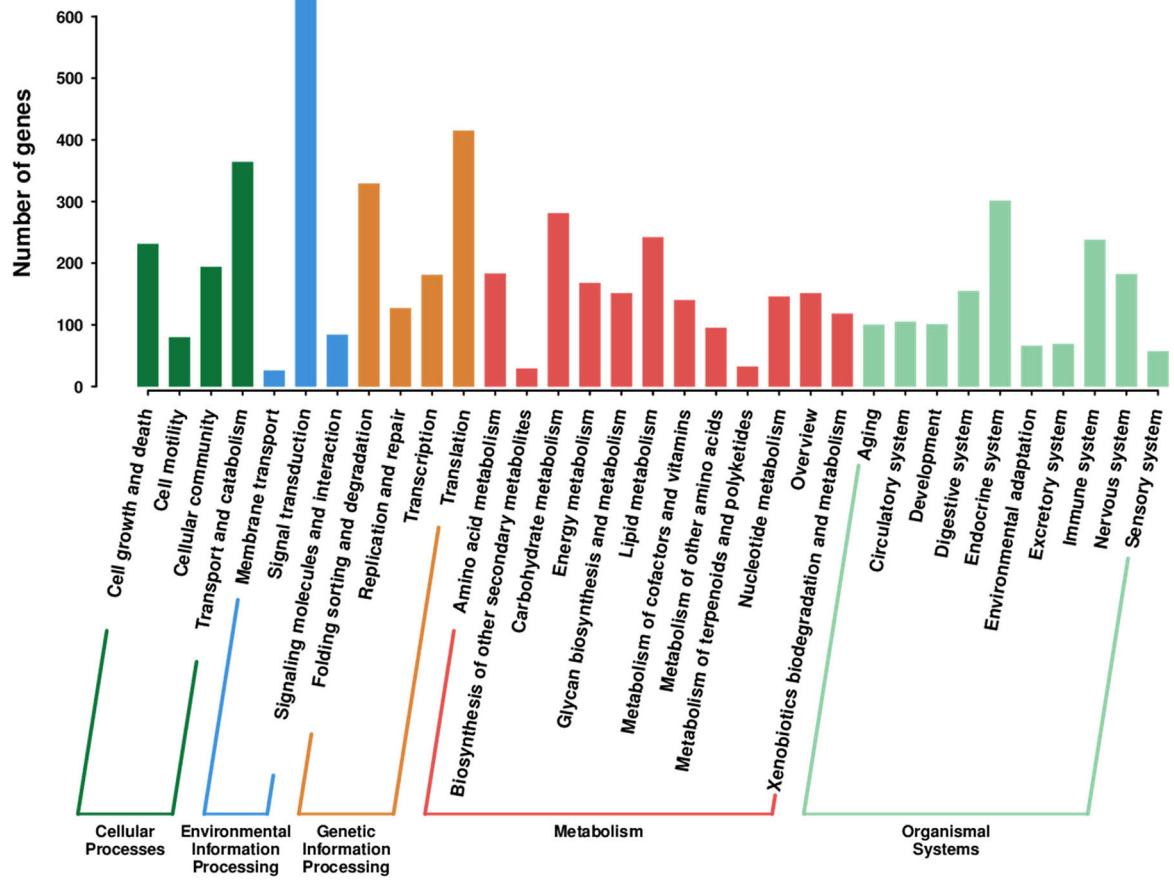

FIGURE 6 | KEGG classifications of unigenes of *M. aurolineatus*.

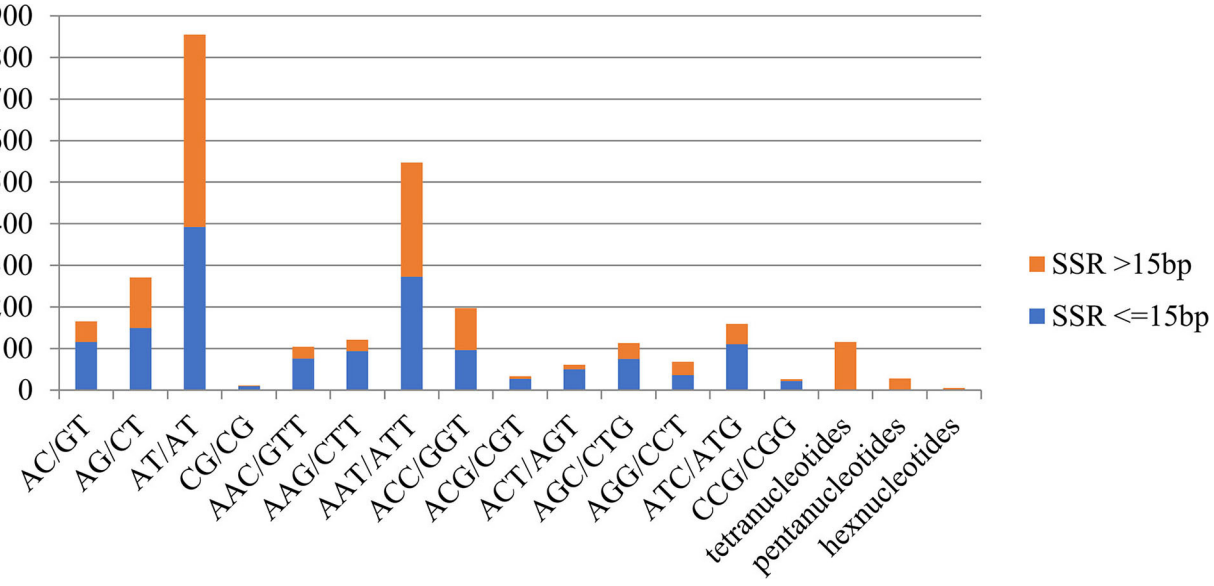

FIGURE 7 | Distribution of simple sequence repeat (SSR) nucleotide classes among different nucleotide types found in the transcriptome of *M. aurolineatus*.

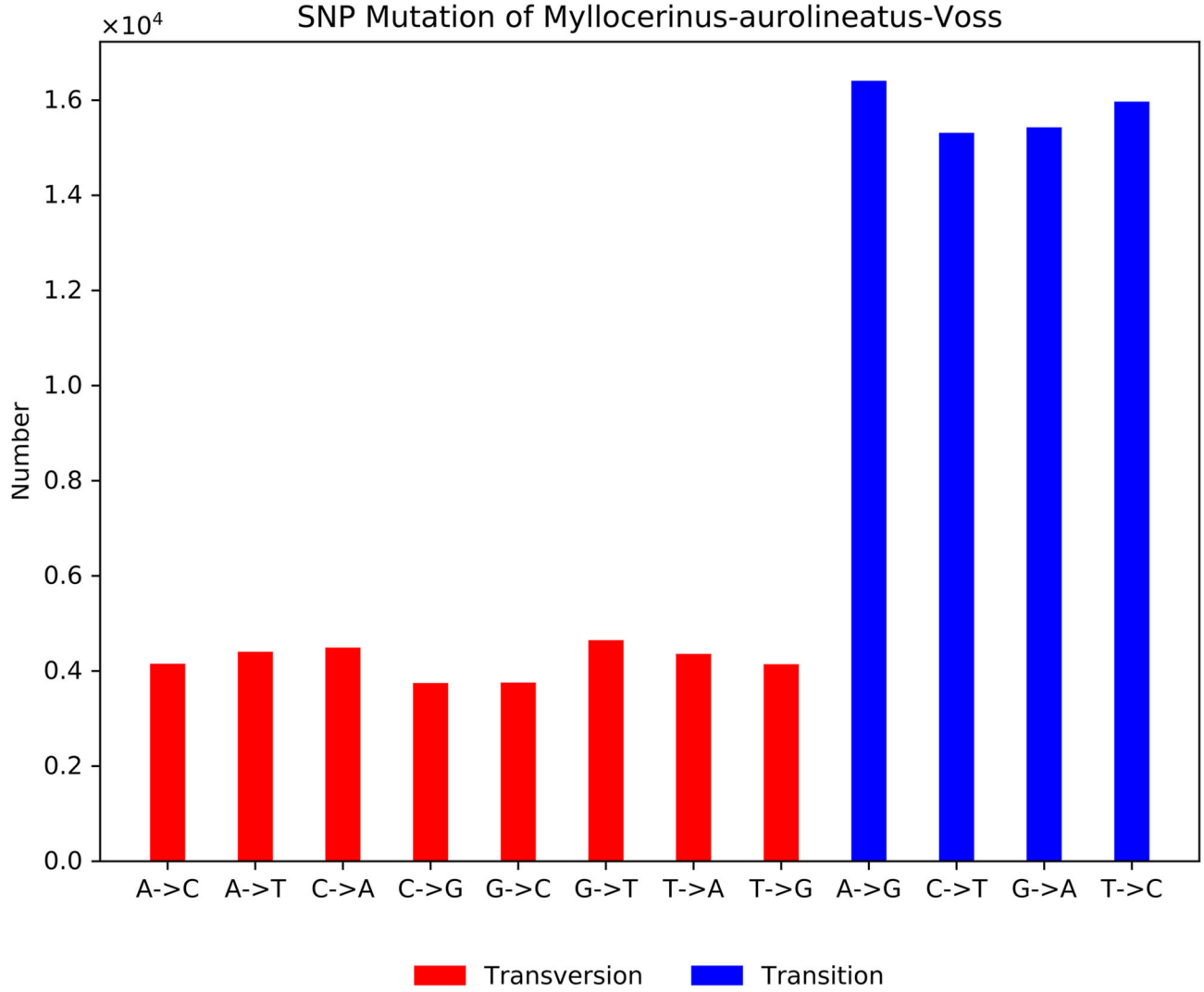

FIGURE 8 | Classification of SNPs identified in the *M. aurolineatus*.

CDS Prediction

BLAST alignment was used to search the coding sequences (CDS) in NR, SwissProt, and TrEMBL databases, and the remaining undefined sequences were assigned by using TransDecoder software. A total of 39,876 CDS sequences were predicted in our data (**Supplementary Tables 4**, **5**). After transcript combination, the gene coverage was searched by BEDTools software. From our data, 63,340 genes can be detected in the 90–100% gene distribution rate, followed by 3,314 genes in the 80–90% gene distribution rate, 1,538 genes in the 70–80% gene distribution rate, 867 genes in the 60–70% gene distribution rate, and only few genes in the gene distribution rate under 50% (**Supplementary Figure 1**).

SSR Discovery

SSRs or microsatellite sequences, represented by 2–6 base pairs in length of core sequences, are polymorphic loci present in genomic DNA (Powell et al., 1996). To date, SSRs have been used to genotype numerous species for functional analysis (Kantety et al., 2002). Our results obtained 13,848 SSRs, including 9.40% dinucleotide repeats, 10.32% trinucleotide repeats, and 1.05% tetra/penta/hexanucleotide repeats. A total of 1,355 SSRs (9.78%) with more than 15 base pairs in length and 1,525 SSRs (11.01%) with <15 base pairs in length were found (**Figure 7**). Among the dinucleotide repeat motifs, (AT/AT)n (855 SSRs) and (AG/CT)n (271 SSRs) were the most common types and significantly outnumbered the other types of dinucleotide repeat motifs. Among the trinucleotide repeat motifs, (AAT/ATT)n (547 SSRs) and (ACC/GGT)n (197 SSRs) were the most common types (**Figure 7**). A total of 6,512 unique sequences with microsatellites flanking sequences on both sides of the microsatellites were obtained after removing the microsatellites that lacked sufficient flanking sequences for primer design, which allows for the design of primers for genotyping.

SNP Identification

The type of variation in the genome was commonly analyzed by using SNPs (Williams et al., 2010; Gimode et al., 2016). SNPs were generated by aligning sequences used for contig assembly. We obtained 96,790 SNPs after removing those that had a base mutation frequency lower than 1% (**Supplementary Table 6**). The proportions of transition substitutions of A->G, T->C, G->A, and C->T were 16.95% (16,408), 16.50% (15,970), 15.94% (15,430), and 15.82% (15,313), respectively (**Figure 8**). A total transition:transversion ratio was 1.87:1. A small proportion of transversion-type SNPs and a large proportion of transition-type SNPs exist because of the differences in the numbers of hydrogen bonds and base structures between different bases.

CONCLUSION

In the present study, we identified a new pest in tea plants in Guizhou, China and first reported the transcriptome of *M. aurolineatus* Voss by using *de novo* assembly technology with next-generation sequencing. We identified 69,439 unigenes, which constitute an important database for future studies on *M. aurolineatus* gene function analysis. Furthermore, we annotated these unigenes in the GO, KOG, and KEGG databases. In addition, to explore the molecular biology research of *M. aurolineatus*, we predicted many SSRs and SNPs that will provide a basal foundation for genetic analysis.

DATA AVAILABILITY STATEMENT

The datasets presented in this study can be found in online repositories. The names of the repository/repositories and accession number(s) can be found below: NCBI BioProject ID: PRJNA694293.

AUTHOR CONTRIBUTIONS

XL: conceptualization. XX: methodology. MC: software. XX: validation. JJ and MH: formal analysis. JJ: investigation. LJ: resources. XX and JJ: writing—original draft preparation. XL: writing—review and editing and project administration. XL and XX: funding acquisition. All authors contributed to the article and approved the submitted version.

FUNDING

This work was supported by the National Key Research and Development Program of China (Grant No. 2016YFD0200902), the Advanced Programs of Guizhou Province for the Returned Overseas Scholars [(2018)02], the Science and Technology Foundation of Guizhou Province [(2019)2408], the Project of Guizhou Province [No. (2018)5781], and the Ph.D. Funding of Guizhou University (No. 201754).

ACKNOWLEDGMENTS

We sincerely thank the reviewer for the constructive criticisms and valuable comments.

SUPPLEMENTARY MATERIAL

The Supplementary Material for this article can be found online at: https://www.frontiersin.org/articles/10.3389/fsufs.2021.631990/full#supplementary-material

Supplementary Figure 1 | Distribution of gene's coverage of *M. aurolineatus*.

Supplementary Table 1 | Gene Ontology (GO) classification of proteins in biological process, cellular component, and molecular function process.

Supplementary Table 2 | euKaryotic Ortholog Groups (KOG) functional categories of *M. aurolineatus* proteins.

Supplementary Table 3 | The annotation of identified unigenes in different biological pathways.

Supplementary Table 4 | The coding sequences (CDS) prediction of identified unigenes.

Supplementary Table 5 | The peptide prediction of identified unigenes.

Supplementary Table 6 | Single nucleotide polymorphism (SNP) identification of identified unigenes.

REFERENCES

Bishnoi, R., and Singla, D. (2017). APMicroDB: a microsatellite database of Acyrthosiphon pisum. *Genom Data* 12, 111–115. doi: 10.1016/j.gdata.2017.03.014

Casida, J. E. (2017). Pesticide interactions: mechanisms, benefits, and risks. *J. Agric. Food Chem.* 65, 4553–4561. doi: 10.1021/acs.jafc.7b01813

Comblain, F., Dubuc, J. E., Lambert, C., Sanchez, C., Lesponne, I., Serisier, S., et al. (2016). Identification of targets of a new nutritional mixture for osteoarthritis management composed by curcuminoids extract, hydrolyzed collagen and green tea extract. *PLoS ONE* 11:e0156902. doi: 10.1371/journal.pone.0156902

Du, J., Li, M., Yuan, Z., Guo, M., Song, J., Xie, X., et al. (2016). A decision analysis model for KEGG pathway analysis. *BMC Bioinformatics* 17:407. doi: 10.1186/s12859-016-1285-1

Ekblom, R., and Galindo, J. (2011). Applications of next generation sequencing in molecular ecology of non-model organisms. *Heredity* 107, 1–15. doi: 10.1038/hdy.2010.152

Gayral, P., Melo-Ferreira, J., Glemin, S., Bierne, N., Carneiro, M., Nabholz, B., et al. (2013). Reference-free population genomics from next-generation transcriptome data and the vertebrate-invertebrate gap. *PLoS Genet.* 9:e1003457. doi: 10.1371/journal.pgen.1003457

Gimode, D., Odeny, D. A., de Villiers, E. P., Wanyonyi, S., Dida, M. M., Mneney, E. E., et al. (2016). Identification of SNP and SSR markers in finger millet using next generation sequencing technologies. *PLoS ONE* 11:e0159437. doi: 10.1371/journal.pone.0159437

Jugulam, M., and Gill, B. S. (2018). Molecular cytogenetics to characterize mechanisms of gene duplication in pesticide resistance. *Pest Manag. Sci.* 74, 22–29. doi: 10.1002/ps.4665

Kanehisa, M., Sato, Y., Kawashima, M., Furumichi, M., and Tanabe, M. (2016). KEGG as a reference resource for gene and protein annotation. *Nucleic Acids Res.* 44, 457–462. doi: 10.1093/nar/gkv1070

Kantety, R. V., La Rota, M., Matthews, D. E., and Sorrells, M. E. (2002). Data mining for simple sequence repeats in expressed sequence tags from barley, maize, rice, sorghum and wheat. *Plant Mol. Biol.* 48, 501–510. doi: 10.1023/A:1014875206165

Kuzniar, A., Lin, K., He, Y., Nijveen, H., Pongor, S., and Leunissen, J. A. (2009). ProGMap: an integrated annotation resource for protein orthology. *Nucleic Acids Res.* 37, 428–434. doi: 10.1093/nar/gkp462

Li, B., Predel, R., Neupert, S., Hauser, F., Tanaka, Y., Cazzamali, G., et al. (2008). Genomics, transcriptomics, and peptidomics of neuropeptides and protein hormones in the red flour beetle *Tribolium castaneum*. *Genome Res.* 18, 113–122. doi: 10.1101/gr.6714008

Li, H., Huang, W., Wang, G. L., Wang, W. L., Cui, X., and Zhuang, J. (2017). Transcriptomic analysis of the biosynthesis, recycling, and distribution of ascorbic acid during leaf development in tea plant (*Camellia sinensis* (L.) O. Kuntze). *Sci Rep.* 7:46212. doi: 10.1038/srep46212

Ma, J. Q., Yao, M. Z., Ma, C. L., Wang, X. C., Jin, J. Q., Wang, X. M., et al. (2014). Construction of a SSR-based genetic map and identification of QTLs for catechins content in tea plant (*Camellia sinensis*). *PLoS ONE* 9:e93131. doi: 10.1371/journal.pone.0093131

Moon, E. K., Chung, D. I., Hong, Y. C., Ahn, T. I., and Kong, H. H. (2008). *Acanthamoeba castellanii*: gene profile of encystation by ESTs analysis and KOG assignment. *Exp. Parasitol.* 119, 111–116. doi: 10.1016/j.exppara.2008.01.001

Mukhopadhyay, M., Mondal, T. K., and Chand, P. K. (2016). Biotechnological advances in tea (*Camellia sinensis* [L.] O. Kuntze): a review. *Plant Cell Rep.* 35, 255–287. doi: 10.1007/s00299-015-1884-8

Powell, W., Machray, G. C., and Provan, J. (1996). Polymorphism revealed by simple sequence repeats. *Trends Plant Sci.* 1, 215–222. doi: 10.1016/S1360-1385(96)86898-0

Regniere, J., and Bentz, B. (2007). Modeling cold tolerance in the mountain pine beetle, *Dendroctonus ponderosae*. *J. Insect Physiol.* 53, 559–572. doi: 10.1016/j.jinsphys.2007.02.007

Roy, S., and Muraleedharan, N. (2014). Microbial management of arthropod pests of tea: current state and prospects. *Appl. Microbiol. Biotechnol.* 98, 5375–5386. doi: 10.1007/s00253-014-5749-9

Smith-Unna, R., Boursnell, C., Patro, R., Hibberd, J. M., and Kelly, S. (2016). TransRate: reference-free quality assessment of *de novo* transcriptome assemblies. *Genome Res.* 26, 1134–1144. doi: 10.1101/gr.196469.115

Sun, X., Zhang, X., Wu, G., Li, X., Liu, F., Xin, Z., et al. (2017). n-Pentacosane Acts as both Contact and Volatile Pheromone in the tea Weevil, *Myllocerinus aurolineatus*. *J. Chem. Ecol.* 43, 557–562. doi: 10.1007/s10886-017-0857-5

Sun, X. L., Wang, G. C., Cai, X. M., Jin, S., Gao, Y., and Chen, Z. M. (2010). The tea weevil, *Myllocerinus aurolineatus*, is attracted to volatiles induced by conspecifics. *J. Chem. Ecol.* 36, 388–395. doi: 10.1007/s10886-010-9771-9

Tarrant, A. M., Baumgartner, M. F., Lysiak, N. S., Altin, D., Storseth, T. R., and Hansen, B. H. (2016). Transcriptional Profiling of Metabolic Transitions during Development and Diapause Preparation in the Copepod *Calanus finmarchicus*. *Integr. Comp. Biol.* 56, 1157–1169. doi: 10.1093/icb/icw060

Williams, L. M., Ma, X., Boyko, A. R., Bustamante, C. D., and Oleksiak, M. F. (2010). SNP identification, verification, and utility for population genetics in a non-model genus. *BMC Genet.* 11:32. doi: 10.1186/1471-2156-11-32

Yang, Z. W., Duan, X. N., Jin, S., Li, X. W., Chen, Z. M., Ren, B. Z., et al. (2013). Regurgitant derived from the tea geometrid Ectropis obliqua suppresses wound-induced polyphenol oxidases activity in tea plants. *J. Chem. Ecol.* 39, 744–751. doi: 10.1007/s10886-013-0296-x

Zhang, H. Z., Li, Y. Y., An, T., Huang, F. X., Wang, M. Q., Liu, C. X., et al. (2018). Comparative Transcriptome and iTRAQ Proteome Analyses Reveal the Mechanisms of Diapause in *Aphidius gifuensis* Ashmead (Hymenoptera: Aphidiidae). *Front. Physiol.* 9:1697. doi: 10.3389/fphys.2018.01697

Zhang, X. X., and Zhang, K. (2017). Complete mitochondrial genome and phylogenetic analysis of the Asian swallowtail, Papilio xuthus. *Mitochondrial DNA A DNA Mapp Seq Anal.* 28, 246–247. doi: 10.3109/19401736.2015.1115862

Zhang, Z. R. (1991). Investigation method of the density of adult groups in *Myllocerinus aurolineatus* Voss. *J. Tea* 3, 32–33.

Conflict of Interest: The authors declare that the research was conducted in the absence of any commercial or financial relationships that could be construed as a potential conflict of interest.

frontiers in Sustainable Food Systems

ORIGINAL RESEARCH
published: 11 March 2021
doi: 10.3389/fsufs.2021.639841

RNA Sequencing Analysis of *Metopolophium dirhodum* (Walker) (Hemiptera: Aphididae) Reveals the Mechanism Underlying Insecticide Resistance

Haifeng Gao[1,2†], Xun Zhu[3†], Guangkuo Li[2], Enliang Liu[2], Yuyang Shen[2], Sifeng Zhao[1] and Feng Ge[1,4*]*

[1] Xinjiang Production and Construction Corps Key Laboratory of Special Fruits and Vegetables Cultivation Physiology and Germplasm Resources Utilization, Agriculture College of Shihezi University, Shihezi, China, [2] Key Laboratory of Integrated Pest Management on Crop in Northwestern Oasis, Institute of Plant Protection, Xinjiang Academy of Agricultural Sciences, Ministry of Agriculture and Rural Affairs, Urumqi, China, [3] Key Laboratory for Biology of Plant Diseases and Insect Pests, Institute of Plant Protection, Chinese Academy of Agricultural Sciences, Beijing, China, [4] State Key Laboratory of Integrated Management of Pest and Rodents, Institute of Zoology, Chinese Academy of Sciences, Beijing, China

OPEN ACCESS

Edited by:
Fang Ouyang,
Chinese Academy of Sciences, China

Reviewed by:
Wen Xie,
Chinese Academy of Agricultural Sciences, China
Litao Guo,
Chinese Academy of Agricultural Sciences, China

***Correspondence:**
Feng Ge
get@ioz.ac.cn
Sifeng Zhao
zhsf_agr@shzu.edu.cn

[†] These authors have contributed equally to this work

Specialty section:
This article was submitted to Agroecology and Ecosystem Services, a section of the journal Frontiers in Sustainable Food Systems

Received: 10 December 2020
Accepted: 08 February 2021
Published: 11 March 2021

Citation:
Gao H, Zhu X, Li G, Liu E, Shen Y, Zhao S and Ge F (2021) RNA Sequencing Analysis of Metopolophium dirhodum (Walker) (Hemiptera: Aphididae) Reveals the Mechanism Underlying Insecticide Resistance. Front. Sustain. Food Syst. 5:639841. doi: 10.3389/fsufs.2021.639841

Xinjiang (XJ) and Ningxia (NX) provinces are important agricultural regions in western China. Aphids are one kind of the most devastating pests in both the provinces. Aphids are typical phloem-feeding insects distributed worldwide and can severely damage crops. In this study, two representative *Metopolophium dirhodum* (Walker) (Hemiptera: Aphididae) populations were collected from the typical agricultural regions of XJ and NX, respectively for a high-throughput transcriptome sequencing analysis. A total of 5,265 differentially expressed genes (DEGs) were identified. The functional annotation of DEGs and the identification of enriched pathways indicated many of the DEGs are involved in processes related to energy metabolism, development, and insecticide resistance. Furthermore, an investigation of insecticide toxicity revealed the NX population is more resistant to insecticide treatments than the XJ population. Thus, the transcriptome data generated in present study can be used for functional gene characterization relevant to aphid development, metabolism, environmental adaptation, and insecticide resistance.

Keywords: RNA-seq, *Metopolophium dirhodum*, insecticide, DEGs, resistance

INTRODUCTION

Aphids, which are typical phloem-feeding insects found worldwide, can severely damage crops and other plants (Powell et al., 2006). The suitability of a plant host for an insect depends on plant surface features, including the wax layers (Walling, 2008) and leaf trichomes (Wang et al., 2001; Rodriguezlopez et al., 2011). Insects use their highly specialized mouthparts to probe vegetative tissue for phloem sap, which contains nutrient compounds including sugars and amino acids (Kaloshian and Walling, 2005). After establishing a feeding site, aphids can continue feeding for a prolonged period. Phloem feeding by aphids depletes crop photo assimilate contents and inhibits plant growth. Previous studies revealed that aphids feeding on phloem deposit honeydew on the leaf surface and encourage the

growth of sooty mold, which can block the light required for photosynthesis and restrict crop growth (Filho and Paiva, 2006; Taylor et al., 2012). Aphids are also the vectors of numerous plant viruses (Chen et al., 2012, 2013). When insects penetrate plants' tissue with their mouthparts to enable phloem feeding, they continuously secrete saliva (Will et al., 2009), which is one of the efficient ways for viruses transmission (Weintraub and Beanland, 2006). To date, aphids are mainly controlled by the frequent application of insecticides, which is relatively inefficient and potentially damaging the environment (Devonshire and Field, 1991).

There are ∼4,700 members of the superfamily Aphidoidea (https://www.aphidoidea.com), including *Metopolophium dirhodum* (Walker) (Hemiptera: Aphididae), which is a very important pest in the crop-growing regions of many countries (Winder et al., 2001; Carver, 2010). Like other aphid species, *M. dirhodum* annually reproduces multiple generations on different hosts. Rosaceae species (e.g., apple and peach) are the primary hosts of *M. dirhodum* in the fall, in which season male and female *M. dirhodum* morphs mate for sexual propagation. In the spring, after hatching from eggs, aphids fly away seeking a secondary host to produce colonies. Poaceae species, including wheat, are the secondary hosts for the summer generation comprising only female and parthenogenic aphids (Argandona et al., 1980; Garratt et al., 2010). During the summer, *M. dirhodum* (virginopara) can produce two or three generations on secondary host plants. The plant sap is the sole source of nutrients for *M. dirhodum* and other aphids. The aphid mouthpart is a highly specialized structure. After probing plants, the mouthpart can reach the phloem to feed on the sap (Kempema et al., 2006). Although sap feeding by aphids decreases the nutrient and water contents of plants, ultimately leading to wilting and yield losses, the collateral damages could be more severe.

An earlier investigation proved that *M. dirhodum* can serve as the vector for several viruses, including barley yellow dwarf virus, maize mosaic virus, and potato virus (Waterhouse and Helms, 1985). The puncturing of the host plant by aphids facilitates the infection of the inner plant parts. During sap feeding, aphids produce honeydew containing a substantial abundance of sugars, which promotes the growth of saprophytic fungi detrimental to plant health (Taylor et al., 2012).

Several kinds of insecticides are used to control *M. dirhodum* for instance beta-cypermethrin *et al*. However, these insecticides can also induce the expression of detoxification and metabolism-related genes in insects. Transcriptome sequencing based on new nucleotide sequencing platforms (e.g., Illumina and PacBio) has considerably enhanced molecular and mechanisms research in various life science fields. High-throughput and deep-sequencing technologies enable the rapid and inexpensive acquisition of massive amounts of data. The bioinformatics-based analysis of the sequencing data [e.g., annotation of gene functions, identification of differentially expressed genes (DEGs), and analyses of gene ontology] may further elucidate the metabolic and signal transduction pathways underlying specific phenotypes.

Xinjiang Uygur Autonomous Region (XJ) and Ningxia Hui Autonomous Region (NX) are very large and agriculturally important provinces in western China. In terms of area, XJ is the biggest province in China. Although parts of these provinces are covered by desert, large areas are used for agricultural production. The similarities in the climate conditions of XJ and NX enable the cultivation of the same crops in both provinces, including wheat, barely, rice, cotton, apple, pear, grape, and sweet melon. *M. dirhodum* has been detected in the agricultural regions of both provinces, resulting in severe damages to crops every year, especially wheat. Unfortunately, *M. dirhodum* genes, genomes, and transcriptomes remain relatively uncharacterized. In this study, we selected two *M. dirhodum* populations from the wheat fields of XJ and NX for a transcriptome analysis under laboratory conditions. The comparison of the resulting transcriptome data revealed the DEGs. Furthermore, differences in metabolic pathways and insecticide tolerance between the two aphid populations were examined and discussed further.

MATERIALS AND METHODS

Insect Culture

Metopolophium dirhodum samples were collected from wheat fields in the XJ (N43°41′14″, E87°22′46″) and NX (N39°5′57″, E106°44′51″) provinces. The collected aphids were sub-cultured on fresh wheat seedlings in insect-rearing cages at 20 ± 1°C, with 60 ± 10% relative humidity and a 16-h light:8-h dark photoperiod, for more than 8 generations.

TABLE 1 | Summary statistics of the *Metopolophium dirhodum* (Walker) transcriptomes.

Sample	XJ_1	XJ_2	XJ_3	XJ_4	NX_1	NX_2	NX_3	NX_4
Raw Read(M)	53.428	44.055	39.195	43.445	10.113	10.05	5.632	10.032
Raw Bases (G)	8.014	6.608	5.879	6.517	1.517	1.507	0.845	1.505
Clean Reads (M)	52.094(97.5%)	43.180(98.0%)	38.151(97.3%)	42.473(97.8%)	9.594(94.9%)	9.650(96.0%)	5.341(94.8%)	9.530(95.0%)
Clean Bases (G)	7.772(97.0%)	6.446(97.5%)	5.683(96.7%)	6.331(97.2%)	1.425(93.9%)	1.435(95.2%)	0.793(93.8%)	1.415(94.1%)
Clean Q30(G)	7.258(93.4%)	6.083(94.4%)	5.311(93.4%)	5.970(94.3%)	1.273(89.3%)	1.303(90.8%)	0.706(89.0%)	1.264(89.3%)
Average Length(bp)	149.2	149.3	149	149.1	148.5	148.7	148.4	148.5
Unigenes#	2,1621							
N50(bp)	2,479							
Size(bp)	31,198,947							

Sample Preparation and RNA Isolation

For the NX and XJ populations, total RNA was extracted from 10 wingless adults with the TRIzol reagent according to the manufacturer instructions (Invitrogen TRIZOL® Reagent) for the subsequent RNA sequencing (RNA-seq) analysis, which was completed with four replicates. The purity of all RNA samples was assessed based on the $OD_{260}/_{280}$ and $OD_{260}/_{230}$ absorbance ratios, which were determined with the NanoDrop 2000 spectrophotometer. Samples with $OD_{260}/_{280}$ and $OD_{260}/_{230}$ ratios exceeding 1.8 and 2.2, respectively, were considered sufficiently pure. The RNA integrity was evaluated by 1% agarose gel electrophoresis. The extracted RNA was treated with DNase I to eliminate any residual genomic DNA.

Library Preparation and Illumina Sequencing

The cDNA libraries were constructed and sequenced by OriGene Technologies, Beijing, China. Specifically, mRNA was isolated from two total RNA samples (Grabherr et al., 2011). To construct the paired-end RNA-seq libraries for the transcriptome analysis, 10 μg total poly(A) mRNA was isolated with Seramag Magnetic Oligo(dT) Beads (Thermo) and then fragmented in fragmentation buffer. The resulting fragments were used as templates for the first-strand cDNA synthesis with a random hexamer primer. The second cDNA strand was synthesized in 20 μl second strand buffer (Invitrogen) supplemented with 10 mM dNTP mix, 5 U/μL RNase H, and 10 U/μL DNA polymerase I. Short fragments were purified with the QIAquick PCR purification kit and resuspended in EB buffer for the end-repair step and addition of a poly(A) tail. Sequencing adapters were then added to the short fragments. After an agarose gel electrophoresis, suitable fragments were selected as templates for a PCR amplification. Finally, paired-end RNA-seq libraries were prepared as recommended by Illumina and then sequenced on the HiSeq™ X Ten platform (Illumina). The Illumina instrument software was used for data analysis and base calling.

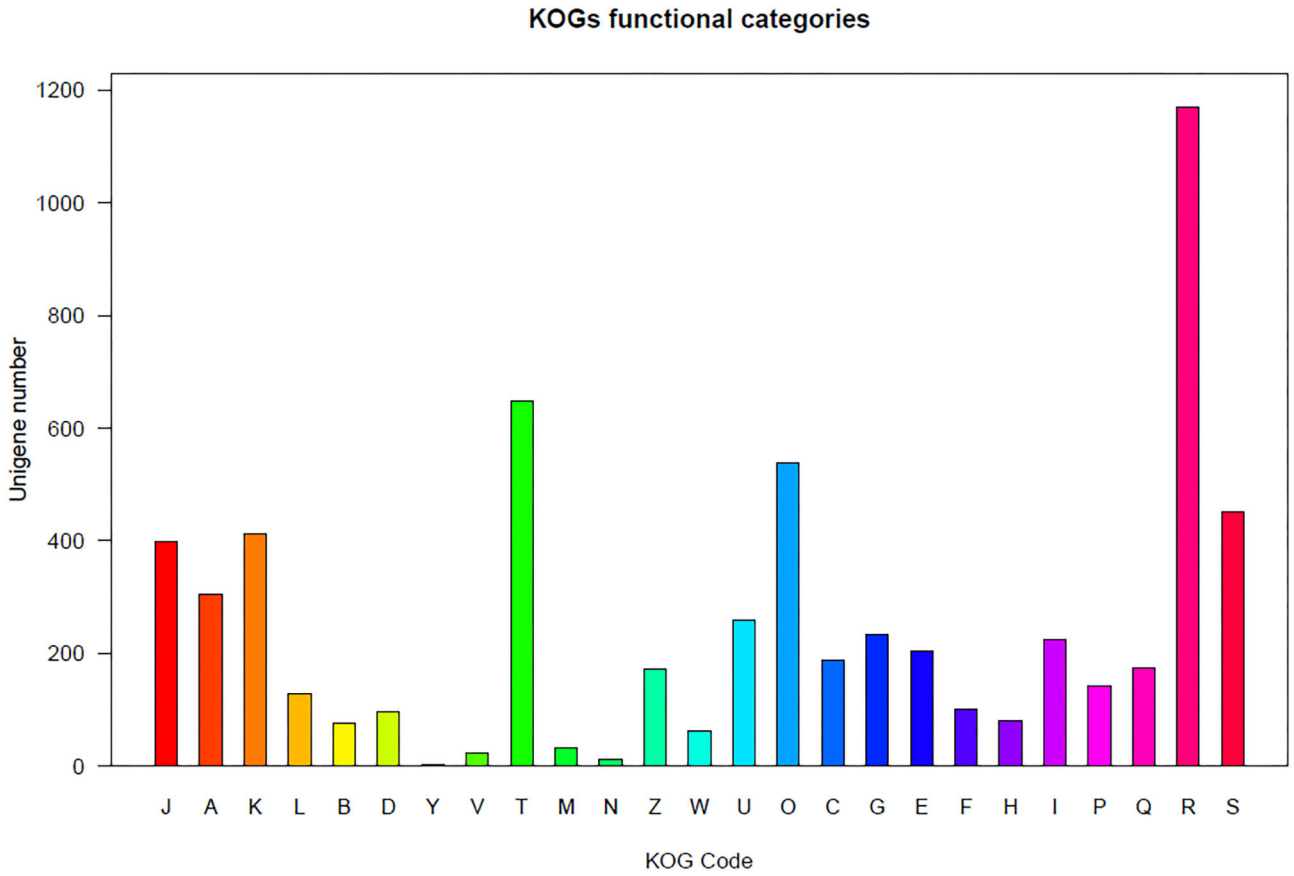

FIGURE 1 | Unigene-function clusterification by KOG. INFORMATION STORAGE AND PROCESSING [J] Translation, ribosomal structure, and biogenesis; [A] RNA processing and modification; [K] Transcription; [L] Replication, recombination, and repair; [B] Chromatin structure and dynamics. CELLULAR PROCESSES AND SIGNALING: [D] Cell cycle control, cell division, chromosome partitioning; [Y] Nuclear structure; [V] Defense mechanisms; [T] Signal transduction mechanisms; [M] Cell wall/membrane/envelope biogenesis; [N] Cell motility; [Z] Cytoskeleton; [W] Extracellular structures; [U] Intracellular trafficking, secretion, and vesicular transport; [O] Posttranslational modification, protein turnover, chaperones. METABOLISM: [C] Energy production and conversion; [G] Carbohydrate transport and metabolism; [E] Amino acid transport and metabolism; [F] Nucleotide transport and metabolism; [H] Coenzyme transport and metabolism; [I] Lipid transport and metabolism; [P] Inorganic ion transport and metabolism; [Q] Secondary metabolites biosynthesis, transport and catabolism. POORLY CHARACTERIZED: [R] General function prediction only; [S] Function unknown.

RNA-seq Data Processing and Analysis

The RNA-seq data were assessed based on the Q30 standard, which confirmed that the sequencing data quality was acceptable. Raw reads with adapters or more than 5% unknown nucleotides as well as low-quality reads were eliminated. The remaining clean reads were used for the *de novo* assembly of the transcriptome with the Trinity short-read assembly program, which connects contigs and generates unigene sequences.

The unigenes were annotated by screening protein databases, including the non-redundant (NR), Swiss-Prot, KOG, KEGG, and GO databases, with the BLASTX algorithm (E-value $< 1 \times 10^{-5}$ and sequence identity >30%). The GO analysis (http://www.geneontology.org) grouped the unigenes into three major categories based on function (i.e., molecular function, cellular component, and biological process). The Blast2GO program was used for the GO annotation of unigenes, after which the WEGO software was used for the GO

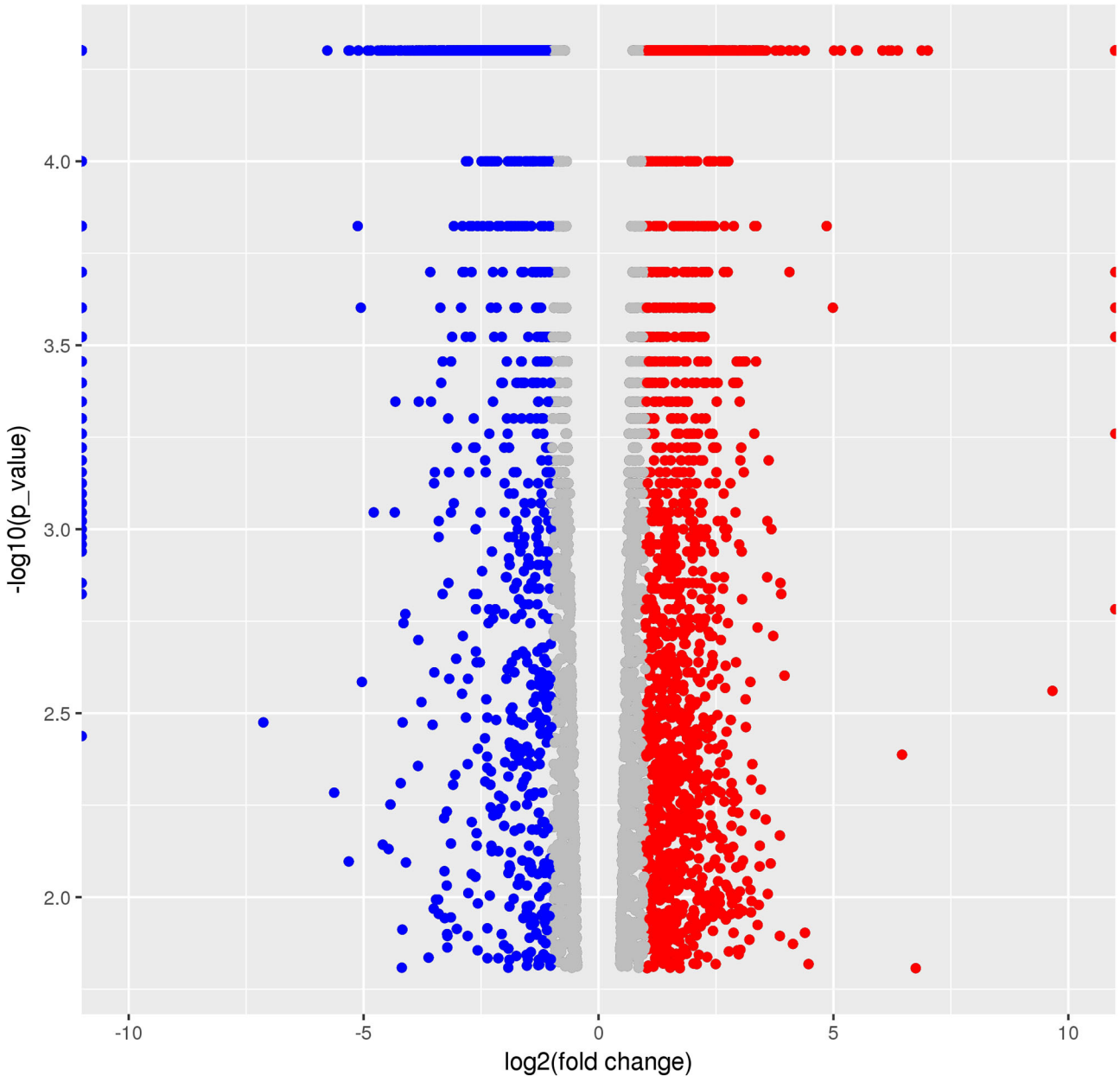

FIGURE 2 | Volcano Graphic. In the figure each dot demonstrated a gene expression in two populations. The horizontal ordinate is the log2 value of folder change between populations (NX/JX). The y-coordinate is the –log10 of the *p*-value. Dots in red indicated the up-regulated, in blue were down-regulated, and in gray were those with no significant change.

functional classification of all unigenes and for clarifying the distribution of gene functions. The KEGG pathway database was used to functionally characterize gene products regarding their effects on metabolic and cellular processes. The KEGG database was also applied to investigate the complex biological behaviors of the gene products. The KEGG pathways enriched among the unigenes were identified with the Blastall algorithm.

The DEGs were identified based on the fold-changes in expression levels ($p < 0.05$), which were determined with Cufflinks (version 2.0.2). The DEGs were clustered according to the KEGG analysis involving the Fisher and Chi-square tests.

Insecticide Toxicity

Insecticide toxicity was evaluated according to a published leaf dip method (Saska et al., 2016). The insecticide (Imidacloprid, Thiamethoxam, Omethoate, Avermectin) stock solutions (10,000 mg/L) were prepared with dimethylformamide. The stock solutions were diluted 5–7 times with 0.1% Tween 80. The 0.1% Tween 80 solution was used as a control. For each insecticide concentration, three replicates of at least 30 aphids were treated. Wheat bran and leaves carrying aphids were immersed in the insecticide solution for 3–5 s and then placed in Petri dishes containing moistened filter paper. The Petri dishes were placed in an incubator set at 20 ± 1°C, with 60 ± 10% relative humidity and a 16-h light:8-h dark photoperiod. After 24 h, the aphids

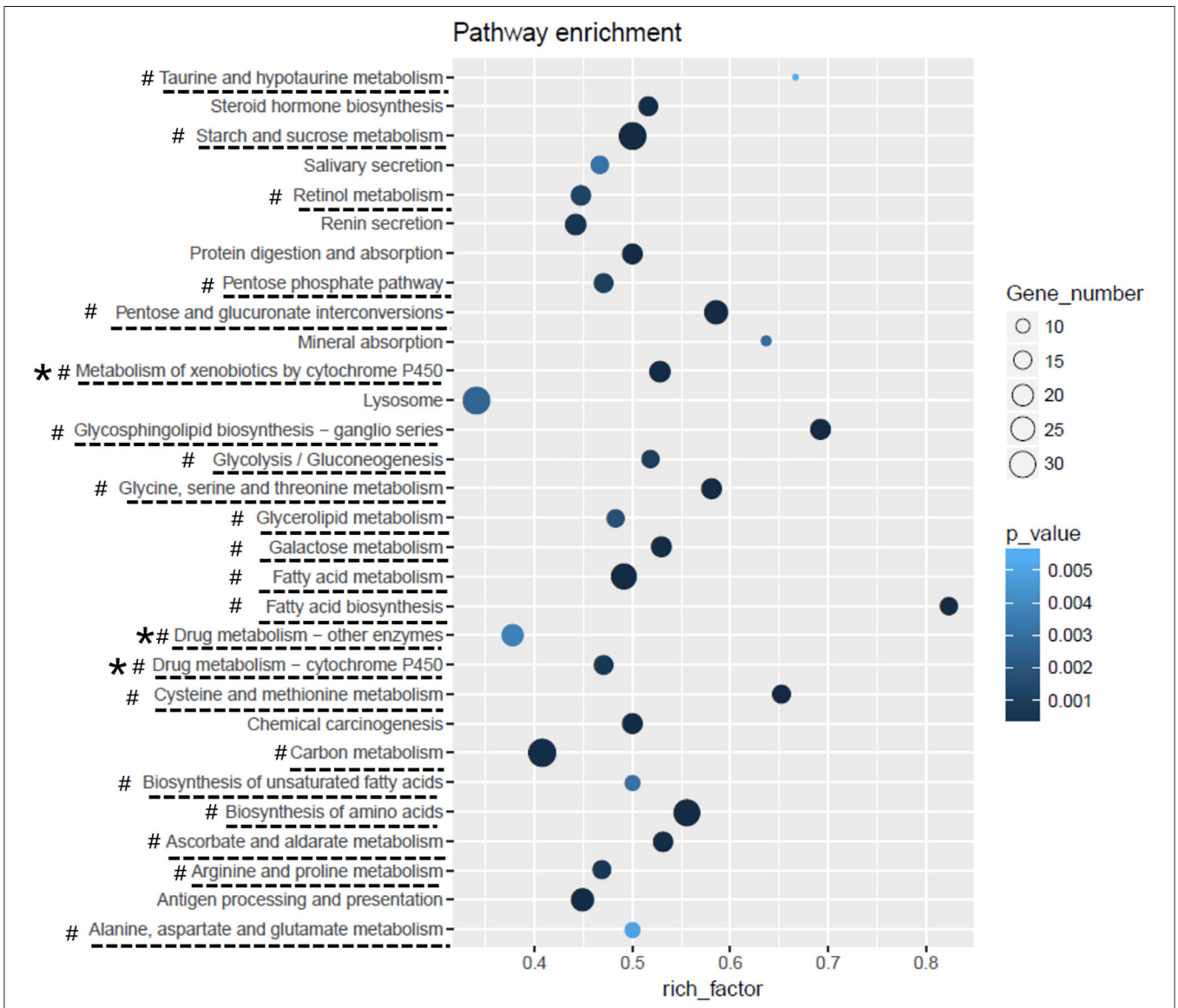

FIGURE 3 | The top-30 pathways of DEGs KEGG enrichment analysis. The pathways list from the bottom to the top were in order of the first letter of the pathway name, from A to Z. Rich_facotor means (number of DEG enriched in the pathway/number of background genes).

were examined with a microscope. They were gently touched with an anatomical needle. Aphids that did not move and aphids with only one foot that moved were considered dead. The total number of aphids and the number of dead aphids were recorded for each Petri dish.

Statistical Analysis

Data were recorded as the average of two replicates ± standard deviation. The data underwent an analysis of variance with SPSS 20.0. In the figures presented herein, significantly different values ($p < 0.05$) are indicated by different lowercase letters (a–d).

RESULTS

Illumina Sequencing and *de novo* Transcriptome Assembly

Each aphid population was analyzed with independently constructed libraries from four biological replicates. A total of 53.4, 44.1, 39.2, and 43.4 million raw reads were obtained for the XJ population, whereas 10.1, 10.1, 5.6, and 10.0 million raw reads were generated for the NX population (**Table 1**). The average raw read length varied from 148.2 to 149.3 bp. After the quality control step (Q30) and filtering of raw reads, the clean reads were used for the *de novo* assembly of 30,262 transcripts. After eliminating redundancies, 22,150 unigenes were retained for the XJ and NX populations, with N50 values of 2,491 and 2,479 bp (XJ population) and 1,356.3 and 1,443.0 bp (NX population). The unigene sequences are provided in **Supplementary File 1**.

Gene Identification and Annotation

The unigenes were used as queries to screen the NR (https://www.ncbi.nlm.nih.gov/refseq/about/nonredundantproteins/), Swiss-Prot (https://www.uniprot.org/), TrEMBL (https://www.uniprot.org/), Pfam (http://pfam.xfam.org/), and KOG databases with BLASTX. A total of 6,961 (32.2% of all distinct sequences), 8,646 (40.0%), 7,409 (34.3%), 6,836 (31.6%), and 4,968 (23.0%) unigenes were annotated based on the Swiss-Prot, NR, KOG, GO, and KEGG databases, respectively.

Regarding the KOG analysis, the orthologs were clustered based on their functions. The unigenes were clustered into the following four groups: information storage and processing, cellular processes and signaling, metabolism, and poorly characterized (**Figure 1**). The unigenes in these four groups were further divided into 24 subgroups. Similar KOG annotation trends were observed for both aphid populations. For example, the three largest subgroups for the two populations were "general function predicted only," "signal transduction mechanism," and

TABLE 2 | Top-10 pathways DEGs involved in based on KEGG enrichment analysis.

Category	*p*_value	*q*_value	numDEInCat	numInCat	Term
#ko01230	8.46E-08	2.50E-05	30	54	Biosynthesis of amino acids
#ko00604	2.88E-07	2.62E-05	18	26	Glycosphingolipid biosynthesis
#ko00040	2.91E-07	2.62E-05	24	41	Pentose and glucuronate interconversions
#ko00500	4.17E-07	2.62E-05	32	64	Starch and sucrose metabolism
#ko00061	4.44E-07	2.62E-05	14	17	Fatty acid biosynthesis
#ko01212	9.87E-06	4.30E-04	28	57	Fatty acid metabolism
#ko00270	1.02E-05	4.30E-04	15	23	Cysteine and methionine metabolism
#ko00260	1.71E-05	6.29E-04	18	31	Glycine, serine and threonine metabolism
* #ko00980	2.12E-05	6.94E-04	19	36	Metabolism of xenobiotics by cytochrome P450
ko04612	2.56E-05	7.55E-04	22	49	Antigen processing and presentation

*Category part show the unique tag of the functional pathway in KEGG database; p-value showed the significance of the enrichment, the smaller the more significant; q-value was the p-value after FDR correction; numDEinCat meant the number of the DEGs enriched into the pathway; numInCat meant the number of total genes involved into the pathway; # marking the pathways concerned with metabolism; * marking the pathway might concerned with insecticide resistance.*

TABLE 3 | Toxicology experiment of pesticides.

Insecticide	Population	Tolerance	*N*	Regression of LC-P line	LC_{50} (95% CL) mg/L
Imidacloprid	Ningxia	Sensitive	842	y = 4.25+0.69x	12.37 (4.36–35.13)
	Xinjiang	Resistant	654	y = 3.79+0.69x	56.63 (14.41–222.56)
Thiamethoxam	Ningxia	Sensitive	1,226	y = 3.57+0.82x	57.24 (37.46–87.47)
	Xinjiang	Resistant	550	y = 2.85+0.78x	572.29 (281.45–1163.67)
Omethoate	Ningxia	Sensitive	811	y = 3.18+0.82x	170.66 (65.90–441.96)
	Xinjiang	Resistant	309	y = 3.52+0.66x	169.53 (39.13–734.52)
Avermectin	Ningxia	Sensitive	1,036	y = 3.63+1.17x	14.61 (7.91–26.97)
	Xinjiang	Resistant	771	y = 4.21+0.81x	9.52 (2.69–33.60)

N – number of bugs for testing.

TABLE 4 | Transcription factor coding DEGs.

Unigene	Name	Definition	Fold change
TR1466|c0_g1	RUNXX	runt-related transcription factor, other	−0.334858
TR3871|c1_g1	SOX2	transcription factor SOX2 (SOX group B)	−0.29796
TR465|c0_g1	TCF4_12	Protein doughterless	1.606357
TR5656|c2_g1	POU3F, OTF	POU domain transcription factor, class 3	−0.422572
TR6180|c5_g2	RUNX2, AML3	runt-related transcription factor 2	−0.315609
TR7327|c1_g1	SOX5_6_13	transcription factor SOX5/6/13 (SOX group D)	−0.429378
TR7993|c1_g1	PBX2	pre-B-cell leukemia transcription factor 2	−0.66574

"post translational modification, protein turnover, chaperones" (**Supplementary File 2**).

Comparison of the Transcriptional Profiles of the XJ and NX Populations

A total of 5,265 DEGs were identified following a comparison of the XJ and NX aphid transcriptomes (XJ/NX), of which 2,447 were up-regulated and 2,791 were down-regulated (**Figure 2**, **Supplementary File 3**). The functional annotations revealed considerable differences between the two aphid populations, 47 KEGG pathways were enriched among the DEGs. The top 30 enriched pathways are presented in **Figure 3**. Among them, 22 pathways were relevant to metabolism, all of them were underlined and marked with hashtag. There were three (marked with an extra asterisk) metabolism pathways concerned with drug/xenobiotics degradation, and two of them were of P450 monooxygenase system. The top 10 most enriched pathways based on the $-\log^2$ *p*-value are listed in **Table 2**, including those related to amino acid biosynthesis, starch and sucrose metabolism, fatty acid biosynthesis and metabolism, and metabolism of xenobiotics by cytochrome P450.

Insecticide Toxicity

We evaluated the tolerance of the two aphid populations to the following beta-cypermethrin-containing insecticides: imidacloprid, thiamethoxam, omethoate, and avermectin. The median lethal dose (LC_{50}) and toxicity regression equations indicated the NX population was substantially more tolerant to imidacloprid and thiamethoxam than the XJ population (**Table 3**). Additionally, the NX aphids were slightly more tolerant to avermectin than the XJ population, whereas there was no difference in the toxicity of omethoate. The LC_{50} of imidacloprid for the NX population was 56.63 mg/L, which was 5-fold higher than that for the XJ population. The LC_{50} of thiamethoxam for the NX aphids was as high as 573.29 mg/L, which was ∼10-fold higher than that for the XJ aphids.

DISCUSSION

In western China, both XJ and NX are large provinces of agriculture. Sustainable wheat production in both provinces is threatened by *M. dirhodum*. In the current study, we collected and analyzed two typical *M. dirhodum* populations reflecting the effects of the geographical and environmental conditions in the main agricultural regions of XJ and NX. The two aphid populations were compared based on a high-throughput transcriptome analysis. A total of 47 Gb data were generated. The subsequent data analysis identified 5,265 DEGs between the populations (XJ/NX).

The DEG functional annotation and pathway enrichment analysis indicated that a considerable proportion of the DEGs involved in the pathways related to energy metabolism, development, and insecticide resistance. There were several clear differences in the metabolic pathways between the two populations. For example, the amino acid biosynthesis (Chen, 1966; Wilson et al., 2010), starch and sucrose metabolism (Kunieda et al., 2006), and fatty acid biosynthesis and metabolism (Crippsc and De Renobales, 1988; Tan et al., 2011) varied between the XJ and NX aphids. This diversity might be due to the differences in the environmental conditions in the two provinces. The DEGs and their associated pathways may provide clues regarding how the aphids adapted to various environmental factors, including temperature, light, humidity, and nutrient availability (Gade, 2004; Contreras and Bradley, 2009). The significant enrichment of development-related pathways, such as the glycosphingolipid biosynthesis pathway, may help clarify the developmental differences between the aphid populations (Wandall et al., 2005), although these differences might also be due to the environment. Among these XJ/NX DEGs, there were only seven coding transcription factors (TFs). Their information was listed in **Table 4**. The one up-regulated DEG is *TCF4_12* encoding a transcription factor (homolog of the *Drosophila melanogaster daughterless* gene) (Caudy et al., 1988). The expression levels of the other transcription factor-encoding DEGs were down-regulated. Of these DEGs, *POU3F* is reportedly important for regulating the neuron-specific expression of the gene encoding the diapause hormone and pheromone biosynthesis-activating neuropeptide in *Bombyx mori* (Zhang et al., 2004).

The 30 most enriched KEGG pathways (**Figure 3**) included several associated with insecticide detoxification (e.g., metabolism of xenobiotics by cytochrome P450, drug metabolism – cytochrome P450, and drug metabolism – other enzymes) (Scott and Wen, 2001; Schwab, 2013). Previous studies revealed that the cytochrome P450 monooxygenase system (Berge et al., 1998; Wang et al., 2018; Zhang et al., 2018; Chiu et al., 2019) and carboxylesterases (Coppin et al., 2012; Zhang et al., 2014) help detoxify xenobiotics. In the current study, the insecticide treatments indicated that the NX aphids are substantially more tolerant to insecticides than the XJ aphids. To date, there is not yet transcriptomic research on *M. dirhodum* reported, neither

any sequencing data available to the public. Accordingly, the transcriptome data generated in this study can enable researchers to further clarify *M. dirhodum* (aphid) gene functions and characterize the molecular mechanisms underlying *M. dirhodum* development, metabolism, adaptation, and insecticide resistance.

CONCLUSION

In the present study, two *M. dirhodum* populations collected from the main agricultural regions in western China underwent a transcriptome analysis. The resulting data suggest the genetic differences between the two aphid populations are primarily related to amino acid, sugar, and fatty acid metabolism as well as development. Moreover, the results also revealed differences in the cytochrome P450-related insecticide metabolism and detoxification. Toxicological experiment demostrated the insecticide resistance of the NX aphids was greater than that of the XJ aphids. These findings imply that the sequencing data can be relevant for future investigations regarding the classification, expression, and function of M. dirhodum detoxification enzyme genes that influence insecticide resistance. The data presented herein will be applicable for future functional genomics research and investigations on insect development, metabolism, environmental adaptation, and insecticide resistance. All the data generated in this study is free and available for any scientific research. The data has been uploaded to NCBI for releasing later (Accession numbers: SRR13447691, SRR13447690, SRR13447689, SRR13447688, SRR13447687, SRR13447686, SRR13447685).

DATA AVAILABILITY STATEMENT

The datasets presented in this study can be found in online repositories. The names of the repository/repositories and accession number(s) can be found below: NCBI BioProject, accession no: PRJNA692554.

AUTHOR CONTRIBUTIONS

HG, XZ, SZ, and FG conceived and designed the research. HG and XZ conducted the experiments. HG, XZ, and YS analyzed the data. HG and XZ wrote the manuscript. SZ, FG, GL, and EL revised the manuscript. All authors have read and approved the manuscript.

FUNDING

This study was sponsored by the National Key Research and Development program of China (2018YFD0200406), Tianshan Yonug Talents (2019Q051), SINOGRAIN II (CHN-17/0019): Technological Innovation to Support Environmentally-Friendly Food Production and Food Safety Under a Changing Climate-Opportunities and Challenges for Norway-China Cooperation, and the Technology Innovation and Key Cultivation Projects of Xinjiang Academy of Agricultural Sciences (xjkcpy-003).

SUPPLEMENTARY MATERIAL

The Supplementary Material for this article can be found online at: https://www.frontiersin.org/articles/10.3389/fsufs.2021.639841/full#supplementary-material

REFERENCES

Argandona, V. H., Luza, J. G., Niemeyer, H. M., and Corcuera, L. J. (1980). Role of hydroxamic acids in the resistance of cereals to aphids. *Phytochemistry* 19, 1665–1668. doi: 10.1016/S0031-9422(00)83790-5

Berge, J. B., Feyereisen, R., and Amichot, M. (1998). Cytochrome P450 monooxygenases and insecticide resistance in insects. *Philosoph. Trans. Royal Soc. B* 353, 1701–1705. doi: 10.1098/rstb.1998.0321

Carver, M. (2010). *Metopolophium dirhodum* (walker) (homoptera: aphididae) newly recorded from australia. *Aust. J. Entomol.* 23, 192–192. doi: 10.1111/j.1440-6055.1984.tb01944.x

Caudy, M., Vassin, H., Brand, M., Tuma, R., Jah, L. Y., and Jan, Y. N. (1988). daughterless, a *Drosophila* gene essential for both neurogenesis and sex determination, has sequence similarities to myc and the achaete-scute complex. *Cell* 55, 1061–1067. doi: 10.1016/0092-8674(88)90250-4

Chen, P. S. (1966). Amino acid and protein metabolism in insect development. *Adv. Insect Phys.* 3, 53–132. doi: 10.1016/S0065-2806(08)60186-1

Chen, X., Vosman, B., Visser, R. G. F., Der Vlugt, R. V., and Broekgaarden, C. (2012). High throughput phenotyping for aphid resistance in large plant collections. *Plant Methods* 8, 33–33. doi: 10.1186/1746-4811-8-33

Chen, X., Zhang, Z., Visser, R. G. F., Broekgaarden, C., and Vosman, B. (2013). Overexpression of IRM1 enhances resistance to aphids in *Arabidopsis thaliana*. *PLoS ONE* 8:e0070914. doi: 10.1371/journal.pone.0070914

Chiu, C. C., Keeling, C. I., and Bohlmann, J. (2019). Cytochromes P450 preferentially expressed in antennae of the mountain pine beetle. *J. Chem. Ecol.* 45, 178–186. doi: 10.1007/s10886-018-0999-0

Contreras, H. L., and Bradley, T. J. (2009). Metabolic rate controls respiratory pattern in insects. *J. Exp. Biol.* 212, 424–428. doi: 10.1242/jeb.024091

Coppin, C. W., Jackson, C. J., Sutherland, T. D., Hart, P. J., Devonshire, A. L., Russell, R. J., et al. (2012). Testing the evolvability of an insect carboxylesterase for the detoxification of synthetic pyrethroid insecticides. *Insect Biochem. Mol. Biol.* 42, 343–352. doi: 10.1016/j.ibmb.2012.01.004

Crippsc, C., and De Renobales, M. (1988). Developmental changes in fatty acid biosynthesis and composition in the house cricket, *Acheta domesticus*. *Arch. Insect Biochem. Physiol.* 9, 357–366. doi: 10.1002/arch.940090409

Devonshire, A. L., and Field, L. M. (1991). Gene amplification and insecticide resistance. *Annu. Rev. Entomol.* 36, 1–23. doi: 10.1146/annurev.en.36.010191.000245

Filho, J. P. D. L., and Paiva, E. A. S. (2006). The effects of sooty mold on photosynthesis and mesophyll structure of mahogany (*Swietenia macrophylla* King., Meliaceae). *Bragantia* 65, 11–17. doi: 10.1590/S0006-87052006000100003

Gade, G. (2004). Regulation of intermediary metabolism and water balance of insects by neuropeptides. *Annu. Rev. Entomol.* 49, 93–113. doi: 10.1146/annurev.ento.49.061802.123354

Garratt, M. P. D., Leather, S. R., and Wright, D. J. (2010). Tritrophic effects of organic and conventional fertilisers on a cereal-aphid-parasitoid system. *Entomol. Exp. Appl.* 134, 211–219. doi: 10.1111/j.1570-7458.2009.00957.x

Grabherr, M., Haas, B. J., Yassour, M., Levin, J. Z., Thompson, D. A., Amit, I., et al. (2011). Full-length transcriptome assembly from RNA-Seq data without a reference genome. *Nat. Biotechnol.* 29, 644–652. doi: 10.1038/nbt.1883

Kaloshian, I., and Walling, L. L. (2005). Hemipterans as plant pathogens. *Annu. Rev. Phytopathol.* 43, 491–521. doi: 10.1146/annurev.phyto.43.040204.135944

Kempema, L. A., Cui, X., Holzer, F. M., and Walling, L. L. (2006). Arabidopsis transcriptome changes in response to phloem-feeding silverleaf Whitefly

Nymphs. Similarities and distinctions in responses to aphids. *Plant Physiol.* 143, 849–865. doi: 10.1104/pp.106.090662

Kunieda, T., Fujiyuki, T., Kucharski, R., Foret, S., Ament, S. A., Toth, A. L., et al. (2006). Carbohydrate metabolism genes and pathways in insects: insights from the honey bee genome. *Insect Mol. Biol.* 15, 563–576. doi: 10.1111/j.1365-2583.2006.00677.x

Powell, G., Tosh, C. R., and Hardie, J. (2006). Host plant selection by aphids: behavioral, evolutionary, and applied perspectives. *Annu. Rev. Entomol.* 51, 309–330. doi: 10.1146/annurev.ento.51.110104.151107

Rodriguezlopez, M. J., Garzo, E., Bonani, J. P., Fereres, A., Fernandezmunoz, R., and Moriones, E. (2011). Whitefly resistance traits derived from the wild tomato Solanum pimpinellifolium affect the preference and feeding behavior of *Bemisia tabaci* and reduce the spread of tomato yellow leaf curl virus. *Phytochemistry* 101, 1191–1201. doi: 10.1094/PHYTO-01-11-0028

Saska, P., Skuhrovec, J., Lukas, J., Chi, H., Tuan, S., and Honěk, A. (2016). Treatment by glyphosate-based herbicide alters life history parameters of the rose-grain aphid Metopolophium dirhodum. *Sci. Rep.* 6:27801. doi: 10.1038/srep27801

Schwab, M. (2013). Cytochrome P450 enzymes in drug metabolism: regulation of gene expression, enzyme activities, and impact of genetic variation. *Pharmacol. Therap.* 138, 103–141. doi: 10.1016/j.pharmthera.2012.12.007

Scott, J. G., and Wen, Z. (2001). Cytochromes P450 of insects: the tip of the iceberg. *Pest Manag. Sci.* 57, 958–967. doi: 10.1002/ps.354

Tan, L., Meesapyodsuk, D., and Qiu, X. (2011). Molecular analysis of Δ6 desaturase and Δ6 elongase from *Conidiobolus obscurus* in the biosynthesis of eicosatetraenoic acid, a ω3 fatty acid with nutraceutical potentials. *Appl. Microbiol. Biotechnol.* 90, 591–601. doi: 10.1007/s00253-010-3060-y

Taylor, S. H., Parker, W. E., and Douglas, A. E. (2012). Patterns in aphid honeydew production parallel diurnal shifts in phloem sap composition. *Entomol. Exp. Appl.* 142, 121–129. doi: 10.1111/j.1570-7458.2011.01206.x

Walling, L. L. (2008). Avoiding effective defenses: strategies employed by phloem-feeding insects. *Plant Physiol.* 146, 859–866. doi: 10.1104/pp.107.113142

Wandall, H. H., Pizette, S., Pedersen, J. W., Eichert, H., Levery, S. B., Mandel, U., et al. (2005). Egghead and brainiac are essential for glycosphingolipid biosynthesis *in vivo*. *J. Biol. Chem.* 280, 4858–4863. doi: 10.1074/jbc.C400571200

Wang, E., Wang, R., Deparasis, J., Loughrin, J. H., Gan, S., and Wagner, G. J. (2001). Suppression of a P450 hydroxylase gene in plant trichome glands enhances natural-product-based aphid resistance. *Nat. Biotechnol.* 19, 371–374. doi: 10.1038/86770

Wang, X., Chen, Y., Gong, C., Yao, X., Jiang, C., and Yang, Q. (2018). Molecular identification of four novel cytochrome P450 genes related to the development of resistance of *Spodoptera exigua* (Lepidoptera: Noctuidae) to chlorantraniliprole. *Pest Manag. Sci.* 74, 1938–1952. doi: 10.1002/ps.4898

Waterhouse, P. M., and Helms, K. (1985). *Metopolophium dirhodum* (Walker): a newly arrived vector of barley yellow dwarf virus in Australia. *Aust. Plant Pathol.* 14, 64–66. doi: 10.1071/APP9850064

Weintraub, P. G., and Beanland, L. (2006). Insect vectors of phytoplasmas. *Annu. Rev. Entomol.* 51, 91–111. doi: 10.1146/annurev.ento.51.110104.151039

Will, T., Kornemann, S. R., Furch, A. C. U., Tjallingii, W. F., and Van Bel, A. J. E. (2009). Aphid watery saliva counteracts sieve-tube occlusion: a universal phenomenon? *J. Exp. Biol.* 212, 3305–3312. doi: 10.1242/jeb.028514

Wilson, A., Ashton, P. D., Calevro, F., Charles, H., Colella, S., Febvay, G., et al. (2010). Genomic insight into the amino acid relations of the pea aphid, *Acyrthosiphon pisum*, with its symbiotic bacterium Buchnera aphidicola. *Insect Mol. Biol.* 19, 249–258. doi: 10.1111/j.1365-2583.2009.00942.x

Winder, L., Alexander, C. J., Holland, J. M., Woolley, C., and Perry, J. N. (2001). Modelling the dynamic spatio-temporal response of predators to transient prey patches in the field. *Ecol. Lett.* 4, 568–576. doi: 10.1046/j.1461-0248.2001.00269.x

Zhang, H., Zhao, M., Liu, Y., Zhou, Z., and Guo, J. (2018). Identification of cytochrome P450 monooxygenase genes and their expression in response to high temperature in the alligatorweed flea beetle *Agasicles hygrophila* (Coleoptera: Chrysomelidae). *Sci. Rep.* 8, 1–13. doi: 10.1038/s41598-018-35993-1

Zhang, J., Li, D., Ge, P., Guo, Y., Zhu, K. Y., Ma, E., et al. (2014). Molecular and functional characterization of cDNAs putatively encoding carboxylesterases from the migratory locust, *Locusta migratoria*. *PLoS ONE* 9:e94809. doi: 10.1371/journal.pone.0094809

Zhang, T.-Y., Kang, L., Zhang, Z.-F., and Xu, W.-H. (2004). Identification of a POU factor involved in regulating the neuron-specific expression of the gene encoding diapause hormone and pheromone biosynthesis-activating neuropeptide in *Bombyx mori*. *Biochem. J.* 380, 255–263. doi: 10.1042/bj20031482

Conflict of Interest: The authors declare that the research was conducted in the absence of any commercial or financial relationships that could be construed as a potential conflict of interest.

The handling editor declared a shared affiliation with one of the authors FG.

frontiers in Sustainable Food Systems

ORIGINAL RESEARCH
published: 19 April 2021
doi: 10.3389/fsufs.2021.663238

Transcriptome Analysis Identified Gene Regulation Networks in Soybean Leaves Perturbed by the Coronatine Toxin

Xiong Zhang[1†], Bin He[2†], Sheng Sun[3], Zhipeng Zhang[3], Tian Li[3], Hehe Wang[4], Zhicheng Liu[1], Ahmed Jawaad Afzal[5] and Xueqing Geng[1]*

[1] School of Agriculture and Biology, Shanghai Jiao Tong University, Shanghai, China, [2] Institute of Quality and Safety Testing Center for Agro-Products, Xining, China, [3] College of Horticulture, Shanxi Agricultural University, Jinzhong, China, [4] Department of Plant and Environmental Sciences, Edisto Research and Education Center, Clemson University, Blackville, SC, United States, [5] Biology Program, Division of Science, New York University Abu Dhabi, Abu Dhabi, United Arab Emirates

OPEN ACCESS

Edited by:
Wei Li,
Chinese Academy of Agricultural Sciences, China

Reviewed by:
Gang Wei,
Fudan University, China
Jinxin Gao,
New York University, United States
Songbiao Chen,
Minjiang University, China

***Correspondence:**
Xueqing Geng
xqgeng@sjtu.edu.cn

[†]These authors have contributed equally to this work and share first authorship

Specialty section:
This article was submitted to Agroecology and Ecosystem Services, a section of the journal Frontiers in Sustainable Food Systems

Received: *02 February 2021*
Accepted: *18 March 2021*
Published: *19 April 2021*

Citation:
Zhang X, He B, Sun S, Zhang Z, Li T, Wang H, Liu Z, Afzal AJ and Geng X (2021) Transcriptome Analysis Identified Gene Regulation Networks in Soybean Leaves Perturbed by the Coronatine Toxin. Front. Sustain. Food Syst. 5:663238. doi: 10.3389/fsufs.2021.663238

The non-host specific *Pseudomonas syringae* phytotoxin Coronatine (COR) causes chlorosis and promotes toxicity by inducing physiological changes in plants. We performed transcriptome analysis to better understand plants' transcriptional and metabolic response to COR. Toward this end, mock-treated and COR-treated soybean plants were analyzed by RNA-Seq. A total of 4,545 genes were differentially expressed between the two treatments, of which 2,170 were up-regulated whereas 2,375 were down-regulated in COR treated samples. Gene annotation and pathway analysis conducted using the Kyoto Encyclopedia of Genes and Genomes (KEGG) and Gene Ontology (GO) databases revealed that the differential genes were involved in photosynthesis, jasmonic acid (JA) synthesis, signal transduction, and phenylpropane metabolism. This study will provide new insights into COR mediated responses and extend our understanding of COR function in plants.

Keywords: soybean, *Pseudomonas syringae*, coronatine, RNA-Seq, differentially expressed genes

INTRODUCTION

Soybean [*Glycine max* (L.) Merr.] is one of the most important economic crops in the world but is vulnerable to various pests and diseases which drastically affect yield and quality. Soybean speck caused by *Pseudomonas syringae* pv. *glycinea* (*Pgy*) is a common disease, threatening soybean yield worldwide (Keen and Buzzell, 1991; Wrather et al., 1997). Pathogenic bacteria inject type three effectors (TTEs) through the type three secretion system (TTSS) in order to inhibit the plant immune response and cause virulence in compatible hosts. Besides effector proteins, pathogens also secrete phytotoxins to increase pathogenicity on plants. Phytotoxins promote pathogen growth by modifying host cell processes and by altering host metabolism (Galán, 2009). Coronatine (COR) is a non-host specific phytotoxin secreted by *Pseudomonas syringae* pathovars *atropurpurea*, *glycinea*, *maculicola*, *morsprunorum,* and *tomato* (Bender et al., 1999). Coronatine can be detected in healthy tissues adjacent to the bacterial lesions, indicating that COR could move systemically (Zhao et al., 2001). The main symptom caused by COR is chlorosis, however, COR does not destroy organelles or membrane systems (Palmer and Bender, 1995). In addition to causing chlorosis in plants, the compound can reopen stomata, which can promote bacterial invasion, proliferation, and development of plant disease symptoms (Geng et al., 2012).

Coronatine ($C_{18}H_{25}NO_4$) has a relative molecular weight of 319 g/mol and is a structural and functional analog of JA-Ile. It is formed by linking the α-amino acid Coronamic Acid (CMA) with the polyketone Coronafacic Acid (CFA) through an amide linkage (Brooks et al., 2004). Coronafacic Acid structure partially mimics the plant hormone jasmonic acid (JAs), and similar to Jasmonate, its activity is mediated by binding to the Coranatine Insensitive1 (COI1) receptor (Feys et al., 1994). The affinity of COR for COI1 is more than 1,000 times that of JA-Ile (Katsir et al., 2008). Coronatine induces JA biosynthesis and inhibits SA signaling, thereby dampening SA-dependent disease resistance (Zheng et al., 2012). The treatment of COR in plants also induces ethylene production and the release rate of ethylene is proportional to the concentration of COR in tobacco leaves (Ferguson and Mitchell, 1985; Kenyon and Turner, 1992). Although CMA is structurally similar to the ethylene precursor 1-aminocyclopropene 1-carboxylic acid (ACC), it does not induce the production of ethylene responsive genes (Uppalapati et al., 2005). Furthermore, treatment with CFA, CMA, MeJA, or ACC does not induce chlorosis, indicating that COR has additional functions than those attributed to either CFA or CMA (Uppalapati et al., 2005).

High-throughput RNA-Seq is a powerful tool to study gene expression changes in plants (Gao et al., 2014). In order to better understand the function of COR in soybean, we treated soybean plant leaves with COR which was followed by transcriptome analysis. The biological annotation of differentially expressed genes (DEGs) under treatment of COR provided new insights into COR mediated plant responses on soybeans, thereby extending our understanding of COR function in plants.

MATERIALS AND METHODS

Plant Material and Treatment

Soybean [*Glycine max* (L.) Merrill cv. Williams 82] was grown under a 12 h light /12 h dark period with light and dark temperatures of 25 and 20°C, respectively. Four-week-old soybean plants were used in the study. Coronatine purchased from Sigma-Aldrich (St. Louis, MO) was dissolved in methanol to make a stock solution (600 μM, stored at −20°C) which was subsequently diluted with water to a final concentration of 3 μM. After the addition of 0.004% Silwet L-77, the working solution was sprayed on soybean leaves and leaf samples were collected 10 h post spray. For control treatment, only water containing 0.004% Silwet L-77 solution was sprayed onto the plant leaves. Harvested samples were immediately frozen in liquid nitrogen and stored at −80°C.

Library Construction and RNA-Seq

Each treatment (COR or mock) was carried out in triplicate. Total RNA was extracted from leaves of COR-treated and control plants using Trizol reagent (Invitrogen, Carlsbad, CA, USA; Rio et al., 2010), and the concentration of RNA was quantified using a NanoDrop-2000 nucleic acid spectrophotometer (Thermo Fisher Scientific, Wilmington, DE). Nucleic acid integrity was assessed by resolving RNA on a 1% (w/v) agarose gel. Quality control and library construction were entrusted to Huada Gene Technology Company (Wuhan, Hubei, China). In brief, from a pool of total RNA, the mRNA fraction was enriched with the help of Oligo-dT magnetic beads (Vazyme Biotech Company, Jiangsu, China). This was followed by RNA fragmentation and first strand cDNA synthesis using the random hexamer primers (Illumina, San Diego, CA, USA). Following second strand cDNA synthesis, the fragments were ligated with adapters and PCR amplified to construct cDNA libraries. BGISEQ-500 platform from Huada Gene Technology Co., Ltd. (Wuhan, Hubei, China) was used to generate raw library reads. The base quaility of the raw data was the ASCII (American standard code for information interchange) value of each character in the fourth line of the FASTQ format minus 64. Reads where more than half of the component bases had a quality score below 15 was considered a low-quality read and removed by Soapnuk. Hierarchical Indexing for Spliced Alignment of Transcripts (HISAT) was used to align the filtered data to the reference genome (GCF_000004515.4_Glycine_max_v2.0; Kim et al., 2015). The RNA-seq data has been uploaded to NCBI gene expression omnibus server (accession number: PRJNA690873, Biosample ID: SAMN17266875, COR SRA ID: SRR13389957, and Mock SRA ID: SRR13389956).

Gene Annotation and Classification

Fragments Per Kilobase of exon model per Million mapped fragments (FPKM) was used to evaluate gene expression levels, and DEGseq R package (Anders and Huber, 2010) was used to determine the DEGs between the two samples. The screening threshold for differential genes was $|\log_2 \text{Fold Change}| \geq 1$, FDR < 0.01, FPKM ≥ 1.

Based on Gene Ontology (GO) (http://www.geneontology.org/) analysis, DEGs were divided into three major functional categories including molecular function, cellular component, and biological process. These genes were further classified

TABLE 1 | Primer Sequence used for RT-PCR validation.

Gene number	Primer sequence	Description
GLYMA_18G057900	GACATCGACTCCATTGCC	Dihydroflavonol reductase
	CCGCCTTCAACACATTAACTG	
GLYMA_05G039900	GACCCAGTTCAAGACACCC	Receptor-like protein kinase
	CCGAGTTCCACAAGTTCAC	
GLYMA_17G023100	AAAGAAAGAGAAGTGATGGTGG	CASP-like protein 5
	GAGGGCAAGGAGTAGAGAC	
GLYMA_04G166900	CCAAACACCAGCCAATCTC	Transcription repressor MYB6
	GTCACTTTCTAACCCAATACCA	
GLYMA_18G072200	GTTCTACACTACACTCACACTG	Vacuolar cation/ proton exchanger 5
	GTTTCCATTCTGACTCTCATCC	
GLYMA _ 20G141600	GTGTAATGTTGGATGTGTTCCC	Polyubiquitin
	ACACAATTGAGTTCAACAC AAACCG	

TABLE 2 | Data quality statistics of mapped and sequenced reads.

Sample	Total reads[a]	Clean reads[b]	Clean reads Q30 (%)[c]	Total mapped reads[d]	Uniquely mapped[e]
COR treat	21,851,267	21,013,001 (95.98%)	90.33	20,319,572 (96.7%)	21,833,299 (72.26%)
H_2O treat	24,011,531	23,048,199 (96.24%)	90.32	22,359,058 (97.01)	16,348,088 (70.93%)

[a] *The number of raw reads obtained by RNA sequencing.*
[b] *The number of reads after filtering low-quality reads (Q ≤ 15 bases), reads with high content of unknown base N and Joint contamination.*
[c] *The number of reads with a read quality score >30.*
[d] *The number of reads uniquely mapped to the reference genome.*
[e] *Number of reads mapped to unique positions in the reference genome.*

TABLE 3 | Distribution of FPKM-quantified expression level of detected genes in COR and mock treated samples.

Sample	0 < FPKM[a]	FPKM ≤ 1	1 < FPKM ≤ 10	10 < FPKM ≤ 100	100 < FPKM
COR treatment	40,505	13,937 (33.824%)	15,189 (39.828%)	10,367 (24.102%)	1,012 (2.245%)
Mock treatment	41,290	13,966 (34.408%)	16,445 (37.499%)	9,952 (25.594%)	927 (2.498%)

[a] *Fragment per kilobase per million reads.*

into biological pathways based on Kyoto Encyclopedia of Genes and Genomes (KEGG) (http://www.genome.jp/kegg/) annotation and the phyper function in R was used for enrichment analysis.

Quantitative Real Time PCR (qRT-PCR) Validation

In order to assess the reliability of the data obtained from RNA-Seq, we measured the relative fold change of five genes by qRT-PCR analysis (Yu et al., 2014). RNA was extracted from frozen leaf tissue using Trizol reagent. In order to determine RNA integrity, the RNA samples were resolved on a 1% (w/v) agarose gel. For first strand cDNA synthesis, the PrimeScript™ RT (TaKaRa, Mountain View, CA), and the gDNA Eraser (TaKaRa, Mountain View, CA) kits were used. For qPCR analysis, the TB Green™ Premix Ex Taq™ (TaKaRa, Mountain View, CA) kit was used under the following set of conditions. A pre-denaturation step of 95°C for 30 s, 40 cycles with each cycle employing a denaturation temperature of 95°C for 5 s, and an annealing/extension step with a temperature of 60°C for 30 s followed by melt curve analysis. For each treatment, we analyzed a total of three biological replicates, each of which included three technical repeats. The $2^{-\Delta\Delta CT}$ method was used for the relative quantification of the five genes. The primers used for the qRT-PCR analysis are listed in **Table 1**. The GLYMA_20G141600 gene that encodes for polyubiquitin served as an internal control.

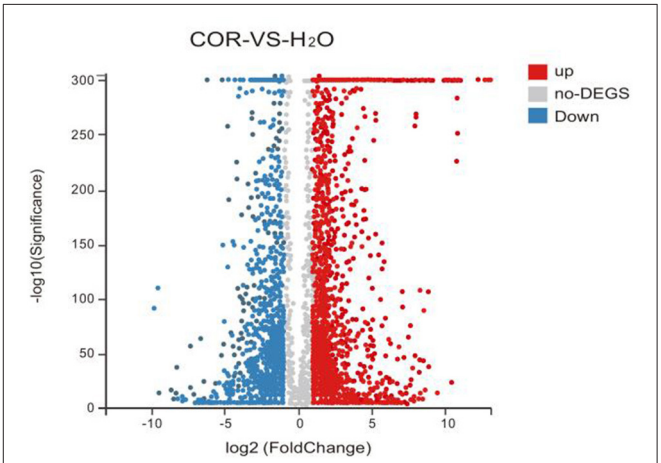

FIGURE 1 | Volcano plot for DEGs. The X-axis represents the log_2-transformed expression changes between COR-treated and mock samples, and the Y-axis represents the –log10-transformed *p*-value denoting the significance of differential expression. The red dots, blue dots, and gray dots denote up-regulated, down-regulated, and non-differential genes, respectively.

RESULTS

Overview of the Soybean Transcriptome

Transcriptome sequencing was performed on samples of COR and mock treated soybean leaves. A high proportion of clean reads (>96%) were obtained after filtration of the raw reads and more than 90% of the total reads had a quality value of 30, suggesting the sequencing reads were of high quality. Hierarchical Indexing for Spliced Alignment of Transcripts (HISAT) was used to align the filtered data to the reference genome, and the mapping result statistics are shown in **Table 2** (Kim et al., 2015).

Gene expression based on fragments per kilobase per million mapped reads (FPKM), generated sequence information for 41,290 and 40,505 reference genes from the COR and mock samples, respectively. Most of the expressed genes were distributed between 10 and 100 FPKM (**Table 3**). Transcriptome sequencing analysis was carried out on soybean leaves from the COR and the mock groups. The overall transcriptome data analysis showed that the transcriptome sequencing data was of high quality and could meet the basic requirements necessary for downstream analysis.

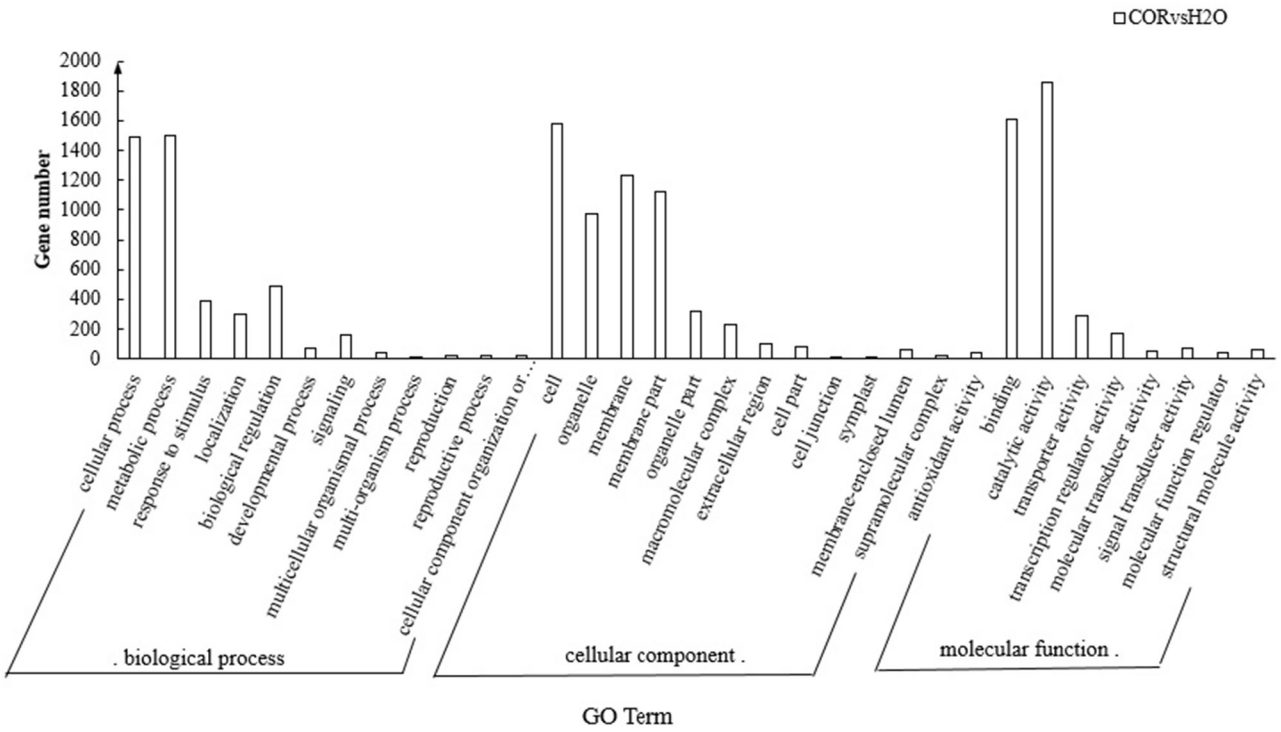

FIGURE 2 | GO functional categories of DEGs in different sub-groups. The GO terms are sorted according to their *P*-values in the cellular component, molecular functions, and biological process categories. The bars represent the number of enriched genes in major sub-categories within each GO category.

Analysis of Differentially Expressed Genes

Our results showed that the COR-vs.-mock comparison yielded 4,531 DEGs. In order to summarize the results obtained from our analysis, and to make visualization of the regulatory patterns more intuitive, we have drawn a volcanic map (**Figure 1**). The volcano diagram clearly and intuitively shows the expression profile of differential genes in soybeans under different treatments. Although COR-treatment resulted in a greater number of down-regulated genes (2,370), most of the genes with large fold differences were up-regulated (2,161; **Figure 1**).

Gene Ontology Enrichment Analysis

The GO database was used to functionally annotate DEGs into the following three major categories: Biological process, Cellular component, and Molecular function. There were 4,545 significant DEGs between COR and mock treated samples. Twelve GO subclasses belonged to biological processes sub-category, 12 subclasses were found within the cellular components category while 9 subclasses were enriched in the molecular function category (**Figure 2**). Within the biological process category, cellular processes, and metabolic processes accounted for a relatively high proportion of hits. In the cell components category, cell, organelle, membrane, and membrane part were the four subclasses with higher percentage representation whereas within the molecular function category, binding, and catalytic activity were the two majorly represented subclasses.

KEGG Annotation of DEGs

The KEGG database integrates gene catalogs obtained from a completely sequenced genome with higher-level system functions at the cell, species, and ecosystem level. The integrative function of the database transforms the expressed gene data into gene networks. By mapping DEGs to the reference genes in the KEGG database, we identified 2,100 DEGs involved in 131 KEGG pathways. Enrichment analysis showed that KEGG enrichment with a *Q*-value <0.05 was reliable, and on the basis of that threshold, a total of 30 KEGGs were found to be significantly enriched (**Figure 3**, **Supplementary Table 3**). The KEGG pathway with the largest number of enriched genes was related to "plant hormone signal transduction" (ko04075), with 181 genes annotated in this pathway. Although there were only 26 genes in the "Photosynthesis—antenna proteins" (ko00196) pathway, the enrichment factor reached 0.764, which was the highest of all annotated pathways. Analysis of the enriched KEGG pathway showed that the vast majority of KEGG genes belonged to the "metabolic branch" and were related to photosynthesis, hormone transduction, and secondary metabolism (**Figure 3**, **Supplementary Table 3**).

Chlorophyll and Photosynthesis Related Genes Were Down-Regulated by COR Treatment

Coronatine treatment resulted in the down-regulation of a large number of genes involved in chloroplast

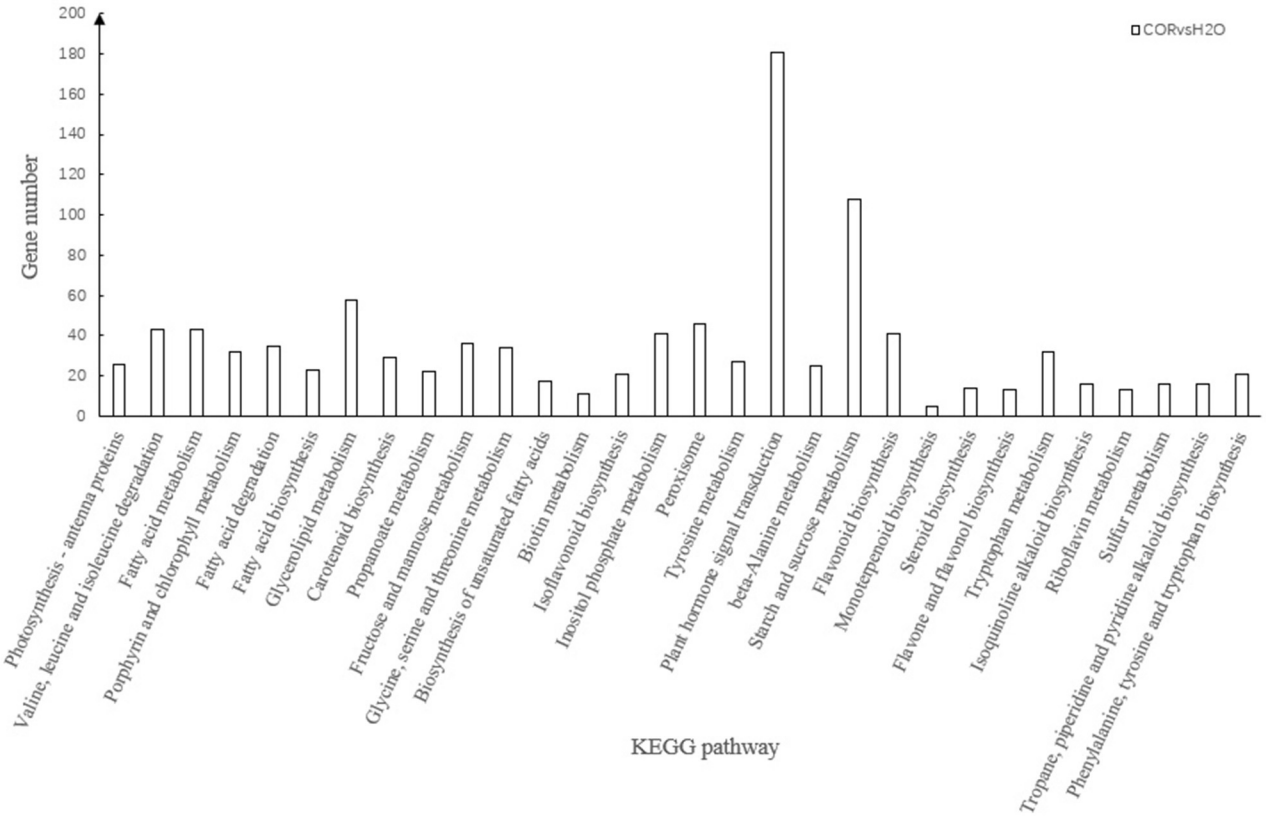

FIGURE 3 | Over-representation of DEGs in KEGG pathways. The X-axis shows different KEGG pathways, and the Y-axis denotes the number of DEGs involved in each category.

metabolism (**Supplementary Table 3**), indicating that COR had a significant influence on plant health. Chlorophyll a/b binding protein was significantly down-regulated, whereas genes related to magnesium removal, such as magnesium dechelatase, chlorophyllase, uroporphyrin-III C-methyltransferase, pheophorbidase, pheophorbide an oxygenase, and glucuronosyltransferase were significantly upregulated (**Supplementary Table 3**). Furthermore, COR induced the expression of chlorophyllase, an enzyme that degrades chlorophyll (Takamiya et al., 2000; Xie et al., 2008). In the three photosynthetic pathways: Photosynthesis-antenna proteins (ko00196), Carbon fixation in photosynthetic organisms (ko00710), Photosynthesis (ko00195), there were 129 genes with significant gene expression changes (**Supplementary Table 1**). Out of these, only 15 genes were up-regulated while 114 genes were down-regulated, indicating that photosynthesis was significantly downregulated upon COR treatment.

Genes Related to ROS Generation Were Upregulated in Response to COR Treatment

When plants are under biological stress, rapid generation of reactive oxygen species (ROS) can be observed (Wojakowska et al., 2013; Gao et al., 2017). While ROS cannot prevent the development of macroscopic symptoms, its production limits the invasiveness of pathogens (Zou et al., 2005). Reactive oxygen species strengthens cell walls through oxidative crosslinking of glycoproteins, and acts as a second messenger in some cell signaling pathways (Lamb and Dixon, 1997). However, ROS also exhibits potential toxicity as its increased accumulation can accelerate membrane lipid peroxidation (Mittler, 2002; Mittler et al., 2004). In order to increase their resistance to oxidative damage, plants require high levels of antioxidant enzymes (Sudhakar et al., 2001). The antioxidant enzymes or ROS scavengers can reduce ROS levels (Keppler and Baker, 1989). Various ROS scavengers, including ascorbic acid peroxidase (PER), glutathione, superoxide dismutase (SOD), and catalase (CAT) maintain ROS homeostasis in different compartments of plant cells (Mittler et al., 2004). Most of the enzymes involved in ROS detoxification, such as glutathione S-transferase (GST), CAT, PER, and glutathione reductase (GR), were up-regulated in COR treated samples, while SOD-related enzymes were down-regulated (**Table 4**).

COR Regulation of JA Biosynthesis and Related Hormone Pathways

Plant hormones not only play an essential role in growth and development, but they also contribute to how plants respond

TABLE 4 | COR induced genes involved in the production of secondary metabolites.

Gene ID	Locus tag	Annotation	$Log_2(COR/H_2O)$	FDR
Glutathione reductase				
LOC100787748	GLYMA_12G188600	Transcription factor LHW	1.574	3.77E-54
Catalase				
LOC100037447	GLYMA_14G223500	Catalase	1.687	2.62E-233
Superoxide dismutase (sod)				
LOC100778673	GLYMA_20G050800	Superoxide dismutase [Fe] 3, chloroplastic	−1.231625701	5.80E-09
LOC100784752	GLYMA_12G081300	Superoxide dismutase [Cu-Zn], chloroplastic	−3.984189485	1.35E-292
LOC100814802	GLYMA_02G087700	Superoxide dismutase [Fe], chloroplastic	−1.193681125	3.71E-13
LOC100815376	GLYMA_11G192700	Superoxide dismutase [Cu-Zn], chloroplastic	−3.066015698	0
Vegetable storage protein (vsp)				
LOC100778379	GLYMA_07G014600	Stem 28 kDa glycoprotein	1.918542343	4.33675E-68
LOC102661443	GLYMA_16G220900	Acid phosphatase 1	2.320167637	6.39352E-40
LOC547483	GLYMA_03G001500	Syringolide-induced protein B15-3-5	1.606397221	1.49774E-25
LOC547669	GLYMA_08G200200	Acid phosphatase	1.366006146	4.70121E-80
LOC547820	GLYMA_08G200100	31 kDa protein	4.912387218	0
LOC547821	GLYMA_07G014500	28 kDa protein	1.147466677	0
Glutathione s-transferase (gst)				
LOC100306196	GLYMA_07G140200	Tau class glutathione S-transferase	1.291766124	1.02E-27
LOC100527851	GLYMA_07G139700	Probable glutathione S-transferase	3.699554209	0
LOC100775492	GLYMA_13G135600	Glutathione S-transferase L3-like	−1.134671536	1.11E-14
LOC100807613	GLYMA_07G139800	Probable glutathione S-transferase	3.763046026	7.75E-292
LOC100808141	GLYMA_07G139900	Probable glutathione S-transferase	3.463748914	4.72E-63
LOC547576	GLYMA_01G040200	Glutathione S-transferase GST 5	−1.347694963	0
LOC547583	PROVISIONAL	Probable glutathione S-transferase	1.775084536	4.89E-81
LOC547584	GLYMA_10G192900	Glutathione S-transferase GST 15	1.087031993	6.91E-14
LOC547586	GLYMA_20G101100	Glutathione S-transferase GST 18	1.307361982	0.000115395
LOC547925	GLYMA_15G252200	Lactoylglutathione lyase	1.897552731	4.66E-71
LOC547951	GLYMA_14G031000	Glutathione S-transf erase 24	1.951303217	1.39E-252
Glucosinolate (gs)				
LOC100785254	GLYMA_11G197300	Isoleucine N-monooxygenase 2	10.83700417	0
LOC100786887	GLYMA_20G065100	Isoleucine N-monooxygenase 1	10.129171	0
LOC100787378	GLYMA_11G197400	Isoleucine N-monooxygenase 1	3.350497247	0.000308612
LOC100787727	GLYMA_03G031400	Cytochrome P450 71A1	1.543542573	2.26E-15
LOC100787855	GLYMA_01G036000	UDP-glycosyltransferase 74B1	2.017147307	2.22E-30
LOC100796528	GLYMA_03G029900	Cytochrome P450 83B1-like	2.407905807	0
LOC100801312	GLYMA_03G030800	Cytochrome P450 83B1	1.391968651	1.11E-11
LOC100805576	GLYMA_03G030400	Cytochrome P450 83B1	1.468980474	6.77E-53
LOC100806069	GLYMA_02G029900	UDP-glycosyltransferase 74B1	2.928916902	6.67E-06
LOC100806470	GLYMA_U013600	Cytochrome P450 83B1	1.438839277	8.12E-31
LOC100809902	GLYMA_13G051600	Isoleucine N-monooxygenase 2	5.526903463	0
LOC102662047			2.862496476	2.18E-05
Lipoxygenase (lox)				
LOC100127399	GLYMA_07G034800	Lipoxygenase-9	2.030088379	0
LOC100782973	GLYMA_20G234000		−1.497573779	8.38E-43
LOC100786646	GLYMA_11G130200	Linoleate 13S-lipoxygenase 2-1, chloroplastic	1.724133299	0
LOC100791000	GLYMA_16G008700	Linoleate 13S-lipoxygenase 3-1, chloroplastic	1.954806341	0
LOC100795276	GLYMA_13G030300	Linoleate 13S-lipoxygenase 2-1, chloroplastic	−1.446819343	4.01E-76
LOC100797626	GLYMA_12G054700	Linoleate 13S-lipoxygenase 2-1, chloroplastic	−1.10523695	2.67E-189
LOC100800451	GLYMA_20G144600	Linoleate 9S-lipoxygenase 5	1.258182041	2.74E-22
LOC100802459	GLYMA_07G034900	Linoleate 9S-lipoxygenase 1	2.606178987	1.93E-135
LOC100803358	GLYMA_15G026400	Linoleate 9S-lipoxygenase	2.558156513	0

(Continued)

TABLE 4 | Continued

Gene ID	Locus tag	Annotation	$Log_2(COR/H_2O)$	FDR
LOC100814410	GLYMA_08G102900	Lipoxygenase 6, chloroplastic	1.060411517	3.25E-08
LOC547835	GLYMA_07G007000	Lipoxygenase	1.029817611	1.42E-35
LOC547836	GLYMA_13G347700	Lipoxygenase	1.74506997	0
LOC547860	GLYMA_13G347800	Lipoxygenase	2.726734875	0
Chalcone synthase (chs)				
LOC100775264	GLYMA_19G105100	Chalcone synthase 13	−1.35841466	3.83E-66
LOC100777949	GLYMA_11G001500	Vacuolar-sorting receptor 1	1.882660553	0
LOC100779649	GLYMA_08G110700	Chalcone synthase 4a	1.803708989	4.99E-25
LOC100789075	GLYMA_08G110300	Chalcone synthase 3	1.167530486	5.39E-05
LOC100791524	GLYMA_08G109300	chalcone synthase 3	2.983647795	1.16E-36
LOC100794652	GLYMA_06G118500	chalcone synthase	−1.979405132	3.27E-203
LOC100803958	GLYMA_10G257300	vacuolar-sorting receptor 1	1.061012921	3.06E-66
LOC100804241	GLYMA_15G242900	Chalcone isomerase	−1.952513213	3.05E-30
LOC100820115	GLYMA_01G242800	Vacuolar-sorting receptor 1	1.618450868	0
LOC106794283	GLYMA_08G110900	Chalcone synthase 3	2.306838759	1.81E-28
LOC732546	GLYMA_20G241700	Chalcone–flavonone isomerase 2-A	−1.376245016	1.11E-05
LOC732575	GLYMA_08G109400	Chalcone synthase 1	3.006533728	8.10E-165
LOC732649	GLYMA_13G262500	Chalcone isomerase 3A1	−1.495076997	1.94E-06
Phenylalanine ammonia lyase (pal)				
LOC100787902	GLYMA_03G181600	Phenylalanine ammonia-lyase 1	1.655913298	5.53E-87
LOC100803857	GLYMA_13G145000	Phenylalanine ammonia-lyase 2.3	1.575001583	0
LOC100811101	GLYMA_19G182300	Phenylalanine ammonia-lyase 1.1	3.09186466	0
LOC100818777	GLYMA_20G180800	Phenylalanine ammonia-lyase 2.2	−2.017000353	1.09E-49

to both biotic and abiotic stressors. For instance, Jasmonate Acid (JA) modulates developmental as well as innate immune responses. Jasmonate Acid belongs to a small class of lipid-derived molecules and acts as a salicylic acid (SA) antagonist and an ethylene (ET) synergist (Gfeller et al., 2010). The first step in JA synthesis is accomplished by lipoxygenase (LOX)-catalyzed oxidation of linolenic acid (Vick and Zimmerman, 1984). In the JA synthesis pathway, 12 genes were up-regulated and only 2 genes were down-regulated. Among the genes encoding LOX, two genes were down-regulated, while five genes were up-regulated. In particular, the genes encoding allene oxide synthase (AOS) and allene oxide cyclase (AOC) were all up-regulated, suggesting that COR induced the activation of the JA biosynthetic pathway (**Supplementary Table 2**). Coronatine treatment also affected the expression of ethylene (ET) synthesis genes (**Supplementary Table 2**). In this study, a total of 14 DEGs involved in ethylene synthesis were identified, of which 13 genes were up-regulated and 1 gene was down-regulated (**Supplementary Table 2**), indicating that COR could promote ethylene biosynthesis.

COR Induced the Expression of Genes Involved in the Production of Stress Associated Proteins and Plant Secondary Metabolites

The accumulation of secondary metabolites constitutes an important component of plant stress response (Dixon et al., 2002). Some secondary metabolites play important defense roles during pathogen invasion (Erb and Kliebenstein, 2020). Vegetable Storage Protein (VSP) can be rapidly synthesized or degraded and plays an important role in the process of plant stress adaptation (Staswick et al., 1991). In our study VSP was up-regulated upon COR treatment (**Table 4**). Glucosinolates (GS) are also defense-related secondary metabolites, and related genes were also up-regulated in the presence of COR (**Table 4**). Coronatine also induced the expression of key enzymes in the phenylpropane pathway such as phenylalanineammonialyase (PAL), chalcone synthase (CHS), and phenylalanineammonialyase (PAL) (**Table 4**, **Supplementary Table 3**). These results suggest that COR may affect plant defense responses by regulating plant secondary metabolism, which is known to play important roles during plant pathogenesis.

qRT-PCR Validation of RNA-Seq Results

A total of 5 DEGs (GLYMA_18G057900, GLYMA_05G039900, GLYMA_17G023100, GLYMA_04G166900, and GLYMA_18G072200) identified through RNA-Seq analysis were selected for qRT-PCR verification. Our comparison results (**Figure 4**) showed that the relative expression levels of these genes in RNA-seq and qRT-PCR followed the same trend, suggesting that the results of RNA-seq were reliable.

DISCUSSION

Bacterial COR has been shown to induce the activation of LOXs, which catalyze the synthesis of JA and MeJA. Through a

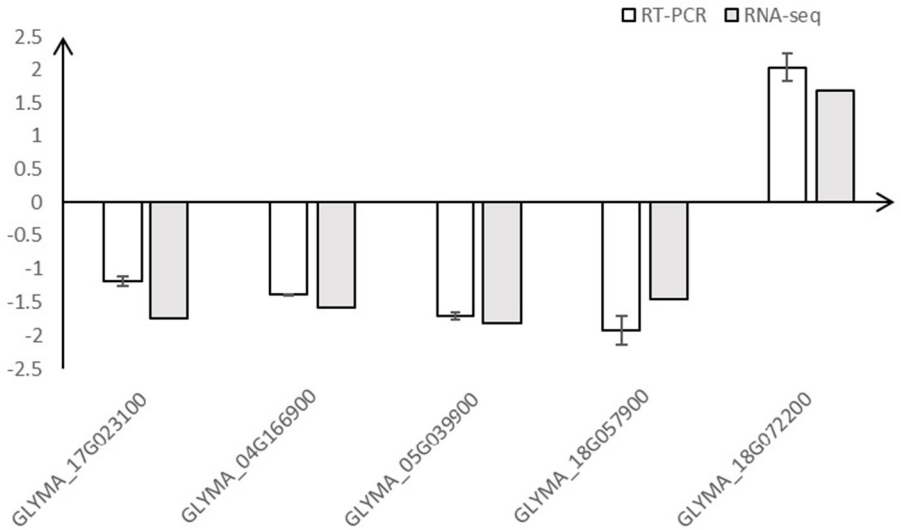

FIGURE 4 | qRT-PCR validation of DEGs identified by RNA-seq. Five differentially expressed genes (GLYMA_18G057900, GLYMA_05G039900, GLYMA_17G023100, GLYMA_04G166900, and GLYMA_18G072200) identified through RNA-Seq analysis were selected for qRT-PCR validation, and the gene expression changes between COR-treated and mock samples detected by RNA-seq and qRT-PCR were compared. The white columns represent the mean fold change of the five genes through qRT-PCR analysis (error bars represent standard error of mean) while the gray bars represent fold changes obtained through RNA-Seq analysis. Pearson correlation coefficient used to measure the strength of the correlation between both methods showed a significant positive correlation ($r = 0.974$, $p = 0.0053$).

positive feedback loop, JA can also activate LOXs and promote JA accumulation even further (Bell and Mullet, 1991). Both COR and JA induce ethylene biosynthesis (Czapski and Saniewski, 1992; Uppalapati et al., 2005) which plays an important role in the development of chlorotic symptoms associated with soybean speck disease (Lund et al., 1998). During plant–pathogen interactions, SA signaling activates resistance against biotrophic and hemi-biotrophic pathogens, whereas JA and ethylene (ET) activate resistance against necrotrophic pathogens while suppressing SA dependent signaling (Glazebrook, 2005). As bacteria expressing COR induce the production of JA and ET, we would expect a dampening of SA-dependent responses and enhanced growth of biotrophic pathogens. Coronatine-induced ethylene has also been shown to accelerate plant senescence and inhibit photosynthesis in a dose-dependent manner (Ueda and Kato, 1980; Stall and Hall, 1985; Kenyon and Turner, 1990; Bleecker and Kende, 2000; He et al., 2002; Uppalapati et al., 2005). Consistent with previous studies, we showed that in COR-treated soybean leaves, photosynthetic related genes were down-regulated, suggesting that COR is involved in inducing chlorotic symptoms through the inhibition of the photosynthetic machinery.

Reactive oxygen species generation is one of the initial responses to pathogen invasion (Lamb and Dixon, 1997). High levels of ROS are produced in plant cells undergoing stress. Superoxide anion (O^{2-}), hydrogen peroxide (H_2O_2), and hydroxyl radical (OH^-) are the main forms of ROS produced during photosynthesis (Karpinski et al., 2003; Apel and Hirt, 2004). *Pseudomonas syringae* infection is reported to result in COR-induced decomposition of chlorophyll, which in turn promotes ROS production (Mur et al., 2010). As high level of ROS leads to cell toxicity (Mittler, 2002), its overproduction usually results in the generation of free radical scavenging enzymes. GST is one such enzyme, which is known to be involved in regulating redox potential of infected tissues (Zhang et al., 2015). Consistent with these findings, COR has been reported to cause GST mRNA accumulation 4–9 h after bacterial inoculation (Greulichi et al., 1995). However, not all antioxidant enzymes are up-regulated upon ROS generation. As some studies show that COR inhibits the expression of thylakoid-localized Cu/Zn SOD (Ishiga et al., 2009). These results may explain why we observed a down-regulation of SOD expression and an upregulation of GSTs upon COR treatment.

In *Arabidopsis*, COR also induces the expression of genes related to phenylpropane metabolism (Attaran et al., 2014). Flavonoids are secondary metabolites that are synthesized via the phenylpropane pathway and are involved in imparting resistance against necrotrophic pathogens. Lamb and Dixon (1997) proposed that the isoflavone phytoalexin pathway may also be the main participant involved in the modulation of oxidative stress responses (Lamb and Dixon, 1997; Winkel-Shirley, 2001). The up-regulation of PAL and CHS indicated that COR targets the phenylpropane metabolic pathway and promotes the synthesis of flavonoids which in turn induce the production of ROS-scavenging enzymes. Of note, ROS scavengers may be beneficial to the host as well as the pathogen. To increase the resistance to oxidative damage induced upon bacterial infection and to improve plant health, plants need high levels of these antioxidants. However, COR can inhibit the early onset of pathogen-associated molecular patterns (PAMP)-triggered immunity (PTI) and induce disease-related necrotic cell death at later stages of disease progression. While COR has

not been shown to function as a ROS scavenger, tomato plants infected with COR-producing bacterial strains have reduced ROS levels through the activity of ROS scavenging enzymes (Ishiga et al., 2009). It is therefore not surprising that most ROS scavenger-related genes were up-regulated in our study.

In addition to ROS scavengers, we focused on other genes that were specifically regulated by COR. These included the vegetative storage proteins (VSP) and glucosinolate (GS). Vegetative storage proteins is known to be upregulated during insect herbivory and is specifically induced by JA (Benedetti et al., 1995). Other plant hormones below a certain concentration threshold do not modulate VSP levels in plant cells (Anderson et al., 1989). In *Arabidopsis*, VSP expression was not detected in the *Arabidopsis coi1* mutant seedlings, and VSP in wild-type *Arabidopsis* seedlings was induced upon MeJA and COR treatments (Benedetti et al., 1995). Thioglucoside and its hydrolyzed metabolites are involved in multiple functions including antioxidant activity, chemical protection, and resistance to biotic and abiotic stressors (Guo et al., 2013). The ability of *coi1* mutants to induce indole-GS through MeJA was severely impaired, suggesting that COI1 plays a positive role in inducing GS production (Mewis et al., 2006; Brader et al., 2007). It is worth noting that GS, VSP, and ethylene expression can be induced by both COR and JA, indicating that these genes may be induced by COR and JA in a similar manner. Interestingly, the ability of COR to induce chlorosis is also achieved through COI1 (Mecey et al., 2011). The above results indicate that COI1 plays a major role in the regulation of COR-induced responses in plants.

The phytotoxin COR plays an important role in promoting the pathogenicity of bacteria, and the virulent activity of bacteria lacking COR is significantly reduced (Geng et al., 2014). Our results showed that COR induced the expression of genes related to JA and ethylene synthesis, suggesting that COR may activate these two hormone pathways to regulate plant defenses. Coronatine also induced expression of Phenylalanine ammonia lyase (PAL), which is the key enzyme involved in the production of phenylpropane metabolites in plants. This indicated that COR could dampen plant defenses through perturbing phenylpropane metabolism. Our comprehensive transcriptional analysis of the interaction between COR and soybean through RNA-Seq would help better understand the non-host resistance (NHR) response in plants and would also provide a theoretical basis for the improvement of soybean resistance against non-adapted pathogens.

DATA AVAILABILITY STATEMENT

The datasets presented in this study can be found in online repositories. The names of the repository/repositories and accession number(s) can be found in the article/**Supplementary Material**.

AUTHOR CONTRIBUTIONS

XZ, BH, and XG designed the research strategy and analyzed the sequenced data. SS, ZZ, and TL conducted part of experiments. XZ, AJA, and XG wrote the manuscript. HW, ZL analyzed part of data. All authors contributed to the article and approved the submitted version.

FUNDING

This work was funded by Shanghai international scientific and technological cooperation foundation (No. 19390743400) and the key R&D and transformation program of Xining city (CN) (No. 2019-y-35).

ACKNOWLEDGMENTS

We would like to thank Huada gene institution in China for providing technical assistance with bioinformatics analysis.

SUPPLEMENTARY MATERIAL

The Supplementary Material for this article can be found online at: https://www.frontiersin.org/articles/10.3389/fsufs.2021.663238/full#supplementary-material

REFERENCES

Anders, S., and Huber, W. (2010). Differential expression analysis for sequence count data. *Genome Biol.* 11, 1–12. doi: 10.1186/gb-2010-11-10-r106

Anderson, J. M., Spilatro, S. R., Klauer, S. F., and Franceschi, V. R. (1989). Jasmonic acid-dependent increase in the level of vegetative storage proteins in soybean. *Plant Sci.* 62, 45–52. doi: 10.1016/0168-9452(89)90188-X

Apel, K., and Hirt, H. (2004). Reactive oxygen species: metabolism, oxidative stress, and signal transduction. *Annu. Rev. Plant Biol.* 55, 373–399. doi: 10.1146/annurev.arplant.55.031903.141701

Attaran, E., Major, I. T., Cruz, J. A., Rosa, B. A., Koo, A. J., Chen, J., et al. (2014). Temporal dynamics of growth and photosynthesis suppression in response to jasmonate signaling. *Plant Physiol.* 165, 1302–1314. doi: 10.1104/pp.114.239004

Bell, E., and Mullet, J. E. (1991). Lipoxygenase gene expression is modulated in plants by water deficit, wounding, and methyl jasmonate. *Mol. Gen. Genet.* 230, 456–462. doi: 10.1007/BF00280303

Bender, C. L., Alarconchaidez, F., and Gross, D. C. (1999). *Pseudomonas syringae* phytotoxins: mode of action, regulation, and biosynthesis by peptide and polyketide synthetases. *Microbiol. Mol. Biol. Rev.* 63, 266–292. doi: 10.1128/MMBR.63.2.266-292.1999

Benedetti, C. E., Xie, D., and Turner, J. G. (1995). COI1-dependent expression of an Arabidopsis vegetative storage protein in flowers and siliques and in response to coronatine or methyl jasmonate. *Plant Physiol.* 109, 567–572. doi: 10.1104/pp.109.2.567

Bleecker, A. B., and Kende, H. (2000). Ethylene: a gaseous signal molecule in plants. *Annu. Rev. Cell Dev. Biol.* 16, 1–18. doi: 10.1146/annurev.cellbio.16.1.1

Brader, G., Djamei, A., Teige, M., Palva, E. T., and Hirt, H. (2007). The MAP kinase kinase MKK2 affects disease resistance in Arabidopsis. *Mol. Plant Microbe Interact.* 20, 589–596. doi: 10.1094/MPMI-20-5-0589

Brooks, D. M., Hernández-Guzmán, G., Kloek, A. P., Alarcón-Chaidez, F., Sreedharan, A., Rangaswamy, V., et al. (2004). Identification and characterization of a well-defined series of coronatine biosynthetic mutants of *Pseudomonas syringae* pv. tomato DC3000. *Mol. Plant Microbe Interact.* 17, 162–174. doi: 10.1094/MPMI.2004.17.2.162

Czapski, J., and Saniewski, M. (1992). Stimulation of ethylene production and ethylene-forming enzyme activity in fruits of the non-ripening nor and

rin tomato mutants by methyl jasmonate. *J. Plant Physiol.* 139, 265–268. doi: 10.1016/S0176-1617(11)80334-2

Dixon, D. P., Lapthorn, A., and Edwards, R. (2002). Plant glutathione transferases. *Genome Biol.* 3:reviews3004. doi: 10.1186/gb-2002-3-3-reviews3004

Erb, M., and Kliebenstein, D. J. (2020). Plant secondary metabolites as defenses, regulators, and primary metabolites: the blurred functional trichotomy. *Plant Physiol.* 184, 39–52. doi: 10.1104/pp.20.00433

Ferguson, I., and Mitchell, R. (1985). Stimulation of ethylene production in bean leaf discs by the pseudomonad phytotoxin coronatine. *Plant Physiol.* 77, 969–973. doi: 10.1104/pp.77.4.969

Feys, B. J., Benedetti, C. E., Penfold, C. N., and Turner, J. G. (1994). Arabidopsis mutants selected for resistance to the phytotoxin coronatine are male sterile, insensitive to methyl jasmonate, and resistant to a bacterial pathogen. *Plant Cell* 6, 751–759. doi: 10.2307/3869877

Galán, J. E. (2009). Common themes in the design and function of bacterial effectors. *Cell Host Microbe* 5, 571–579. doi: 10.1016/j.chom.2009.04.008

Gao, J.-X., Yu, C.-J., Wang, M., Sun, J.-N., Li, Y.-Q., and Chen, J. (2017). Involvement of a velvet protein ClVelB in the regulation of vegetative differentiation, oxidative stress response, secondary metabolism, and virulence in *Curvularia lunata*. *Sci. Rep.* 7, 1–13. doi: 10.1038/srep46054

Gao, S., Li, Y., Gao, J., Suo, Y., Fu, K., Li, Y., et al. (2014). Genome sequence and virulence variation-related transcriptome profiles of *Curvularia lunata*, an important maize pathogenic fungus. *BMC Genomics* 15:627. doi: 10.1186/1471-2164-15-627

Geng, X., Cheng, J., Gangadharan, A., and Mackey, D. (2012). The coronatine toxin of *Pseudomonas syringae* is a multifunctional suppressor of *Arabidopsis defense*. *Plant Cell* 24, 4763–4774. doi: 10.1105/tpc.112.105312

Geng, X., Jin, L., Shimada, M., Kim, M. G., and Mackey, D. (2014). The phytotoxin coronatine is a multifunctional component of the virulence armament of Pseudomonas syringae . *Planta* 240, 1149–1165. doi: 10.1007/s00425-014-2151-x

Gfeller, A., Liechti, R., and Farmer, E. E. (2010). Arabidopsis jasmonate signaling pathway. *Sci. Signal.* 3:cm4. doi: 10.1126/scisignal.3109cm4

Glazebrook, J. (2005). Contrasting mechanisms of defense against biotrophic and necrotrophic pathogens. *Annu. Rev. Phytopathol.* 43, 205–227. doi: 10.1146/annurev.phyto.43.040204.135923

Greulichi, F., Yoshihara, T., and Ichihara, A. (1995). Coronatine, a bacterial phytotoxin, acts as a stereospecific analog of jasmonate type signals in tomato cells and potato tissues. *J. Plant Physiol.* 147, 359–366. doi: 10.1016/S0176-1617(11)82168-1

Guo, R., Shen, W., Qian, H., Zhang, M., Liu, L., and Wang, Q. (2013). Jasmonic acid and glucose synergistically modulate the accumulation of glucosinolates in *Arabidopsis thaliana*. *J. Exp. Bot.* 64, 5707–5719. doi: 10.1093/jxb/ert348

He, Y., Fukushige, H., Hildebrand, D. F., and Gan, S. (2002). Evidence supporting a role of jasmonic acid in Arabidopsis leaf senescence. *Plant Physiol.* 128, 876–884. doi: 10.1104/pp.010843

Ishiga, Y., Uppalapati, S. R., Ishiga, T., Elavarthi, S., Martin, B., and Bender, C. L. (2009). Involvement of coronatine-inducible reactive oxygen species in bacterial speck disease of tomato. *Plant Signal. Behav.* 4, 237–239. doi: 10.4161/psb.4.3.7915

Karpinski, S., Gabrys, H., Mateo, A., Karpinska, B., and Mullineaux, P. M. (2003). Light perception in plant disease defence signalling. *Curr. Opin. Plant Biol.* 6, 390–396. doi: 10.1016/S1369-5266(03)00061-X

Katsir, L., Schilmiller, A. L., Staswick, P. E., He, S. Y., and Howe, G. A. (2008). COI1 is a critical component of a receptor for jasmonate and the bacterial virulence factor coronatine. *Proc. Natl. Acad. Sci. U.S.A.* 105, 7100–7105. doi: 10.1073/pnas.0802332105

Keen, N., and Buzzell, R. (1991). New disease resistance genes in soybean against *Pseudomonas syringae* pv *glycinea*: evidence that one of them interacts with a bacterial elicitor. *Theor. Appl. Genet.* 81, 133–138. doi: 10.1007/BF00226123

Kenyon, J., and Turner, J. (1990). Physiological changes in *Nicotiana tabacum* leaves during development of chlorosis caused by coronatine. *Physiol. Mol. Plant Pathol.* 37, 463–477. doi: 10.1016/0885-5765(90)90037-X

Kenyon, J. S., and Turner, J. G. (1992). The stimulation of ethylene synthesis in *Nicotiana tabacum* leaves by the phytotoxin coronatine. *Plant Physiol.* 100, 219–224. doi: 10.1104/pp.100.1.219

Keppler, L. D., and Baker, C. J. (1989). O_2-initiated lipid peroxidation in a bacteria-induced hypersensitive reaction in tobacco cell suspensions. *Phytopathology* 79, 555–562. doi: 10.1094/phyto-79-555

Kim, D., Langmead, B., and Salzberg, S. L. (2015). HISAT: a fast spliced aligner with low memory requirements. *Nat. Methods* 12, 357–360. doi: 10.1038/nmeth.3317

Lamb, C., and Dixon, R. A. (1997). The oxidative burst in plant disease resistance. *Annu. Rev. Plant Biol.* 48, 251–275. doi: 10.1146/annurev.arplant.48.1.251

Lund, S. T., Stall, R. E., and Klee, H. J. (1998). Ethylene regulates the susceptible response to pathogen infection in tomato. *Plant Cell* 10, 371–382. doi: 10.2307/3870595

Mecey, C., Hauck, P., Trapp, M., Pumplin, N., Plovanich, A., Yao, J., et al. (2011). A critical role of STAYGREEN/Mendel's I locus in controlling disease symptom development during *Pseudomonas syringae* pv tomato infection of Arabidopsis. *Plant Physiol.* 157, 1965–1974. doi: 10.1104/pp.111.181826

Mewis, I., Tokuhisa, J. G., Schultz, J. C., Appel, H. M., Ulrichs, C., and Gershenzon, J. (2006). Gene expression and glucosinolate accumulation in *Arabidopsis thaliana* in response to generalist and specialist herbivores of different feeding guilds and the role of defense signaling pathways. *Phytochemistry* 67, 2450–2462. doi: 10.1016/j.phytochem.2006.09.004

Mittler, R. (2002). Oxidative stress, antioxidants and stress tolerance. *Trends Plant Sci* 7, 405–410. doi: 10.1016/S1360-1385(02)02312-9

Mittler, R., Vanderauwera, S., Gollery, M., and Van Breusegem, F. (2004). Reactive oxygen gene network of plants. *Trends Plant Sci.* 9, 490–498. doi: 10.1016/j.tplants.2004.08.009

Mur, L. A. J., Aubry, S., Mondhe, M., Kingstonsmith, A. H., Gallagher, J., Timmstaravella, E., et al. (2010). Accumulation of chlorophyll catabolites photosensitizes the hypersensitive response elicited by *Pseudomonas syringae* in Arabidopsis. *New Phytol.* 188, 161–174. doi: 10.1111/j.1469-8137.2010.03377.x

Palmer, D., and Bender, C. (1995). Utrastructure of tomato leaf tissue treated with the pseudomonad phytotoxin coronatine and comparison with methyl jasmonate. *Mol. Plant Microbe Interact.* 8, 683–692. doi: 10.1094/MPMI-8-0683

Rio, D. C., Ares, M., Hannon, G. J., and Nilsen, T. W. (2010). Purification of RNA using TRIzol (TRI reagent). *Cold Spring Harb. Protoc.* 2010:pdb.prot5439. doi: 10.1101/pdb.prot5439

Stall, R., and Hall, C. (1985). Chlorosis and ethylene production in pepper leaves infected by *Xanthomonas campestris* pv. vesicatoria. *Phytopathology* 74, 373–375.

Staswick, P. E., Huang, J.-F., and Rhee, Y. (1991). Nitrogen and methyl jasmonate induction of soybean vegetative storage protein genes. *Plant Physiol.* 96, 130–136. doi: 10.1104/pp.96.1.130

Sudhakar, C., Lakshmi, A., and Giridarakumar, S. (2001). Changes in the antioxidant enzyme efficacy in two high yielding genotypes of mulberry (*Morus alba* L.) under NaCl salinity. *Plant Sci.* 161, 613–619. doi: 10.1016/S0168-9452(01)00450-2

Takamiya, K.-I., Tsuchiya, T., and Ohta, H. (2000). Degradation pathway (s) of chlorophyll: what has gene cloning revealed? *Trends Plant Sci.* 5, 426–431. doi: 10.1016/S1360-1385(00)01735-0

Ueda, J., and Kato, J. (1980). Isolation and identification of a senescence-promoting substance from wormwood (*Artemisia absinthium* L.). *Plant Physiol.* 66, 246–249. doi: 10.1104/pp.66.2.246

Uppalapati, S. R., Ayoubi, P., Weng, H., Palmer, D. A., Mitchell, R. E., Jones, W., et al. (2005). The phytotoxin coronatine and methyl jasmonate impact multiple phytohormone pathways in tomato. *Plant J.* 42, 201–217. doi: 10.1111/j.1365-313X.2005.02366.x

Vick, B. A., and Zimmerman, D. C. (1984). Biosynthesis of jasmonic acid by several plant species. *Plant Physiol.* 75, 458–461. doi: 10.1104/pp.75.2.458

Winkel-Shirley, B. (2001). Flavonoid biosynthesis. A colorful model for genetics, biochemistry, cell biology, and biotechnology. *Plant Physiol.* 126, 485–493. doi: 10.1104/pp.126.2.485

Wojakowska, A., Muth, D., Narozna, D., Madrzak, C., Stobiecki, M., and Kachlicki, P. (2013). Changes of phenolic secondary metabolite profiles in the reaction of narrow leaf lupin (*Lupinus angustifolius*) plants to infections with *Colletotrichum lupini* fungus or treatment with its toxin. *Metabolomics* 9, 575–589. doi: 10.1007/s11306-012-0475-8

Wrather, J. A., Anderson, T., Arsyad, D., Gai, J., Ploper, L., Porta-Puglia, A., et al. (1997). Soybean disease loss estimates for the top 10 soybean producing countries in 1994. *Plant Dis.* 81, 107–110. doi: 10.1094/PDIS.1997.81.1.107

Xie, Z., Duan, L., Tian, X., Wang, B., Eneji, A. E., and Li, Z. (2008). Coronatine alleviates salinity stress in cotton by improving the antioxidative defense system and radical-scavenging activity. *J. Plant Physiol.* 165, 375–384. doi: 10.1016/j.jplph.2007.06.001

Yu, C., Fan, L., Wu, Q., Fu, K., Gao, S., Wang, M., et al. (2014). Biological role of Trichoderma harzianum-derived platelet-activating factor acetylhydrolase (PAF-AH) on stress response and antagonism. *PLoS ONE* 9:e100367. doi: 10.1371/journal.pone.0100367

Zhang, Z., Zhang, X., Hu, Z., Wang, S., Zhang, J., Wang, X., et al. (2015). Lack of K-dependent oxidative stress in cotton roots following coronatine-induced ROS accumulation. *PLoS ONE* 10:e0126476. doi: 10.1371/journal.pone.0126476

Zhao, Y., Jones, W., Sutherland, P., Palmer, D., Mitchell, R., Reynolds, P., et al. (2001). Detection of the phytotoxin coronatine by ELISA and localization in infected plant tissue. *Physiol. Mol. Plant Pathol.* 58, 247–258. doi: 10.1006/pmpp.2001.0334

Zheng, X. Y., Spivey, N. W., Zeng, W., Liu, P. P., Fu, Z. Q., Klessig, D. F., et al. (2012). Coronatine promotes *Pseudomonas syringae* virulence in plants by activating a signaling cascade that inhibits salicylic acid accumulation. *Cell Host Microbe* 11, 587–596. doi: 10.1016/j.chom.2012.04.014

Zou, J., Rodriguez-Zas, S., Aldea, M., Li, M., Zhu, J., Gonzalez, D. O., et al. (2005). Expression profiling soybean response to *Pseudomonas syringae* reveals new defense-related genes and rapid HR-specific downregulation of photosynthesis. *Mol. Plant Microbe Interact.* 18, 1161–1174. doi: 10.1094/MPMI-18-1161

Conflict of Interest: The authors declare that the research was conducted in the absence of any commercial or financial relationships that could be construed as a potential conflict of interest.

frontiers in Sustainable Food Systems

ORIGINAL RESEARCH
published: 14 May 2021
doi: 10.3389/fsufs.2021.675177

Genome Identification and Expression Analysis of GRAS Family Related to Development, Hormone and Pathogen Stress in *Brachypodium distachyon*

Zejun Tang[1,2†], *Na Song*[1,2†], *Weiye Peng*[1,2], *Yang Yang*[1,2], *Tian Qiu*[1,2], *Chenting Huang*[1,2], *Liangying Dai*[1,2*] *and Bing Wang*[1,2*]

[1] Hunan Provincial Key Laboratory for Biology and Control of Plant Diseases and Insect Pests, Hunan Agricultural University, Changsha, China, [2] College of Plant Protection, Hunan Agricultural University, Changsha, China

OPEN ACCESS

Edited by:
Wen Xie,
Chinese Academy of Agricultural Sciences, China

Reviewed by:
Yong Liu,
Hunan Academy of Agricultural Sciences (CAAS), China
Suprasanna Penna,
Bhabha Atomic Research Centre (BARC), India

***Correspondence:**
Bing Wang
zhufu@hunau.edu.cn
Liangying Dai
daily@hunau.net

[†] *These authors have contributed equally to this work*

Specialty section:
This article was submitted to Agroecology and Ecosystem Services, a section of the journal Frontiers in Sustainable Food Systems

Received: *02 March 2021*
Accepted: *12 April 2021*
Published: *14 May 2021*

Citation:
Tang Z, Song N, Peng W, Yang Y, Qiu T, Huang C, Dai L and Wang B (2021) Genome Identification and Expression Analysis of GRAS Family Related to Development, Hormone and Pathogen Stress in Brachypodium distachyon. Front. Sustain. Food Syst. 5:675177. doi: 10.3389/fsufs.2021.675177

GRAS transcription factors are widely present in the plant kingdom and play important roles in regulating multiple plant physiological processes. *Brachypodium distachyon* is a model for grasses for researching plant-pathogen interactions. However, little is known about the *BdGRAS* family genes involved in plant response to biotic stress. In this study, we identified 63 genes of the GRAS family in *B. distachyon*. The phylogenetic analysis showed that *BdGRAS* genes were divided into ten subfamilies and unevenly distributed on five chromosomes. qRT-PCR results showed that the *BdGRAS* family genes were involved in the growth and development of *B. distachyon*. Moreover, the expression of the HAM subfamily genes of *BdGRAS* changed during the interaction between *B. distachyon* and *Magnaporthe oryzae*. Interestingly, *BdGRAS31* in the HAM subfamily was regulated by miR171 after inoculation with *M. oryzae*. These results provide insight into the potential functions of the *BdGRAS* family in disease resistance.

Keywords: GRAS family, transcription factor, *Brachypodium distachyon*, *Magnaporthe oryzae*, HAM subfamily

INTRODUCTION

The GRAS protein family is an important transcription factor family named after the function of three members: Gibberellic acid insensitive (GAI), Repressor of GAI (RGA), and Scarecrow (SCR; Chen et al., 2019). Genome-wide analysis of the family showed that GRAS genes are also widely distributed in the plant kingdom (Tian et al., 2004). GRAS proteins typically consist of 400–700 amino acids. The sequences at the C-terminus are highly conserved and are divided into five conserved motifs: LHRI, VHIID, LHRII, PFYRE, and SAW (Pysh et al., 1999; Tian et al., 2004). VHIID, PFYRE, and SAW are important for maintaining the structural stability and function of GRAS proteins (Itoh et al., 2002; Smit et al., 2005; Hofmann, 2016; Li et al., 2016); the VHIID sequence can interact with other proteins (Gao et al., 2004). LHRI and VHIID have abundant leucine repeats, which affect protein dimerization. The N-terminal sequence is highly variable and can be used as bait in molecular research activities (Tian et al., 2004). Some GRAS proteins contain the DELLA domain, which plays important roles in gibberellin signaling (Silverstone et al., 1998).

The GRAS family is widely involved in regulating plant growth and development, including gibberellin signaling (Peng et al., 1997; Ikeda et al., 2001; Hirsch and Oldroyd, 2009), formation of

axillary meristems (Greb et al., 2003; Li et al., 2006), root radial patterning (Helariutta et al., 2000), photosensitive signal transduction (Bolle et al., 2000), and male gametogenesis (Morohashi et al., 2003). For example, two GRAS proteins are required for root rot formation in legumes (Kaló et al., 2005; Heckmann et al., 2006). Moreover, the GRAS family has been shown to participate in the hormone signaling pathway that regulates plant growth and development (Davière and Achard, 2016; Van De Velde et al., 2017). DELLA proteins also participate in the signaling pathways of auxin, brassinosteroids (BRs), abscisic acid (ABA), and ethylene (Chen et al., 2019). *AtSCL3* (an *Arabidopsis thaliana* GRAS gene) mediates the gibberellic acid pathway by attenuating the DELLA repressors during root development (Heo et al., 2011). In addition, GRAS genes participate in the regulation of jasmonic acid (JA) signaling by interacting with the JAZ1 protein (repressor of JA signal pathway) (De Lucas et al., 2008; Feng et al., 2008; Hou et al., 2010).

GRAS genes also participate in the process of stress resistance. For example, the expression of *GRAS6*, *GRAS37*, *GRAS50*, *GRAS68*, and *GRAS69* was significantly induced in sweet potato under salt stress treatment (Chen et al., 2019). *OsGRAS23*-overexpressing plants demonstrated less H_2O_2 accumulation under antioxidant stress and enhanced drought resistance (Xu et al., 2015). Moreover, GRAS genes are involved in the interaction between plants and fungi. The GRAS transcription factor CIGR2 activates *OsHsf23* to cause hypersensitive cell death and inhibits excessive cell death in the incompatible interaction between rice (*Oryza sativa*) and *Magnaporthe oryzae* (Tanabe et al., 2016).

Brachypodium distachyon is a new model of gramineous plants and has a short growth cycle, small plant size, small genome, and easy growth. *B. distachyon* can be infected by *M. oryzae*, which causes rice blast, a devastating disease of rice. In the process of *M. oryzae* infecting *B. distachyon*, conidia first germinated and formed appressoriaand invaded epidermal cells. Invasive hyphae were found in the cells, and the hyphae continued to develop and spread to adjacent cells, causing cell death (Routledge et al., 2004). The infection process and symptoms developed on *B. distachyon* were very similar to those in rice, including the degree of occurrence, time of emergence, size of the lesions, and growth rate (Routledge et al., 2004).

In this study, we performed chromosomal mapping, constructed a phylogenetic tree, and performed gene structure analysis of the *BdGRAS* family. Furthermore, we analyzed the expression levels of *BdGRAS* family of *B. distachyon* after inoculation with *M.oryzae*. Our results will provide evidence for further study of GRAS gene function in disease resistance.

MATERIALS AND METHODS

Experimental Materials and Treatments

B. distachyon (Bd21-3 genotype) seeds were grown in the soil (nutrient soil and stone 1:1) in a greenhouse under a 16 h light/8 h dark photoperiod, at a constant temperature of 23°C and humidity of 60%. Two-month-old *B. distachyon* seedlings were used in the experiment (Wang et al., 2015). Four different *B. distachyon* tissues (roots, stems, leaves, and seeds) were used for total RNA extraction.

The seedlings were treated with jasmonic acid(JA100 μmol/mL), salicylic acid (SA, 100 μmol/mL), indoleacetic acid (IAA, 100 μmol/mL), and abscisic acid (ABA, 100 μmol/mL). Fifteen seedlings were used for each treatment. Three leaves from the treated samples were harvested at 0 and 1 h post-treatment (hpt).

The rice blast fungus (*M. oryzae*) strain RO1-1 was grown on an oat medium at 28°C in the light in an incubator. After 20 days, the spores were washed with sterile water and filtered through gauze. The seedlings were challenged with *M. oryzae* spore (1×10^5 spores mL^{-1}) by spraying (Wei et al., 2013). Inoculated leaves were harvested at 0, 24, and 48 h post inoculation (hpi).

Identification of *BdGRAS* Genes and Phylogenetic Analysis

All *B. distachyon* GRAS genes were derived from the Plant Transcription Factor Database (http://planttfdb.gao-lab.org/). The sequences of the GRAS genes of rice, wheat and *A. thaliana* for analysis of the phylogeny of the *BdGRAS* family were also obtained from the Plant Transcription Factor Database (**Supplementary Table 1**).

The protein sequences of the *BdGRAS, OsGRAS*, and *AtGRAS* family were analyzed to generate a phylogenetic tree using MEGA7.0 (Kumar et al., 2016). ClustalW was used for sequence alignment to infer the evolutionary history of multiple sequences. The neighbor-joining method was used to set the parameters to the P-distance model, and 1,000 bootstrap replicates were used to generate phylogenetic trees (Wu et al., 2021). We performed miRNA target analysis using the webtool psRNATarget (http://plantgrn.noble.org/psRNATarget/).

Analysis of Conserved Domains and Motifs for the Chromosomal Location of BdGRAS Protein

We used NCBI to search for each gene annotation in the *BdGRAS* family to confirm the specific location of each gene on the chromosome. The genetic map of the *BdGRAS* family was visualized using MapChart software. We used Multiple Em for Motif Elicitation Version 5.1.1 (MEME) (http://meme-suite.org/tools/meme) to analyze BdGRAS family motifs. For the analysis of the conserved motifs of BdGRAS family genes, we first used the NCBI Web CD-search Tool (https://www.ncbi.nlm.nih.gov/Structure/bwrpsb/bwrpsb.cgi) to predict the conserved domains of genes and then used TBtools to realize visualization. We also performed *cis*-acting regulatory element analysis, found the 2000 bp DNA promoter sequence upstream of the start site of each gene, and used PlangtCare (http://bioinformatics.psb.ugent.be/webtools/plantcare/html/).

RT-PCR and qRT-PCR Analysis

Total RNA (roots, stems, leaves and seeds, and leaves treated by hormone and rice blast) was extracted using TRIzol Reagent (Ambion, Waltham, USA). cDNA synthesis was performed using TranScript One-Step gDNA Removal and cDNA Synthesis

SuperMix (TransGen Biotech, Beijing, China) for RT-PCR (reverse transcription-polymerase chain reaction). The specific primers for *BdGRAS* family genes were designed using Primer5.0 (Singh et al., 1998) (**Supplementary Table 2**). The *BdUBC* gene (*Bradi4g00660*) was used as the internal reference. For PCR amplification, 2× EasyTaq PCR SuperMix (+dye) (TransGen Biotech, Beijing, China) was used. The reaction procedure was as follows: 94°C for 3 min, 34 cycles of 15 s at 94°C, 30 s at 56°C, and 72°C for 1 min (Chen et al., 2015).

First-strand cDNA was synthesized using the RevertAid First Stand cDNA Synthesis Kit (Thermo Fisher Scientific, Waltham, USA) for qRT-PCR. The qRT-PCR reaction sample adopts 20 μl systems, of which 10 μM forward and reverse primers are 0.4 μl each, TransStart Tip Green qPCR SuperMix 10 μl, template 2 μl, 7.2 μl ddH_2O. qRT-PCR conditions were as follows: 94°C for 1 min, 30 cycles (94°C for 20 s, 56°C for 15 s, and 1 min at 72°C), and 72°C for 5 min. qRT-PCR was performed using the CFX 96 qPCR instrument (BioRad, California, USA) (Tong et al., 2020). The *BdUBC* gene was used as the internal reference. Similar results were obtained from three biological replicates.

Transcriptional Activation Assay

The GRAS genes were constructed on the pGBKT7 vector and then transformed into AH109 yeast competent cells. Transformed cells were streaked onto SD/-Trp and SD/-Trp-His-Ade medium. The growth status of AH109 transformed cells was evaluated after incubation at 30°C for 2 days. Transformed cells (OD_{600} = 1.0) were tested on the selection medium (SD/-Trp and SD/-Trp-His-Ade medium). The α-galactosidase activity assay was performed using X-α-Gal as a substrate (Wang et al., 2018a).

RESULTS

Phylogenetic Evolution Analysis and Chromosome Location of GRAS Family

Through in *silico* prediction, 63 candidate *GRAS* genes were identified in *B. distachyon*. The proteins of the BdGRAS family ranged from 185 to 806 amino acids with molecular weights ranging from 30 to 89 kDa. The isoelectric point of BdGRAS was between 4.6 and 9.8, with an average of 6.7 (**Supplementary Table 3**). A phylogenetic tree was constructed using 60 *GRAS* genes from *B. distachyon*, 50 *GRAS* genes from *O. sativa*, and 33 *GRAS* genes from *A. thaliana*. Atypical *GRAS* family genes, including, 3 *BdGRAS* genes, 10 *OsGRAS* genes, and 1 *AtGRAS* gene, were also observed and were not included in the phylogenetic tree. The phylogenetic analysis showed they were divided into ten subfamilies, namely, DELLA, SCL3, SCL4/7, LAS, SCR, HAM, PAT1, SHR, DLT, and LISCL. Among these, the LISCL subfamily contained the greatest number of *BdGRAS* genes (11 members), the DLT subfamily contained only three genes. Moreover, 16 *BdGRAS* family genes were not classified into any subfamilies (**Figure 1A**). According to the clade support values and the classification of orthologs in wheat and *B. distachyon*. They can also be divided into 10 subfamilies using the phylogenetic analysis

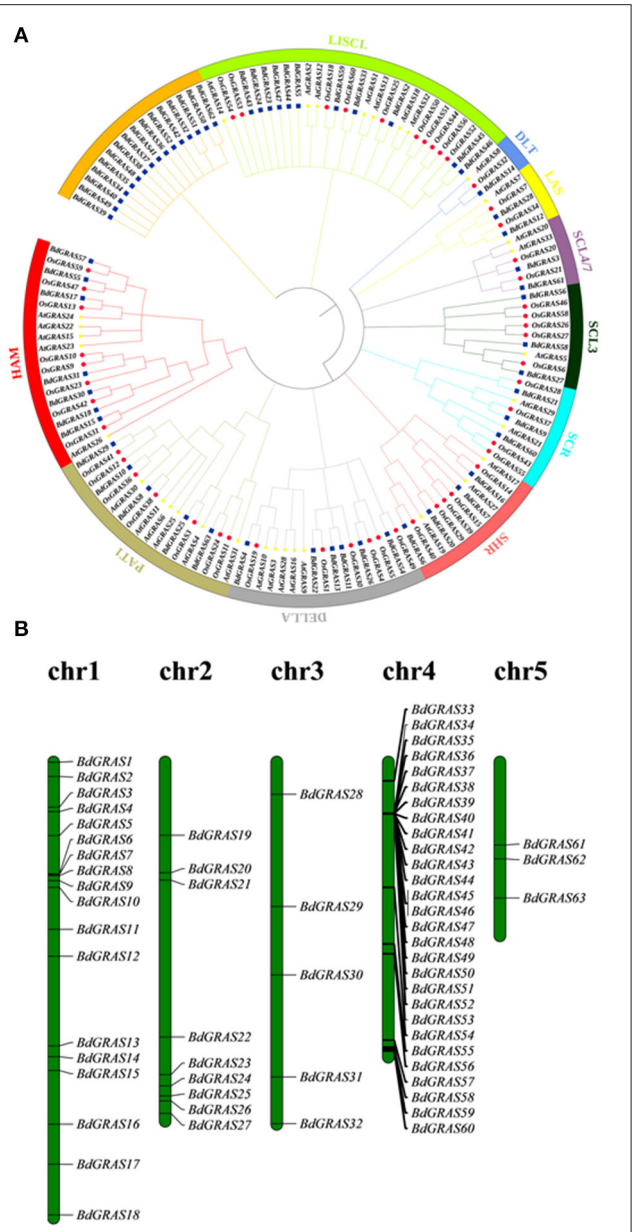

FIGURE 1 | Phylogenetic analysis of GRAS proteins in *Arabidopsis thaliana*, *Oryza sativa* and *Brachypodium distachyon* and chromosomal mapping of *GRAS* gene in *Brachypodium distachyon*. **(A)** The phylogenetic tree is divided into 10 different subfamilies, and the different subfamilies are shown with branches and outer ring of different colors. The blue solid square represents *B. distachyon* GRAS protein, the red solid circle represents *O. sativa* protein, and the yellow five-pointed star represents *Arabidopsis* protein. **(B)** Chromosomal locations of *GRAS* genes in *B. distachyon*.

(**Supplementary Figure 1**).These *BdGRAS* genes were unevenly distributed on five chromosomes. Chr4 contained the greatest number of *BdGRAS* genes ($n = 28$), followed by Chr1 ($n = 18$). Furthermore, nine genes were distributed on Chr2, and five genes were distributed on Chr3. Only three genes were distributed on Chr5 (**Figure 1B**).

B. distachyon GRAS Family Collinearity Analysis and Structural Domain Analysis

Protein domain analysis showed that most members contained typical GRAS regions (**Supplementary Figure 2**). In each subfamily, the amino acid sequences of BdGRAS proteins showed high homology. All BdGRAS proteins have five conserved motifs in the C-terminus, namely, LHRI, VHIID, LHRII, PFYRE, and SAW; meanwhile, the N-terminus of BdGRAS proteins was highly variable (**Figure 2B**). To compare the genetic relationship of *BdGRAS* in *B. distachyon*, we used TBtools to identify paralogous genes in the *B. distachyon* genome. Five pairs of homologous genes were identified in *BdGRAS*, indicating that *B. distachyon* has experienced genome replication events during evolution (**Figure 2A**). Through the analysis of the transcriptional regulation mechanism of *GRAS* gene, it is found that *BdGRAS* gene mainly involves 15 biological pathways, most of which are involved in stress response, such as low temperature and light signal. It has been detected that *BdGRAS* gene is related to hormones, such as salicylic acid and jasmonic acid (**Supplementary Figure 3**).

Expression Profiles of the *BdGRAS* Family Genes in Different Tissues and Hormone Treatments

We tested the expression levels of *BdGRAS* family genes in different tissues of *B. distachyon*, including the roots, stems, leaves, and seeds, by RT-PCR. It was found that most of the genes were identified in a wide range of tissues, such as *BdGRAS33*, *BdGRAS57*, and *BdGRAS58* (**Figure 3**). Moreover, some genes were highly expressed in some tissues. For instance, the expression of *BdGRAS34* to *BdGRAS40* was high in the roots and seeds. In contrast, the expression of *BdGRAS31* was low in the seeds.

We also investigated the expression levels of *BdGRAS* genes under four different hormone treatments by qRT-RCR (SA, JA, IAA, and ABA). The expression levels of *BdGRAS48*, *BdGRAS49*, *BdGRAS51*, *BdGRAS52*, and *BdGRAS55* significantly increased after SA hormone treatment at 1 hpt; *BdGRAS2*, *BdGRAS8*, *BdGRAS10*, *BdGRAS23*, *BdGRAS47*, and *BdGRAS59* were significantly induced after JA hormone treatment. Moreover, *BdGRAS47* expression levels significantly increased after ABA

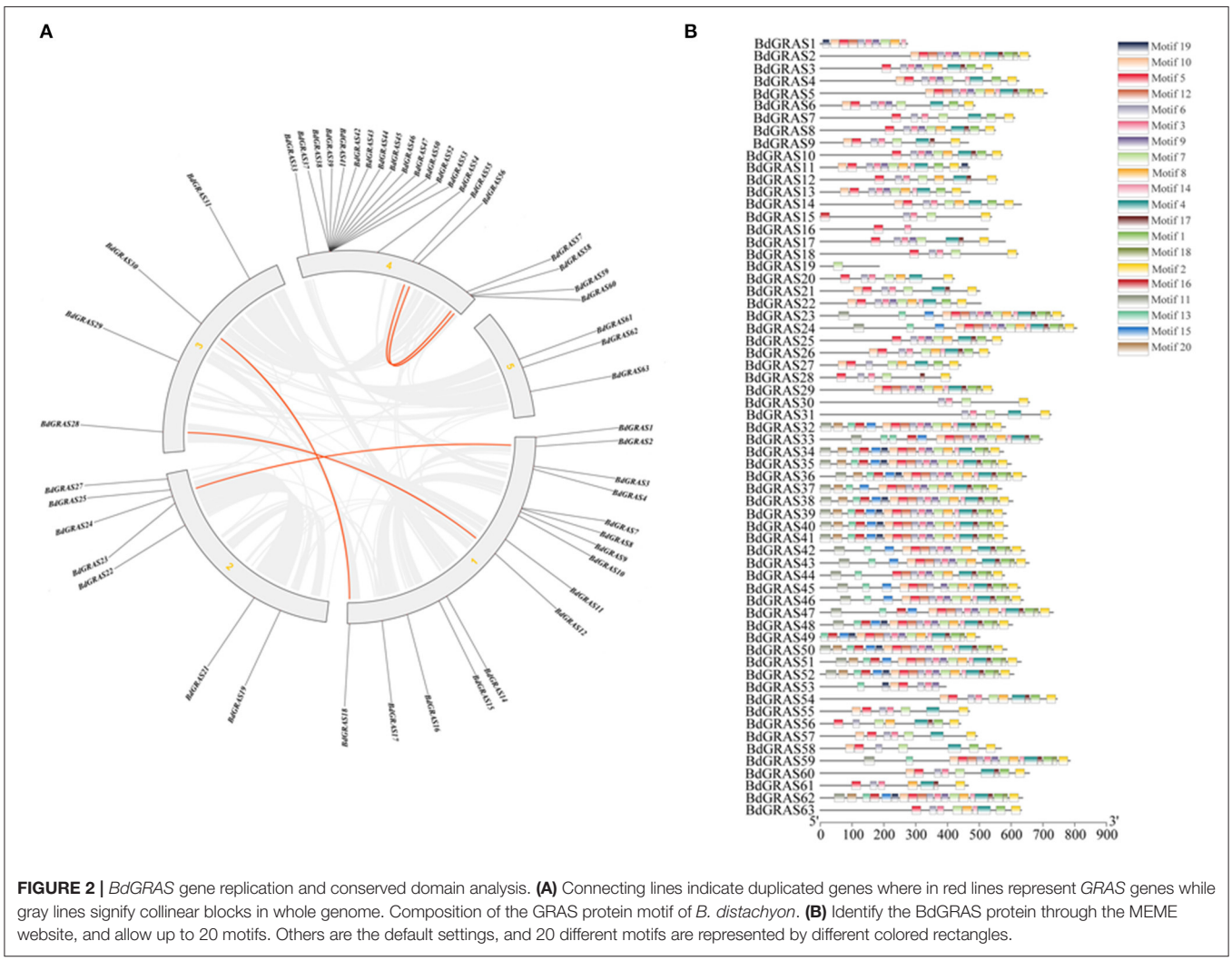

FIGURE 2 | *BdGRAS* gene replication and conserved domain analysis. **(A)** Connecting lines indicate duplicated genes where in red lines represent *GRAS* genes while gray lines signify collinear blocks in whole genome. Composition of the GRAS protein motif of *B. distachyon*. **(B)** Identify the BdGRAS protein through the MEME website, and allow up to 20 motifs. Others are the default settings, and 20 different motifs are represented by different colored rectangles.

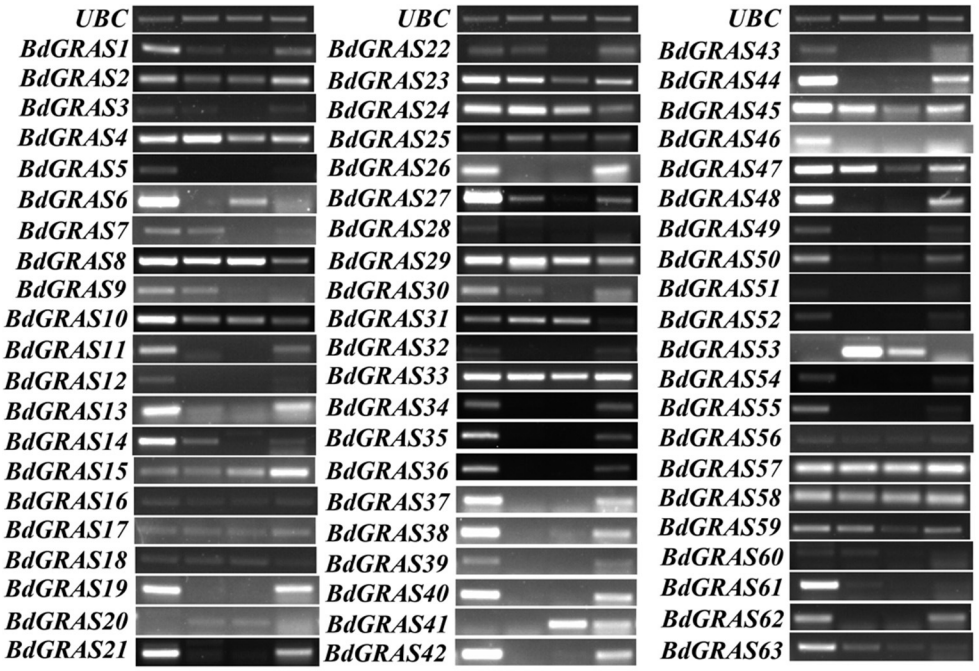

FIGURE 3 | The *GRAS* genes expression pattern in different tissues of *Brachypodium distachyon*. The expression level of the *BdGRAS* gene in the root, stem, leaf, and seeds of *B. distachyon*, using *UBC* as a control.

hormone treatment. After IAA treatment, the expression levels of most *GRAS* genes significantly reduced. The expression of *BdGRAS34*, *BdGRAS36*, *BdGRAS37*, *BdGRAS38*, *BdGRAS39*, *BdGRAS40*, *BdGRAS41*, *BdGRAS42*, and *BdGRAS45* was inhibited under all four different hormone treatments (**Figure 4**). These results indicated that the *GRAS* family genes participate in different hormone signaling pathways.

Expression Levels of *BdGRAS* Family Genes in *B. distachyon* and *M. oryzae* Interaction

To investigate the roles of *BdGRAS* genes in response to biotic stress, we analyzed the expression levels of *BdGRAS* genes in *B. distachyon* inoculated with *M. oryzae* RO1-1 at 0, 24, and 48 hpi. The results showed that the expression of *BdGRAS4*, *BdGRAS8*, *BdGRAS10*, *BdGRAS30*, and *BdGRAS31* gradually decreased after inoculation with *M. oryzae*. Moreover, expression levels of *BdGRAS2*, *BdGRAS9*, *BdGRAS18*, *BdGRAS23*, *BdGRAS33*, *BdGRAS34*, *BdGRAS47*, *BdGRAS48*, *BdGRAS49*, *BdGRAS51*, *BdGRAS52*, *BdGRAS57*, and *BdGRAS58* significantly increased at 24 hpi (**Figure 5**). These results indicate that the *BdGRAS* family participates in the interaction between *B. distachyon* and *M. oryzae,* and plays a role in the resistance of *B. distachyon* to rice blast.

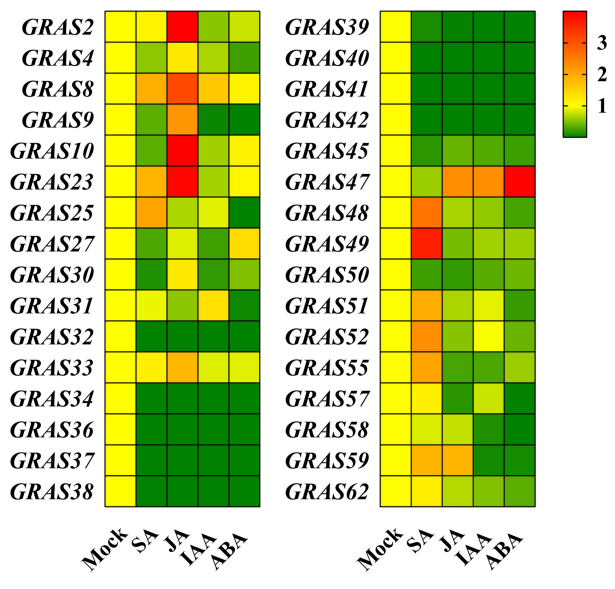

FIGURE 4 | *BdGRAS* genes transcription level expression analysis under different hormone treatments. The changes of *BdGRAS* genes expression levels in *B. distachyon* under salicylic acid (SA), jasmonic acid (JA), indoleacetic acid (IAA), and abscisic acid (ABA) treatments at 1 hpi. Green and red represent relatively low and high expression levels.

BdGRAS31 Is the Target of miR171 in *B. distachyon*

Some members of the *GRAS* gene family are potential regulatory targets of miRNAs. We predicted that 23 *BdGRAS* genes were targeted by six miRNA families (**Supplementary Table 4**). Furthermore, we identified that *BdGRAS15*, *BdGRAS18*, and

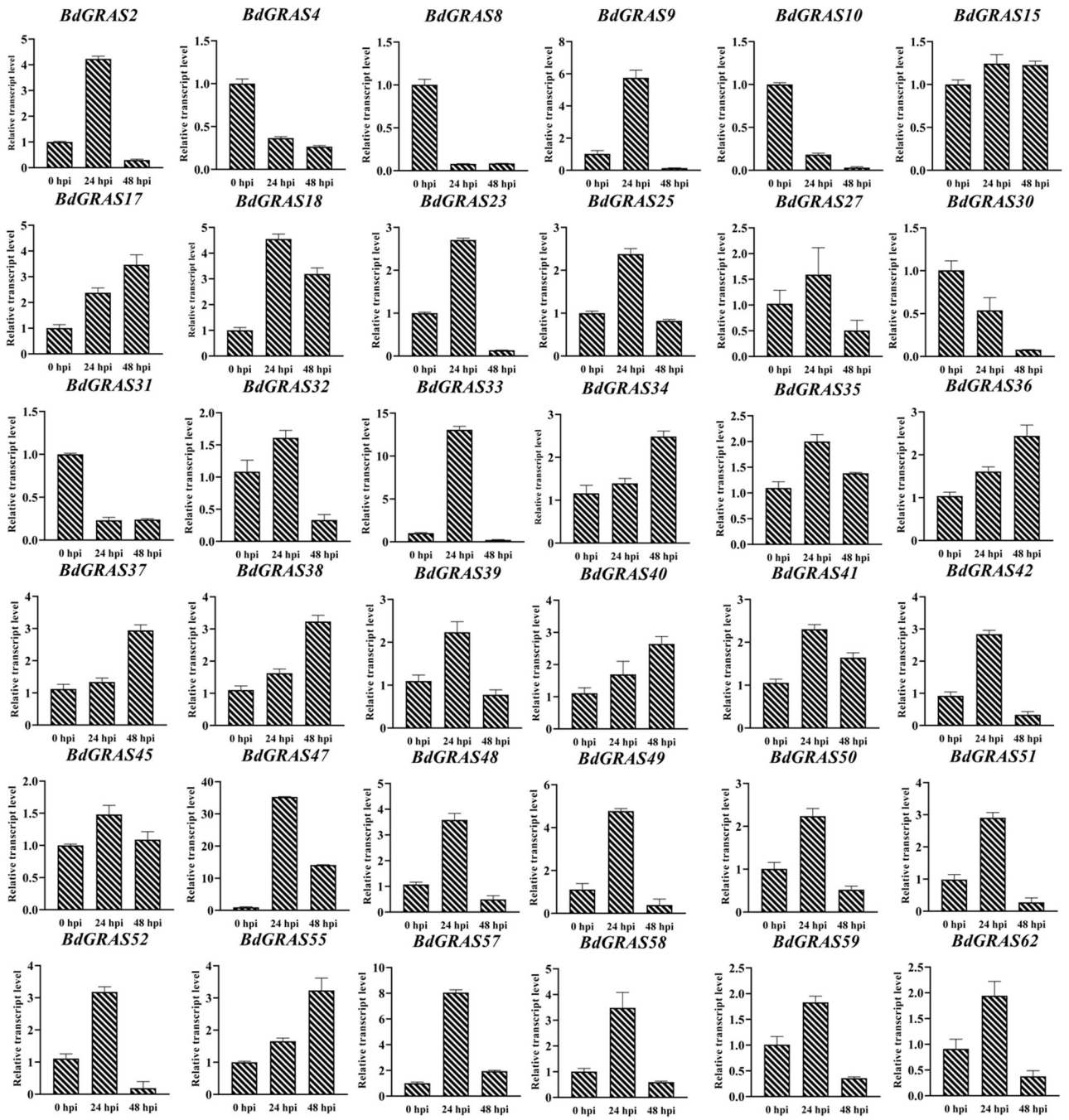

FIGURE 5 | qRT-PCR analysis of the expression pattern of *BdGRAS* gene after inoculation with *Magnaporthe oryzae*. The Y-axis is the relative expression of *BdGRAS* gene, and the X-axis is different time points after inoculation with *M. oryzae*, including 0, 24, and 48 hpi. *UBC* is used as an internal control (hour post inoculation, hpi).

BdGRAS31 were candidate targets of *Bd-miR171* by degradome deep sequencing (**Figure 6A**). We used qRT-PCR to detect the expression levels of the three candidate target genes and Bd-miR171 after inoculation with *M. oryzae* (**Figure 6B**). The expression of Bd-miR171 gradually increased within 48 hpi with RO1-1, while that of *BdGRAS31* gradually decreased within 48 hpi. The expression level of *BdGRAS15* did not change significantly, and the expression of *BdGRAS18* increased at 24 hpi and began to decrease at 48 hpi (**Supplementary Figure 4**). Therefore, we inferred that *BdGRAS31* is regulated by Bd-miR171 in the interactions between *B. distachyon* and *M. oryzae*.

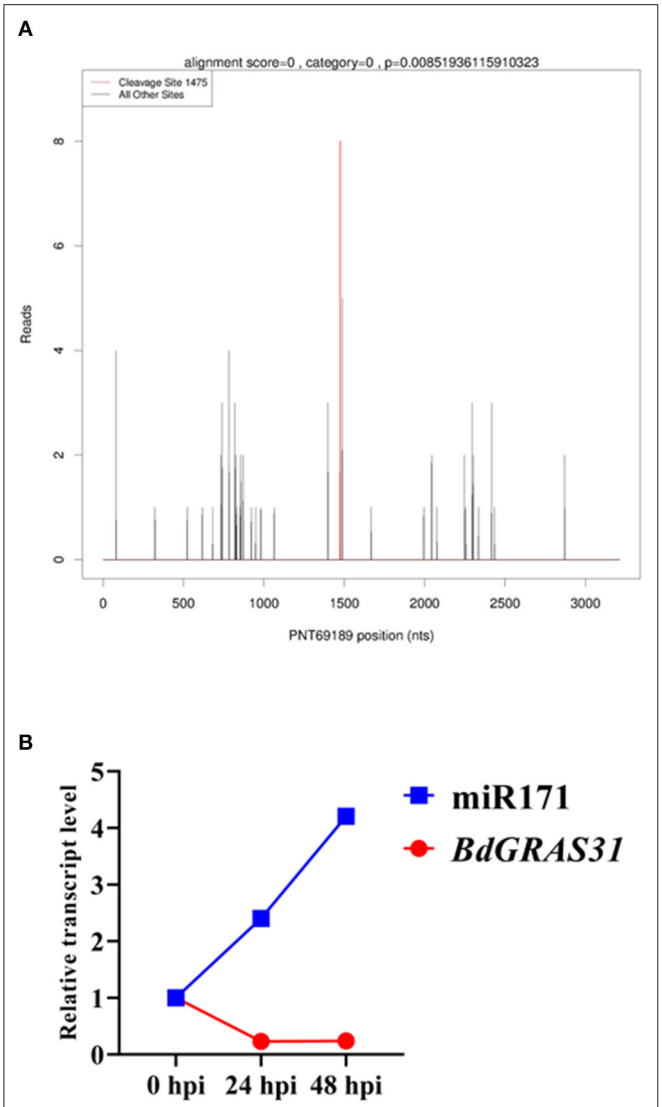

FIGURE 6 | *BdGRAS31* is the target gene of miR171. **(A)** Identification of *BdGRAS31* was the target of Bd-miR171 by degradome sequencing. **(B)** The expression of miR171 and *BdGRAS31* in *Brachypodium distachyon* after inoculation with *M. oryzae*.

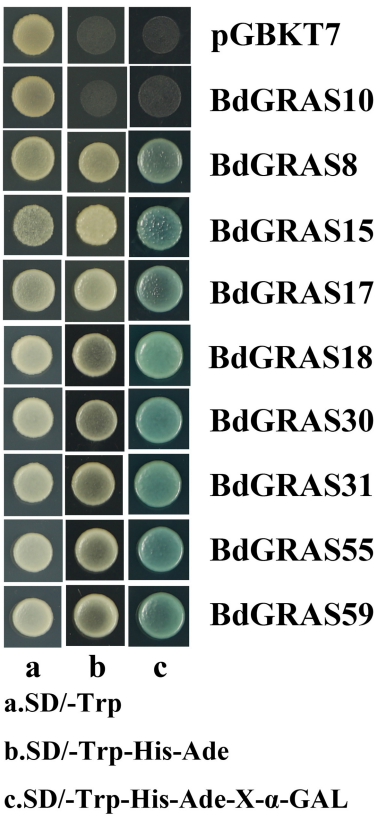

FIGURE 7 | Analysis of *Brachypodium distachyon* GRAS protein transcription activity.

Verification of Transcriptional Activity of *BdGRAS* Genes

To detect whether the *BdGRAS* family has transcriptional activity, we selected nine genes-*BdGRAS8*, *BdGRAS10*, *BdGRAS515*, *BdGRAS17*, *BdGRAS18*, *BdGRAS30*, *BdGRA31*, *BdGRA55*, and *BdGRA59* for testing transcriptional activation. It was found that eight transformants harboring *BdGRAS* genes could grow on SD/-Trp and SD/-Trp-His-Ade and turned blue on SD-Trp-His-Ade-X-α-GAL, indicating that BdGRAS8, BdGRAS15, BdGRAS17, BdGRAS18, BdGRAS30, BdGRA31, BdGRA55, and BdGRA59 show transcriptional activity (**Figure 7**). However, BdGRAS10 did not show transcriptional activity.

DISCUSSION

The GRAS family is an important plant-specific transcription factor family divided into multiple subfamilies (Bolle, 2004). Recent studies have divided the GRAS family into 10–17 subfamilies in multiple plants (Bolle, 2016; Wang et al., 2018b,c). It is reported there were 48 *BdGRAS* genes, which were divided into ten known subfamilies (Niu et al., 2019). In this study, 63 *BdGRAS* family genes were identified by domain analysis. The phylogenetic tree showed that *BdGRAS* family genes were divided into ten subfamilies according to their genetic relationship. Moreover, most *B. distachyon* GRAS genes are divided into the same clade as that of *Arabidopsis* or rice (Niu et al., 2019). For example, the LISCL subfamily contains 11 *BdGRAS* genes. The conserved function of putative orthologs in each subfamily was indicated by the functional characterization of GRAS proteins. Therefore, we inferred that *BdGRAS* genes are also involved in multiple plant physiological processes by different regulation.

Each subfamily of *GRAS* genes has specific functions in plant development (Chen et al., 2019). For example, in *Lilium longiflorum,* the *LISCL* gene is involved in regulating microsporogenesis (Morohashi et al., 2003). The LISCL subfamily members were identified in a wide range of tissues in *Brassica napus* (Guo et al., 2019). The HAM subfamily

is considered to play an important role in the growth and development of root tips, stem tips, and shoot apex meristem (Stuurman et al., 2002). In this study, we identified some *LISCL* genes, such as *BdGRAS2*, *BdGRAS23*, *BdGRAS45*, and *BdGRAS59*, in multiple tissues. Moreover, we found that members of the HAM subfamily showed differences in tissue expression. *BdGRAS55* is only highly expressed in roots. Therefore, the results suggested that *BdGRAS* genes play an important role in controlling the growth and development of *B. distachyon*.

Multiple plant physiological processes are regulated by a diverse group of hormones (Huang et al., 2015). IAA is involved in almost all aspects of plant growth and development. JA and SA play important roles in biotic stresses. The *HcSCL13* gene of *Halostachys Caspica* was overexpressed in *Arabidopsis*, under the treatment of hormone ABA, the *HcSCL13* gene was induced rapidly, reached the highest peak at 1 h, and then decreased to the control level (Zhang et al., 2020). In the potato, the expression levels of *StGRAS34*, *StGRAS36*, and *StGRAS46* are increased under the treatment of IAA, ABA, and GA_3 hormones (Wang et al., 2019). In this study, we observed that *BdGRAS47* expression increased significantly under ABA and IAA treatment; this gene may play important roles in plant development. Moreover, the expression of *BdGRAS2*, *BdGRAS8*, *BdGRAS10*, *BdGRAS23*, and *BdGRAS47* increased significantly under JA treatment. The expression of *BdGRAS48*, *BdGRAS49*, *BdGRAS51*, *BdGRAS52*, and *BdGRAS55* significantly increased after SA treatment. These results suggest that *BdGRAS* genes may be involved in the plant response to biotic stress.

GRAS genes play important roles in the plant response to pathogens. For example, *VviRGA5* is upregulated in grape berries at the initial stage of fungal infection (Agudelo-Romero et al., 2014). *SlGRAS1* is involved in the plant response to biotic stress (Mayrose et al., 2006). CIGR2 negatively regulated resistance to *M. oryzae* in rice (Tanabe et al., 2016). In this study, the expression levels of 28 *BdGRAS* genes changed after inoculation with rice blast fungus. We found that the expression levels of most members of the HAM subfamily, including *BdGRAS17*, *BdGRAS18*, *BdGRAS55*, and *BdGRAS57*, increased significantly after inoculation with *M. oryzae*, while the expression levels of *BdGRAS30* and *BdGRAS31* significantly decreased. In *B. napus*, HAM subfamilies comprise two clades and perform different functions (Guo et al., 2019). We inferred that *BdGRAS* genes of HAM subfamilies may play multiply function in *B. distachyon* and *M. oryzae* interaction. Moreover, HAM genes are candidate targets of miR171 (Fan et al., 2015). We found 4 HAM subfamilies genes as candidate targets of Bd-miR171, and confirmed that *BdGRAS31* could be regulated by degradome deep sequencing and qRT-PCR. We also identified the transcriptional activity of the members of *GRAS* genes. Most *BdGRAS* genes showed transcriptional activity, except *BdGRAS10*. These results suggested that *BdGRAS* regulated target genes through multiple approaches.

In this study, we found that the HAM subfamily of *BdGRAS* genes may play essential roles in disease resistance. These results provide a basis for further research on the *BdGRAS* family and also provide a reference for the study of disease resistance and stress resistance of grasses.

DATA AVAILABILITY STATEMENT

The data presented in the study are deposited in the Plant Transcription Factor Database (http://planttfdb.gao-lab.org/index.php) repository, accession number Bradi1g00219.1.p-Bradi5g19190.1.p; LOC_Os01g45860-LOC_Os12g38490; AT1G07520-AT5G67411; TRAES3BF021600230CFD_t1-Traes_7DL_44FCA17C4.1, see **Supplementary Table 1** for details.

AUTHOR CONTRIBUTIONS

ZT and NS are the experimental designers and executors of the experimental research, completing data analysis, and writing the first draft of the paper. WP, YY, TQ, and CH participated in the experimental design and analysis of the experimental results. LD and BW are the creators and leaders of the project, directing experimental design, data analysis, thesis writing, and revision.

FUNDING

This study was supported by grants from the National Natural Science Foundation of China (31801721; 31672017), National Key Research and Development Project (2016YFD0200800; 2016YFD0300707), the Natural Science Foundation of Hunan Province, China (2020JJ5240), the Scientific Research Fund of Hunan Provincial Education Department (19B247), Commonweal Plan Project of Ningbo City (202002N3004), and the Youth Fund Project of Hunan Agricultural University (19QN31).

SUPPLEMENTARY MATERIAL

The Supplementary Material for this article can be found online at: https://www.frontiersin.org/articles/10.3389/fsufs.2021.675177/full#supplementary-material

Supplementary Figure 1 | Phylogenetic analysis of GRAS proteins in *Triticum aestivum* and *Brachypodium distachyon*.

Supplementary Figure 2 | The composition of the GRAS protein domain of *Brachypodium distachyon*. Green represents the GRAS domain, yellow represents the GRAS superfamily domain, pink represents the DELLA domain, and blue represents the PA28_alpha superfamily domain.

Supplementary Figure 3 | *Brachypodium distachyon* GRAS *cis*-acting regulatory element analysis.

Supplementary Figure 4 | The expression level of candidate targets of Bd-miR171.

Supplementary Table 1 | GRAS family genes in wheat, rice and *Arabidopsis thaliana*.

Supplementary Table 2 | *Brachypodium distachyon GRAS* family genes specific primers for qRT-PCR and RT-PCR analysis.

Supplementary Table 3 | Parameters of *Brachypodium distachyon GRAS* family genes.

Supplementary Table 4 | Prediction of target RNA of GRAS family in *Brachypodium distachyon*.

REFERENCES

Agudelo-Romero, P., Ali, K., Choi, Y. H., Sousa, L., Verpoorte, R., Tiburcio, A. F., et al. (2014). Perturbation of polyamine catabolism affects grape ripening of Vitis vinifera cv. *Trincadeira*. *Plant Physiol. Biochem.* 74, 141–155. doi: 10.1016/j.plaphy.2013.11.002

Bolle, C. (2016). Structure and evolution of plant GRAS family proteins. *Plant Transcription Factors* 153–161. doi: 10.1016/B978-0-12-800854-6.00010-5

Bolle, C. (2004). The role of GRAS proteins in plant signal transduction and development. *Planta* 218, 683–692. doi: 10.1007/s00425-004-1203-z

Bolle, C., Koncz, C., and Chua, N. H. (2000). PAT1, a new member of the GRAS family, is involved in phytochrome A signal transduction. *Genes Dev.* 14, 1269–1278. doi: 10.1101/gad.14.10.1269

Chen, H., Li, H., Lu, X., Chen, L., Liu, J., and Wu, H. (2019). Identification and expression analysis of GRAS transcription factors to elucidate candidate genes related to stolons, fruit ripening and abiotic stresses in woodland strawberry (*Fragaria vesca*). *Int. J. Mol. Sci.* 20:4593. doi: 10.3390/ijms20184593

Chen, Y. Q., Tai, S. S., Wang, D. W., Ding, A. M., Sun, T. T., Wang, W. F., et al.(2015). Homology-based analysis of the GRAS gene family in tobacco. *Genet. Mol. Res.* 14, 15188–15200. doi: 10.4238/2015.November.25.7

Davière, J. M., and Achard, P. (2016). A pivotal role of DELLAs in regulating multiple hormone signals. *Mol. Plant* 9, 10–20. doi: 10.1016/j.molp.2015.09.011

De Lucas, M., Daviere, J. M., Rodríguez-Falcón, M., Pontin, M., Iglesias-Pedraz, J. M., Lorrain, S., et al. (2008). A molecular framework for light and gibberellin control of cell elongation. *Nature* 451, 480–484. doi: 10.1038/nature06520

Fan, T., Li, X., Yang, W., Xia, K., Ouyang, J., and Zhang, M. (2015). Rice osa-miR171c mediates phase change from vegetative to reproductive development and shoot apical meristem maintenance by repressing four OsHAM transcription factors. *PLoS ONE* 10:e0125833. doi: 10.1371/journal.pone.0125833

Feng, S., Martinez, C., Gusmaroli, G., Wang, Y., Zhou, J., Wang, F., et al. (2008). Coordinated regulation of *Arabidopsis thaliana* development by light and gibberellins. *Nature* 451, 475–479. doi: 10.1038/nature06448

Gao, M. J., Parkin, I., Lydiate, D., and Hannoufa, A. (2004). An auxin-responsive SCARECROW-like transcriptional activator interacts with histone deacetylase. *Plant Mol. Biol.* 55, 417–431. doi: 10.1007/s11103-004-0892-9

Greb, T., Clarenz, O., Schäfer, E., Müller, D., Herrero, R., Schmitz, G., et al. (2003). Molecular analysis of the *LATERAL SUPPRESSOR* gene in *Arabidopsis* reveals a conserved control mechanism for axillary meristem formation. *Genes Dev.* 17, 1175–1187. doi: 10.1101/gad.260703

Guo, P., Wen, J., Yang, J., Ke, Y., Wang, M., Liu, M., et al. (2019). Genome-wide survey and expression analyses of the *GRAS* gene family in *Brassica napus* reveals their roles in root development and stress response. *Planta* 250, 1051–1072. doi: 10.1007/s00425-019-03199-y

Heckmann, A. B., Lombardo, F., Miwa, H., Perry, J. A., Bunnewell, S., Parniske, M., et al. (2006). *Lotus japonicus* nodulation requires two GRAS domain regulators, one of which is functionally conserved in a non-legume. *Plant Physiol.* 142, 1739–1750. doi: 10.1104/pp.106.089508

Helariutta, Y., Fukaki, H., Wysocka-Diller, J., Nakajima, K., Jung, J., Sena, G., et al. (2000). The *SHORT-ROOT* gene controls radial patterning of the *Arabidopsis* root through radial signaling. *Cell* 101, 555–567. doi: 10.1016/S0092-8674(00)80865-X

Heo, J. O., Chang, K. S., Kim, I. A., Lee, M. H., Lee, S. A., Song, S. K., et al. (2011). Funneling of gibberellin signaling by the GRAS transcription regulator scarecrow-like 3 in the *Arabidopsis* root. *Proc. Natl. Acad. Sci. U.S.A.* 108, 2166–2171. doi: 10.1073/pnas.1012215108

Hirsch, S., and Oldroyd, G. E. (2009). GRAS-domain transcription factors that regulate plant development. *Plant Signal. Behav.* 4, 698–700. doi: 10.4161/psb.4.8.9176

Hofmann, N. R. (2016). A structure for plant-specific transcription factors. *Plant Cell* 28, 993–994. doi: 10.1105/tpc.16.00309

Hou, X., Lee, L. Y. C., Xia, K., Yan, Y., and Yu, H. (2010). DELLAs modulate jasmonate signaling via competitive binding to JAZs. *Dev. Cell* 19, 884–894. doi: 10.1016/j.devcel.2010.10.024

Huang, W., Xian, Z., Kang, X., Tang, N., and Li, Z. (2015). Genome-wide identification, phylogeny and expression analysis of *GRAS* gene family in tomato. *BMC Plant Biol.* 15, 1–18. doi: 10.1186/s12870-015-0590-6

Ikeda, A., Ueguchi-Tanaka, M., Sonoda, Y., Kitano, H., Koshioka, M., Futsuhara, Y., et al. (2001). *slender* rice, a constitutive gibberellin response mutant, is caused by a null mutation of the *SLR1* gene, an ortholog of the height-regulating gene *GAI/RGA/RHT/D8*. *Plant Cell* 13, 999–1010. doi: 10.1105/tpc.13.5.999

Itoh, H., Ueguchi-Tanaka, M., Sato, Y., Ashikari, M., and Matsuoka, M. (2002). The gibberellin signaling pathway is regulated by the appearance and disappearance of SLENDER RICE1 in nuclei. *Plant Cell* 14, 57–70. doi: 10.1105/tpc.010319

Kaló, P., Gleason, C., Edwards, A., Marsh, J., Mitra, R. M., Hirsch, S., et al. (2005). Nodulation signaling in legumes requires NSP2, a member of the GRAS family of transcriptional regulators. *Science* 308, 1786–1789. doi: 10.1126/science.1110951

Kumar, S., Stecher, G., and Tamura, K. (2016). MEGA7: molecular evolutionary genetics analysis version 7.0 for bigger datasets. *Mol. Biol. Evol.* 33, 1870–1874. doi: 10.1093/molbev/msw054

Li, S., Zhao, Y., Zhao, Z., Wu, X., Sun, L., Liu, Q., et al. (2016). Crystal structure of the GRAS domain of SCARECROW-LIKE7 in *Oryza sativa*. *Plant Cell* 28, 1025–1034. doi: 10.1105/tpc.16.00018

Li, X., Duan, X., Jiang, H., Sun, Y., Tang, Y., Yuan, Z., et al. (2006). Genome-wide analysis of basic/helix-loop-helix transcription factor family in rice and *Arabidopsis*. *Plant Physiol.* 141, 1167–1184. doi: 10.1104/pp.106.080580

Mayrose, M., Ekengren, S. K., Melech-Bonfil, S. H. I. R. I., Martin, G. B., and Sessa, G. (2006). A novel link between tomato *GRAS* genes, plant disease resistance and mechanical stress response. *Mol. Plant Pathol.* 7, 593–604. doi: 10.1111/j.1364-3703.2006.00364.x

Morohashi, K., Minami, M., Takase, H., Hotta, Y., and Hiratsuka, K. (2003). Isolation and characterization of a novel *GRAS* gene that regulates meiosis-associated gene expression. *J. Biol. Chem.* 278, 20865–20873. doi: 10.1074/jbc.M301712200

Niu, X., Chen, S., Li, J., Liu, Y., Ji, W., and Li, H. (2019). Genome-wide identification of *GRAS* genes in *Brachypodium distachyon* and functional characterization of *BdSLR1* and *BdSLRL1*. *BMC Genomics* 20, 1–18. doi: 10.1186/s12864-019-5985-6

Peng, J., Carol, P., Richards, D. E., King, K. E., Cowling, R. J., Murphy, G. P., et al. (1997). The *Arabidopsis GAI* gene defines a signaling pathway that negatively regulates gibberellin responses. *Genes Dev.* 11, 3194–3205. doi: 10.1101/gad.11.23.3194

Pysh, L. D., Wysocka-Diller, J. W., Camilleri, C., Bouchez, D., and Benfey, P. N. (1999). The *GRAS* gene family in *Arabidopsis*: sequence characterization and basic expression analysis of the *SCARECROW-LIKE* genes. *Plant J.* 18, 111–119. doi: 10.1046/j.1365-313X.1999.00431.x

Routledge, A. P., Shelley, G., Smith, J. V., Talbot, N. J., Draper, J., and Mur, L. A. (2004). *Magnaporthe grisea* interactions with the model grass *Brachypodium distachyon* closely resemble those with rice (*Oryza sativa*). *Mol. Plant Pathol.* 5, 253–265. doi: 10.1111/j.1364-3703.2004.00224.x

Silverstone, A. L., Ciampaglio, C. N., and Sun, T. P. (1998). The *Arabidopsis RGA* gene encodes a transcriptional regulator repressing the gibberellin signal transduction pathway. *Plant Cell* 10, 155–169. doi: 10.1105/tpc.10.2.155

Singh, V. K., Mangalam, A. K., Dwivedi, S., and Naik, S. (1998). Primer premier: program for design of degenerate primers from a protein sequence. *Biotechniques* 24, 318–319. doi: 10.2144/98242pf02

Smit, P., Raedts, J., Portyanko, V., Debellé, F., Gough, C., Bisseling, T., et al. (2005). NSP1 of the GRAS protein family is essential for rhizobial Nod factor-induced transcription. *Science* 308, 1789–1791. doi: 10.1126/science.1111025

Stuurman, J., Jäggi, F., and Kuhlemeier, C. (2002). Shoot meristem maintenance is controlled by a *GRAS*-gene mediated signal from differentiating cells. *Genes Dev.* 16, 2213–2218. doi: 10.1101/gad.230702

Tanabe, S., Onodera, H., Hara, N., Ishii-Minami, N., Day, B., Fujisawa, Y., et al. (2016). The elicitor-responsive gene for a GRAS family protein, *CIGR2*, suppresses cell death in rice inoculated with rice blast fungus via activation of a heat shock transcription factor, *OsHsf23*. *Biosci. Biotechnol. Biochem.* 80, 145–151. doi: 10.1080/09168451.2015.1075866

Tian, C., Wan, P., Sun, S., Li, J., and Chen, M. (2004). Genome-wide analysis of the *GRAS* gene family in rice and *Arabidopsis*. *Plant Mol. Biol.* 54, 519–532. doi: 10.1023/B:PLAN.0000038256.89809.57

Tong, J., Walk, T. C., Han, P., Chen, L., Shen, X., Li, Y., et al. (2020). Genome-wide identification and analysis of high-affinity nitrate transporter 2 (*NRT2*) family genes in rapeseed (*Brassica napus L.*) and their responses to various stresses. *BMC Plant Biol.* 20, 1–16. doi: 10.1186/s12870-020-02648-1

Van De Velde, K., Ruelens, P., Geuten, K., Rohde, A., and Van Der Straeten, D. (2017). Exploiting DELLA signaling in cereals. *Trends Plant Sci.* 22, 880–893. doi: 10.1016/j.tplants.2017.07.010

Wang, B., Wei, J., Song, N., Wang, N., Zhao, J., and Kang, Z. (2018a). A novel wheat NAC transcription factor, *TaNAC30*, negatively regulates resistance of wheat to stripe rust. *J. Integrative Plant Biol.* 60, 432–443. doi: 10.1111/jipb.12627

Wang, L., Hu, W., Sun, J., Liang, X., Yang, X., Wei, S., et al. (2015). Genome-wide analysis of *SnRK* gene family in *Brachypodium distachyon* and functional characterization of *BdSnRK2. 9*. *Plant Sci.* 237, 33–45. doi: 10.1016/j.plantsci.2015.05.008

Wang, M., Xu, Z., Ding, A., and Kong, Y. (2018b). Genome-wide identification and expression profiling analysis of the xyloglucan endotransglucosylase/hydrolase gene family in tobacco (*Nicotiana tabacum L.*). *Genes* 9:273. doi: 10.3390/genes9060273

Wang, S., Zhang, N., Zhu, X., Yang, J., Li, S., Che, Y., et al. (2019). Identification and expression analysis of *StGRAS* gene family in potato (*Solanum tuberosum L.*). *Comput. Biol. Chem.* 80, 195–205. doi: 10.1016/j.compbiolchem.2019.03.020

Wang, Y. X., Liu, Z. W., Wu, Z. J., Li, H., Wang, W. L., Cui, X., et al. (2018c). Genome-wide identification and expression analysis of GRAS family transcription factors in tea plant (*Camellia sinensis*). *Sci. Rep.* 8, 1–19. doi: 10.1038/s41598-018-22275-z

Wei, T., Ou, B., Li, J., Zhao, Y., Guo, D., Zhu, Y., et al. (2013). Transcriptional profiling of rice early response to *Magnaporthe oryzae* identified OsWRKYs as important regulators in rice blast resistance. *PLoS ONE* 8:e59720. doi: 10.1371/journal.pone.0059720

Wu, J., Liu, H., Lu, S., Hua, J., and Zou, B. (2021). Identification and expression analysis of chloroplast ribonucleoproteins (*cpRNPs*) in *Arabidopsis* and rice. *Genome* 99, 1–10. doi: 10.1139/gen-2020-0007

Xu, K., Chen, S., Li, T., Ma, X., Liang, X., Ding, X., et al. (2015). *OsGRAS23*, a rice GRAS transcription factor gene, is involved in drought stress response through regulating expression of stress-responsive genes. *BMC Plant Biol.* 15, 1–13. doi: 10.1186/s12870-015-0532-3

Zhang, S., Li, X., Fan, S., Zhou, L., and Wang, Y. (2020). Overexpression of *HcSCL13*, a *Halostachys caspica* GRAS transcription factor, enhances plant growth and salt stress tolerance in transgenic *Arabidopsis*. *Plant Physiol. Biochem.* 151, 243–254. doi: 10.1016/j.plaphy.2020.03.020

Conflict of Interest: The authors declare that the research was conducted in the absence of any commercial or financial relationships that could be construed as a potential conflict of interest.

frontiers in Sustainable Food Systems

ORIGINAL RESEARCH
published: 29 June 2021
doi: 10.3389/fsufs.2021.697864

A Comparison of Flower and Grass Strips for Augmentation of Beneficial Arthropods in Apple Orchards

Zhaoke Dong[1], Mengjing Xia[2], Cheng Li[2], Baofeng Mu[2] and Zhiyong Zhang[2]**

[1] College of Plant Health and Medicine, Qingdao Agricultural University, Qingdao, China, [2] Beijing Key Laboratory of New Technology in Agricultural Application, Beijing University of Agriculture, Beijing, China

Sowing plants that provide food resources in orchards is a potential habitat management practice for enhancing biological control. Flowering plants (providing pollen and nectar) and grasses (providing alternative prey) can benefit natural enemies in orchards; however, little is known about their relative importance. We studied the effect of management practices (flower strips, grass strips, and spontaneous grass) on arthropod predators under organic apple management regimes in apple orchards in Beijing, China. Orchards located at two different sites were assessed for 3 years (2017–2019). The cover crops had a significant impact on the abundance and diversity of arthropod predators. The grass treatment consistently supported significantly greater densities of alternative prey resources for predators, and predators were more abundant in the grass than in the other treatments. The Shannon–Wiener diversity was significantly higher for the cover crop treatment than for the control. Community structure was somewhat similar between the grass and control, but it differed between the flower treatment and grass/control. Weak evidence for an increase in mobile predators (ladybirds and lacewings) in the orchard canopy was found. Ladybirds and lacewings were more abundant in the grass treatment than in the other treatments in 2019 only, while the aphid abundance in the grass treatment was lowest. The fact that grass strips promoted higher predator abundance and stronger aphid suppression in comparison to the flower strips suggests that providing alternative prey for predators has great biocontrol service potential. The selection of cover crops and necessary management for conserving natural enemies in orchards are discussed in this paper.

Keywords: cover crops, understory, habitat management, strip sown, predator, conservation biological control

OPEN ACCESS

Edited by:
Fang Ouyang,
Institute of Zoology, Chinese Academy of Sciences (CAS), China

Reviewed by:
Hongying Cui,
China Agricultural University, China
Weiyi He,
Fujian Agriculture and Forestry University, China

****Correspondence:***
Zhiyong Zhang
zzy@bua.edu.cn
Zhaoke Dong
zhaoke_dong@126.com

Specialty section:
This article was submitted to Agroecology and Ecosystem Services, a section of the journal Frontiers in Sustainable Food Systems

Received: *20 April 2021*
Accepted: *03 June 2021*
Published: *29 June 2021*

Citation:
Dong Z, Xia M, Li C, Mu B and Zhang Z (2021) A Comparison of Flower and Grass Strips for Augmentation of Beneficial Arthropods in Apple Orchards. Front. Sustain. Food Syst. 5:697864. doi: 10.3389/fsufs.2021.697864

INTRODUCTION

Agriculture intensification has led to the loss of ecological heterogeneity, consequently threatening farmland biodiversity (Benton et al., 2003). Implementing management practices that increase agricultural biodiversity is important for mediating the negative impacts of intensive agriculture. At landscape scales, diversified landscapes hold the most potential for the conservation of biodiversity and sustaining pest control function (Bianchi et al., 2006). At local scales, the allocation of habitats to enhance local diversity in agroecosystems may compensate for local high-intensity management (Tscharntke et al., 2005). To enhance pest control, habitats have been managed to conserve natural enemies (Tscharntke et al., 2007; Fiedler et al., 2008; Isaacs et al., 2009). Habitat management that

intentionally conserves non-crop habitats and establishes flower strips can reduce pest density by enhancing functional biodiversity and associated ecosystem services (Landis et al., 2000; Gurr et al., 2017; Lundin et al., 2019).

Orchards are susceptible to damage by a wide range of arthropod pests. Moreover, orchards are often characterized by an intense use of pesticides. The reduced pesticide use in organic orchards can reduce disturbance intensity and promote arthropod predators (Galloway et al., 2021). Predators and parasitoids that are natural enemies of orchard pests can potentially suppress pests to below damaging levels if they are present in sufficient numbers at the appropriate time. The potential for ecosystem services provided by natural enemies has been highlighted in orchards (Simon et al., 2010). Creating diversified hedgerows and cover crops in alleys or the understory may improve the level of biodiversity and ecosystem services (Demestihas et al., 2017). Previous studies have confirmed the role of functional agrobiodiversity as a means of potentially reducing insecticide use in orchards (Cahenzli et al., 2019; Penvern et al., 2019), and manipulating orchard habitat vegetation to promote natural enemies is a pest management practice that has gained increasing interest in recent decades.

Cover crops, grass cover, ecological infrastructures, flowering plants, island habitats, and hedgerows have been used to boost natural enemy diversity and abundance in orchards (Bugg and Waddington, 1994; English-Loeb et al., 2003; Fernández et al., 2008; Bone et al., 2009; Geldenhuys et al., 2021). However, the agroecological principles and practical applications are poorly understood (Duru et al., 2015), and thus scientific support and experiential knowledge could help in the design of diversified farming systems and landscapes.

The selection of optimal plant species for the promotion of natural predators is based on information on the ecological mechanisms of how they benefit the predators. Based on their functions and characteristics, cover crops can be divided into two types: (1) flowering plants that provide pollen and nectar (Gontijo et al., 2013; Lu et al., 2014), and (2) grass plants that provide alternative prey/hosts (Wyss, 1996; Gomez-Marco et al., 2016). Floral resources could benefit the longevity and fecundity of predators (Robinson et al., 2008; He et al., 2021) and also increase the natural enemy assemblages (Cloyd, 2020). However, few studies have considered both criteria when selecting suitable cover plants. The choice of optimal plants for use as cover crops in orchards should be considered a key decision that requires adequate research at the local scale. A comparison of the effects of grass strips and flower strips is necessary, as their performance in the same orchard is not known.

The aim of this study was to evaluate the potential effects of flower strips and grass strips on natural enemies and aphid pests in apple orchards in North China. We conducted a 3-year field experiment in apple orchards by sowing two types of cover crops, including flower strips sown with marigold (*Tagetes erecta*) and China aster (*Callistephus chinensis*) and grass strips sown with alfalfa (*Medicago sativa*) and ryegrass (*Lolium perenne*). Marigold is a fragrant plant species that has been tested as a cover crop in apple orchards (Song and Han, 2020). We also added an untested flowering plant, namely China aster, to the flower strips. The selection of ryegrass was based on its supply of alternative prey for ladybirds in field crops (Dong et al., 2012), and alfalfa is also reported as a traditional cover crop (Yan et al., 1997). Our primary objective was to evaluate the performance of these crops on the conservation of natural enemies and aphid suppression.

MATERIALS AND METHODS

Site Descriptions and Experimental Design

The study was carried out in two commercial organic apple orchards. One orchard was located in Yanqing district (Beijing city, 116°6′ 5″ E, 40°35′38″ N) in North China, which consisted of 12-year-old trees. In this orchard, field experiments were conducted during 2017 and 2018. The other orchard was located in Changping district (Beijing city, 116°7′50″ E, 40°12′59″ N) in North China, consisting of 5-year-old trees, where the study was conducted in 2019. Both sites had <700 mm mean annual rainfall.

At Yanqing, the study area was ∼3.4 ha (68 m long, 50 m wide). There were three treatments with four replicates per treatment, arranged in a randomized block design. Each plot was 283 m^2. Apple trees of the "Guoguang" variety were planted with a tree spacing of 5 × 1.8 m. At Changping, three replicates of each of three treatments were established in a randomized block design. The study area in the Changping orchard was ∼1.2 ha (40 m long, 30 m wide). Each plot was 135 m^2 and included the apple cultivar "Red Fuji" planted in five rows, with row distances of 3 m and a distance of 1 m between single trees.

Flower mixture and grass mixture were sown in the between-row space at each site (**Figure 1**). Seeds of the flowers (marigold and China aster) and grasses (alfalfa and ryegrass) were separately mixed with garden sand to ease handling and distribution. These mixes were drilled manually in the spring of 2017, 2018, and 2019 (**Table 1**). The area within tree rows was left natural. The weed management was according to the local practices. The naturally growing wild grass underneath the trees was mowed three times per year in spring and summer. In the control (CK) plots, the native vegetation consisted mainly of four species: *Echinochloa crus-galli, Setaria viridis, Artemisia lavandulaefolia,* and *Rorippa dubia*. The percentage of ground cover was assessed every month during the plant growing season in one of the between-row spaces of each assessment plot.

Arthropod Sampling and Monitoring

To assess the influence of treatments on natural enemies in the cover crops and tree canopy, two approaches were used: sweep netting (38 cm diameter) and yellow sticky cards (240 × 100 mm). The sweep net was used to sample arthropods fortnightly in the cover crops. Thirty sweeps in each plot were conducted on each sample date. The sampled arthropods were delivered to the laboratory and identified to the species or genus level based on morphological characteristics. Sticky trap sampling was repeated over 5 months from June through October, with sticky traps placed out for the first week of each month. Yellow sticky cards were suspended on the branches at a height of 1.5 m. The main observed predators were ladybirds and

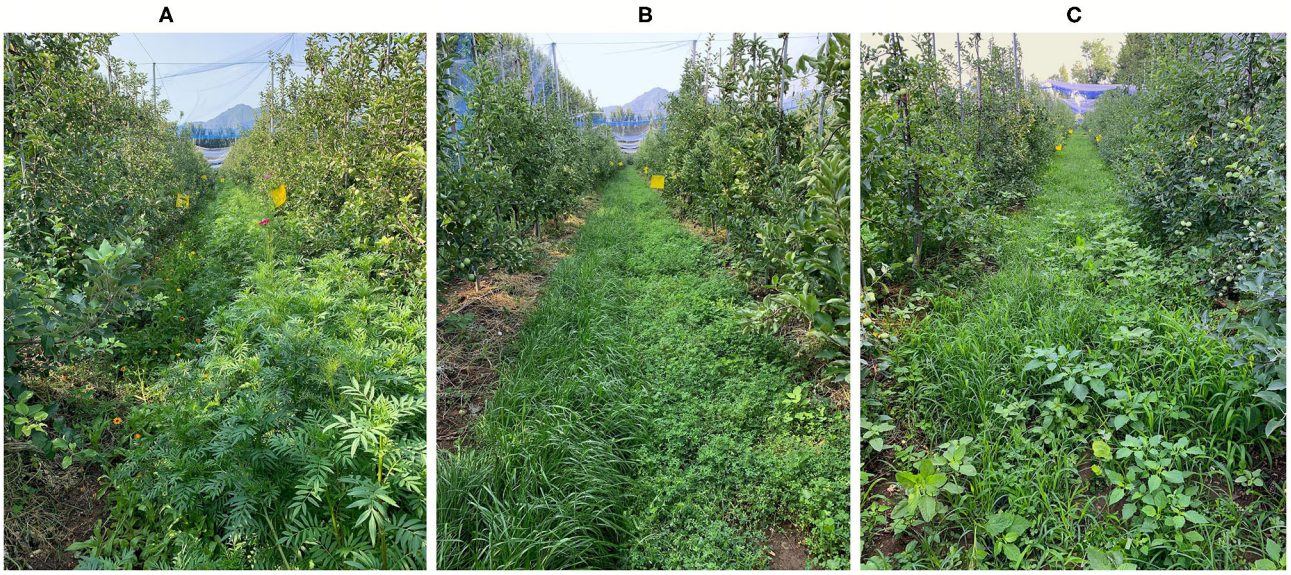

FIGURE 1 | Example of the cover plants in the three treatments: the sown flower strip **(A)**, the sown grass strip **(B)**, and the control **(C)**.

TABLE 1 | Date of cover crop planting and percent area occupied by cover crops in the between-row space of orchards in Yanqing and Changping at 8 weeks after planting (July).

	Date of crop planting			Coverage (%)		
	2017	2018	2019	2017	2018	2019
Control	–	–	–	92.8 ± 4.2	61.7 ± 12.8	74.0 ± 0.0
Flower	May 6	May 23	April 29	47.0 ± 3.3	74.4 ± 5.5	100.0 ± 0.0
Grass	May 6	May 23	April 29	67.3 ± 6.1	57.2 ± 6.1	100.0 ± 0.0

Dashes indicate that the plants in the control plots were spontaneous.

lacewings. Some hoverflies were also seen but were not included in the analysis due to their low numbers.

Aphid density on the tree leaves was measured by directly searching for aphids each week. Within each plot, four apple trees were selected at random as sampling points, and each tree was sampled from four directions (east, south, west, and north). On each side of the tree, 20 leaves were observed, and the numbers of aphids and natural enemies (ladybirds and lacewings) were recorded. However, the densities of ladybirds and lacewings detected on the leaves were low, and therefore these data were not analyzed further.

Data Analysis

Arthropod abundance and percentage of plant cover are presented as means ± standard error of the mean. All of the statistical analyses were completed using R 3.6.3 (R Core Team, 2020).

To determine whether crop type affected the composition of the predator community, we used non-metric multidimensional scaling (NMDS, based on Bray-Curtis dissimilarity) with the *vegan* package (Oksanen et al., 2020). The assemblages of arthropod predators were compared between the plots with cover and the controls by PERMANOVA using the adonis function, and the Euclidean distances were calculated using the vegdist function; these two functions are available in the *vegan* package. The Shannon–Wiener diversity index of predators for each sample date was calculated using the total number of captures of each of the taxa using the diversity function in the *vegan* package. Linear mixed-effects models (LMMs) in the *lme4* package (Bates et al., 2015) were used to estimate the effect of the cover crops on the Shannon–Wiener diversity index. Sampling date was introduced in the models as a random factor.

To determine if crop type affected arthropod abundances in cover crops, we used general linear mixed effects models (GLMM) fitted to a poisson distribution. The models included the abundance of total predators (or each group of predators) as dependent variables and year as fixed effects, with date as a random effect. The χ^2- and *P*-values were obtained using the ANOVA function in the *car* package (Fox and Weisberg, 2019). We then used the glht function in the package *multcomp* (Hothorn et al., 2008) for *post-hoc* pairwise comparisons. The effects of cover crops on the aphid abundance on apple tree leaves and herbivore in cover crops were also tested using GLMM with a poisson distribution. Each response variable (aphid and herbivores) included the data of 2017 and 2019. The data of aphid

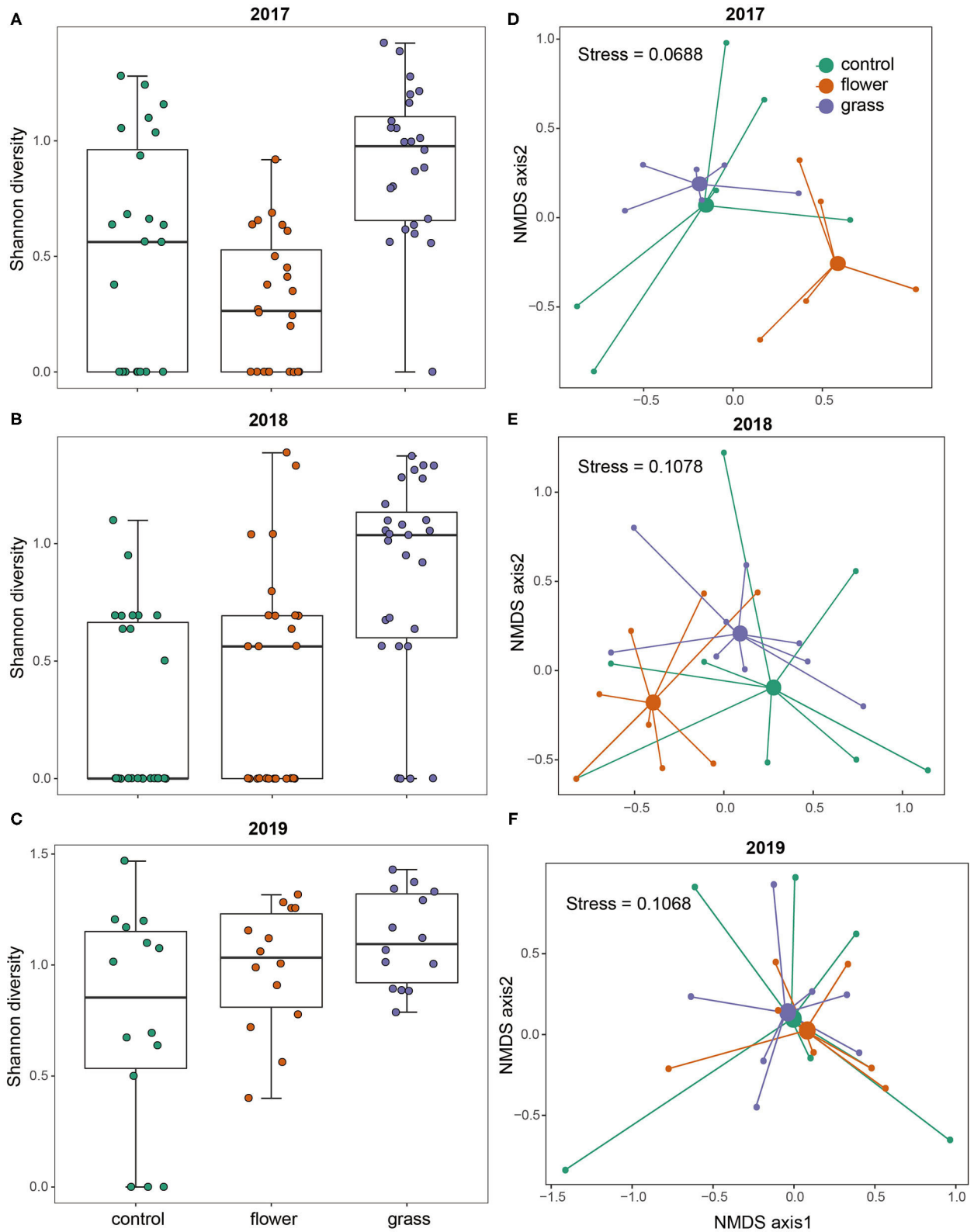

FIGURE 2 | Diversity and community structure of the predators in the control, flower, and grass cover plants during the 3 years (2017–2019). Each year is presented separately: 2017 **(A,D)**, 2018 **(B,E),** and 2019 **(C,F)**. NMDS plots are presented based on Bray–Curtis similarity.

and herbivores in 2018 was not available because no specific counting was recorded.

RESULTS

Percentage of Ground Cover

The cover crop planting dates varied among the 3 years. The planting date in 2019 was a week earlier than in 2017 and 3 weeks earlier than in 2018. The cover crop percentage increased as the growing season progressed. Eight weeks after planting, the mean percentage of cover crops almost exceeded 50.0% and varied across the 3 years (**Table 1**). In contrast to the coverage in 2017 and 2018, the percentage of cover crops in 2019 had already reached 100.0% after 8 weeks.

Predator Community and Abundance

Overall, we observed arthropod predators in the cover crops from four different families. The observed predators included ladybirds (Coccinellidae), lacewings (Chrysopidae), hoverflies (Syrphidae), and spiders (mainly Philodromidae). The complete list of dominant species can be read in in the **Supplementary Table 1**.

The two-dimensional NMDS plots of the predator community in 2017, 2018, and 2019 had stress values of 0.069, 0.108, and 0.107, respectively (**Figure 2**). The PERMANOVA analysis indicated that the community composition in 2017 varied significantly among treatments ($P = 0.001$). The *post-hoc* analysis indicated that communities occurring in the three treatments differed from one another (flower vs. grass: $P = 0.045$, grass vs. control: $P = 0.006$, flower vs. control: $P = 0.018$). The community composition in 2018 also differed significantly among treatments ($P = 0.002$). *Post-hoc* analysis indicated that communities occurring in the flowers differed from the control ($P = 0.036$) and grass ($P = 0.009$), while the control and grass did not differ from each other ($P = 0.081$). In 2019, the community composition was not affected by treatment ($P = 0.739$).

Predator diversity varied significantly with treatment ($\chi^2 = 63.803$, df = 2, $P < 0.0001$) and year ($\chi^2 = 19.837$, df = 2, $P < 0.0001$). The mean predator diversity was higher in the grass treatment than in the flower and control treatments. Through analyzing the data in each year separately, the *post-hoc* tests showed that predator diversity in the grass was consistently higher than in the control in the 3 years (all $P < 0.001$, **Figure 2**). On the contrary, the flower treatment had a similar predator diversity with the control in the 3 years (all $P > 0.05$, **Figure 2**).

Treatment and year significantly affected predator abundances (**Table 2**). The results from the *post-hoc* tests showed that the abundances of total predators were highest in the grass, followed by the flowers, and lowest in the control (**Figure 3C**). The interactions of treatment and year were significant in most cases (**Table 2**). Both the grass and flower treatments possessed more predators than the control. Hoverflies, lacewings, and ladybirds were higher in the grass than in the flowers, while the spiders were high in the flower as well as in the grass (**Figure 3**). Herbivore abundance was significantly higher in the grass treatment than in the flower and control treatments (**Table 2**; **Figure 3F**). In 2017 and 2019, the lowest abundance was recorded in the flower treatment. Both the grass treatment and the control exhibited relatively high abundance of herbivores. The herbivores were mainly composited of small sucking insect, such as Aphididae, Miridae, and Delphacidae.

TABLE 2 | Coefficients and statistics of the generalized linear mixed effects models (GLMM) to test for the effect of the cover plant type and year on the abundance of natural enemies and herbivores collected from the sweep net.

Natural enemy	Effects	χ^2	df	*P*
Total predators	Treatment	120.809	2	<0.0001
	Year	65.194	2	<0.0001
	Treatment × year	11.939	4	0.018
Hoverfly	Treatment	39.382	2	<0.0001
	Year	6.410	2	0.041
	Treatment × year	4.632	4	0.327
Spider	Treatment	75.505	2	<0.0001
	Year	166.106	2	<0.0001
	Treatment × year	3.875	4	0.423
Ladybird	Treatment	60.104	2	<0.0001
	Year	36.070	2	<0.0001
	Treatment × year	8.497	4	0.075
Lacewing	Treatment	12.546	2	0.002
	Year	68.780	2	<0.0001
	Treatment × year	4.215	4	0.378
Herbivores	Treatment	1442.671	2	<0.0001
	Year	83.012	1	<0.0001
	Treatment × year	3.020	2	0.221

Main Predators in Tree Canopy

For the canopy sampling, we used yellow sticky cards to monitor the abundance of flying predators. Ladybirds and lacewings were the most abundant taxa in the sticky card samples. There were three species of ladybird (*Harmonia axyridis*, *Propylaea japonica*, and *Chilocorus kuwanae*) and one species of lacewing (*Chrysoperla sinica*).

We observed 2,857 individual predators during the 3 years (2017: 802, 2018: 556, 2019: 1499). Ladybirds and lacewings accounted for 72% and 28% of the number of predators captured, respectively. A low number of hover flies (Syrphidae) were captured but were not included in the analysis.

There were significant differences in the occurrence of predators (lacewings and ladybirds) (**Table 3**). The abundance of ladybirds in the tree canopy in 2019 varied significantly by cover crop treatment ($\chi^2 = 1688.3$, $P = 0.003$). *Post-hoc* analysis indicated that the abundances of ladybirds in the flowers and grass were higher than in the control treatment. In 2017 and 2018, ladybird abundance did not differ among the treatments. Lacewings consistently exhibited similar abundances across the three treatments, with the exception of 2018. Lacewing abundance was highest in the flower treatment, followed by the grass and control, and no differences in lacewing abundance were detected between the grass and control (**Figure 4**).

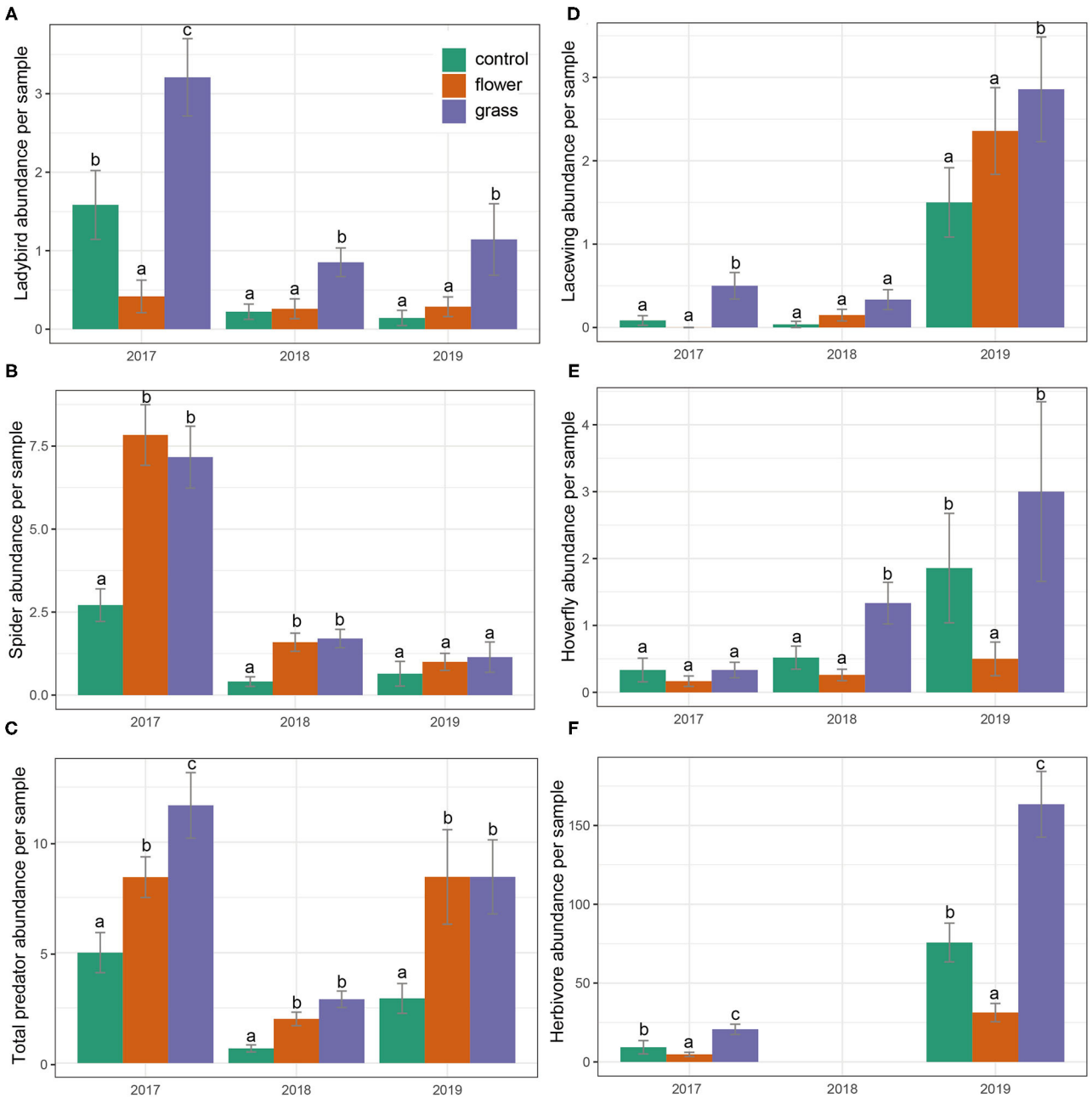

FIGURE 3 | (A-F) Predator and herbivore abundances (mean ± SE) in the cover crops during the 3 years (2017–2019). Within each year, bars capped with the different letter are significantly different ($P < 0.05$).

Aphid Suppression

The aphid abundance in 2017 did not differ significantly among the treatments ($\chi^2 = 2.391$, df = 2, $P = 0.303$). On the contrary, aphid abundance in 2019 differed among the three treatments ($\chi^2 = 58.031$, df = 2, $P < 0.001$), with the abundances in the grass and flower treatments being significantly lower than in the control. As the growing season progressed, the aphid abundance increased and peaked in June and July, following which it declined gradually. In 2019, aphid abundance in the grass treatment was constantly lower than in the flower treatment and control (**Figure 5**).

DISCUSSION

The overall impact of cover crops on predator abundance in apple orchards was significant in comparison to the impact of spontaneous grasses (control). We hypothesized that different cover crops had a differential impact on the conservation

TABLE 3 | Coefficients and statistics of the generalized linear mixed effects models (GLMM) to test for the effect of the cover plant type and year on the abundance of predators collected from the yellow sticky card trap.

	Ladybird			Lacewing		
	χ^2	df	*p*	χ^2	df	*P*
Treatment	35.882	2	<0.001	2.510	2	0.285
Year	19.807	2	<0.001	19.725	2	<0.001
Treatment * year	8.353	4	0.079	17.310	4	0.002

of natural enemies. We found that the mean abundance of total predators was higher in the grass treatment than in the flower treatment. Moreover, predator diversity was also higher in the grass treatment than in the flower treatment. In theory, the composition and size of the pool of natural enemies available for orchard pest suppression could vary significantly with the composition of cover crops in orchards. In cover crop management, a mix of herbaceous plants or flowering plants is often used to house natural enemies in orchards (Eric, 1995; Marliac et al., 2016; de Pedro et al., 2020). For example, it is suggested that perennial flower strips should be placed in orchards to maintain natural enemies (Cahenzli et al., 2019). Considering the functional differences in cover crops, relatively little information on the comparison between flower strips and grass strips is available. Our results suggest that grass strips might offer a promising approach for augmenting natural enemy abundance and diversity.

The grass treatment demonstrated higher predator abundance and diversity than the control and flower treatments. A number of factors may contribute to the increase in predator abundance in the grass treatment. One explanation is that the alternative prey benefits predators during periods of food shortage or disturbance (Happe et al., 2018). In the present study, the herbivores in the grasses were more abundant than in the flowering plants and may have provided food resources to predators. The microclimate created by cover crops has also been cited as a mechanism behind increased predator abundance and suppressed prey populations (Bugg and Waddington, 1994). In our apple orchards, the control treatment (spontaneous grass) was also under organic management. Wild grass on the ground would likely provide microclimate benefits to natural enemies. The community structure of the predators showed similarity in the grass treatment and control, but these treatments differed from the flower treatment. This might be explained by the microclimate, which was similar in the grass treatment and control. However, the spontaneous grass under organic management did not perform as well as the cover crop treatment. Higher predator abundances were observed in the cover crops than in the control. This supports the idea that in organic orchards, a promising approach for conserving natural enemies is the use of functional plants.

Flower strips may have limited capacity to influence predators in our region due to the relatively late planting date of the cover crop. Flowering plants have often been grown in orchards, vegetables, and field crops to improve biological control and reduce dependence on chemical pesticides (Lu et al., 2014). Previous results suggest that flower strips that include fragrant plants favor an increase in natural enemy abundance in orchards (Song et al., 2012; Albert et al., 2017). However, we should also note that nectar or pollen is a limited resource that is usually available for only a short time in the plant growing season. We expected the flowers in the cover crop to attract natural enemies, providing a source of predators that would enhance biocontrol in the orchard. However, if the pest density in orchards is low, the predators will move to other habitats instead of staying in the orchards. Therefore, herbivore populations acting as alternative prey are critical for maintaining a certain number of predators. As most of the predators are highly mobile, the time and duration that they respectively arrive and stay are both important.

Although the cover crops in the apple orchards had a strong impact on the predator abundance and communities in the cover crops, we found weak evidence of an increase in mobile predators in the orchard canopy. Only in 2019 was the predator abundance in the canopy associated with more ladybirds in the grass treatment and flower treatment than in the control. A similar situation was reported by Bone et al. (2009), who found no increase in natural enemies in the orchard canopy when using cover crops. An increase in cover crop benefits did not translate into increases in canopy numbers in the orchards. Such unexpected results may be partly due to the high mobility of ladybirds and lacewings, which might blur the impacts of cover crop. Mobile predators (e.g., ladybirds and lacewings) can offer local population sources of predators. Although the cover crop is not necessarily related to canopy predators, the functions of cover crops are potentially large, especially regarding how they adjust the behavior of predators in orchards. We hypothesized that cover crops could increase biocontrol services in apple orchards by offering food resources for predators. However, only in 1 year did the cover crop improve aphid suppression. It was also reported that increases in natural enemies in cover crops often do not translate into the control of pests in the crop itself (Bone et al., 2009; Markó et al., 2013).

Many studies favor the use of perennial plants to reduce planting costs (Cahenzli et al., 2019), and annual cover crops are also intensive to sow. In the present study, the growing conditions in 2017 and 2018 were not as good as in 2019. This may have resulted from the management practices in these regions, which were inadequate for the cultivation of cover crops. Habitat management through cover crops may be more successful when careful field management can be implemented, e.g., by facilitating the establishment of cover crops by watering dry areas. A greater cover crop biomass may produce greater opportunities for predators and their prey resources to colonize cover crop fields. Vegetative density has been correlated with predator abundance (Rebek et al., 2005). The percentage of ground cover was 100% higher in 2019 than the other years. Implementing practices to plant cover crops earlier

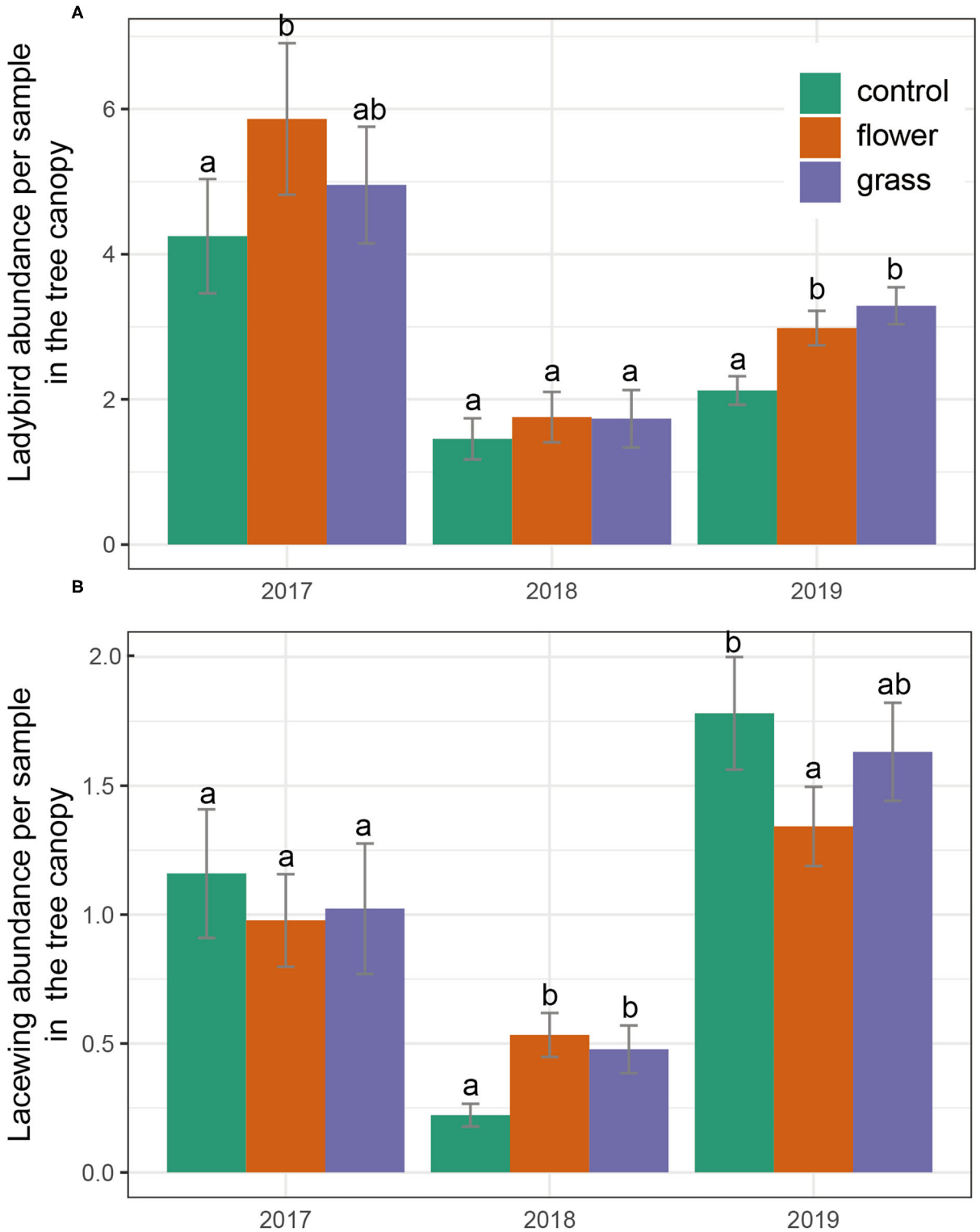

FIGURE 4 | (A,B) Predator abundances (mean ± SE) in the tree canopy during the 3 years (2017–2019). Within each year, bars capped with the different letter are significantly different ($P < 0.05$).

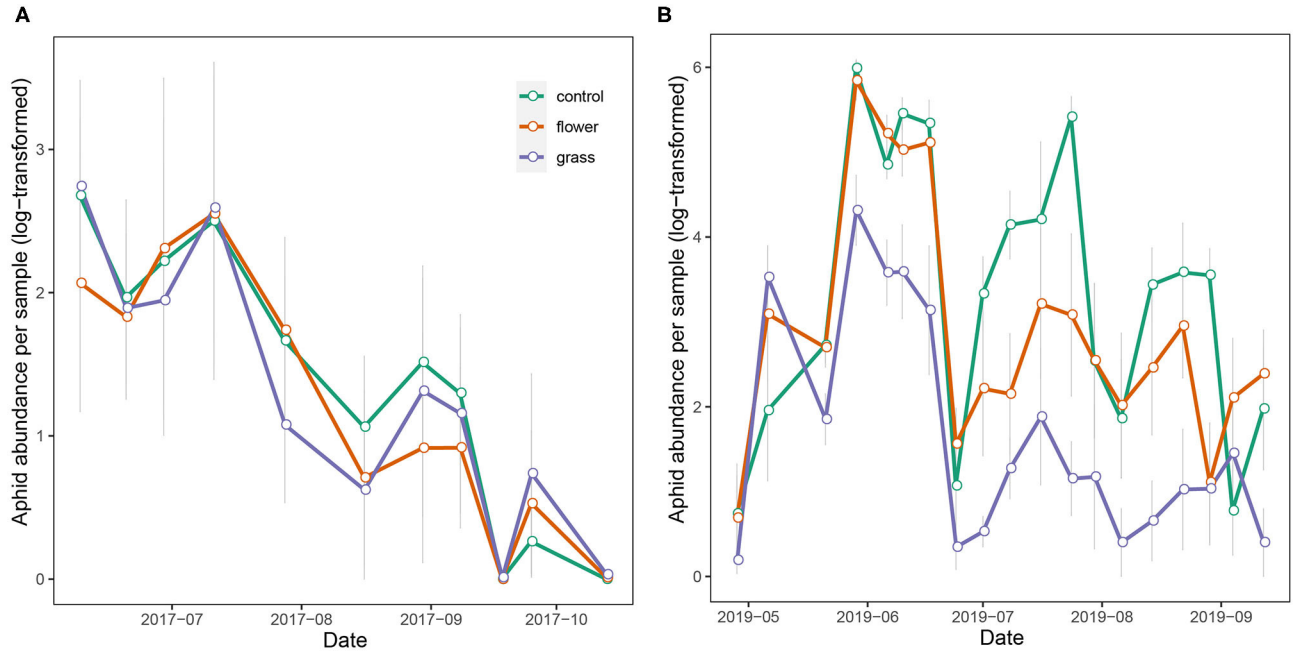

FIGURE 5 | Temporal abundance of aphid (mean ± SE) in the treatments of the apple trees during 2017 **(A)** and 2019 **(B)**.

may increase the cover crop percentage and potentially increase biocontrol efficiency.

DATA AVAILABILITY STATEMENT

The raw data supporting the conclusions of this article will be made available by the authors, without undue reservation.

AUTHOR CONTRIBUTIONS

ZD and ZZ conceived and designed the research. CL and BM conducted experiments. MX contributed to the research design. ZD wrote the manuscript. All of the authors read and approved the manuscript.

FUNDING

This study was supported by the National Key R&D Program of China (2017YFD0200307) and National Natural Science Foundation of China (No. 31501646).

ACKNOWLEDGMENTS

We thank Shifeng Liu, Hongru Kou, Yanchao Sun, and Pengyuan Sun for field and lab assistance.

SUPPLEMENTARY MATERIAL

The Supplementary Material for this article can be found online at: https://www.frontiersin.org/articles/10.3389/fsufs.2021.697864/full#supplementary-material

REFERENCES

Albert, L., Franck, P., Gilles, Y., and Plantegenest, M. (2017). Impact of agroecological infrastructures on the dynamics of *Dysaphis plantaginea* (Hemiptera: Aphididae) and its natural enemies in apple orchards in Northwestern France. *Environ. Entomol.* 46, 528–537. doi: 10.1093/ee/nvx054

Bates, D., Mächler, M., Bolker, B., and Walker, S. (2015). Fitting linear mixed-effects models using *lme4*. *J. Stat. Softw.* 67:i01. doi: 10.18637/jss.v067.i01

Benton, T. G., Vickery, J. A., and Wilson, J. D. (2003). Farmland biodiversity: is habitat heterogeneity the key? *Trends Ecol. Evol.* 18, 182–188. doi: 10.1016/S0169-5347(03)00011-9

Bianchi, F. J., Booij, C. J., and Tscharntke, T. (2006). Sustainable pest regulation in agricultural landscapes: a review on landscape composition, biodiversity, and natural pest control. *Proc. R. Soc. B Biol. Sci.* 273, 1715–1727. doi: 10.1098/rspb.2006.3530

Bone, N. J., Thomson, L. J., Ridland, P. M., Cole, P., and Hoffmann, A. A. (2009). Cover crops in Victorian apple orchards: effects on production, natural enemies, and pests across a season. *Crop Prot.* 28, 675–683. doi: 10.1016/j.cropro.2009.03.021

Bugg, R. L., and Waddington, C. (1994). Using cover crops to manage arthropod pests of orchards: a review. *Agric. Ecosyst. Environ.* 50, 11–28. doi: 10.1016/0167-8809(94)90121-X

Cahenzli, F., Sigsgaard, L., Daniel, C., Herz, A., Jamar, L., Kelderer, M., et al. (2019). Perennial flower strips for pest control in organic apple orchards–a pan-European study. *Agric. Ecosyst. Environ.* 278, 43–53. doi: 10.1016/j.agee.2019.03.011

Cloyd, R. A. (2020). How effective is conservation biological control in regulating insect pest populations in organic crop production systems? *Insects* 11:15. doi: 10.3390/insects11110744

de Pedro, L., Perera-Fernández, L. G., López-Gallego, E., Pérez-Marcos, M., and Sanchez, J. A. (2020). The effect of cover crops on the biodiversity and abundance of ground-dwelling arthropods in a Mediterranean pear orchard. *Agronomy* 10:580. doi: 10.3390/agronomy10040580

Demestihas, C., Plénet, D., Génard, M., Raynal, C., and Lescourret, F. (2017). Ecosystem services in orchards. A review. *Agron. Sustain. Dev.* 37:12. doi: 10.1007/s13593-017-0422-1

Dong, Z. K., Gao, F. J., and Zhang, R. Z. (2012). Use of ryegrass strips to enhance biological control of aphids by ladybirds in wheat fields. *Insect Sci.* 19, 529–534. doi: 10.1111/j.1744-7917.2011.01499.x

Duru, M., Therond, O., Martin, G., Martin-Clouaire, R., Magne, M.-A., Justes, E., et al. (2015). How to implement biodiversity-based agriculture to enhance ecosystem services: a review. *Agron. Sustain. Dev.* 35, 1259–1281. doi: 10.1007/s13593-015-0306-1

English-Loeb, G., Rhainds, M., Martinson, T., and Ugine, T. (2003). Influence of flowering cover crops on *Anagrus* parasitoids (Hymenoptera: Mymaridae) and *Erythroneura* leafhoppers (Homoptera: Cicadellidae) in New York vineyards. *Agric. For. Entomol.* 5, 173–181. doi: 10.1046/j.1461-9563.2003.00179.x

Eric, W. (1995). The effects of weed strips on aphids and aphidophagous predators in an apple orchard. *Entomol. Exp. Appl.* 75, 43–49. doi: 10.1111/j.1570-7458.1995.tb01908.x

Fernández, D. E., Cichón, L. I., Sánchez, E. E., Garrido, S. A., and Gittins, C. (2008). Effect of different cover crops on the presence of arthropods in an organic apple (*Malus domestica* Borkh) orchard. *J. Sustain. Agric.* 32, 197–211. doi: 10.1080/10440040802170624

Fiedler, A. K., Landis, D. A., and Wratten, S. D. (2008). Maximizing ecosystem services from conservation biological control: the role of habitat management. *Biol. Control* 45, 254–271. doi: 10.1016/j.biocontrol.2007.12.009

Fox, J., and Weisberg, S. (2019). *An R Companion to Applied Regression*. Thousand Oaks, CA: Sage.

Galloway, A. D., Seymour, C. L., Gaigher, R., and Pryke, J. S. (2021). Organic farming promotes arthropod predators, but this depends on neighbouring patches of natural vegetation. *Agric. Ecosyst. Environ.* 310:107295. doi: 10.1016/j.agee.2020.107295

Geldenhuys, M., Gaigher, R., Pryke, J. S., and Samways, M. J. (2021). Diverse herbaceous cover crops promote vineyard arthropod diversity across different management regimes. *Agric. Ecosyst. Environ.* 307:10. doi: 10.1016/j.agee.2020.107222

Gomez-Marco, F., Urbaneja, A., and Tena, A. (2016). A sown grass cover enriched with wild forb plants improves the biological control of aphids in citrus. *Basic Appl. Ecol.* 17, 210–219. doi: 10.1016/j.baae.2015.10.006

Gontijo, L. M., Beers, E. H., and Snyder, W. E. (2013). Flowers promote aphid suppression in apple orchards. *Biol. Control* 66, 8–15. doi: 10.1016/j.biocontrol.2013.03.007

Gurr, G. M., Wratten, S. D., Landis, D. A., and You, M. S. (2017). Habitat management to suppress pest populations: progress and prospects. *Annu. Rev. Entomol.* 62, 91–109. doi: 10.1146/annurev-ento-031616-035050

Happe, A. K., Roquer-Beni, L., Bosch, J., Alins, G., Mody, K., and Rroll Dp, J. O. E. E. V. P. (2018). Earwigs and woolly apple aphids in integrated and organic apple orchards: responses of a generalist predator and a pest prey to local and landscape factors. *Agric. Ecosyst. Environ.* 268, 44–51. doi: 10.1016/j.agee.2018.09.004

He, X. Q., Kiaer, L. P., Jensen, P. M., and Sigsgaard, L. (2021). The effect of floral resources on predator longevity and fecundity: a systematic review and meta-analysis. *Biol. Control* 153:11. doi: 10.1016/j.biocontrol.2020.104476

Hothorn, T., Bretz, F., and Westfall, P. (2008). Simultaneous inference in general parametric models. *Biom. J.* 50, 346–363. doi: 10.1002/bimj.200810425

Isaacs, R., Tuell, J., Fiedler, A., Gardiner, M., and Landis, D. (2009). Maximizing arthropod-mediated ecosystem services in agricultural landscapes: the role of native plants. *Front. Ecol. Environ.* 7, 196–203. doi: 10.1890/080035

Landis, D. A., Wratten, S. D., and Gurr, G. M. (2000). Habitat management to conserve natural enemies of arthropod pests in agriculture. *Annu. Rev. Entomol.* 45, 175–201. doi: 10.1146/annurev.ento.45.1.175

Lu, Z. X., Zhu, P. Y., Gurr, G. M., Zheng, X. S., Read, D. M., Heong, K. L., et al. (2014). Mechanisms for flowering plants to benefit arthropod natural enemies of insect pests: prospects for enhanced use in agriculture. *Insect Sci.* 21, 1–12. doi: 10.1111/1744-7917.12000

Lundin, O., Ward, K. L., and Williams, N. M. (2019). Identifying native plants for coordinated habitat management of arthropod pollinators, herbivores and natural enemies. *J. Appl. Ecol.* 56, 665–676. doi: 10.1111/1365-2664.13304

Markó, V., Jenser, G., Kondorosy, E., Ábrahám, L., and Balázs, K. (2013). Flowers for better pest control? the effects of apple orchard ground cover management on green apple aphids (*Aphis* spp.) (Hemiptera: Aphididae), their predators and the canopy insect community. *Biocontrol Sci. Technol.* 23, 126–145. doi: 10.1080/09583157.2012.743972

Marliac, G., Mazzia, C., Pasquet, A., Cornic, J. F., Hedde, M., and Capowiez, Y. (2016). Management diversity within organic production influences epigeal spider communities in apple orchards. *Agric. Ecosyst. Environ.* 216, 73–81. doi: 10.1016/j.agee.2015.09.026

Oksanen, J., Blanchet, F. G., Friendly, M., Kindt, R., Legendre, P., McGlinn, D., et al. (2020). *vegan: Community Ecology Package. R package version 2.5-7*. Available online at: https://CRAN.R-project.org/package=vegan.

Penvern, S., Fernique, S., Cardona, A., Herz, A., Ahrenfeldt, E., Dufils, A., et al. (2019). Farmers' management of functional biodiversity goes beyond pest management in organic European apple orchards. *Agric. Ecosyst. Environ.* 284:11. doi: 10.1016/j.agee.2019.05.014

R Core Team (2020). *R: A Language and Environment for Statistical Computing*. Vienna: R Foundation for Statistical Computing.

Rebek, E. J., Sadof, C. S., and Hanks, L. M. (2005). Manipulating the abundance of natural enemies in ornamental landscapes with floral resource plants. *Biol. Control* 33, 203–216. doi: 10.1016/j.biocontrol.2005.02.011

Robinson, K. A., Jonsson, M., Wratten, S. D., Wade, M. R., and Buckley, H. L. (2008). Implications of floral resources for predation by an omnivorous lacewing. *Basic Appl. Ecol.* 9, 172–181. doi: 10.1016/j.baae.2007.01.002

Simon, S., Bouvier, J. C., Debras, J. F., and Sauphanor, B. (2010). Biodiversity and pest management in orchard systems. A review. *Agron. Sustain. Dev.* 30, 139–152. doi: 10.1051/agro/2009013

Song, B. Z., and Han, Z. H. (2020). Assessment of the biocontrol effects of three aromatic plants on multiple trophic levels of the arthropod community in an agroforestry ecosystem. *Ecol. Entomol.* 45, 831–839. doi: 10.1111/een.12858

Song, B. Z., Zhang, J., Wiggins, N. L., Yao, Y. C., Tang, G. B., and Sang, X. S. (2012). Intercropping with aromatic plants decreases herbivore abundance, species richness, and shifts arthropod community trophic structure. *Environ. Entomol.* 41, 872–879. doi: 10.1603/EN12053

Tscharntke, T., Bommarco, R., Clough, Y., Crist, T. O., Kleijn, D., Rand, T. A., et al. (2007). Conservation biological control and enemy diversity on a landscape scale. *Biol. Control* 43, 294–309. doi: 10.1016/j.biocontrol.2007.08.006

Tscharntke, T., Klein, A. M., Kruess, A., Steffan-Dewenter, I., and Thies, C. (2005). Landscape perspectives on agricultural intensification and biodiversity–ecosystem service management. *Ecol. Lett.* 8, 857–874. doi: 10.1111/j.1461-0248.2005.00782.x

Wyss, E. (1996). The effects of artificial weed strips on diversity and abundance of the arthropod fauna in a Swiss experimental apple orchard. *Agric. Ecosyst. Environ.* 60, 47–59. doi: 10.1016/S0167-8809(96)01060-2

Yan, Y. H., Yu, Y., Du, X. G., and Zhao, B. G. (1997). Conservation and augmentation of natural enemies in pest management of Chinese apple orchards. *Agric. Ecosyst. Environ.* 62, 253–260. doi: 10.1016/S0167-8809(96)01130-9

Conflict of Interest: The authors declare that the research was conducted in the absence of any commercial or financial relationships that could be construed as a potential conflict of interest.

frontiers in Sustainable Food Systems

ORIGINAL RESEARCH
published: 10 January 2022
doi: 10.3389/fsufs.2021.782425

Biocontrol of Anthracnose Disease on Chili Pepper Using a Formulation Containing *Paenibacillus polymyxa* C1

*Dewa Ngurah Suprapta**

Laboratory of Biopesticide, Faculty of Agriculture Udayana University, Denpasar, Indonesia

Anthracnose disease on chili pepper has been known to seriously interfere with the plant growth and obviously reduce the yield. The disease is caused by *Colletotrichum* spp. In Bali, Indonesia, six species of *Colletotrichum* have been identified: *Colletotrichum scovillei, C. acutatum, C. nymphaeae, C. gloeosporioides, C. truncatum,* and *C. fructicola.* However, among them the *C. scovillei* was found to be the most prevalent cause of anthracnose on chili pepper in Bali. Two species of antagonist against *C. scovillei,* namely *Paenibacillus polymyxa* C1 and *Bacillus siamensis* C7B, have been identified. In this study the effectiveness of *P. polymyxa* C1 formulation was evaluated under greenhouse condition on chili pepper cultivars *Cabe Besar.* Application of formulation was conducted by a mini hand sprayer once to five times with a week interval. Results of the study showed that treatment with five applications significantly ($p < 0.05$) reduced the disease incidence, disease intensity, and the yield loss of chili pepper cultivar *Cabe Besar*. Alose relationship was observed between the number of applications with disease intensity, with coefficient of determination (R^2) at 0.929. These results revealed that the formulation of *P. polymyxa* C1 effectively control the anthracnose disease on chili pepper, particularly on chili pepper cultivar *Cabe Besar,* and thus can be recommended for field testing to confirm its stability under field conditions.

Keywords: biocontrol, anthracnose disease, chili pepper, formulation, *Paenibacillus polymyxa* C1

OPEN ACCESS

Edited by:
Xingyuan Men,
Shandong Academy of Agricultural Sciences, China

Reviewed by:
Yong Liu,
Hunan Academy of Agricultural Sciences (CAAS), China
Durgesh Kumar Jaiswal,
Savitribai Phule Pune University, India

***Correspondence:**
Dewa Ngurah Suprapta
ngurahsuprapta@unud.ac.id

Specialty section:
This article was submitted to Agroecology and Ecosystem Services, a section of the journal Frontiers in Sustainable Food Systems

Received: *24 September 2021*
Accepted: *08 December 2021*
Published: *10 January 2022*

Citation:
Suprapta DN (2022) Biocontrol of Anthracnose Disease on Chili Pepper Using a Formulation Containing Paenibacillus polymyxa C1. Front. Sustain. Food Syst. 5:782425. doi: 10.3389/fsufs.2021.782425

INTRODUCTION

Cultivation of chili pepper in Bali, Indonesia, is frequently affected by anthracnose disease, caused by *Colletotrichum* spp. The incidence of the disease in this region was reported at 84% and disease intensity varied from 22 to 78% (Khalimi et al., 2019). A study done by Khalimi et al. (2019) identified six species of *Colletotrichum* as the cause of anthracnose disease on chili pepper in Bali: *Colletotrichum scovillei*, *C. acutatum*, *C. nymphaeae*, *C. gloesporioides*, *C. truncatum*, and *C. fructicola*. Among them, *C. scovillei* was the most prevalent, with rates of 55%. The disease causes 10 to 80% of yield losses depending on cultivation areas (Poonpolgul and Kumphai, 2007; Asare-Badiako et al., 2015; Diao et al., 2017).

Development of a resistant chili cultivar is expected to be effective in controlling the disease, however the resistance against *Colletotrichum* spp. is often broken down under field conditions

(Park, 2007). Synthetic fungicides are generally used by farmers to control anthracnose disease; however, this measure is not always effective to reduce the disease incidence. Other alternative measures are needed to overcome the problem of anthracnose disease on chili pepper, while remaining safe for the consumers and environment.

Because of the increased preference of consumers for organic agricultural products in Indonesia, organic farming systems are becoming popular among farmers and consumers (Shiotsu et al., 2015). To develop organic farming, it is important to provide bio-control agents to manage plant diseases. The use of bio-agents to control plant fungal diseases may reduce the use of synthetic chemical fungicides and hence reduce the adverse effect to the environment. Several bio-agents have been found and reported to possess inhibitory activities against plant pathogens. *Piriformospora indica*, *Trichoderma viride*, *Acremonium lolii*, and *Colletotrichum lindemuthianum* protected against leaf rust of wheat caused by *Puccinia recondite* (Anwaar et al., 2019), *Bacillus cereus* SSB1 effectively controlled *Pectobacterium* infection in potato (Sarfraz et al., 2019) and *Bacillus amyloliquesfaciens* BA-16-8 inhibited the growth of *Penicillium expansum,* which is the cause of postharvest decay in apple (Fu et al., 2020).

One type of bio-agent that could potentially be used for plant fungal disease control is rhizobacteria. Rhizobacteria are bacteria that colonize the plant root and give beneficial effect to the plant through growth promotion (Saharan and Nehra, 2011). *Enterobacter cloacae* KtB3 isolated from the rhizosphere of groundnut were proven to effectively control the damping-off disease on soybean caused by *Sclerotium rolfsii* (Mahartha and Suprapta, 2018). Rhizobacteria are able to produce phyto-hormones such as *indole acetic acid* (IAA), ACC deaminase to fix atmospheric nitrogen and act as antagonistic microbes against plant pathogen through the production of siderophores, and β-1,3-glucanase, chitinase, cellulase, and antibiotics, which are able to dissolve phosphate and other nutrients in the soil (Soesanto, 2008; Guo et al., 2015; Saleem et al., 2015). For example, *Pseudomonas fluorescens* produced 2, 4-*diacetyl phloroglucinol* that effectively suppressed plant fungal pathogens (Nowak-Thompson et al., 1994). *Pseudomonas stutzeri* produced extracellular chitinase enzyme and laminarinase that were able to decompose the mycelia of *Fusarium solani* (Mauch et al., 1988). Our previous study showed that two species of antagonist, namely *Paenibacillus polymyxa* C1 and *Bacillus siamensis* C7B, were proven to possess strong antifungal activities against *C. scovillei* (Darmadi et al., 2020).

Based on the above-mentioned consideration, this study was done to evaluate the effectiveness of the formulation of *P. polymyxa* C1 to reduce the disease incidence and intensity of anthracnose on chili pepper as well as to reduce the yield losses of chili cultivar *Cabe Besar*.

MATERIALS AND METHODS

Preparation of Formulation

Paenibacillus polymyxa isolate C1 was used to develop the formulation. In general the formulation contained the following components: potato broth 3–5% (v/v), dextrose 1–3% (w/v), yeast extract 0.2–0.4% (w/v), extract of green bean sprouts 2–5% (v/v), spore's suspension of *P. polymyxa* C1 (10^6 CFU/ml) 0.2–0.5% (v/v), and distilled water to bring the total volume to one liter. Seven formulations were prepared with the components as shown in **Table 1**.

TABLE 1 | Detail components of formulation of *P. polymyxa* C1.

Components	Formulations						
	F1	F2	F3	F4	F5	F6	F7
Potato dextrose (%, v/v)	3	3	3	4	4	4	5
Dextrose (%, w/v)	1	1	2	2	3	3	3
Yeast extract (%, w/v)	0.1	0.1	0.2	0.2	0.2	0.3	0.3
Green bean sprout (%, v/v)	2	3	3	4	5	5	5
Suspension of *P. polymyxa* C1 (%, v/v)	0.2	0.2	0.3	0.3	0.3	0.4	0.4
Distilled water (%, v/v)	93.7	92.7	91.5	89.5	87.5	87.3	86.3

All components of the formulation (except for suspension of *P. polymyxa* C1) were put into 1.000 ml Erlenmeyer, covered with aluminum foil, and autoclaved for 20 min at 121°C. After the formulation reached room temperature, suspension of *P. polymyxa* C1 was added aseptically in a laminar air flow. Each formulation was made in four replications (four L). These cultures were incubated for 72 h in the dark at room temperature (28 ± 2°C. Population of bacteria in each formulation was counted. A serial of dilution ($10^{-1} - 10^{-9}$) was made using sterile distilled water. Each 0.2 ml of respective dilution was grown in NA medium on Petri dishes and incubated in the dark under room temperature for 48 h. The number of colonies were counted and compared among formulations. The formulation with the highest number of colonies was used for further tests.

Application of Formulation on Chili Pepper Fruit

Formulation F6 was selected and used for testing on fruits of chili pepper cultivar *Cabe Besar*. This experiment was done to know the optimum concentration to control anthracnose disease. Six levels of concentration (v/v) were tested: Control (0%, with distilled water only) (K0), concentration 1% (K1), 3% (K3), 5% (K5), 7% (K7), and 9% (K9). Each concentration was replicated four times. Thus, there are 24 experimental units consisting of 10 chili pepper fruits placed on plastic trays.

Inoculum Preparation

Colletotrichum scovillei SGCR was provided by the Laboratory of Biopesticide Faculty of Agriculture Udayana University, Bali that previously was identified based on 18S rRNA gene analysis (Khalimi et al., 2019). The fungus was transferred onto slant PDA medium for 7 days and the spores were harvested using sterile distilled water by wire loop. The suspension was then sieved with No. 1 Whatman filter paper to separate the mycelia and hyphae. The spore's density was determined on hemocytometer under light microscope. The spore's density was adjusted into 10^6 spores/ml by adding sterile distilled water.

Preparation of Chili Pepper Fruits

The mature fruits of chili pepper cultivar *Cabe Besar* obtained directly from the farmers with similar size and maturity were selected; they were then washed with tap water to remove the surface contaminants and then were washed with sterile distilled water and wiped with sterile tissue paper. All fruits were then surface sterilized using alcohol 70% for about 2 min, then rinsed in sterile distilled water, and wiped with tissue paper. Fruits were divided into 10 fruits then put in a plastic tray (17.5 x 22.5 cm in size) with wet towel tissue on the bottom.

Application of Formulation and Inoculation

The chili pepper fruits were pierced with needles on the upper surface at three sites. Application of formulation was done by spraying the formulation at six levels of concentration: 0% (K0), 1% (K1), 3% (K3), 5% (K5), 7% (K7), and 9% (K9). Each concentration was replicated four times, thus there are 24 experimental units consisting of plastic tray with chili pepper fruits. Thirty minutes after formulation application, all fruit were inoculated with spore's suspension of *C. scovillei* with 10^7 spores/ml. Inoculation was done over the upper surface of chili pepper fruit using a mini hand sprayer. After inoculation the trays were covered with cling plastic wrap to maintain the humidity. All trays were incubated in the dark under room temperature (28 ± 2°C) for 5 days. Number of inoculation sites developed into anthracnose lesions were counted and compared among treatments.

Green House Experiment

As the best concentration was determined based on *in vivo* experiment of chili pepper fruits to be 5%, in the greenhouse experiment the frequency of application was evaluated. Frequencies of application varied from 0 to 5 times, namely 0 (F0 = Control), once (F1), twice (F2), three times (F3), four times (F4), and five times (F5). Each frequency was replicated four times, thus, there are 24 experimental units consisting of 10 polybags of chili pepper plants. All treatment was allocated based on randomized block design (CRD).

Parameters observed in this experiment included disease incidence, disease intensity, and weight of consumable fruits per plant.

Observation of disease intensity on chili pepper fruit was done three days after formulation application according to formula developed by Sinaga (2006), as follows:

Description:

$$DI = \frac{\sum_{i=0}^{i} (n_i . v_i)}{N.V} \times 100\%$$

DI = disease intensity
ni = number of fruits for each category
vi = score of each category
N = the highest score of each category
V = number of observed fruits/plant

The score for each category is determined as follows:

0 = no Symptom Observed
1 = Very Light Symptom (0–10% Fruit Surface Destroyed)
2 = Light Symptom (10–30% Fruit Surface Destroyed)
3 = Medium Symptom (30–50% Fruit Surface Destroyed)
4 = Severe Symptom (50–75% Fruit Surface Destroyed)
5 = Very Severe Symptom (75–100% Fruit Surface Destroyed)

TABLE 2 | Population of *Paenibacillus polymyxa* C1 in respective formulation.

No.	Formulation	Density ± Sd (x 10^7 CFU/ml)
1	F1	10.98 ± 2,23*
2	F2	11.77 ± 1,78
3	F3	12.89 ± 1,07
4	F4	16.47 ± 2,08
5	F5	20.55 ± 1,98
6	F6	26.25 ± 2,02
7	F7	17.87± 2,37

*Sd, Standard deviation. *Average of 5 (five) replications.*

Data Analysis

All data obtained in this experiment were subjected to the analysis of variance (ANOVA) and followed by Duncan's Multiple Range Test (DMRT) at 5% to determine significant difference. This statistical analysis was done using software SPSS for windows version 17.0 year 2009.

RESULTS

Among seven formulations tested, formulation F6 showed the highest number of *P. polymyxa* C1 colonies. This formulation containing 4% (v/v) potato broth, 3% (w/v) dextrose, 0.3% (w/v) yeast extract, 5% (v/v) green bean sprout extract, 0.4% (v/v) suspension of *P. polymyxa* C1, and 87.3% (v/v) distilled water resulted in 26.25 x 10^7 CFU/ml superior among others, as presented in **Table 2**.

Effectiveness of F6 to Control Anthracnose Symptom on Chili Pepper Fruit

Six levels of concentration of formulation F6 were evaluated for their effectiveness to suppress anthracnose symptom *in vivo* on fruits of chili pepper cultivar *Cabe Besar*. Results of this experiment showed that concentration at 5, 7, and 9% (v/v) totally inhibited the development of anthracnose symptom on *Cabe Besar* as presented in **Table 3**. This result suggested that formulation F6 at a concentration of 5% (v/v) is enough to suppress the growth of *C. scovillei* and the development of anthracnose disease.

Effectiveness of Formulation in a Green House

Result of the experiment under greenhouse condition showed that treatment with formulation F6 significantly ($p < 0.05$) reduced the disease incidence, disease intensity, and consumable chili pepper fruits per plant. Treatment of five times application (F5) showed the disease incidence to be only 1.88% with disease intensity at 2.12%, but it is not significantly different from the treatment of F4 (four applications). While in the Control

TABLE 3 | Effects of concentration of formulation F6 on the number of anthracnose lesions on chili pepper fruit cultivar *Cabe Besar in vivo*.

No.	Treatment	Number of anthracnose lesions ± Sd*	Percentage of inhibitory activity against K0 (Control)
1	K0	11.75d** ± 2.87	-
2	K1	8.50c ± 2.03	27.66
3	K3	1.75b ± 0.87	85.11
4	K5	0a ± 0.00	100
5	K7	0a ± 0.00	100
6	K9	0a ± 0.00	100

Sd, Standard deviation.
**Average of 4 (four) replications.*
***Values followed by the same letter did not significantly different according to Duncan's Multiple Range Test at 5% level.*

TABLE 4 | Effect of frequency of application of F6 to the incidence of anthracnose disease on chili pepper cultivar *Cabe Besar*.

No.	Treatment	Disease incidence (%) ± Sd*	Inhibitory activity compared to F0 (%)
1	F0	70.68a** ± 12.24	-
2	F1	49.20b ± 10.76	30.38
3	F2	31.28c ± 7.89	55.73
4	F3	18.43d ± 3.45	68.70
5	F4	4.96e ± 1.98	92.98
6	F5	1.88e ± 0.87	97.34

Sd, Standard deviation.
**Average of 4 (four) replications.*
***Values followed by the same letter did not significantly different according to Duncan's Multiple Range Test at 5% level.*

TABLE 5 | Effect of frequency of application of F6 to the disease intensity on chili pepper cultivar *Cabe Besar*.

No.	Treatment	Disease intensity (%) ± Sd*	Inhibitory activity compared to F0 (%)
1	F0	69.80a** ± 18.17	-
2	F1	45.85b ± 16.78	34.31
3	F2	29.49c ± 8.65	57.75
4	F3	12.49d ± 5.42	82.11
5	F4	3.11e ± 2.74	95.54
6	F5	2.12e ± 1.88	96.96

Sd, Standard deviation.
**Average of 4 (four) replications.*
***Values followed by the same letter did not significantly different according to Duncan's Multiple Range Test at 5% level.*

TABLE 6 | Effect of frequency of application of F6 to the weight of healthy fruits/plant on chili pepper cultivar *Cabe Besar*.

No.	Treatment	Weight of healthy fruits (g/plant) ± Sd*	Estimated yield (ton/ha)**
1	F0	43.93a*** ± 9.26	1.05
2	F1	107.15b ± 24.47	2.55
3	F2	210.10c ± 23.78	5.00
4	F3	283.92d ± 32.46	6.76
5	F4	447.56e ± 52.78	10.66
6	F5	476.98e ± 48.93	11.36

Sd = Standard deviation.
**Average of 4 (four) replications.*
***Planting spacing was 60 x 70 cm, with estimated number of plants 23,809/ha.*
****Values followed by the same letter did not significantly different according to Duncan's Multiple Range Test at 5% level.*

(F0) the disease incidence and intensity were 70.68 and 69.80% respectively (**Tables 4**, **5**). The frequency of application also significantly ($p < 0.05$) affected the weight of healthy fruits per plant. The weight of healthy fruits on Control (F0) was only 43.93 g/plant while for that of F5 was 476.98 g/plant (**Table 6**). This result suggested that the formulation of *P. polyxyxa* C1 effectively reduced the disease incidence and intensity on the one hand, and on the other obviously avoided yield losses.

There was a close relationship between the frequency of application and disease intensity, and the disease intensity with the weight of healthy fruits per plant. The coefficient determination for those relationships were 0.929 and 0.905 respectively (**Figures 1**, **2**).

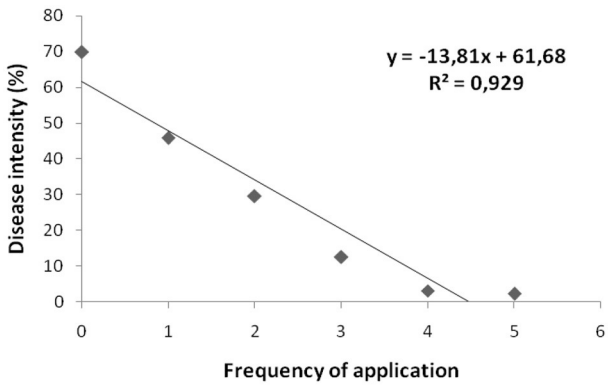

FIGURE 1 | Relationship between frequency of application of formulation F6 with the disease intensity on chili pepper cultivar *Cabe Besar*.

DISCUSSION

Paenibacillus polymyxa C1 was proven to be a potential bioagent against *C. scovillei,* the prominent cause of anthracnose disease on chili pepper in Bali, Indonesia (Khalimi et al., 2019). In the present study the effectiveness of a formulation containing suspension of *P. polymyxa* C1 was tested in a greenhouse to control anthracnose disease on chili pepper cultivar *Cabe Besar*. Some species of microbes have been proven to possess potential antagonistic activities against plant fungal pathogens. Several of them have been successfully used as biocontrol agents against

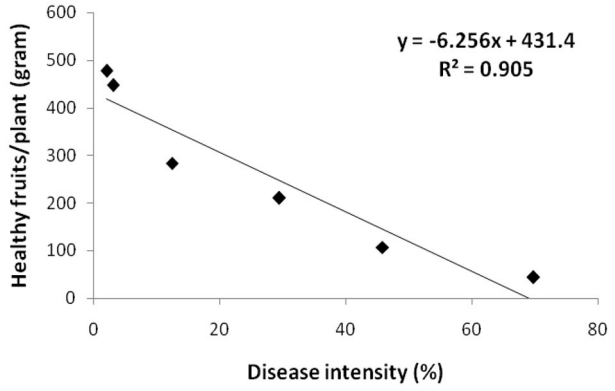

FIGURE 2 | Relationship between disease intensity with the weight of healthy fruits per plant on chili pepper cultivar *Cabe Besar*.

plant fungal diseases (Suprapta, 2012; Widnyana et al., 2013; Parwati et al., 2014; Suprapta et al., 2014; Guo et al., 2015; Hudge, 2015; Adame-Garcia et al., 2016).

In our previous study we detected three compounds in the cell-free filtrate of *P. polymixa* C1: 3-hydroxy-2-butanone, 2, 3-Butanediol, and 2, 3-Butanediol (Darmadi et al., 2020). Other researchers proved that 3-hydroxy-2-butanone is a volatile compound with antifungal activity (Lim et al., 2017). Arrebola et al. (2010) also proved that 3-hydroxy-2-butanone is a volatile compound with antifungal activity against *Penicillium crustosum*. A compound 2,3-butanediol extracted from a culture of *P. polymyxa* was proven to induce systemic acquired resistance against *Phytophthora parasitica* var. *nicotianae* (Park et al., 2018). Scanning electron microscopy showed that serious damage on the mycelia of *C. scovillei* was observed. Wrinkles were observed on the mycelia of *C. scovillei* grown side by side with *P. polymyxa* C1, whereas no such wrinkle was observed on *C. scovillei* grown alone (Darmadi et al., 2020). A study done by Shahbazi et al. (2014) showed that antagonistic *Streptomyces rochei* strain P14 caused hyphal tip lyses, folding back, stunted mycelium, disintegrated hyphae, and curling of hyphae on *Colletotrichum,* the cause of anthracnose on chili pepper. This strain, P14, produced chitinase (Shahbazi et al., 2014).

In this study the best formulation was F6 containing 4% (v/v) potato broth, 3% (w/v) dextrose, 0.3% (w/v) yeast extract, 5% (v/v) green bean sprout extract, 0.4% (v/v) suspension of *P. polymyxa* C1, and 87.3% (v/v) distilled water. This formulation resulted in the highest population of bacteria. In a greenhouse test on chili pepper cultivars *Cabe Besar*, treatment with formulation containing suspension of *P. polymyxa* C1 effectively reduced the disease incidence and intensity, as well as increased the weight of healthy fruit per plant. A close relationship was observed between frequency of application (1 to 5 times) and the disease intensity of anthracnose on chili fruit with coefficient of determination (R^2) = 0.929, suggesting that the higher frequency of application resulted in less disease intensity. A close relationship was also observed between disease intensity with number of healthy fruits per plant, suggesting that disease intensity is the main factor influencing number of healthy fruits per plant. Although the test was done under greenhouse conditions, our present results revealed that formulation F6 is promising for controlling the anthracnose disease on chili pepper. This result is similar to the result obtained by Shahbazi et al. (2014) where *Streptomyces rochei* strain P14 significantly decreased disease severity and increased fresh fruit weight of chili when compared with control (treatment with *Colletotrichum* only). The average disease severity reduction from 75% (on control) to 10% (treatment with strain P14). Raghunandan et al. (2019) tested the efficacy of antagonistic yeasts (*Pichia guilliesmondii* Y-12, *Hanseniaspora uvarum* Y-73), fungus (*Trichoderma asperellum* Th-3), and bacterium (*Pseudomonas fluorescens* Pf-1) to control fruit rot/anthracnose disease on chili under field conditions over two seasons. All bio-agents significantly reduced the disease intensity and increased the fruit yield per hectare. The disease intensities on treated plants varied from 13.42 to 16.38%, while fruits yield obtained on plants treated with bio-agents varied from 7.36 to 80.89 ton/ha, while for that of control was only 4.35 ton/ha.

Several other bioagents have been studied in relation to their antifungal activity against *Colletotrichum* as well as their efficacy to control anthracnose disease on chili pepper. The use of *Trichoderma viridae* and *Pseudomonas fluorescens* individually or in combination significantly lowers the anthracnose disease incidence (Reddy et al., 2011). An antagonistic yeast, *Pichia guilliermondii* strain R13, was reported to reduce the disease incidence of anthracnose in chili pepper incited by *C. truncatum* as low as 6.5% (Chanchaichaovivat et al., 2008). Kim and Yun (2011) reported that under greenhouse conditions, treatment with *Myxococcus* sp. KYC 1126 obviously lowered the incidence of anthracnose in hot pepper. The incidence of anthracnose in control seedlings was 74%, while for treated seedlings was only 29%. Prihatiningsing et al. (2019) proved that microencapsulates containing *Bacillus subtilis* B298 reduced anthracnose disease intensity by 48%. This microencapsulated *B. Subtilis* B298 is considered to induce systemic resistance on chili as total phenol in the treated plants increased.

In the present study it is proven that a formulation containing suspension of *P. polymyxa* C1 significantly reduced both disease incidence and disease intensity on chili pepper, and thus can be considered an environmentally friendly measure to protect chili pepper from anthracnose disease.

CONCLUSION

This study confirmed that treatment with a formulation containing suspension of *P. polymyxa* C1 effectively reduced the disease incidence, disease intensity, and the yield loss of chili pepper cultivar *Cabe Besar*. Alose relationship was observed

between the number of applications with disease intensity, and the disease intensity with the number of healthy fruits. These results suggested that the formulation of *P. polymyxa* C1 effectively controlled the anthracnose disease on chili pepper cultivar *Cabe Besar*, and can be recommended for field testing before it is used widely in the field.

DATA AVAILABILITY STATEMENT

The raw data supporting the conclusions of this article will be made available by the authors, without undue reservation.

AUTHOR CONTRIBUTIONS

The author confirms being the sole contributor of this work and has approved it for publication.

ACKNOWLEDGMENTS

I wish to express a high appreciation to the Institute of Research and Community Services, Udayana University for providing the research grant in the fiscal year 2020 under the scheme of Penelitian Percepatan Guru Besar (P2GB).

REFERENCES

Adame-Garcia, J., Luna-Rodriguez, M., and Iglesias-Andreu, L. G. (2016). Vanilla rhizobacteria as antagonists against *Fusarium oxysforum* f.sp. *vanillae. Int. J. Agric. Biol*. 18, 23–30. doi: 10.17957/IJAB/15.0053

Anwaar, H. A., Ali, S., Sahi, S. T., and Siddiqui, M. T. (2019). Evaluating the antagonistic role of fungal endophytes against leaf rust of wheat caused by *Puccinia recondita. Int. J. Agric. Biol*. 21, 333–337. doi: 10.17957/IJAB/15.0898

Arrebola, E., Sivakumar, D., and Korsten, L. (2010). Effect of volatile compounds produced by *Bacillus* strains on postharvest decay in citrus. *Biol. Control*. 53, 122–128. doi: 10.1016/j.biocontrol.2009.11.010

Asare-Badiako, E., Addo-Quaye, A., Boakye, B., Sarbah, J. M., Asante, P., and Dorm, E. (2015). Incidence and severity of viral and fungal diseases of Chili pepper (*Capsicum frutescens*) in some districts in Chana. *Int. J. Plant and Soil Sci*. 1, 147–159. doi: 10.9734/IJPSS/2015/16830

Chanchaichaovivat, A., Panijpan, B., and Ruenwongsa, P. (2008). Putative modes of action of *Pichia guilliermondii* strain R13 in controlling chili anthracnose after harvest. *Biol. Control*. 47, 207–215. doi: 10.1016/j.biocontrol.2008.07.018

Darmadi, A. A. K., Suprapta, D. N., and Khalimi, K. (2020). Potential antagonistic rhizobacteria to control *Colletotrichum scovillei*, the cause of anthracnose disease in chili pepper. *Biodiversitas* 21, 2727–2734. doi: 10.13057/biodiv/d210648

Diao, Y. Z., Zhang, C., Liu, F., Wang, W. Z., Liu, L., Cai, L., et al. (2017). *Colletotrichum* species causing anthracnose disease of chili in China. *Persoonia* 38, 20–37. doi: 10.3767/003158517X692788

Fu, R., Zhang, H., Chang, H., Zhang, F., and Chen, W. (2020). Evaluation of antifungal mechanism of *Bacillus amyloliquefaciens* BA-16-8. *Int. J. Agric. Biol.* 23, 405–408. doi: 10.17957/IJAB/15.1302

Guo, J. H., Jiang, C. H., Xie, P., Huang, Z. Y., and Fa, Z. H. (2015). The plant healthy and safety guards plant growth promoting rhizobacteria (PGPR). *Transcriptomics* 3:109. doi: 10.4172/2329-8936.1000109

Hudge, B. V. (2015). Management of damping-off disease on soybean caused by *Pythium ultimum* Trow. *Int. J. Curr. Microbiol. Appl. Sci*. 4, 799–808.

Khalimi, K., Darmadi, A. A. K., and Suprapta, D. N. (2019). First report on the prevalence of *Colletotrichum scovillei* associated with anthracnose on chili pepper in Bali, Indonesia. *Int. J. Agric. Biol*. 22, 363–368. doi: 10.17957/IJAB/15.1072

Kim, S. T., and Yun, S. C. (2011). Biocontrol with *Myxococcus* sp. KYC 1126 against anthracnose in hot pepper. *Plant Pathol. J*. 27, 156-163. doi: 10.5423/PPJ.2011.27.2.156

Lim, S. M., Yoon, M. Y., Choi, G. J., Choi, Y. H., Jang, K. S., Shin, T. S., et al. (2017). Diffusible and volatile antifungal compounds produced by an antagonistic *Bacillus vezelensis* G341 against various phytopathogenic fungi. *Plant Pathol. J*. 33, 488–498. doi: 10.5423/PPJ.OA.04.2017.0073

Mahartha, K. A., and Suprapta, D. N. (2018). Efficacy of *Enterobacter cloacae* KtB3 to control damping-off disease on soybean caused by *Sclerotium rolfsii*. *Int. J. Agric. Biol*. 20, 871–876. doi: 10.17957/IJAB/15.0578

Mauch, F., Mauch-Mani, B., and Boller, T. (1988). Antifungal hydrolases in pea tissue. II. Inhibition of fungal growth by combinations of chitinase and 3-1,3 glucanase. *Plant Physiol.* 88, 936–942. doi: 10.1104/pp.88.3.936

Nowak-Thompson, B., Gould, S. J., Kraus, J., and Loper, J. E. (1994). Production of 2,4-diacetylphloroglucinol by the biocontrol agent *Pseudomonas fluorescens* Pf-5. *Can. J. Microbiol*. 40, 1064–1066. doi: 10.1139/m94-168

Park, H. G. (2007). "Problems of anthracnose in pepper and prospects for its management," in *Abstracts of the First International Symposium on Chilli Anthracnose*, eds D. G. Oh, K. T. Kim (Seoul: National Horticultural Research Institute, Rural Development of Administration), 19.

Park, K. Y., Seo, S. Y., Oh, B. R., Seo, J. W., and Kim, Y. J. (2018). 2, 3-butanediol induces systemic acquired resistance in the plant immune response. *J. Plant Biol*. 61, 424–434. doi: 10.1007/s12374-018-0421-z

Parwati, G. A. K. C., Khalimi, K., and Adiartayasa, W. (2014). Efficacy test of *Pantoea agglomerans* GTA24 formulation in controlling damping off disease on soybean caused by *Sclerotium rolfsii*. *Agroekoteknologi Tropika* 3, 218–229 (in Indonesian language).

Poonpolgul, S., and Kumphai, S. (2007). "Chilli pepper anthracnose in Thailand. Country report," in *Abstracts of the First International Symposium on Chili Anthracnose*, eds D. G. Oh, K. T. Kim (Suwon: National Horticultural Research Institute, Rural Development of Administration, Republic of Korea), 23.

Prihatiningsing, N., Djatmiko, H. A., and Erminawati, W. (2019). Bio-management of anthracnose disease in chili with microencapsulates containing Bacillus subtilis B298. *IOP Conf. Series: Earth Environ. Sci.* 250:012041. doi: 10.1088/1755-1315/250/1/012041

Raghunandan, B. L., Patel, M. V., M. N., Patel, M. N., and Mehta, D.M. (2019). Bio-efficacy of different biological agents for management of chili fruit rot/anthracnose disease. *J. Biol. Control.* 33, 163–168. doi: 10.18311/jbc/2019/22716

Reddy, Y. N. P., Jakhar, S. S., and Dahiya, O. S. (2011). Efficiency of bio-fungicides (Trichoderma spp. and *Pseudomonas fluorescens)* on seedling emergence, vigor and health of infected chili seeds (*Capsicum annuum*) by anthracnose fungus *Colletotrichum gloeosporioides* (Penz.) of chili. *Arch. Phytopathol. Plant Prot.* 44, 287–297.

Saharan, B. S., and Nehra, V. (2011). Plant growth promoting rhizobacteria: a critical review. *LSMR*. 21, 1–30.

Saleem, A. R., Bangash, N., Mahmood, T., Khalid, A., Centritto, M., and Siddique, M. T. (2015). Rhizobacteria capable of producing ACC deaminase promote growth of velvet bean (*Mucuna pruriens*) under water stress condition. *Int. J. Agric. Biol*. 17, 663–667. doi: 10.17957/IJAB/17.3.14.788

Sarfraz, S., Sahi, S. T., Ali, M. A., Khan, S. H., and Faure, D. (2019). Antagonistic potential of N-acyl-homoserine lactone degrading *Bacillus* species for controlling *Pectobacterium* based infections in potato. *Int. J. Agric. Biol*. 22, 639–646. doi: 10.17957/IJAB/15.1110

Shahbazi, P., M. Y., Musa, M. Y., Tan, G. Y. A., Avin, F. A., Teo, W. F. A., et al. (2014). *In vitro* and *in vivo* evaluation of *Streptomyces* suppression against anthracnose in chili caused by *Colletotrichum*. *Sains Malaysiana* 43, 697–705.

Shiotsu, F., Sakagami, N., Asagi, N., Suprapta, D. N., N., Agustiani, N., et al. (2015). Initiation and dissemination of organic rice cultivation in Bali, Indonesia. *Sustainability*. 7, 5171–5181. doi: 10.3390/su7055171

Sinaga, M. S. (2006). *Fundamental of Plant Diseases*. Bogor: Penebar Swadaya Publisher. Indonesia (in Indonesian language).

Soesanto, L. (2008). *Introduction to Biological Control of Plant Diseases*. Jakarta: Raja Grafindo Persada.

Suprapta, D. N. (2012). Potential of microbial antagonists as biocontrol agents against plant fungal pathogens. *J. ISSAAS*. 18, 1–18.

Suprapta, D. N., Quintao, V., and Khalimi, K. (2014). Effectiveness of rhizobacteria to reduce rice blast disease intensity. *J. Biol. Agric. Healthcare* 4, 35–41.

Widnyana, I. K., Suprapta, D. N., Sudana, I. M., and Temaja, I. G. R. M. (2013). Pseudomonas alcaligenes, potential antagonist against Fusarium oxysforum f.sp. *lycopersici* the cause of Fusarium wilt disease on tomato. *J. Biol. Agric. and Healthcare*. 3, 163–169.

Conflict of Interest: The author declares that the research was conducted in the absence of any commercial or financial relationships that could be construed as a potential conflict of interest.

Publisher's Note: All claims expressed in this article are solely those of the authors and do not necessarily represent those of their affiliated organizations, or those of the publisher, the editors and the reviewers. Any product that may be evaluated in this article, or claim that may be made by its manufacturer, is not guaranteed or endorsed by the publisher.

frontiers in Sustainable Food Systems

ORIGINAL RESEARCH
published: 08 March 2022
doi: 10.3389/fsufs.2022.857760

Tryptamine 5-Hydroxylase Is Required for Suppression of Cell Death and Uncontrolled Defense Activation in Rice

*Wangxin Shen[1†], Zhiming Feng[1,2†], Keming Hu[1,2], Wenlei Cao[1,2], Mengchen Li[1], Ran Ju[1], Yafang Zhang[1], Zongxiang Chen[1,2] and Shimin Zuo[1,2,3]**

[1] Key Laboratory of Plant Functional Genomics of the Ministry of Education, Jiangsu Key Laboratory of Crop Genomics and Molecular Breeding, Agricultural College of Yangzhou University, Yangzhou, China, [2] Key Laboratory of Crop Genetics and Physiology of Jiangsu Province, Co-innovation Center for Modern Production Technology of Grain Crops of Jiangsu Province, Yangzhou University, Yangzhou, China, [3] Joint International Research Laboratory of Agriculture and Agri-Product Safety, The Ministry of Education of China, Institutes of Agricultural Science and Technology Development, Yangzhou University, Yangzhou, China

OPEN ACCESS

Edited by:
Wei Li,
Hunan Agricultural University, China

Reviewed by:
Jiangbo Fan,
Shanghai Jiao Tong University, China
Xuli Wang,
Chinese Academy of Agricultural Sciences (CAAS), China
Mawsheng Chern,
University of California, Davis, United States

***Correspondence:**
Shimin Zuo
smzuo@yzu.edu.cn

[†] *These authors have contributed equally to this work*

Specialty section:
This article was submitted to Agroecology and Ecosystem Services, a section of the journal Frontiers in Sustainable Food Systems

Received: *19 January 2022*
Accepted: *07 February 2022*
Published: *08 March 2022*

Citation:
Shen W, Feng Z, Hu K, Cao W, Li M, Ju R, Zhang Y, Chen Z and Zuo S (2022) Tryptamine 5-Hydroxylase Is Required for Suppression of Cell Death and Uncontrolled Defense Activation in Rice. Front. Sustain. Food Syst. 6:857760. doi: 10.3389/fsufs.2022.857760

Lesion-mimic mutants are useful materials to dissect mechanisms controlling programmed cell death (PCD) and defense response in plants. Although dozens of lesion-mimic mutant genes have been identified in plants, the molecular mechanisms underlying PCD and defense response remain to be extensively elucidated. Here, we identified a rice lesion mimic mutant, named *lesion mimic 42* (*lm42*), from an ethylmethylsulfone (EMS)-induced mutant population. The *lm42* mutant displayed flame-red spots on the leaves and sheaths at the 3-leaf developmental stage and exhibited impaired photosynthetic capacity with decreased chlorophyll content and decomposed chloroplast thylakoids. The lesion development of *lm42* was light- and temperature-dependent. We identified a single base mutation (T38A), changing a Leu to Gln, in the first exon of *LOC_Os12g16720* (*LM42*), which encodes a tryptamine 5-hydroxylase, by map-based cloning. We carried out transgenic complementation to confirm that this mutation caused the *lm42* phenotype. We further knocked out the *LM42* gene by CRISPR/Cas9 to recreate the *lm42* phenotype. *LM42* is highly expressed in leaves, leaf sheaths and roots. Loss-of-function of *LM42* activated expression of ROS-generating genes and inhibited expression of ROS-scavenging genes, leading to ROS accumulation and eventually cell death. Furthermore, its disruption induced expression of defense-response genes and enhanced host resistance to both fungal pathogen *Magnaporthe oryzae* and bacterial pathogen *Xanthomonas oryzae pv. oryzae*. Our transcriptomic data suggested that the way *lm42* led to lesion-mimic was probably by affecting ribosome development. Overall, our results demonstrate that tryptamine 5-hydroxylase-coding gene *LM42* is required for suppression of cell death and uncontrolled activation of defense responses in rice.

Keywords: *Oryza sativa*, lesion mimic mutant, defense responses, map-based cloning, programmed cell death, RNA-seq

INTRODUCTION

Plants have developed sophisticated mechanisms to prevent pathogen attack, including hypersensitive response (HR) which triggers rapid programmed cell death (PCD) at infection sites to inhibit further pathogen invasion or spread to adjacent cells (Heath, 2000; Williams and Dickman, 2008). Typical physiological events associated with HR include bursts of reactive oxygen species (ROS), followed by accumulation of antibacterial compounds, expression of *pathogenesis-related* (*PR*) genes, and cell wall strengthening through callose deposition or lignin reinforcement (Shirsekar et al., 2014). Although HR plays a critical role in plant immunity, its molecular mechanisms have not been fully clarified.

Lesion-mimic mutants (LMMs) or spotted-leaf (spl) mutants that spontaneously produce HR-like cell death lesions in the absence of biotic stresses or mechanical damage have been reported in a range of plant species (Zhu et al., 2020; Yang et al., 2021). It has been reported that cell death in LMMs mainly results from increased accumulation of ROS including hydrogen peroxide (H_2O_2), superoxide anion (O^{2-}), and singlet oxygen (Qiao et al., 2010; Huang et al., 2016; Chen et al., 2018), which are widely known to kill cells when excessively accumulated. In many cases, LMMs constitutively activate immune responses without pathogen infection, suggesting that most of LMM genes are negative regulators of PCD and defense response (Zhu et al., 2020). Therefore, LMMs are considered ideal materials for deciphering the mechanisms underlying PCD and defense response, providing a useful tool to the development of broad-spectrum disease resistance in plants (Wang et al., 2015).

The first rice LMM named *sekiguchi lesio*n (*sl*) was discovered and confirmed to be controlled by a single recessive gene in 1970 (Kiyosawa, 1970). Since then, various LMMs have been identified based on different lesion phenotypes, including spotted leaf (spl), cell death and resistance (cdr), brown leaf spot (bl), blast lesion mimic mutants (blm), zebra necrosis (zn), probenazol (pbz) and yellow leaf spot (ysl) (Qian et al., 2021). To date, at least 41 genes have been cloned from LMMs in rice that encode a broad range of proteins, such as E3 ubiquitin ligase, protein kinase, chlorophyll synthesis enzyme, ATPase protein, transcription factors, fatty acids/lipids biosynthesis eEF1A-like protein and so on (Zeng et al., 2004; Vega-Sánchez et al., 2008; Sakuraba et al., 2013; Fekih et al., 2015; Matsui et al., 2015; Liu et al., 2017; Hu et al., 2021; Ma et al., 2021; Qiu et al., 2021). Thus, the molecular mechanisms triggering LMMs phenotypes and associated defense responses are not uniform, indicating that the complex network regulating PCD and defense responses needs more investigation.

Here, we identified a stably inherited LMM named *lesion mimic 42* (*lm42*) generated by ethylmethylsulfone (EMS) mutagenesis. At the 3-leaf stage, *lm42* showed flame-red pots on leaves and leaf sheaths and significantly lower quality on main yield-related agronomic traits than wild-type (WT). Through map-based cloning, we identified a single base substitution (T38A) in the first exon of *LOC_Os12g16720*. We further confirmed this single base substitution was the cause of the lesion mimic phenotype of *lm42* by transgenic complementation and CRISPR/Cas9-mediated knockout of *LM42*. Loss-of-function of *LM42* led to cell death, ROS accumulation and enhanced resistance to blast and bacterial blight diseases. RNA-seq data showed that the ribosome abnormality in *lm42* that likely led to its lesion mimic phenotype. Our study provides in-depth insights to the molecular mechanism that regulates PCD and disease resistance in rice.

MATERIALS AND METHODS

Plant Materials

The rice (*Oryza sativa* L) *lm42* mutant was obtained from *japonica* rice Taigeng 394 (T394) mutagenized with EMS treatment. For morphological and genetic analysis, all plants were grown under natural conditions with temperature between 28 and 37°C in Yangzhou City, Jiangsu Province.

Determination of Chlorophyll and Carotenoid Contents

The leaves of WT and *lm42* at tillering stage were harvested to determine chlorophyll and carotenoid contents. Weigh fresh chopped leaves with 0.1 g quartz sand (veins removed), calcium carbonate and 95% ethanol were grinded in a mortar. Add 95% ethanol and continue grinding until the tissues turn white. Let stand at room temperature for 5 min. Filter with a filter paper and funnel, use 95% ethanol to 25 mL, shake well. The chloroplast pigment extract was poured into a colorimetric dish. Using 95% ethanol as blank, the absorbance was measured by spectrophotometer at wavelengths of 470, 646, and 663 nm. Formula for calculating chlorophyll and carotenoid contents: Chla = (12.21* D663-2.81*D646) *0.025/w Chlb = (20.13*D646-5.03* D663) *0.025/w; Chl (a+b) = (17.32*D646-7.18*D663) *0.025/w; Car = (1000*D470-3.27* Chla-104* Chlb)/229*0.025/w.

DNA Extraction and Molecular Marker Development

Genomic DNA was extracted from frozen young leaves using the cetyltrimethylammonium bromide (CTAB) method. Insertion and deletion (InDel) markers were developed and listed in **Supplementary Tables 3**, **4**.

Histochemical Analysis

Leaves of *lm42* and WT were used in histochemical assays at different leaf stages. A lactic acid-phenol-trypan blue solution was used to evaluate cell death, and 3,3'-diaminobenzidine (DAB) solution and tetranitro blue tetrazolium chloride (NBT) solution was used to evaluate H_2O_2 and O^{2-} accumulation, respectively. Staining was conducted as previously described (Wang et al., 2017).

Physiological and Biochemical Analysis

POD and CAT enzyme activities and H_2O_2 and O^{2-} contents at different leaf stages of WT and mutant were measured using kits purchased from Solarbio, Beijing, following manufacturer's instructions.

Temperature and Light Treatment Experiment

For temperature treatment, WT and *lm42* plants growing to the 2-leaf stage were treated at 25, 30, and 35°C separately. At the booting stage, the number of leaves with lesion mimics was continuously identified and recorded, with three repetitions. For light treatment, leaves of WT and mutant at the tillering stage were shaded with 2 cm aluminum foil for 10 days, observed and photos taken.

RNA Extract and RT-qPCR Analysis

RNA samples were extracted using a Trizol reagent (Vazyme). Reverse transcription and fluorescence quantitative PCR analysis were performed using a RT-qPCR system from the company. Primers for RT-qPCR analysis are listed in **Supplementary Table 5**.

Map-Based Cloning, Complementation, and Knock-Out Tests

For genetic analysis, the mapping population was generated from a cross between the *lm42* mutant and the *indica* cultivar 9311. Individuals with lesion-visible leaves from the F_2 generation were selected for initial mapping. For fine mapping, we used SSR markers and designed Indel markers in the localized regions (**Supplementary Tables 2**, **3**). For complementation of the *lm42* mutant, the promoter and coding region of the *LM42* gene were inserted into the pCAMBIA2300 vector, and the resulting plasmid (pCAMBIA-2300-*LM42*) was introduced into the *lm42* mutant. To knock out the *LM42* gene, an 18-bp gene-specific guide RNA sequence targeting *LM42* was cloned into the binary vector containing a Cas9 expression cassette using the Vazyme Enzyme mix. The primers are listed in **Supplementary Table 6**.

Inoculation of Rice Blast and Bacterial Blight

Isolates of 2 *Magnaporthe oryzae* pathotypes (2018-263 and XZ602-3), virulent to WT rice, were used to infect *lm42* plants. Inoculum preparation and seedling inoculation with the isolates followed a previously described procedure (Li et al., 2008). The disease index was calculated as described previously (Wang et al., 2013). *Xanthomonas oryzae pv. oryzae* (*Xoo*) isolate PX099A, virulent to WT rice, was used to evaluate resistance to bacterial blight in *lm42* plants as previously described (Chen et al., 2018). Lesion lengths were measured two weeks after inoculation.

RNA-Seq and Functional Classification of Differentially Expressed Genes

RNA-seq was used to compare transcriptomic differences between WT and *lm42* at the 3-4 leaf stage when the mutant showed visible lesions. The screening criteria for differentially expressed genes were "FC=2" and "p-value < 0.05." Gene Ontology (GO) analysis and Kyoto Encyclopedia of Genes and Genomes (KEGG) were performed using the DAVID Resources 6.7 (http://david.abcc.ncifcrf.gov/) and KEGG analysis website (http://www.kegg.jp/), respectively (Wei et al., 2009; Minoru et al., 2014).

RESULTS

Phenotypic Characterization of the *lm42* Mutant

We identified a stable rice mutant, *lm42*, from an EMS mutagenized population of *japonica* rice Taigeng 394 (T394). The *lm42* mutant carries random flame-red spots that appear on leaves and leaf sheaths starting at the 3-leaf stage (**Figures 1a,b**). At the tillering stage, the distribution and size of spots on *lm42* leaves appears random and follows no particular orders (**Figure 1c**). Lower leaves and leaf sheaths dry out significantly earlier in *lm42* than in WT (**Figure 1d**). The *lm42* mutation also affects agronomic traits, including plant height, effective panicle number, panicle length, grain number per panicle, seed setting rate and 1,000-grain weight, significantly decreasing their yield-related performance in field tests (**Figure 1d**, **Supplementary Table 1**).

To explore whether the photosynthetic capacity of *lm42* was affected, we examined chlorophyll and carotenoid contents, and found that chlorophyll a, chlorophyll b and carotenoid contents in *lm42* were significantly lower than in WT (**Figure 1e**). In addition, RT-qPCR showed that the expression levels of four photosynthesis-related genes *cab2R*, *PsbB*, *Pabc*, and *PsbA* were significantly lower in *lm42* than in WT (**Figures 1f–i**). Examination with transmission electron microscopy (TEM) showed that the number of thylakoid and thylakoid grana decreased, demonstrating the chloroplast thylakoids decomposed after the appearance of lesions in *lm42* leaves at the tillering stage (**Figures 1j,k**). These results suggest that the reduction on photosynthetic ability in *lm42* is likely due to the abnormal chloroplasts with decreased chlorophyll and carotenoid contents.

Lesion Occurrence in *lm42* Depends on Light and Temperature

The lesion initiation of many LMMs depends on light or temperature (Huang et al., 2010). In order to determine whether the lesion phenotype of *lm42* was affected by light and temperature, we first treated *lm42* and WT at 2-3 leaf stage (before appearance of lesions) at 25, 30, and 35°C separately (**Figure 2a**). We found that although all three temperatures caused the lesion phenotype at the 3rd day, high temperature produced significantly more leaves with lesions than low temperature (**Figures 2b–e**). Shading treatment was then performed on *lm42* leaves by covering *lm42* leaves with a piece of 2 cm aluminum foil for 7 days. The results showed that lesions did not appear in the shaded leaf areas, while lesions emerged in the unshaded leaf areas in *lm42* (**Figure 2f**). These data indicate that the lesion formation in *lm42* was regulated by light and temperature.

Map-Based Cloning Identified a Single Base Substitution in *lm42*

To assess the genetic nature of the *lm42* lesion phenotype, we carried out a cross between *lm42* and WT, and found that the hybrid F_1 plants all exhibited WT phenotype during the whole growth period, suggesting a recessive nature for the phenotype. In the self-pollinated progeny (F_2 population) of F_1 plants, we

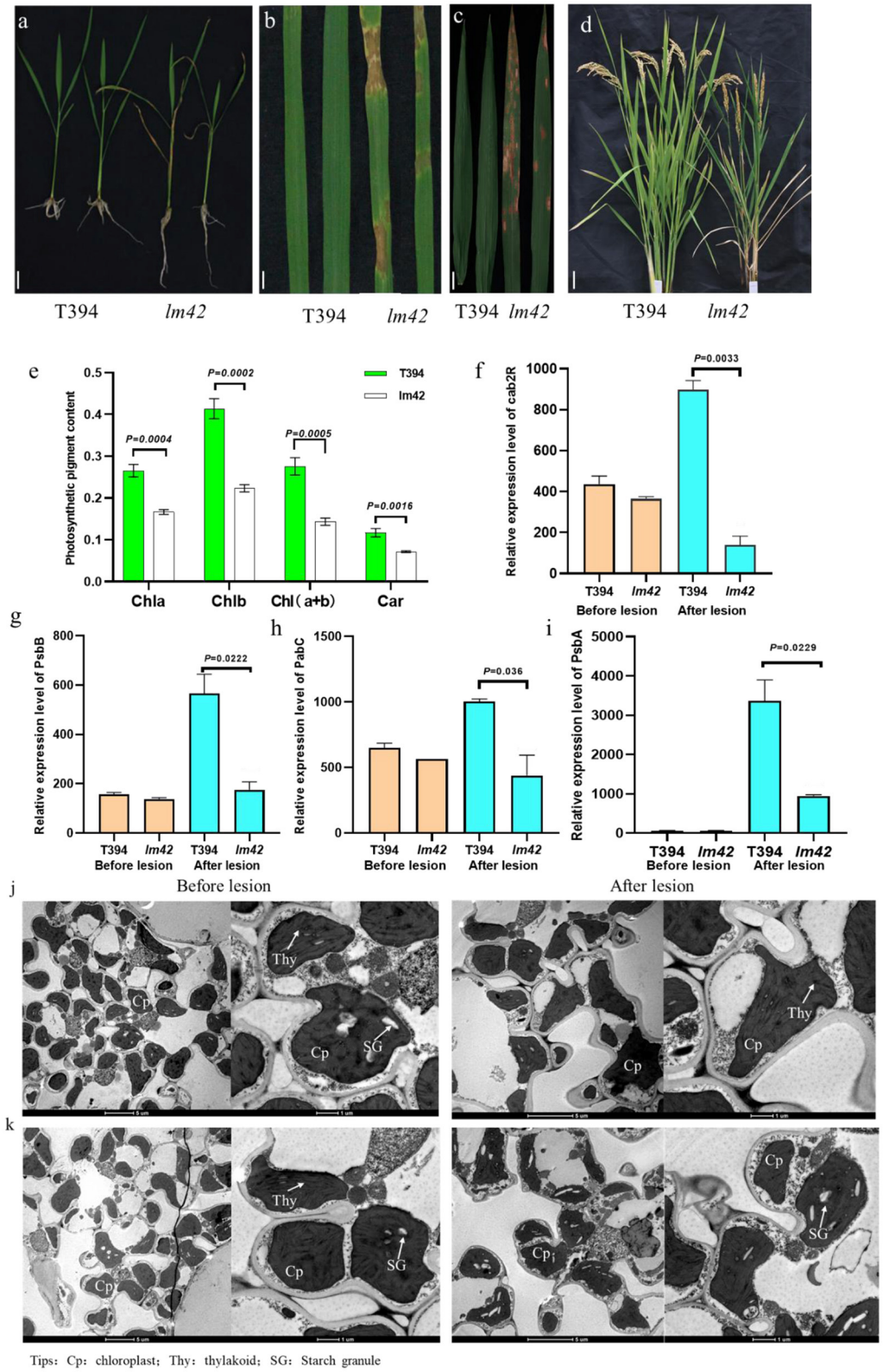

FIGURE 1 | Phenotypic characterization of *lm42*. **(a,b)** The *lm42* lesion mimic phenotype at seedling stage. **(c)** Location and size of lesions on *lm42* leaves at tillering stage. **(d)** Plant stature and leaf senescence of *lm42* at maturity stage, scale bars, 1 cm. **(e)** Contents of photosynthetic pigments at tillering stage. **(f–i)** RNA levels of photosynthesis-related genes determined by RT-qPCR. **(j,k)** Observation of chloroplasts by TEM in WT **(j)** and *lm42* **(k)**, scale bars, 5 and 1 μm.

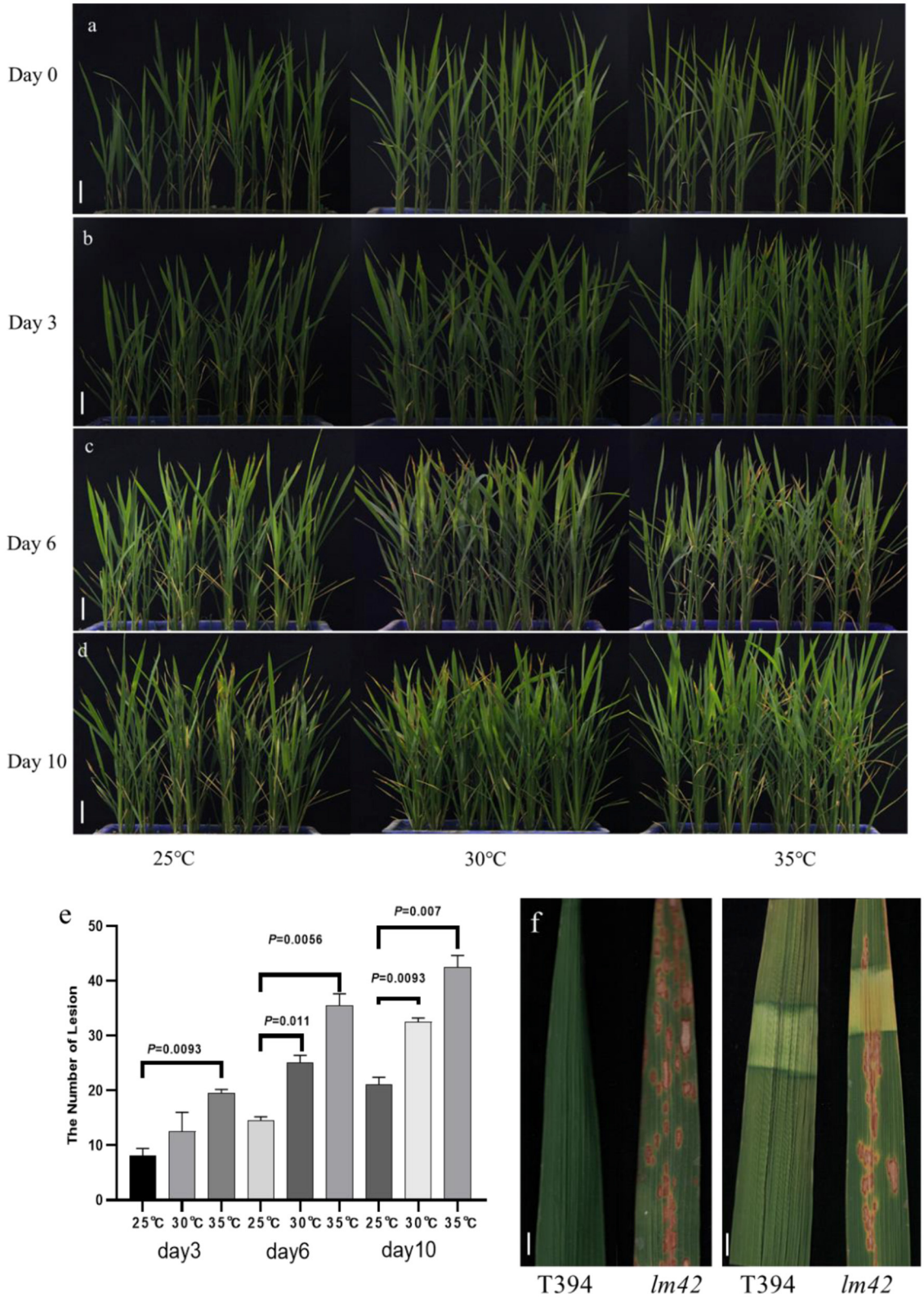

FIGURE 2 | Light and temperature influence lesion formation in *lm42*. **(a–d)** The phenotypes of WT and *lm42* were observed at 0 **(a)**, 3 **(b)**, 6 **(c)**, and 10 **(d)** days at different temperatures. **(e)** Number of lesion mimic leaves in *lm42* at 3, 6, and 10 days at different temperatures. **(f)** Effects of shading treatment on lesion formation, scale bars, 1 cm.

observed a segregation of WT and *lm42* phenotypes in a 3:1 ratio (**Supplementary Table 2**). These data indicate that the *lm42* phenotype is conferred by a single recessive gene.

To map the *LM42* locus, we developed an F_2 population from the cross of *lm42* and *indica* cv. 9311. We first genotyped 15 F_2 individuals with WT phenotype and another 15 with mutant phenotype using 280 SSR markers randomly distributed on the rice genome, yielding a preliminary map region containing *LM42* located between markers RM27808 and RM1337 on chromosome 12 (**Figure 3A**, **Supplementary Table 3**). We further developed 6 polymorphic Indel markers to fine-map the *LM42* gene with a total of 745 F_2 plants with mutant phenotype, which allowed us to finally narrowed down the *LM42* gene to a 30 kb region between markers Indel13 and Indel38 (**Figure 3B**, **Supplementary Table 4**). According to the rice Genome Interpretation database (https://www.gramene.org/), seven open reading frames (ORFs) were annotated in this region (**Figure 3C**). Comparison of our sequencing data revealed that the fourth ORF (*LOC_Os12g16720*) carried a single-base substitution (T38A) in *lm42* (**Supplementary Table 5**), leading to a single amino acid change from leucine (Leu) to glutamine (Gln). The other six ORFs showed no differences between *lm42* and WT (**Figure 3D**). We subsequently developed a dCAPs marker for this T/A SNP: the PCR product from *lm42* is digested by the Alu I enzyme into two fragments (126 and 39 bp), whereas the WT PCR product is not cut. A screen of the F2 population with this dCAPs marker confirmed the association of this SNP with the phenotype (**Supplementary Figure 1**). Therefore, *LOC_Os12g16720*, encoding a tryptamine 5-hydroxylase/cytochrome P450 monooxygenase, is the candidate gene for *LM42*.

Transgenic Complementation and CRISPR/Cas9-Mediated Knockout Validate the *LM42* Gene

In order to verify the candidate gene, we generated a construct (pCAMBIA-2300-*LM42*) containing the upstream 2.5 kb promoter and the full-length coding region genomic DNA of *LM42* from WT for complementation. We introduced the *LM42* gene into the *lm42* mutant through *Agrobacterium*-mediated transformation, and obtained 4 T_0 transgenic plants confirmed by PCR genotyping. We found that all four independent transformants showed WT phenotype exhibiting no lesion mimics across the whole life cycle, whereas negative controls regenerated from the same tissue culture containing no transgene exhibited the mutant phenotype (**Figures 3E,F**). Also, the overall agronomic traits of the positive transformants were similar with that of WT (**Supplementary Figure 2A**, **Supplementary Table 8**). This result demonstrated that the WT candidate gene can rescue the lesion phenotype of the *lm42* mutant.

Furthermore, we generated two *LM42* knockout plants in the *japonica* variety Nipponbare (NIP) background using the CRISPR/Cas9 technology. After sequencing candidate transgenic lines, we obtained two *LM42* knockout (ko) T_0 plants: one contained a heterozygous two-base insertion and the other a one-base insertion, both causing loss-of-function due to frameshifts (**Supplementary Figure 2B**). For the two heterozygous LM42-ko T0 plants, we observed no lesion mimics throughout the whole growth stage, whereas we found that some T_1 plants of each line showed clear lesion mimic phenotype, like the *lm42* mutant (**Figure 3G**). What's more, the major agronomic phenotype of LM42-ko lines were similar with that of *lm42* mutant (**Supplementary Figure 2C**, **Supplementary Table 9**). This result indicates that knockouts of *LOC_Os12g16720* cause the *lm42* lesion mimic phenotype. Together, these results demonstrate that the *lm42* lesion mimic phenotype is caused by mutations that block the function of *LOC_Os12g16720*.

ROS Accumulation and Cell Death Occur in the *lm42* Mutant

To assess the expression pattern of *LM42*, we ran RT-qPCR to monitor *LM42* transcript levels and found that *LM42* was mainly expressed in roots, leaves and leaf sheaths (**Figure 3H**). To detect whether cell death occurred in *lm42*, we firstly carried out trypan blue staining (Qiao et al., 2010) and observed more and darker blue spots on *lm42* than on WT leaves (**Figure 4A**), indicating that severe cell death occurred in *lm42*. We next assessed expression levels of *metacaspase* family genes that are usually associated with PCD (Fagundes et al., 2015) and found changes in their expression levels: *OSMC1-OSMC4* were down-regulated whereas *OSMC5-OSMC7* were up-regulated in *lm42* (**Supplementary Figure 3A**).

ROS are major signal molecules in plant PCD and may lead to cellular damage (Khanna-Chopra, 2012). To determine ROS levels in *lm42*, we firstly carried out 3,3'-diaminobenzidine (DAB) staining, an indicator of H_2O_2 accumulation, and found more brown precipitates around lesion sites in *lm42* leaves than in WT leaves (**Figure 4B**). In agreement with DAB staining, H_2O_2 contents were significantly higher in *lm42* than in WT when quantified (**Supplementary Figure 3B**). In addition, we found that the content of CAT in mutant was higher than that in WT, indicating that the increased content of CAT was not enough to remove excessive ROS in mutant (**Supplementary Figure 3C**). We next assessed O^{2-} contents by staining leaves with tetranitro blue tetrazolium chloride (NBT), an indicator of O^{2-} accumulation. We observed much more blue spots on *lm42* than on WT leaves (**Figure 4C**), indicating higher O^{2-} contents in *lm42* (**Supplementary Figures 3D,E**). We further found that genes encoding ROS-scavenging enzymes (*CATC* and *SODCC1*) were significantly down-regulated whereas ROS-generating enzymes (*NOX2* and *PAO*) were upregulated in *lm42* compared to WT (**Figures 4D–G**). Together, these results indicate excess accumulation of ROS in *lm42*, which likely causes cell death in *lm42*.

lm42 Confers Enhanced Resistance to Bacterial Blight and Blast Diseases

The lesion mimic phenotype of *lm42* resembles the HR that occurs in plants following infection by many pathogens. Many LMMs show enhanced resistance to fungal and bacterial pathogens (Zhu et al., 2020). Thus, we tested whether *lm42*

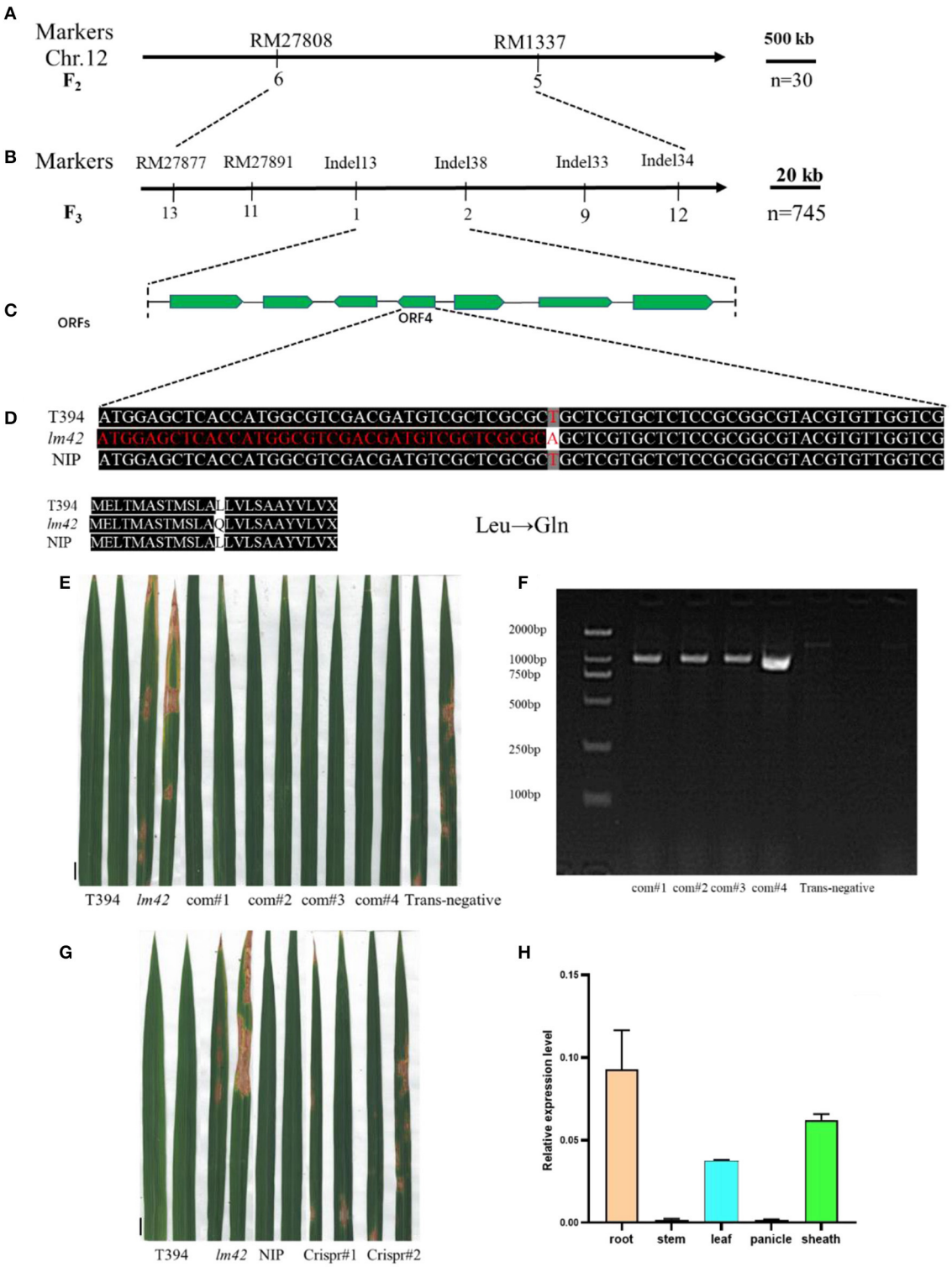

FIGURE 3 | Map-based identification of the *LM42* gene. **(A)** *LM42* was initially mapped on chromosome 12 between markers RM27808 and RM1337. **(B)** The *LM42* locus was fine-mapped to a 30-kb genomic region between markers Indel13 and Indel38; the number below a primer represents the number of recombinants. **(C)** Seven putative ORFs are located in the ~30-kb identified region. **(D)** Sequence comparison at the mutation site for wild type and the *lm42* mutant; a T-to-A point mutation is present, resulting in a substitution of Leu by Gln. **(E)** Lesion mimic phenotype of *LOC_Os12g16720* knock-out lines. **(F)** Lesion mimic phenotype of *LOC_Os12g16720* complemented lines, scale bars, 1 cm. **(G)** PCR products of *LOC_Os12g16720* for positive complementation lines, scale bars, 1 cm. **(H)** *LM42* RNA expression in various tissues.

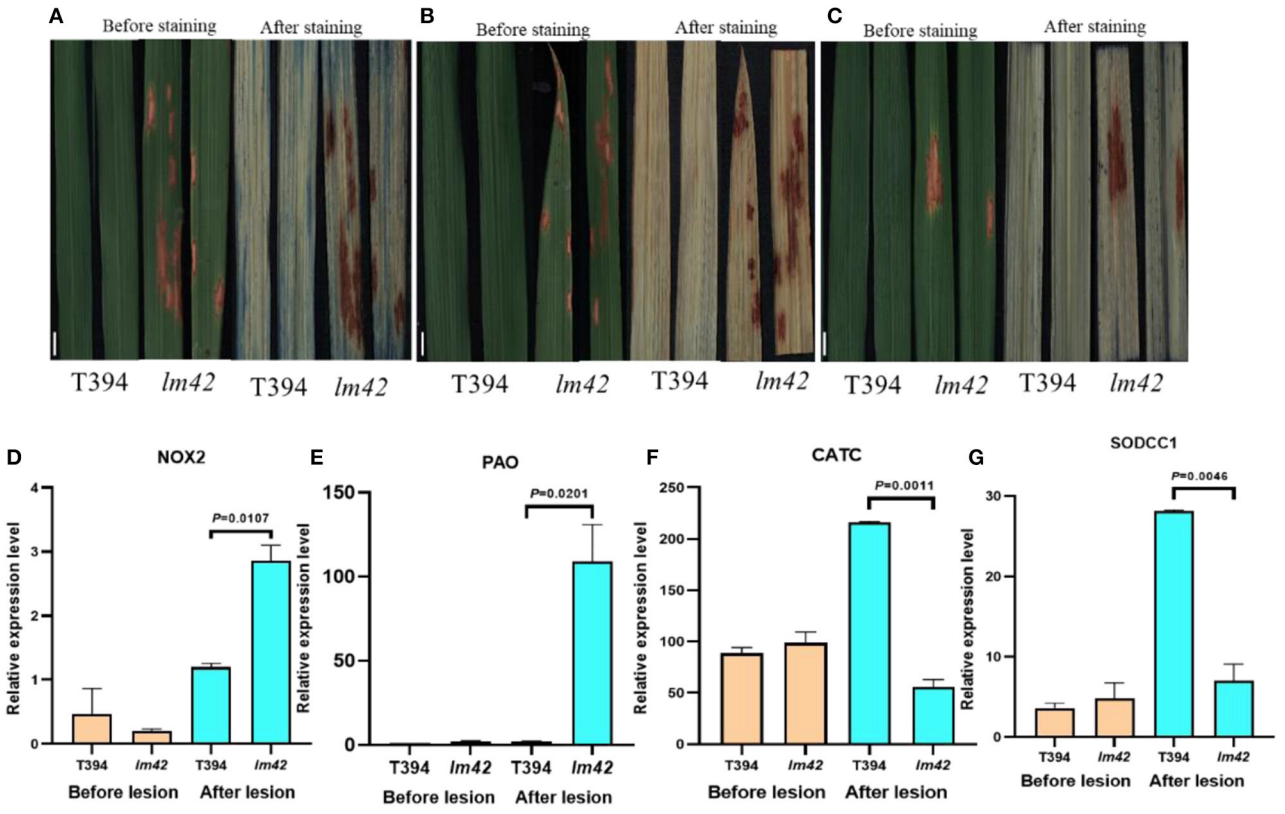

FIGURE 4 | Cell death and ROS accumulation occur in *lm42*. **(A)** Comparison of trypan blue staining between WT and *lm42* leaves at tillering stage, scale bars, 1 cm. **(B)** Comparison of DAB staining between WT and *lm42* leaves at tillering stage, scale bars, 1 cm. **(C)** Comparison of NBT staining between WT and *lm42* leaves at tillering stage, scale bars, 1 cm. **(D,E)** Expression levels of genes encoding ROS-generating enzymes NOX2 and PAO. **(F,G)** Expression levels of genes encoding ROS-scavenging enzymes CATC and SODCC1.

also gained disease resistance. We inoculated *lm42* and WT plants with two common rice fungal and bacterial pathogens: two *M. oryzae* isolates and a *Xoo* pathotype that are virulent on WT plants. Compared with WT, we found that *lm42* developed significantly shorter lesion lengths than WT for all isolates of the two pathogens, demonstrating that the *lm42* mutant significantly enhanced resistance to the two common rice bacterial and fungal pathogens (**Figures 5A–D**).

To determine whether defense response genes were induced in *lm42*, we assessed the expression levels of defense-related genes *PBZ1, PR1, PR1a, POX22.3, PAL1*, and *PR10* (Hou et al., 2012) in *lm42* and WT plants at 2-leaf stage (before appearance of visible lesions) and 3-4 leaf stage (clearly visible lesions) by RT-qPCR. At 2-leaf stage, we found that these genes showed similar expression levels in WT and *lm42*. In contrast, at 3-4 leaf stage, their expression levels were significantly elevated in *lm42* than in WT (**Figures 5E–J**). These results suggest that *LM42/LOC_Os12g16720* functions to suppress the defense response and disease resistance.

LM42 Affects Multiple Biological Pathways

To probe the molecular basis underlying the cell death and defense activation in *lm42*, we performed RNA-seq to assess transcriptomes of *lm42* and WT at the 3-4 leaf stage when mutant plants showed visible lesions. Based on our RNA-seq data, we identified 6,409 differentially expressed genes (DEGs) comparing *lm42* to WT, including 3,789 up-regulated and 2,620 down-regulated genes (**Figures 6A,B**). GO functional enrichment including cellular components, biological processes and molecular functions was performed on these 6,409 DEGs (**Figure 6B**). For cellular components, ribosome was the most prevalent class including 164 DEGs, followed by proteasome complex, photosynthesis synthesis and mitochondrial inner membrane. For biological processes, translation was the most prevalent class including 144 DEGs, followed by glycolysis and photosynthesis. For molecular function, structural constituent of ribosome and iron ion binding were the two most prevalent classes each including nearly 150 DEGs, followed by oxidoreductase activity of degrading ROS, metal ion binding, transferase activity, magnesium ion binding and pyridoxal phosphate binding.

To further explore the biological pathways in which *LM42* may be involved, we performed KEGG enrichment analysis for the DEGs, and found that 9 pathways were significantly ($P < 0.01$) enriched (**Figure 6B**). The highly enriched pathways are mainly related to protein

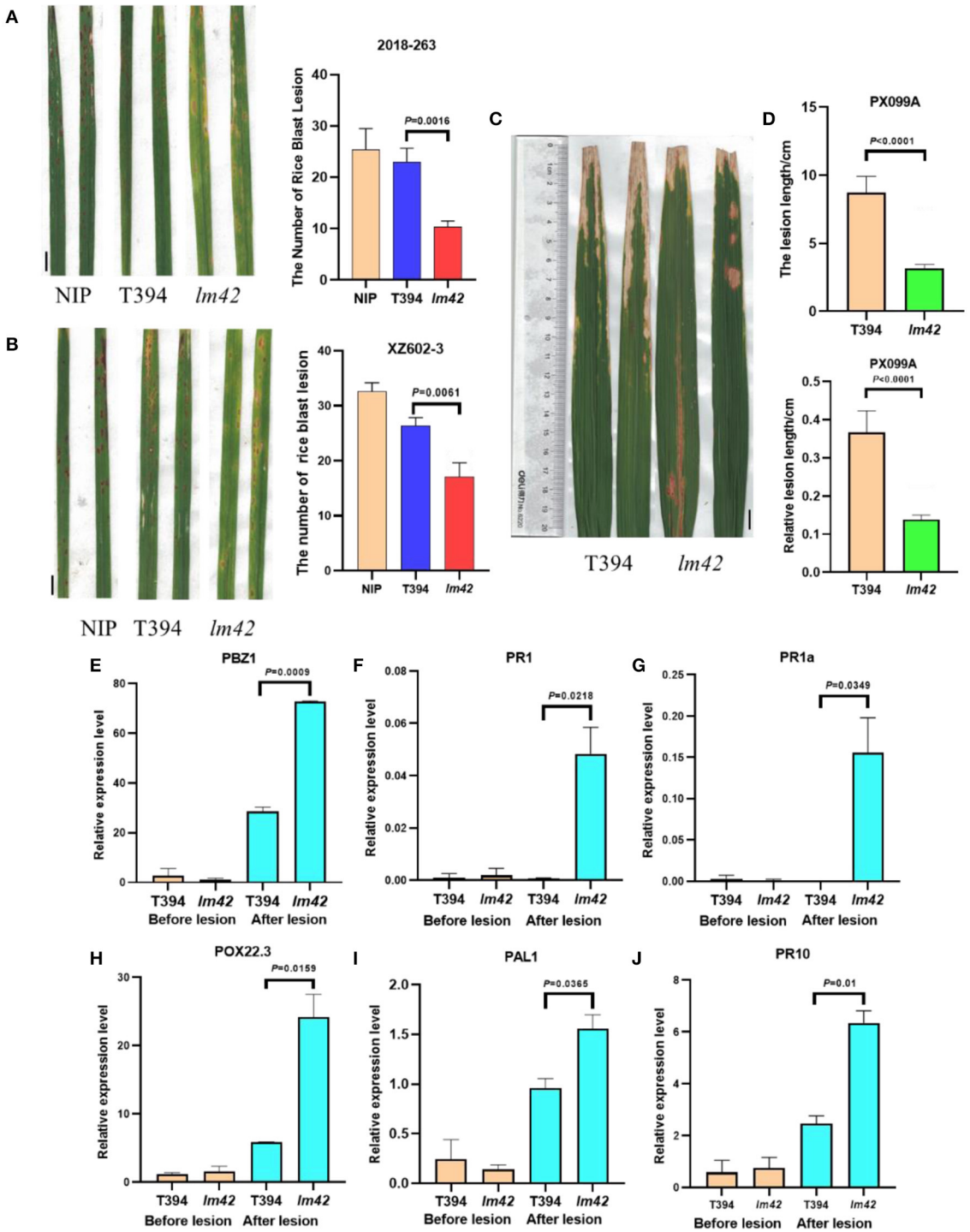

FIGURE 5 | Defense responses are activated in *lm42*. **(A,B)** Lesions on WT and *lm42* leaves developed after infection with rice blast races 2018-263 **(A)** and XZ602-3 **(B)**, scale bars, 1 cm. **(C,D)** Lesion lengths on WT and *lm42* leaves developed 14 days post inoculation with bacterial blight race PX099A, scale bars, 1 cm. **(E–J)** Expression levels of defense-related genes before (orange bars) and after (cyan bars) the appearance of lesions in *lm42*.

synthesis (including ribosome and biosynthesis of amino acids), redox (including oxidative phosphorylation and glutathione metabolism), carbon metabolism (including carbon fixation in photosynthetic organisms, glyoxylate and dicarboxylate metabolism and pentose phosphate pathway), and photosynthesis. Together, these results suggest that *LM42* likely regulates cell death and plant defense through affecting these functional pathways.

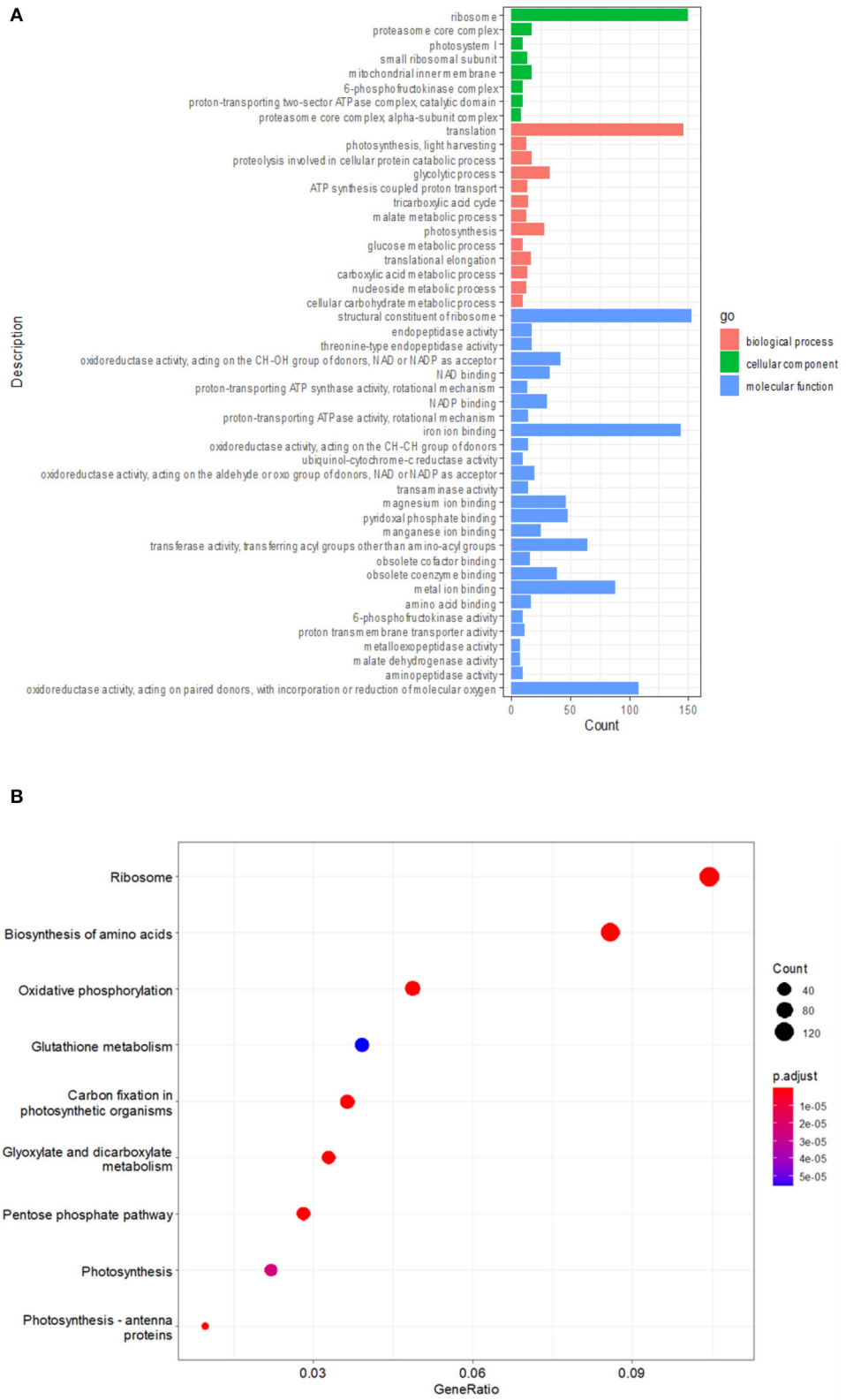

FIGURE 6 | Multiple biological pathways affected in *lm42* as revealed by RNA-seq. **(A)** GO enrichment analysis of differentially expressed genes before and after lesion appearance. **(B)** KEGG analysis of differentially expressed genes before and after lesion appearance.

DISCUSSION

LMMs are often used as a tool to study plant PCD and defense response because they autonomously form necrotic lesions resembling activation of the immune response in the absence of pathogen attack (Sun et al., 2011). In this study, a mutant allele of the previously characterized gene *SL* was identified (Fujiwara et al., 2010). We named the mutant *lm42* and cloned the *LM42* gene *via* a map-based cloning strategy. *SL* encodes a cytochrome P450 monooxygenase, which has tryptamine 5-hydroxylase activity and can catalyze the conversion of tryptamine to 5-hydroxytryptamine. However, previous report showed no detailed analysis on how this gene caused lesion mimic symptoms (Fujiwara et al., 2010). Through various staining analyses and physiological and biochemical tests, we confirmed that irreversible ROS bursts and PCD occurred in mutant leaves after the appearance of lesions. In the same leaf, ROS accumulation and PCD only occurred at the lesion sites, but not at areas without lesions, indicating that the occurrence of lesions in *lm42* is tightly associated with ROS bursts (**Figures 4B,C**). Recently, Cui et al. (2020) identified another mutant allele of the *SL* gene in the *ell1* mutant and also detected excessive accumulation of ROS, which is consistent with our results. However, the mechanism underlying how *lm42/ell1/sl* mutations cause excessive accumulation of ROS and PCD remains unclear. Therefore, we performed the transcriptomic sequencing for WT and *lm42* at the 3-4 leaf stage when lesions are clearly visible (**Figure 6**). Combined with the functional analysis results of DEGs, we hypothesize that the *lm42* mutation may lead to ribosome abnormality which ultimately triggers PCD. This hypothesis is based on two aspects: First, LM42/ELL1/SL is located in the endoplasmic reticulum (ER) rather than in chloroplasts (Cui et al., 2020). Ribosomes are attached to the membranes of the ER. Second, our GO and KEGG functional enrichment analyses of DEGs showed that DEGs involved in ribosome function or assembly were most prevalent (**Figures 6C,D**). Ribosomes are the key organelle for the biosynthesis and transport of all proteins. If damaged, it will in particular affect the biosynthesis and transport of many ion binding proteins, which are necessary for the maintenance of oxidoreductase activities associated with ROS-scavenging and photosynthesis (Suo et al., 2020). As a result, ROS were excessively accumulated, and toxic substances produced in the process of photosynthesis could not be timely degraded either, which ultimately cause damages in chloroplasts leading to cell death.

Mutations in many *LMM* genes lead to significantly enhanced disease resistance and their molecular mechanisms regulating defense response are very diverse and complicated (Zhu et al., 2020; Qian et al., 2021). Previous research found that *LM42/ELL1/SL* was induced by the chitin elicitor and by infection with *Magnaporthe oryzae*. Also, application of 5-hydroxytryptamine induced expression of defense genes and cell death in rice (Fujiwara et al., 2010; Tian et al., 2020). In this study, we further confirmed that *LM42* negatively regulates defense-response gene expression and resistance to both fungal pathogen *M. oryzae* and bacterial pathogen *Xoo* (**Figures 5A–D**). However, to date, the molecular mechanism of *LM42/ELL1/SL*-mediated immune response is not all clear. It was reported that there is mutual antagonistic regulation between 5-hydroxytryptamine biosynthesis and salicylic acid (SA) biosynthesis. Their biosynthesis pathways share the common source substance—chorismic acid, and they actively inhibit the activity of biosynthesis genes of the other pathway (Lu et al., 2018). SA is a well-known defense signal against biotrophic pathogens (Zavaliev et al., 2020). Thus, we reason that the molecular mechanism underlying the *lm42/ell1/sl*-mediated immune response is likely related to a release of the suppression of SA biosynthesis and signaling when the 5-hydroxytryptamine biosynthesis pathway is blocked due to the *lm42* mutation. Whether this is true or not requires further investigation.

DATA AVAILABILITY STATEMENT

The datasets presented in this study can be found in online repositories. The names of the repository/repositories and accession number(s) can be found in the article/**Supplementary Material**.

AUTHOR CONTRIBUTIONS

WS, ZF, KH, WC, ML, and RJ conceived and designed the experiments. WS, ZF, ML, and RJ performed the experiments and analyzed the data. ZC was responsible for material plant and field management. WS and ZF wrote the manuscript. SZ revised the manuscript. All authors read and approved the manuscript.

FUNDING

This study was supported by the Natural Science Foundation of China (31872013 and 32000362) and of Jiangsu Province (BK20200930), a Project Funded by the Priority Academic Program Development of Jiangsu Higher Education Institutions (PAPD), and the Scientific Research Innovation Practice Project for postgraduate students of Jiangsu (KYCX21_3248).

SUPPLEMENTARY MATERIAL

The Supplementary Material for this article can be found online at: https://www.frontiersin.org/articles/10.3389/fsufs.2022.857760/full#supplementary-material

REFERENCES

Chen, Z., Chen, T., Sathe, A., He, Y., Zhang, X., and Wu, J. (2018). Identification of a novel semi-dominant spotted-leaf mutant with enhanced resistance to *Xanthomonas oryzae pv*. oryzae in rice. *Int. J. Mol. Sci*. 19:3766. doi: 10.3390/ijms19123766

Cui, Y., Peng, Y., Zhang, Q., Xia, S., Ruan, B., Xu, Q., et al. (2020). Disruption of Early Lesion Leaf 1, encoding a cytochrome P450 monooxygenase,

induces ROS accumulation and cell death in rice. *Plant J*. 105, 942–956. doi: 10.1111/tpj.15079

Fagundes, D., Bohn, B., Cabreira, C., Leipelt, F., Dias, N., Bodanese-Zanettini, M., et al. (2015). Caspases in plants: metacaspase gene family in plant stress responses. *Funct. Integr. Genom*. 15, 639–649. doi: 10.1007/s10142-015-0459-7

Fekih, R., Tamiru, M., Kanzaki, H., Kanzaki, H., Abe, A., Yoshida, K., et al. (2015). The rice (*Oryza sativa* L.) lesion mimic resembling, which encodes an AAA-type ATPase, is implicated in defense response. *Mol. Genet. Genom*. 29, 611–622. doi: 10.1007/s00438-014-0944-z

Fujiwara, T., Maisonneuve, S., Isshiki, M., Mizutani, M., Chen, L., Wong, H., et al. (2010). Sekiguchi lesion gene encodes a cytochrome P450 monooxygenase that catalyzes conversion of tryptamine to serotonin in rice. *J. Biol. Chem*. 285, 11308–11313. doi: 10.1074/jbc.M109.091371

Heath, M. (2000). Hypersensitive response-related death. *Plant Mol. Biol*. 44, 77–90. doi: 10.1023/A:1026592509060

Hou, M., Xu, W., Bai, H., Liu, Y., Li, L., Liu, L., et al. (2012). Characteristic expression of rice pathogenesis-related proteins in rice leaves during interactions with *Xanthomonas oryzae pv*. oryzae. *Plant Cell Rep*. 31, 895–904. doi: 10.1007/s00299-011-1210-z

Hu, H., Ren, D., Hu, J., Jiang, H., Chen, P., Zeng, D., et al. (2021). White and Lesion-mimic leaf1, encoding a lumazine synthase, affects ROS balance and chloroplast development in rice. *Plant J*. 108, 1690–1703. doi: 10.1111/tpj.15537

Huang, Q., Shi, Y., Zhang, X., Song, L., Feng, B., Wang, H., et al. (2016). Single base substitution in OsCDC48 is responsible for premature senescence and death phenotype in rice. *J. Integr. Plant Biol*. 58, 12–28. doi: 10.1111/jipb.12372

Huang, Q., Yang, Y., Shi, Y., Chen, J., and Wu, J. (2010). Spotted-leaf mutants of rice (*Oryza sativa*). *Rice Sci*. 17, 247–256. doi: 10.1016/S1672-6308(09)60024-X

Khanna-Chopra, R. (2012). Leaf senescence and abiotic stresses share reactive oxygen species-mediated chloroplast degradation. *Protoplasma* 249, 469–481. doi: 10.1007/s00709-011-0308-z

Kiyosawa, S. (1970). Inheritance of a particular sensitivity of the rice variety, Sekiguchi-Asahi, to pathogens and chemicals, and linkage relationship with blast resistance. *Nogyo Gijutsu Kenkyusho Hokoku* 21, 61–71.

Li, W., Lei, C., Cheng, Z., Jia, Y., Huang, D., Wang, J., et al. (2008). Identification of SSR markers for a broad-spectrum blast resistance gene Pi20(t) for marker-assisted breeding. *Mol. Breed*. 22, 141–149. doi: 10.1007/s11032-008-9163-9

Liu, Q., Ning, Y., Zhang, Y., Yu, N., Zhao, C., Zhan, X., et al. (2017). OsCUL3a negatively regulates cell death and immunity by degrading OsNPR1 in rice. *Plant Cell* 292, 345–359. doi: 10.1105/tpc.16.00650

Lu, H., Luo, T., Fu, H., Wang, L., Tan, Y., Huang, J., et al. (2018). Resistance of rice to insect pests mediated by suppression of serotonin biosynthesis. *Nat. Plants* 4, 338–344. doi: 10.1038/s41477-018-0152-7

Ma, H., Li, J., Ma, L., Wang, P., Xue, Y., Yin, P., et al. (2021). Pathogen-inducible OsMPKK10.2-OsMPK6 cascade phosphorylates the Raf-like kinase OsEDR1 and inhibits its scaffold function to promote rice disease resistance. *Mol. Plant* 14, 620–632. doi: 10.1016/j.molp.2021.01.008

Matsui, H., Takahashi, A., Hirochika, H. (2015). Rice immune regulator, OsPti1a, is specifically phosphorylated at the plasma membrane. *Plant Signal. Behav*. 10:e991569. doi: 10.4161/15592324.2014.991569

Minoru, K., Susumu, G., Yoko, S., Kawashima, M., Furumichi, M., and Tanabe, M. (2014). Data, information, knowledge and principle: back to metabolism in KEGG. *Nucl. Acids Res*. 42, 199–205. doi: 10.1093/nar/gkt1076

Qian, J., Liu, F., Qu, C., and Yue, W. (2021). Research progress on cloning and mechanism of rice lesion mimic mutation gene. *Mol. Plant Breed*. 19, 3274–3280. doi: 10.5376/rgg.2020.11.0002

Qiao, Y., Jiang, W., Lee, J., Park, B., Choi, M., Piao, R., et al. (2010). SPL28 encodes a clathrinassociated adaptor protein complex 1, medium subunit micro 1 (AP1M1) and is responsible for spotted leaf and early senescence in rice (*Oryza sativa*). *N. Phytologist* 18, 258–274. doi: 10.1111/j.1469-8137.2009.03047.x

Qiu, T., Zhao, X., Feng, H., Qi, L., Yang, J., Penget, Y., et al. (2021). OsNBL3, a mitochondrion-localized pentatricopeptide repeat protein, is involved in splicing nad5 intron 4 and its disruption causes lesion mimic phenotype with enhanced resistance to biotic and abiotic stresses. *Plant Biotechnol. J*. 19, 2277–2290. doi: 10.1111/pbi.13659

Sakuraba, Y., Rahman, M., Cho, S., Kim, Y., Koh, H., Yoo, S., et al. (2013). The rice faded green leaf locus encodes protochlorophyllide oxidoreductase B and is essential for chlorophyll synthesis under high light conditions. *Plant J*. 74, 122–133. doi: 10.1111/tpj.12110

Shirsekar, G., Vega-Sanchez, M., Bordeos, A., Baraoidan, M., Swisshelm, A., Fan, J., et al. (2014). Identification and characterization of suppressor mutants of spl11-mediated cell death in rice. *Mol. Plant Microbe Interact*. 27, 528–536. doi: 10.1094/MPMI-08-13-0259-R

Sun, C., Liu, L., Tang, J., Lin, A., Zhang, F., Fang, J., et al. (2011). RLIN1, encoding a putative coproporphyrinogen III oxidase, is involved in lesion initiation in rice. *J. Genet. Genom*. 38, 29–37. doi: 10.1016/j.jcg.2010.12.001

Suo, J., Zhang, H., Zhao, Q., Zhang, N., Zhang, Y., Li, Y., et al. (2020). Na_2CO_3-responsive photosynthetic and ROS scavenging mechanisms in chloroplasts of alkaligrass revealed by phosphoproteomics. *Genom. Proteom. Bioinformat*. 18, 271–288. doi: 10.1016/j.gpb.2018.10.011

Tian, D., Fang, F., Niu, Y., Lin, Y., Chen, Z., Li, G., et al. (2020). Loss function of SL (sekiguchi lesion) in the rice cultivar Minghui 86 leads to enhanced resistance to (hemi)biotrophic pathogens. *BMC Plant Biol*. 20:507. doi: 10.1186/s12870-020-02724-6

Vega-Sánchez, M., Zeng, L., Chen, S., Leung, H., and Wang, G. (2008). SPIN1, a komology domain protein negatively regulated and ubiquitinated by the E3 ubiquitin ligase SPL11, is involved in flowering time control in rice. *Plant Cell* 20, 1456–1469. doi: 10.1105/tpc.108.058610

Wang, S., Lei, C., Wang, J., Ma, J., Tang, S., Wang, C., et al. (2017). SPL33, encoding an eEF1A-like protein, negatively regulates cell death and defense responses in rice. *J. Exp. Bot*. 68, 899–913. doi: 10.1093/jxb/erx001

Wang, Y., Liu, S., Mao, X., Zhang, Z., Jiang, H., Chai, R., et al. (2013). Identification and characterization of rhizosphere fungal strain MF-91 antagonistic to rice blast and sheath blight pathogens. *J. Appl. Microbiol*. 114, 1480–1490. doi: 10.1111/jam.12153

Wang, Z., Wang, Y., Hong, X., Hu, D., Liu, C., Yang, J., et al. (2015). Functional inactivation of UDP-N-acetylglucosamine pyrophosphorylase 1 (UAP1) induces early leaf senescence and defence responses in rice. *J. Exp. Bot*. 66, 973–987. doi: 10.1093/jxb/eru456

Wei, H., Sherman, B., and Lempicki, R. (2009). Bioinformatics enrichment tools: paths toward the comprehensive functional analysis of large gene lists. *Nucl. Acids Res*. 37, 1–13. doi: 10.1093/nar/gkn923

Williams, B., and Dickman, M. (2008). Plant programmed cell death: can't live with it; can't live without it. *Mol. Plant Pathol*. 9, 534–544. doi: 10.1111/j.1364-3703.2008.00473.x

Yang, Y., Lin, Q., Chen, X., Liang, W., Fu, Y., Xu, Z., et al. (2021). Characterization and proteomic analysis of novel rice lesion mimic mutant with enhanced disease resistance. *Rice Sci*. 28, 466–487. doi: 10.1016/j.rsci.2021.07.007

Zavaliev, R., Mohan, R., Chen, T., and Dong, X. (2020). Formation of NPR1 condensates promotes cell survival during the plant immune response. *Cell* 182, 1093–1108. doi: 10.1016/j.cell.2020.07.016

Zeng, L., Qu, S., Bordeos, A., Yang, C., Baraoidan, M., Yan, H., et al. (2004). Spotted leaf 11, a negative regulator of plant cell death and defense, encodes a U-box/armadillo repeat protein endowed with E3 ubiquitin ligase activity. *Plant Cell* 16, 2795–2808. doi: 10.1105/tpc.104.025171

Zhu, X., Ze, M., Chern, M., Chen, X., and Wang, J. (2020). Deciphering rice lesion mimic mutants to understand molecular network governing plant immunity and growth. *Rice Sci*. 27, 279–294. doi: 10.1016/j.rsci.2020.05.004

Conflict of Interest: The authors declare that the research was conducted in the absence of any commercial or financial relationships that could be construed as a potential conflict of interest.

Publisher's Note: All claims expressed in this article are solely those of the authors and do not necessarily represent those of their affiliated organizations, or those of the publisher, the editors and the reviewers. Any product that may be evaluated in this article, or claim that may be made by its manufacturer, is not guaranteed or endorsed by the publisher.

frontiers in Sustainable Food Systems

ORIGINAL RESEARCH
published: 25 March 2022
doi: 10.3389/fsufs.2022.809008

Identification and Gene Mapping of the Lesion Mimic Mutant *lm8015-3*

Chen Wang[1], *Beifang Wang*[1], *Liyong Cao*[1,2], *Yingxin Zhang*[1], *Yu Gao*[1], *Yongrun Cao*[1], *Yue Zhang*[1], *Qunen Liu*[1]* *and Xiaohui Zhang*[1,3]*

[1] *State Key Laboratory of Rice Biology, Key Laboratory for Zhejiang Super Rice Research, China National Rice Research Institute, Fuyang, China,* [2] *Northern Center of China National Rice Research Institute, China National Rice Research Institute, Fuyang, China,* [3] *Zhejiang Guodao High-Tech Seed Industry Co., Ltd., Fuyang, China*

Lesion mimic mutants (*LMM*s) exhibit spots on leaves without fungal infection pressure. The spots confer variable resistance to pathogens in different *LMM*, making them useful research materials. It is unclear how the rice immune system responds to infection with the fungal pathogen *Magnaporthe oryzae* (*M. oryzae*). Here, we identified a rice *LMM*, *lm8015-3*, which shows reduced resistance to *M. oryzae*. We used Quantitative Real-Time PCR (qRT-PCR) to observe the immune system response to *M. oryzae*–induced *lm8015-3*. *Lm8015-3*, obtained from an ethyl methane sulfonate (EMS)–induced Zhonghui8015 (ZH8015) library, showed orange-yellow spots starting in the seedling stage and accumulated more H_2O_2, resulting in severe degradation of the chloroplast. With map-based cloning, the target gene was located on chromosome 12. Once inoculated with *M. oryzae*, the expression level of pathogen-related genes of *lm8015-3* was downregulated between 48 and 72 h. In addition, more germinating spores appeared in *lm8015-3*. Therefore, we conclude that *M. oryzae* weakening the immune system of *lm8015-3* from 48 to 72 h makes *lm8015-3* more susceptible to *M. oryzae*. These results suggested that understanding how *LMM*s defend against *M. oryzae* infection will contribute to improving rice breeding.

Keywords: rice, *LMM*, ZH8015, *lm8015-3*, defense

OPEN ACCESS

Edited by:
Wei Li,
Hunan Agricultural University, China

Reviewed by:
Yuese Ning,
Institute of Plant Protection (CAAS), China
Shimin Zuo,
Yangzhou University, China
Zhiqiang Li,
Institute of Plant Protection (CAAS), China

***Correspondence:**
Qunen Liu
liuqunen202@163.com
Xiaohui Zhang
zhangxiaohui02@caas.cn

Specialty section:
This article was submitted to Agroecology and Ecosystem Services, a section of the journal Frontiers in Sustainable Food Systems

Received: *04 November 2021*
Accepted: *03 February 2022*
Published: *25 March 2022*

Citation:
Wang C, Wang B, Cao L, Zhang Yx, Gao Y, Cao Y, Zhang Y, Liu Q and Zhang X (2022) Identification and Gene Mapping of the Lesion Mimic Mutant lm8015-3. Front. Sustain. Food Syst. 6:809008. doi: 10.3389/fsufs.2022.809008

INTRODUCTION

Rice is the staple food for the majority of people in China. Improving its grain production has thus been a major research focus for many years. However, many factors reduce rice yield production, especially rice blast fungus, *M. oryzae*. *M. oryzae* is considered the most threatening pathogen to rice production, partly because it develops into spots to spread and infect more plants.

Plants have developed a strict defense response to restrict pathogens from spreading. The pathogen-associated molecular pattern (PAMP)–triggered immunity and effector-triggered immunity are two barriers in the plant defense system. The conserved PAMPs or specific effectors of microbes are essential for the plant to identify the pathogen. In the interaction between plants and pathogens (Jones and Dangl, 2006; Bent and Mackey, 2007), many molecular reactions are activated to assist the immune system, such as the production of reactive oxygen species (ROS), the secondary messengers of plant–pathogen interactions (Cheval et al., 2013; Hetmann and Kowalczyk, 2018). Hypersensitive response (HR), a symptom of programmed cell death, finally occurs within the infected area to avoid infection (Chen et al., 2012).

Lesion mimic mutants (*LMM*s) display spontaneous spots on leaves similar to the HR and usually exhibit differential resistance to pathogens without external stresses (Yoshimura et al., 1997). The first *LMM*, *sl*, was found in 1965 (Fujiwara et al., 2010), and since then, researchers have identified more rice mutants to explain the function of immune system genes in responding to pathogens. Most *LMM*s have enhanced resistance to *Pyricularia oryzae* or *Xanthomonas oryzae* pv. *oryzae* except for *spl3* and *spl6* (Kang et al., 2007; Zhang et al., 2011), which means that the immune mechanism of *LMM*s still needs to be substantiated.

RESULTS

Phenotypic Characterization of *lm8015-3*

The rice *LMM lm8015-3* was obtained from the ethyl methane sulfonate (EMS)–induced Zhonghui8015 (ZH8015) mutant library. The lower leaves first exhibited small orange-yellow spots in the seedling stage. The spots gradually spread throughout the leaves from the early tillering stage to the active tillering stage. During the harvest period, the initial spots fused into a few big spots, resulting in the death of leaves (**Figures 1A–F**). In addition, the plant height, number of productive tillers per plant, and the lengths of flag leaves of *lm8015-3* were significantly smaller than in ZH8015 (**Figures 1G–I**). These results revealed that the occurrence of leaf spots affected the growth of *lm8015-3*.

Light-Dependent Formation and Chloroplast Degradation of *lm8015-3*

Light influences spot formation of *LMM*s. Therefore, we covered part of the leaf tip of *lm8015-3* with foil to avoid exposure to natural light when the spots did not appear. One week later, we found spots on the *lm8015-3* leaves exposed to sunlight, whereas no spots formed in the leaves without exposure (**Figures 2A,B**), indicating that spot formation of *lm8015-3* was induced by natural light. Photosynthetic pigments are essential to plant growth, so we measured their contents. Compared with ZH8015, the contents of chlorophyll (Chl) and carotenoid (Car) of *lm8015-3* were significantly decreased at the tillering stage (**Figure 2C**), suggesting a deficiency in the photosynthetic pigments. By transmission electron microscopy (TEM), the chloroplast structure of leaves of *lm8015-3* was disrupted, whereas it was normal in ZH8015 (**Figures 2D,E**).

ROS Accumulation and Cell Death in *lm8015-3*

*LMM*s always correspond with abnormal antioxidation metabolism, such as the accumulation of H_2O_2 or O^{2-}. We observed H_2O_2 accumulation and apoptosis of *lm8015-3* with diaminobenzidine (DAB) and Evans Blue (EB) staining. Compared with ZH8015, more H_2O_2 and dead cells accumulated in the leaves of *lm8015-3* (**Figures 3A,B**).

Furthermore, we detected data of changes in physiological indices. The contents of soluble protein (SP) and malondialdehyde (MDA) are two key indexes that describe the extent of lipid peroxidation damage to plants. Compared with ZH8015, the SP content of *lm8015-3* decreased significantly, whereas the MDA and H_2O_2 contents increased significantly (**Figures 3C–E**). These results mean that the excessive H_2O_2 accumulation seriously damaged the lipid peroxidation in *lm8015-3* leaves. Superoxide dismutase (SOD) converts O^{2-} into H_2O_2, and catalase (CAT) and peroxidase (POD) immediately convert H_2O_2 into water. However, CAT activity decreased significantly in the leaves of *lm8015-3*, opposite to the changes in SOD and POD (**Figures 3F–H**). The abnormal enzyme activity and metabolic product content of *lm8015-3* indicated that SOD accumulation in *lm8015-3* destroyed its metabolic system.

Gene Mapping of *lm8015-3*

To identify the candidate gene related to spot formation of *lm8015-3*, we crossed 02428 and *lm8015-3* to generate F_1 individuals. All F_1 individuals showed a normal phenotype. The F_2 generation displayed a 3:1 ratio between typical plants and spotted plants, indicating that a single nuclear recessive gene controlled the spotted phenotype of *lm8015-3*. Then, we used 96 F_2 individuals with spots to generate primers over the 12 rice chromosomes (from our laboratory), and found the target gene on chromosome 12 (**Figure 4A**). We designed a series of primers to shorten the linkage interval, including C35-16, W35-6, W35-7, and W35-1 (**Figure 4B**). Finally, *lm8015-3* was localized to a 544-kb interval between C35-16 and W35-6. The sequencing results showed a single base substitution (T to A) in the first exon of *LOC_Os12g16720*, which resulted in the substitution of aspartic acid to valine (**Figure 4C**). To verify the mutation, we constructed knockout plants under the Nipponbare background. The knockout plants showed the same orange spots on leaves similar to *lm8015-3* (**Figure 4D**), as a result of the deletion or insertion of a single base in *LOC_Os12g16720*.

Reduced Resistance of *lm8015-3* to *M. oryzae*

In *LMM*s, changes in the expression levels of some defense gene always accompany the appearance of spots. We examined the expression levels of defense genes between the leaves with spots and the leaves with no spots. *PR10* and *WRKY45* were highly expressed in the leaves without spots and downregulated in leaves of *lm8015-3* with spots. The expression level of *PR1b* decreased in the leaves without spots, opposite to other genes, whereas it also displayed the same decreased tendency in general (**Figures 5A,B**). These results indicated that the appearance of spots in *lm8015-3* leads to downregulated expression of defense genes.

*LMM*s have differential resistance to pathogens. Using the spray method to induce *M. oryzae* infection, 3-week-old *lm8015-3* exhibited a more significant lesion area than ZH8015 (**Figures 5C,D**), meaning that formation of spots reduced the resistance of *lm8015-3* to *M. oryzae*. The lesions of *lm8015-3* appeared at 72 h after inoculation (HAI), earlier than in ZH8015. It seemed that 72 h is needed for *M. oryzae* to infect *lm8015-3*. After inoculation, we used the leaves of *lm8015-3* and ZH8015, ranging from 0 to 96 HAI, for qRT-PCR of defense genes (*PR10*/*PR5*/*WRKY45*). The expression levels of all three genes decreased over time (**Figures 5E–G**), suggesting that the infection of *M. oryzae* suppressed the expression of defense genes. Expression levels of defense genes in *lm8015-3* decreased before

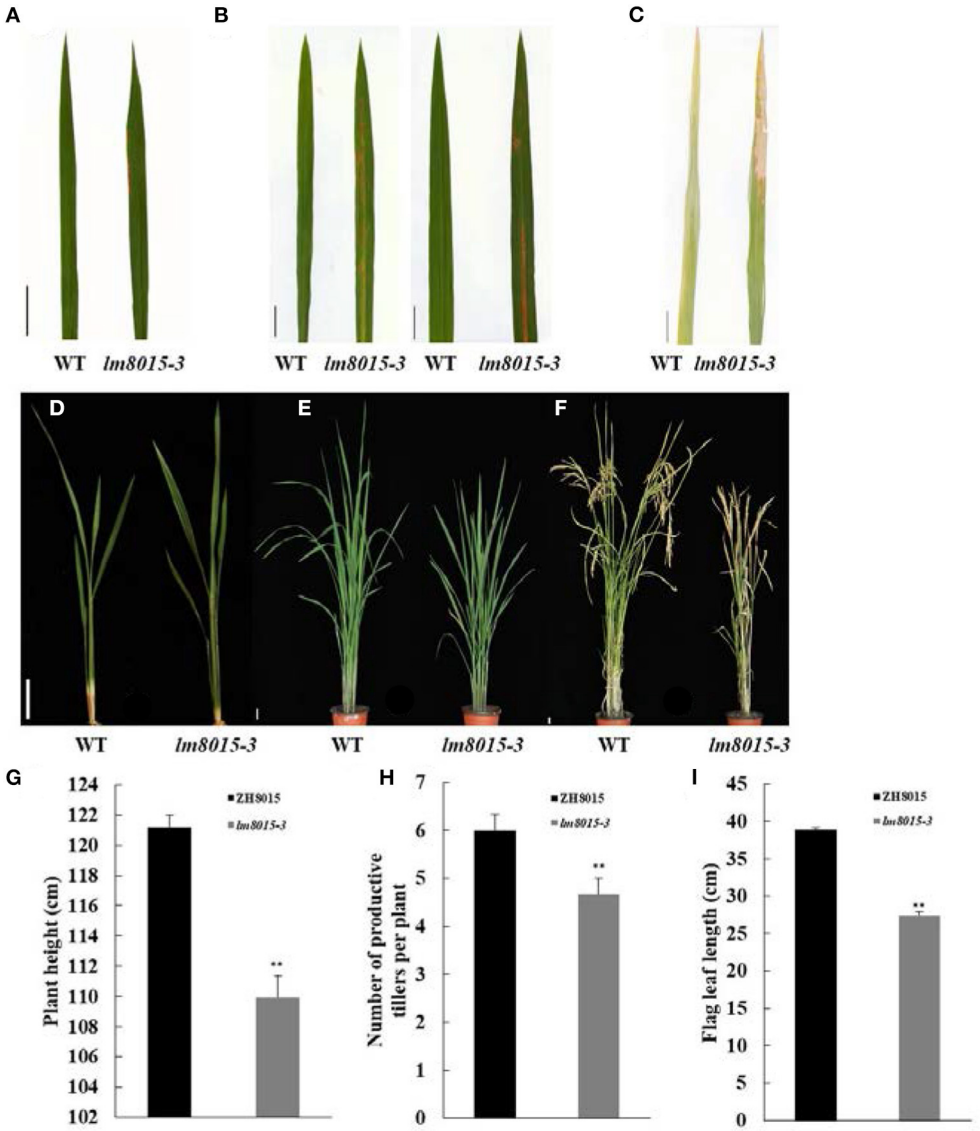

FIGURE 1 | Phenotypic characterization of the *lm8015-3* mutant. **(A–C)** Leaf phenotypes of ZH8015 and *lm8015-3* at the seedling stage, tillering stage, and mature stage. **(D–F)** Plant architecture of ZH8015 and *lm8015-3* at the seedling stage, tillering stage, and mature stage. Scale bar = 2 cm. **(G–I)** Bar graphs of plant height, number of productive tillers per plant, and flag leaf lengths of ZH8015 and *lm8015-3* measured at the mature stage. **Significant at $P < 0.01$ (*t*-test); Error bars represent SD ($n = 3$).

24 h and gradually approached ZH8015 within 48 HAI, indicating that the early defense reaction of *lm8015-3* was more sensitive than ZH8015. Expression levels of defense genes in *lm8015-3* were significantly lower than those in ZH8015 from 48 to 72 HAI, resulting in the successful infection of *lm8015-3* with *M. oryzae*. The expression level decreased from 72 to 96 HAI, which explained the delayed defense reaction of ZH8015. Therefore, *lm8015-3* was susceptible to *M. oryzae*.

As mentioned before, 72 h is required for *M. oryzae* to infect *lm8015-3*. We used leaf-sheath inoculation to determine the *M. oryzae* growth conditions in ZH8015 and *lm8015-3* at 72 h. The number of spores in *lm8015-3* was higher than in ZH8015 (**Figure 6A**) under the identified growth conditions. Most of the spores were germinating, and there were more germinating conidia in the leaves of *lm8015-3* (**Figures 6B,C**). However, the numbers of uninfected conidia and the successfully infected conidia were lower in *lm8015-3* than in ZH8015.

DISCUSSION

Previous studies have demonstrated that *sl* encodes a cytochrome P450 monooxygenase. Cytochrome P450 monooxygenase is a large family of self-oxidizing ferrous hemeprotein enzymes, named for their specific absorption peaks at 450 nm. They

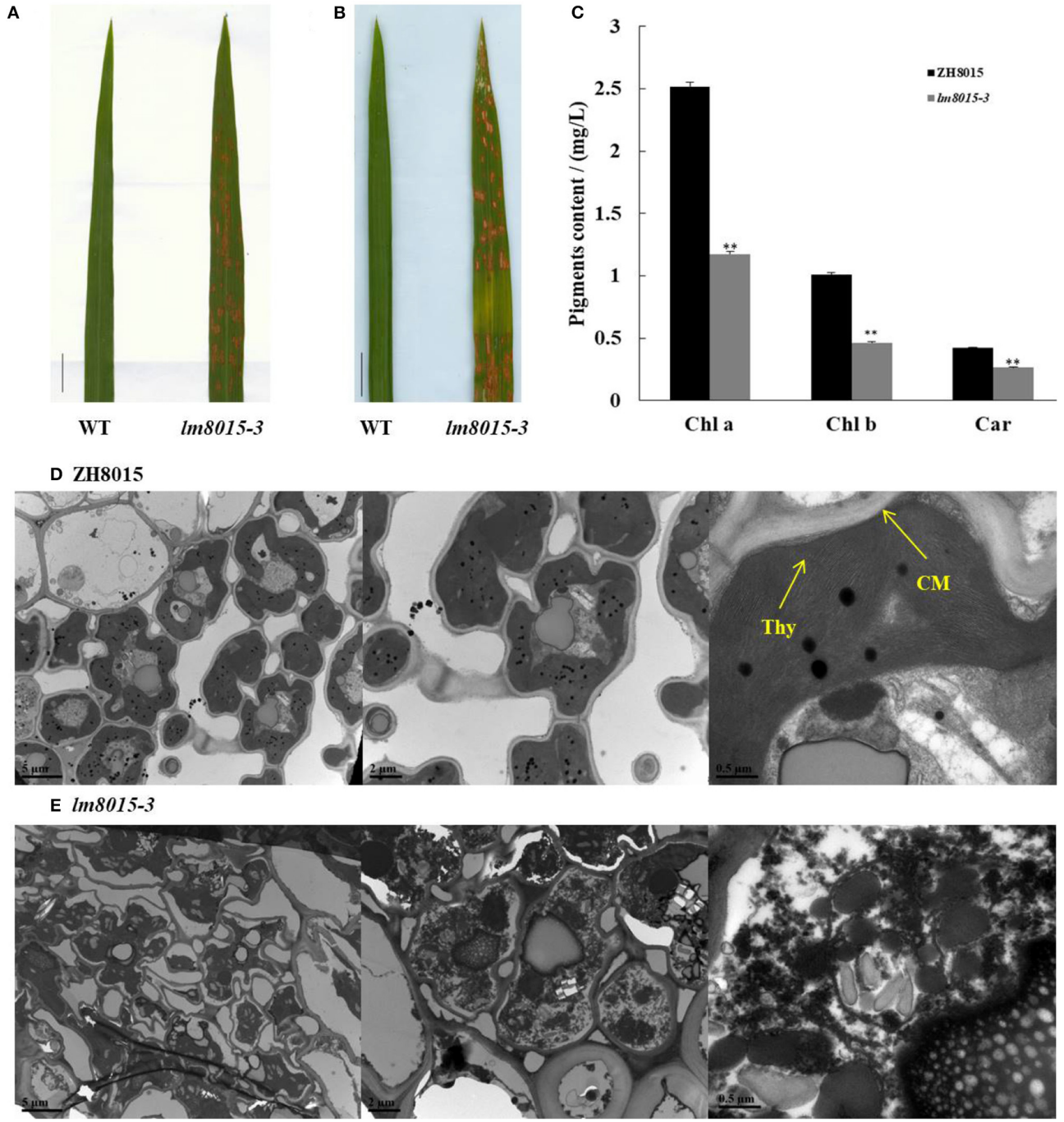

FIGURE 2 | Identification of leaves of *lm8015-3*. **(A,B)** Shading experiment of the second top leaves of ZH8015 and *lm8015-3* at the tillering stage. The leaves were exposed to light, and the leaves in **(B)** were covered with foil for 7 days; scale bar = 2 cm. **(C)** Determination of pigment contents of ZH8015 and *lm8015-3* at the tillering stage. **Significant at $P < 0.01$ (*t*-test); Error bars represent SD ($n = 3$). **(D,E)** TEM observation of the chloroplasts in ZH8015 **(D)** and *lm8015-3* **(E)** at the tillering stage. Thy, thylakoid lamellae; CM, chloroplast membrane.

are involved in the metabolism of endogenous and exogenous substances, including drugs and environmental compounds. Fujiwara et al. (2010) found that sl possesses tryptamine 5-hydroxylase activity, catalyzing tryptamine conversion to serotonin. However, the serotonin and salicylic acid (SA) pathways are antagonistic and trace back to chorismate (Maeda and Dudareva, 2012). As Lu et al. (2018) found, insect damage suppresses serotonin while inducing SA biosynthesis. Moreover,

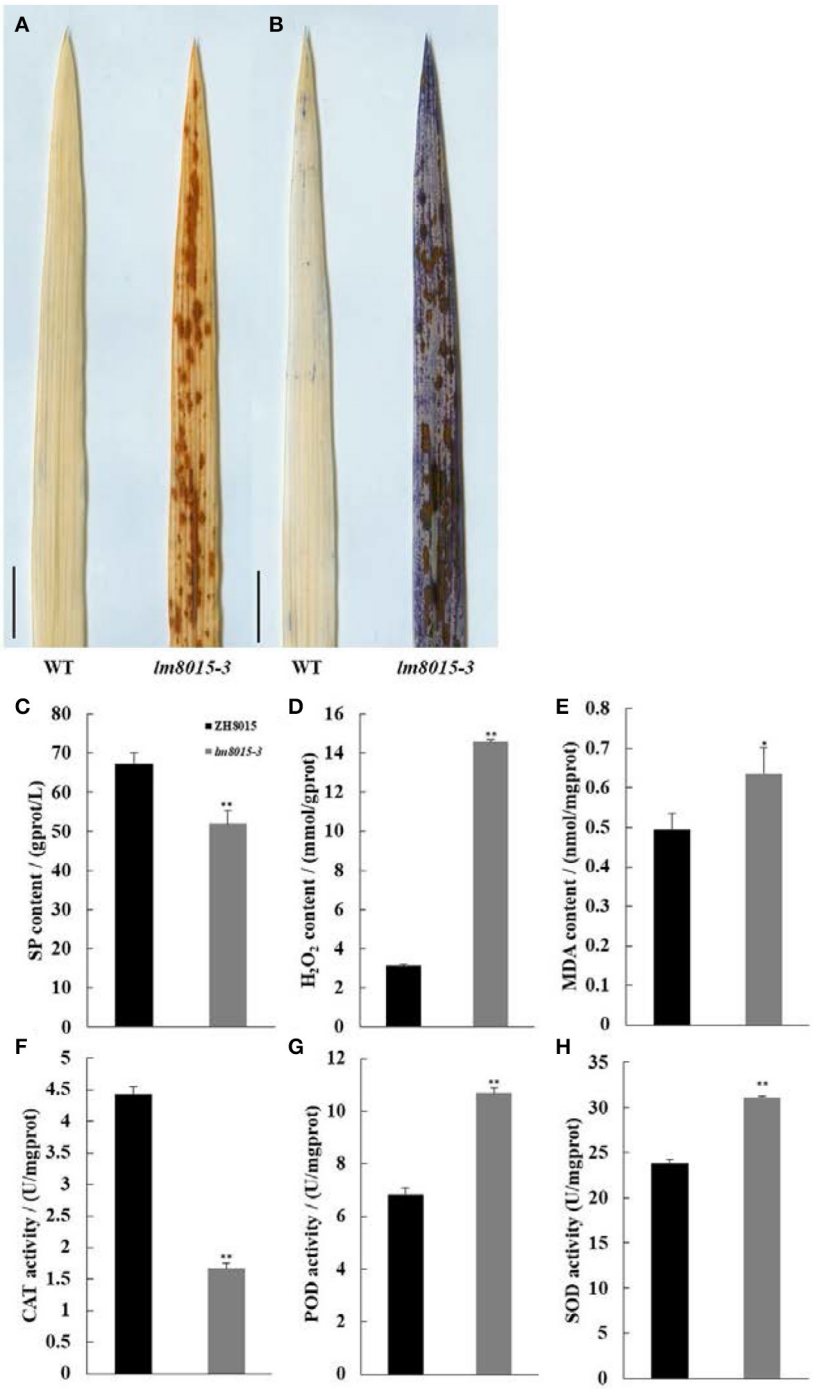

FIGURE 3 | Staining and physiological indices of ZH8015 and *lm8015-3*. **(A,B)** DAB staining and EB staining of the leaves of the wild type (ZH8015) and *lm8015-3* at the tillering stage. Scale bar = 2 cm. **(C–H)** Measurements of SP content, H_2O_2 content, MDA content, CAT activity, POD activity, and SOD activity of ZH8015 and *lm8015-3* at the tillering stage. *Significant at $P < 0.05$ (*t*-test); **Significant at $P < 0.01$ (*t*-test); Error bars represent SD ($n = 3$).

serotonin has high antioxidant activity, which could function as an oxygen radical scavenger to restrict the *M. oryzae*-induced lesion area from expanding (Hayashi et al., 2016).

Researchers previously identified more than five mutants related to *LOC_Os12g16720*; however, they exhibited differential resistance to *M. oryzae*. For example, *sl* showed reduced

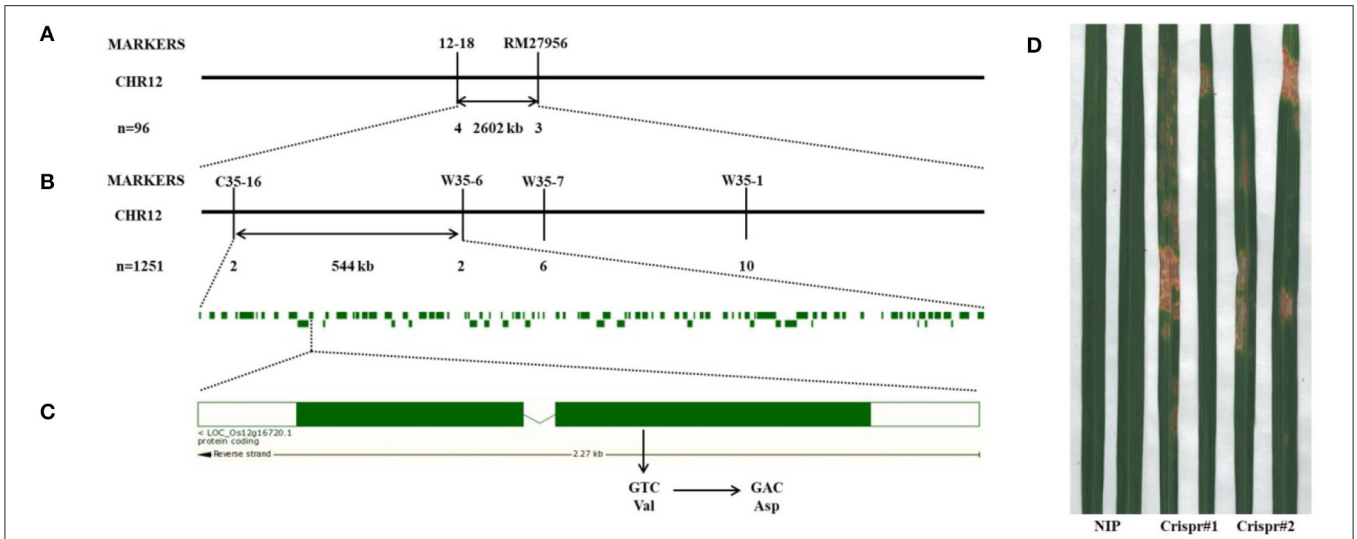

FIGURE 4 | Map-based cloning of *lm8015-3*. **(A)** *LM8015-3* was first mapped on chromosome 12 between markers 12–18 and RM27956 with 96 F_2 individuals. **(B)** *LM8015-3* was finally mapped between markers C35-16 and W35-6 with 1,251 F_2 individuals. **(C)** A single base substitution (T to A) occurred in the first exon of *LOC_Os12g16720* resulting in the mutation of Val to Asp. **(D)** The knockout plant of *LOC_Os12g16720* in Nipponbare showed the same phenotype with *lm8015-3*.

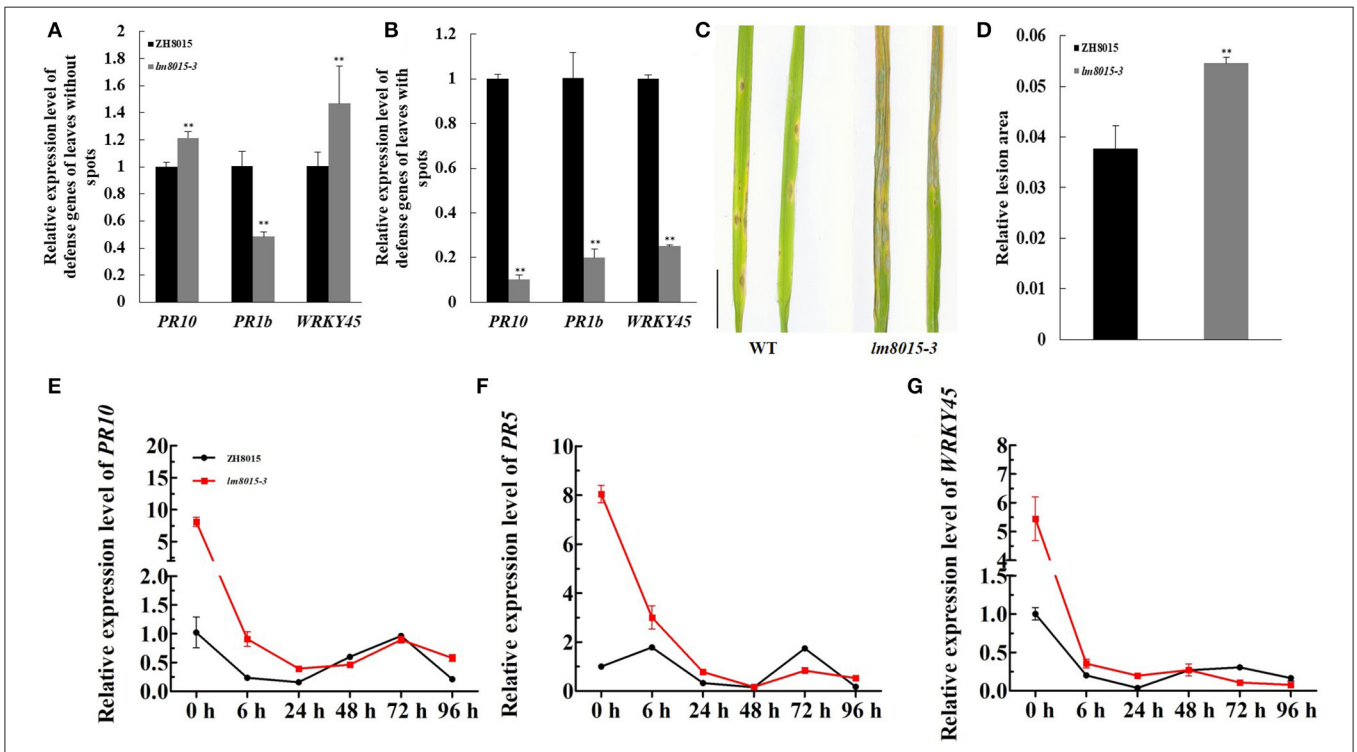

FIGURE 5 | *M. oryzae* resistance of ZH8015 and *lm8015-3*. **(A,B)** Relative expression analysis of defense genes of the leaves with and without spots. The leaves without spots were younger leaves of *lm8015-3* with no lesions at the tillering stage, whereas the leaves with spots were older leaves of *lm8015-3* with lesions at the tillering stage. **(C,D)** Spray inoculation and statistics of relative lesion area of the 3-week-old wild type (ZH8015) and *lm8015-3*. **(E–G)** Analysis of relative expression levels of *PR10*, *PR5*, and *WRKY45* of the 3-week-old ZH8015 and *lm8015-3* after inoculation. **Significant at $P < 0.01$ (*t*-test); Error bars represent SD ($n = 3$).

resistance, whereas *sl-MH* did not (Tian et al., 2020). We speculate that there are two main reasons for this phenomenon. One is the background differences between the wild type used, which might influence the genome sequence. The other more important reason is the mutation sites, which change the expression activity of *LOC_Os12g16720*. As mentioned

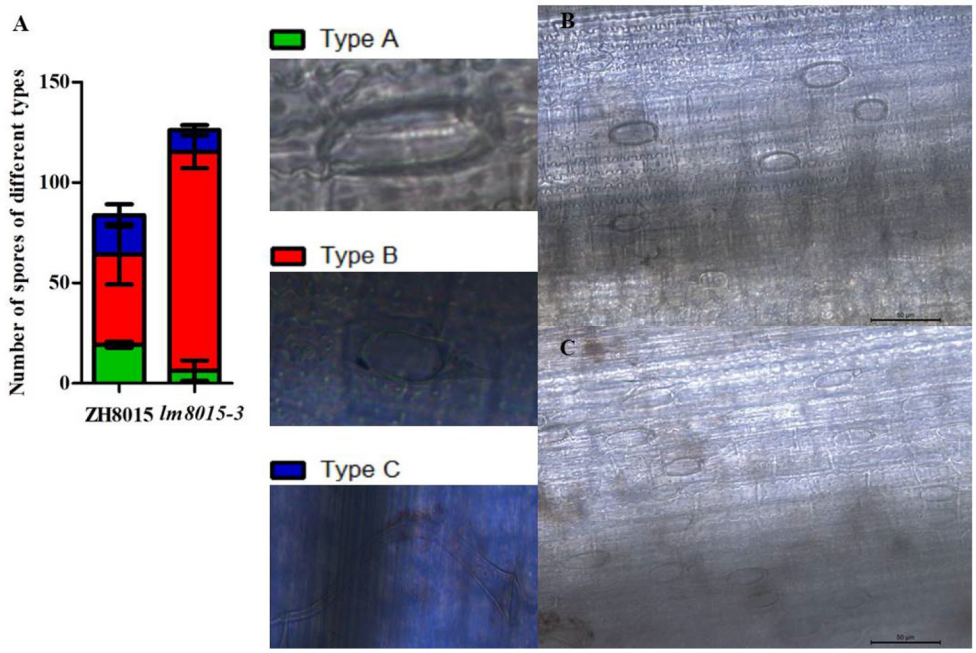

FIGURE 6 | Statistics of different spore types of ZH8015 and *lm8015-3* at 72 h after inoculation. **(A)** Graph of different types of spores of 3-week-old ZH8015 and *lm8015-3* at 72 h after inoculation; Error bars represent SD ($n = 3$). **(B,C)** The 72-h–inoculated leaf sheath of 3-week-old ZH8015 and *lm8015-3*. Type A, uninfected conidium; Type B, germinating conidium; Type C, successfully infected conidium.

before, 72 h is required for *M. oryzae* to infect *lm8015-3*. From 48 to 72 HAI, the pathogen-related genes of *lm8015-3* were downregulated compared to ZH8015, a symbol of an ineffective immune system response. *Os4CL5* and *PAL* genes are essential for lignin biosynthesis (Gui et al., 2011; Zhou et al., 2018), and *OsbHLH6* encodes a factor to regulate the signal antagonism of SA and JA (Meng et al., 2020). *Os4CL5* and *PAL7* of *lm8015-3* were downregulated, whereas *OsbHLH6* had the opposite pattern (**Supplementary Figure S1**). The biosynthesis pathways of SA, serotonin, and melatonin were identified to be involved by Lu et al. (2018), so we speculated that the SA pathway of chorismate was damaged, which means that the serotonin pathway is active. The increased level of serotonin might be the real reason for the reduced resistance of *lm8015-3*. However, the mechanism of how *M. oryzae* induces serotonin accumulation in *lm8015-3* is still unsubstantiated.

CONCLUSION

Pathogen resistance is an essential issue for rice breeding, as it can severely affect crop yield. This study identified the *LMM lm8015-3*, which exhibited reduced resistance to *M. oryzae*. The expression levels of most defense genes in *lm8015-3* were downregulated when spots appeared. The defense reaction of *lm8015-3* thus appears to be sensitive to *M. oryzae*. After the inoculation with *M. oryzae*, *lm8015-3* was easier to infect than ZH8015. Furthermore, the infected lesions on *lm8015-3* appeared 2 days earlier than ZH8015 because of the disordered immune system from 48 to 72 HAI in *lm8015-3*.

METHODS

Plant Materials and Blast Isolates

ZhongHui8015, an indica rice restorer line, was bred at the China National Rice Research Institute (CNRRI), Hangzhou, Zhejiang, China. The *LMM lm8015-3* was isolated from the ZH8015 EMS-induced library. The F_2 population derived from 02428/*lm8015-3* was used for genetic analysis and fine mapping. We measured the agronomic characteristics of *lm8015-3* and ZH8015 at the harvest period with three biological replicates, including plant height, numbers of productive tillers per plant, and flag leaf length. All materials were grown in the FuYang experimental base of CNRRI. The *M. oryzae* strain 14-1 was virulent to ZH8015.

Shading Experiment

At the tillering stage, the second top leaves without lesions of *lm8015-3* and ZH8015 were shaded with 4-cm-wide foil for 7 days, and then, the foil was removed and the leaves were photographed.

Measurements of Photosynthetic Pigment Contents

As described before (Arnon, 1949; Schippers et al., 2015), the second top leaves of plants with lesions at the tillering stage were used to measure the contents of photosynthetic pigments. Each

experiment was performed with three biological replicates. We used the means of three replicates for the *t*-test.

Chloroplast Structure Observation

For the TEM observation of chloroplast structure, the leaves of *lm8015-3* and ZH8015 at the tillering stage were first soaked in 2.5% glutaraldehyde for 24 h. Then, we sent samples to Zhejiang University for subsequent treatments.

Histochemical Analysis

The leaves of *lm8015-3* and ZH8015 at the tillering stage were stained with DAB and EB to observe the H_2O_2 accumulation and cell death as described previously (Thordal-Christensen et al., 1997; Li et al., 2004).

Physiological Indexes

Following the instructions of kits from the Nanjing JianCheng Bioengineering Institute, we ground the leaves of *lm8015-3* and ZH8015 at the tillering stage into homogenates to test the content of SP, MDA, H_2O_2, and the activities of SOD, POD, and CAT. Three replications were used for each group. The means of three replicates were used for the *t*-test.

Gene Mapping

As described previously (Rogers and Bendich, 1985), DNA of the mapping group was extracted using Cetrimonium Bromide (CTAB). Genome sequences of rice cultivars were downloaded from http://ensembl.gramene.org/ and http://rice.genomics.org.cn/, and differences between the genome sequences of the japonica cultivar Nipponbare and the indica cultivar 9311 were used to design primers for map-based cloning of *lm8015-3*. With the databases GRAMENE (http://ensembl.gramene.org/) and MSU (http://rice.uga.edu/), we designed primers for genes and analyzed the sequence differences. The PCR followed the instructions of Vazyme (P222-01). To construct knockout plants of *LOC_Os12g16720*, we used pCAMBIA1305.1 vector to delete or insert a single base in the exon. The primers for gene mapping and confirmation are listed in **Supplementary Table S1**.

qRT-PCR Analysis

Following kit instructions for Invitrogen TRIzol (Thermo Fisher), all RNA samples were extracted. To determine whether lesion occurrence changed the expression levels of defense genes, we extracted RNA of the leaves with or without lesions of *lm8015-3* at the tillering stage. In the qRT-PCR of defense genes after inoculation, the 3-week-old leaves RNA of *lm8015-3* and ZH8015 at 0, 6, 24, 48, 72, and 96 HAI were extracted. With SYBR qPCR Master Mix of Vazyme (Q511-02), three replicates were used for each group. The means of three replicates were used for the *t*-test. The primers for qRT-PCR are listed in **Supplementary Table S1**.

Blast Inoculation

M. oryzae strain 14-1, which was virulent to ZH8015, was cultured on oatmeal agar medium for 2 weeks under light for sporulation. We sprayed the 3-week-old leaves of *lm8015-3* and ZH8015 with a conidial suspension of 2×10^5 spores/ml in the growth chamber. We measured the relative infected-lesion area of *lm8015-3* and ZH8015 by relative pixels with Photoshop. The detached sheath of 3-week-old *lm8015-3* and ZH8015 leaves was injected with a conidial suspension of 1×10^6 spores/ml in the growth chamber by leaf sheath inoculation (Li et al., 2011). After 72 h, the sample was placed under a microscope and observed with a 40× objective. The number of each spore type, observed in 10 random fields of view, was used to calculate one biological replicate. Three biological replicates were used for each group. The means of three replications were used for the *t*-test.

DATA AVAILABILITY STATEMENT

The datasets presented in this study can be found in online repositories. The names of the repository/repositories and accession number(s) can be found in the article/**Supplementary Material**.

AUTHOR CONTRIBUTIONS

XZ and QL contributed to conception and design of the study. CW finished all the experiments and wrote the manuscript. BW, LC, YXZ, YG, YC, and YZ contributed to the completion of the study. All authors contributed to manuscript revision, read, and approved the submitted version.

FUNDING

This study was supported by grants from the National Natural Science Foundation of China (31871236 and 31801726) and the Agricultural Science and Technology Innovation Program of the Chinese Academy of the Agricultural Sciences (CAAS-ASTIP-2013-CNRRI).

SUPPLEMENTARY MATERIAL

The Supplementary Material for this article can be found online at: https://www.frontiersin.org/articles/10.3389/fsufs.2022.809008/full#supplementary-material

REFERENCES

Arnon, D. I. (1949). Copper enzymes in isolated chloroplasts. Polyphenoloxidase in beta vulgaris. *Plant Physiol.* 24, 1–15. doi: 10.1104/pp.24.1.1

Bent, A. F., and Mackey, D. (2007). Elicitors, effectors, and R genes: the new paradigm and a lifetime supply of questions. *Annu. Rev. Phytopathol.* 45, 399–436. doi: 10.1146/annurev.phyto.45.062806.094427

Chen, M., Zeng, H., Qiu, D., Guo, L., Yang, X., Shi, H., Zhou, T., and Zhao, J. (2012). Purification and characterization of a novel hypersensitive response-inducing elicitor from *Magnaporthe oryzae* that triggers defense response in rice. *PLoS ONE.* 7, e37654. doi: 10.1371/journal.pone.0037654

Cheval, C., Aldon, D., Galaud, J. P., and Ranty, B. (2013). Calcium/calmodulin-mediated regulation of plant immunity. *Biochim. Biophys. Acta.* 1833, 1766–1771. doi: 10.1016/j.bbamcr.2013.01.031

Fujiwara, T., Maisonneuve, S., Isshiki, M., Mizutani, M., Chen, L., Wong, H. L., et al. (2010). Sekiguchi lesion gene encodes a cytochrome P450 monooxygenase that catalyzes conversion of tryptamine to serotonin in rice. *J. Biol. Chem*. 285, 11308–11313. doi: 10.1074/jbc.M109.091371

Gui, J., Shen, J., and Li, L. (2011). Functional characterization of evolutionarily divergent 4-coumarate:coenzyme a ligases in rice. *Plant Physiol*. 157, 574–586. doi: 10.1104/pp.111.178301

Hayashi, K., Fujita, Y., Ashizawa, T., Suzuki, F., Nagamura, Y., and Hayano-Saito, Y. (2016). Serotonin attenuates biotic stress and leads to lesion browning caused by a hypersensitive response to *Magnaporthe oryzae* penetration in rice. *Plant J*. 85, 46–56. doi: 10.1111/tpj.13083

Hetmann, A., and Kowalczyk, S. (2018). Membrane receptors recognizing MAMP/PAMP and DAMP molecules that activate first line of defence in plant immune system. *Postepy Biochem*. 64, 29–45. doi: 10.18388/pb.2018_103

Jones, J. D., and Dangl, J. L. (2006). The plant immune system. *Nature*. 444, 323–329. doi: 10.1038/nature05286

Kang, S. G., Matin, M. N., Bae, H., and Natarajan, S. (2007). Proteome analysis and characterization of phenotypes of lesion mimic mutant spotted leaf 6 in rice. *Proteomics*. 7, 2447–2458. doi: 10.1002/pmic.200600961

Li, R., Lqn, S. Y., and Xu, Z. X. (2004). Studies on the programmed cell death in rice during starchy endosperm development. *Agric. Sci. China*. 3, 663–670.

Li, W., Zhong, S., Li, G., Li, Q., Mao, B., Deng, Y., et al. (2011). Rice RING protein OsBBI1 with E3 ligase activity confers broad-spectrum resistance against *Magnaporthe oryzae* by modifying the cell wall defence. *Cell Res*. 21, 835–848. doi: 10.1038/cr.2011.4

Lu, H. P., Luo, T., Fu, H. W., Wang, L., Tan, Y. Y., Huang, J. Z., et al. (2018). Resistance of rice to insect pests mediated by suppression of serotonin biosynthesis. *Nat. Plants*. 4, 338–344. doi: 10.1038/s41477-018-0152-7

Maeda, H., and Dudareva, N. (2012). The shikimate pathway and aromatic amino acid biosynthesis in plants. *Annu. Rev. Plant Biol*. 63, 73–105. doi: 10.1146/annurev-arplant-042811-105439

Meng, F., Yang, C., Cao, J., Chen, H., Pang, J., Zhao, Q., et al. (2020). A bHLH transcription activator regulates defense signaling by nucleo-cytosolic trafficking in rice. *J. Integr. Plant Biol*. 62, 1552–1573. doi: 10.1111/jipb.12922

Rogers, S. O., and Bendich, A. J. (1985). Extraction of DNA from milligram amounts of fresh, herbarium and mummified plant tissues. *Plant Mol. Biol*. 5, 69–76. doi: 10.1007/BF00020088

Schippers, J. H., Schmidt, R., Wagstaff, C., and Jing, H. C. (2015). Living to die and dying to live: the survival strategy behind leaf senescence. *Plant Physiol*. 169, 914–930. doi: 10.1104/pp.15.00498

Thordal-Christensen, H., Zhang, Z. G., Wei, Y. D., and Collinge, D. B. (1997). Subcellular localization of H_2O_2 in plants. H_2O_2 accumulation in papillae and hypersensitive response during the barley-powdery mildew interaction. *Plant J*. 11, 1187–1194. doi: 10.1046/j.1365-313X.1997.11061187.x

Tian, D., Yang, F., Niu, Y., Lin, Y., Chen, Z., Li, G., et al. (2020). Loss function of SL (sekiguchi lesion) in the rice cultivar Minghui 86 leads to enhanced resistance to (hemi) biotrophic pathogens. *BMC Plant Biol*. 20, 507. doi: 10.1186/s12870-020-02724-6

Yoshimura, A., Ideta, O., and Iwata, N. (1997). Linkage map of phenotype and RFLP markers in rice. *Plant Mol. Biol*. 35, 49–60. doi: 10.1023/A:1005764026871

Zhang, H., Liu, K., Zhang, X., Tang, W., Wang, J., Guo, M., et al. (2011). Two phosphodiesterase genes, PDEL and PDEH, regulate development and pathogenicity by modulating intracellular cyclic AMP levels in *Magnaporthe oryzae*. *PLos ONE*. 6, e17241. doi: 10.1371/journal.pone.0017241

Zhou, X., Liao, H., Chern, M., Yin, J., Chen, Y., Wang, J., et al. (2018). Loss of function of a rice TPR-domain RNA-binding protein confers broad-spectrum disease resistance. *Proc. Natl. Acad. Sci. USA*. 115, 3174–3179. doi: 10.1073/pnas.1705927115

Conflict of Interest: XZ was employed by the Zhejiang Guodao High-Tech Seed Industry Co., Ltd.

The remaining authors declare that the research was conducted in the absence of any commercial or financial relationships that could be construed as a potential conflict of interest.

Publisher's Note: All claims expressed in this article are solely those of the authors and do not necessarily represent those of their affiliated organizations, or those of the publisher, the editors and the reviewers. Any product that may be evaluated in this article, or claim that may be made by its manufacturer, is not guaranteed or endorsed by the publisher.

frontiers | Frontiers in Sustainable Food Systems

ORIGINAL RESEARCH
published: 24 June 2022
doi: 10.3389/fsufs.2022.868870

Climate-Smart Agriculture and Trade-Offs With Biodiversity and Crop Yield

Hemant G. Tripathi[1,2]*, *William E. Kunin*[2], *Harriet E. Smith*[3], *Susannah Mary Sallu*[3], *Sixbert Maurice*[4], *Suzan D. Machera*[4], *Rhiannon Davies*[2], *Mosha Florence*[5], *Samuel Eze*[6], *J. H. Galani Yamdeu*[7,8] *and Steven Mark Sait*[2]

[1] UN Environment Programme World Conservation Monitoring Centre (UNEP-WCMC), Cambridge, United Kingdom, [2] Faculty of Biological Sciences, School of Biology, University of Leeds, Leeds, United Kingdom, [3] Faculty of Environment, School of Earth and Environment, Sustainability Research Institute, University of Leeds, Leeds, United Kingdom, [4] Pest Management Centre, Sokoine University of Agriculture, Morogoro, Tanzania, [5] Muheza District Council, Tanga, Tanzania, [6] Department of Life Sciences, College of Science, University of Lincoln, Lincoln, United Kingdom, [7] Section of Natural and Applied Sciences, Canterbury Christ Church University, Canterbury, United Kingdom, [8] School of Food Science and Nutrition, University of Leeds, Leeds, United Kingdom

Biophysical evaluations of climate-smart agriculture (CSA) often overlook the potential interactions with and implications for biodiversity and ecosystem services, which are important determinants of food system resilience and sustainability. Drawing on a case study in the East Usambara Mountains, Tanzania, we compare the impacts of CSA with other agricultural management practices on invertebrate pest and natural enemy diversity, and the associated effects on crop damage and crop yield. We found that the most common CSA practices in the region, terracing and trenching with live and compost mulches, provided the best outcomes for crop production, pest suppression and agricultural income. However, greater diversity of pests was observed when neighboring fields planted improved crop varieties, suggesting that the use of improved varieties by farmers creates increased vulnerability to pest damage among neighboring farmers that used local varieties. Also, greater natural enemy diversity was found when neighboring fields were either intercropped or left fallow highlighting spatial flows of ecosystem services between fields. Landcover heterogeneity was positively correlated with pest diversity, whilst landcover richness was positively associated with higher pest volume, highlighting the importance of landscape characteristics in pest and natural enemy dynamics. Finally, we found that crop damage was most severe when pest communities had low species richness, suggesting that a small number of key crop pests contribute to most yield losses. Our findings illustrate that those varied combinations of agricultural management practices lead to heterogeneous biodiversity outcomes and trade-offs, and highlight the importance of local management, neighborhood effects and landscape characteristics. CSA evaluations must therefore look beyond productivity as a measure for success, as trade-offs with invertebrate biodiversity, food production, and environmental sustainability often interact and feedback in complex and unexpected ways.

Keywords: crop pests, natural enemies, food security, neighborhood effects, East Usambara Mountains, Tanzania, Africa

OPEN ACCESS

Edited by:
Wen Xie,
Insititute of Vegetables and Flowers (CAAS), China

Reviewed by:
Fang Ouyang,
Institute of Zoology (CAS), China
Yang Zeng,
Hubei Normal University, China

****Correspondence:***
Hemant G. Tripathi
hgtripathi05@gmail.com

Specialty section:
This article was submitted to Agroecology and Ecosystem Services, a section of the journal Frontiers in Sustainable Food Systems

Received: *03 February 2022*
Accepted: *16 May 2022*
Published: *24 June 2022*

Citation:
Tripathi HG, Kunin WE, Smith HE, Sallu SM, Maurice S, Machera SD, Davies R, Florence M, Eze S, Yamdeu JHG and Sait SM (2022) Climate-Smart Agriculture and Trade-Offs With Biodiversity and Crop Yield. Front. Sustain. Food Syst. 6:868870. doi: 10.3389/fsufs.2022.868870

INTRODUCTION

Climate change poses a significant threat to the future of global food production with implications for agricultural productivity and food system sustainability (Lobell et al., 2011; Dang and Dabalen, 2017; Ray et al., 2019). In addition to climate change, there is widespread global concern about biodiversity loss due to agricultural expansion and intensification (Newbold, 2018; Beckmann et al., 2019). Besides its inherent, intrinsic value, biodiversity underpins vital ecosystem services that support food production (Dainese et al., 2019), such as the biological control of crop pests and diseases by natural enemies (Bommarco et al., 2018). As with food production, biodiversity and biodiversity-based ecosystem services are fundamentally dependent on climate and, hence, vulnerable to climate change (Pecl et al., 2017; Nunez et al., 2019).

Climate smart agriculture (CSA) has been developed as a climate adaptation framework for multiple aspects of agriculture, from field-level practices to food supply chains (Venkatramanan and Shah, 2019). CSA implementation has targeted developing regions such as the sub-Saharan Africa (SSA) (Neufeldt et al., 2013), which are most vulnerable to climate change and have limited capacity to cope, and invest in adaptive institutions and technologies (Fankhauser and McDermott, 2014; Porter et al., 2015; van Wijk et al., 2020). The primary goal of CSA is to achieve triple wins by contributing to three objectives; increasing productivity, increasing the resilience of food production, and mitigating greenhouse gas emissions (Lipper et al., 2018). However, there are gaps in evaluating the success of CSA approaches as studies have predominantly focussed on productivity outcomes (Dinesh et al., 2015; Rosenstock et al., 2019; van Wijk et al., 2020). In a limited number of cases, investigations of the resilience benefits have also been linked to productivity gains, where surplus food minimized the effects of climate impacts and increased the resilience of farmers (Dinesh et al., 2015; van Wijk et al., 2020). With such a narrow agricultural productivity and food security focus, the possible impact of CSA practices on other components that affect agricultural system resilience and environmental sustainability, such as biodiversity and ecosystem service provisioning (Thornton et al., 2018), is a crucial knowledge gap. Evaluation of these broader components would help develop a better understanding of the system-level effectiveness of, and trade-offs associated with the CSA framework. This is critical to enable the identification of agricultural strategies that improve food system multifunctionality necessary for building resilience to climate change (Thornton et al., 2018; van Wijk et al., 2020).

Here, we evaluate the effects of local-scale farm management, including CSA practices, on invertebrate diversity and agricultural yields, focusing on pest prevalence and suppression in the East Usambara Mountains of Tanzania. Specifically, we examine relationships among (i) invertebrate richness, abundance and volume of crop pests and natural enemies, (ii) percentage crop damage and, (iii) annual income from crops (USD ha^{-1}) under varying combinations of CSA and traditional farm management practices. Landcover diversity and configuration around the fields (Duarte et al., 2018; Zhang et al., 2020), and management practices in the neighboring fields affect the invertebrate diversity, pests, and natural enemies through spatial flow and interactions (Redlich et al., 2018). The understanding of the effects of the landscape context and the associated processes on local agrobiodiversity and related ecosystem services is mainly based on studies in large-scale and commercial farming systems in temperate ecosystems (Rusch et al., 2016; Woodcock et al., 2016; Aguilera et al., 2021). Only a few studies have examined the ecosystem services in biodiverse smallholder farming landscapes in SSA (Mkenda et al., 2019). Hence, we also account for the effects of landscape context and the influence of management in the neighboring fields on invertebrate richness, crop damage and income.

Our study provides new insights into the implications of CSA farm management for biodiversity and ecosystem services at local and landscape scales in SSA, which can inform future agricultural transformation strategies in the region and beyond.

METHODS

Study Site and Experimental Design

The study was conducted in the East Usambara Mountains, Tanzania (**Figure 1**), where CSA was introduced as part of the 'Integrated Approaches for Climate Change Adaptation Project' (IACCA), which ran between 2015 and 2019 as part of the European Union-funded Global Climate Change Alliance (GCCA+) programme (Ongawa, 2019). The project established farmer field schools (FFS) and provided training and capacity building of farmer communities in CSA.

Farming communities in the region predominantly comprise highly diverse but low-input, mixed cropping, livestock (primarily zero-grazing dairy cattle and poultry) and agroforestry smallholder systems. Food crops include maize, beans, yams, banana, and cassava, while commercial crops include spices (cardamom, cinnamon, clove, and black pepper), sugarcane, fruits (jackfruit), and some horticultural produce (tomatoes, onions, leafy vegetables).

We sampled invertebrate diversity and abundance during five sampling occasions at approximately 2-month intervals – September and November 2019, January, March, and May in 2020, in 82 fields across an elevation gradient from 200-400m (lowlands) to 800-1200m (highlands) above sea level. The fields were selected from a dataset of 150 areas containing agronomic details prepared by two local extension officers from the Muheza District Agriculture Office. The selection of the fields was based on the availability and willingness of farmers to participate in this study. We used the agronomic background information to select fields so that 50% of our sampled fields had at least two climate-smart management activities (**Table 1**) practiced for 2 years or more (as defined by the IAACA project). During each field visit, we recorded information about local management practices in the focal field (i.e., the field we were sampling) and in the nearest neighboring field. The information comprised farm size, the number of crop species in the field, and the presence or absence of the following practices: improved crop variety,

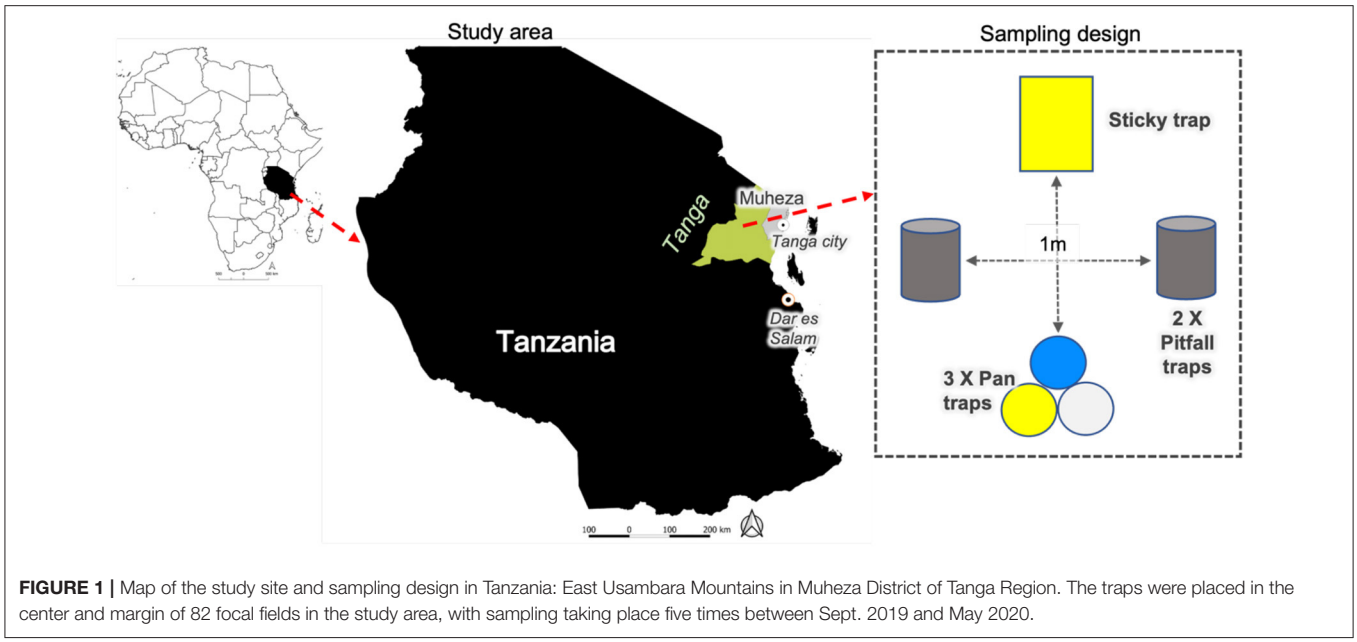

FIGURE 1 | Map of the study site and sampling design in Tanzania: East Usambara Mountains in Muheza District of Tanga Region. The traps were placed in the center and margin of 82 focal fields in the study area, with sampling taking place five times between Sept. 2019 and May 2020.

TABLE 1 | Agronomic background of fields used in the study.

Farm size	0.8 (± 0.1) ha	0.2 to 6 ha
Crop richness	2.4 (±0.14) crop species	1 to 5 crop species
Commonly cultivated crops (*n* = number of fields)	Maize (*n* = 64), Cassava (42), Beans (26), Cloves (17), Banana (14), Cardamom (7)	
Times cultivated per year	Single season – 37, Two seasons – 45	
Field categories – based on clustering of management practices with >1 year of implementation:		
Monocrop-Trench (n = 15)	Local variety Maize monocrops and *Fanya juu* trenching	
Spice-Intercrop-Cropdiv (19)	Local variety intercrops (Maize with Cassava or Bean) and spice plantations (≥ 4-year-old plantations)	
Mulch-Trench (11)	Compost mulches used along with *Fanya juu* trenching and terracing, with Napier (*Pennisetum purpureum)* plantation as live mulches on *Fanya juu* terrace and trench systems to stabilize the soil. *Fanya juu* involves digging of ditches and throwing excavated soil upslope. Napier grass is generally used as fodder and as "pull" crop to attract crop pests toward it and away from crops. Here, it was used only to stabilize the upslope soil and for fodder rather for the purposes of pulling crop pests.	
Spacing-Intercrop (13)	Designated 70–100 cm inter-row spacing between plants along with intercropping of Maize with Cassava or Beans. Traditional spacing generally had 50–60 cm between crop plants.	
CS-Intercrop-Cropdiv (24)	Maximum number of CSA activities including improved variety of crops, intercropping, spice cultivation and agroforestry	

mulching, spice plantation, row spacing, trenching, intercrop, agroforestry, and fallow.

Sampling of Management Practices, Yields, Crop Damage and Invertebrates

Management Practices and Landscape Variables

As the number, type and combination of management practices varied considerably between fields, we applied the k-means hierarchical clustering algorithm (Qi et al., 2017; **Figure 2**) to the management practices data to characterize them. This resulted in 5 distinct field categories (**Figure 2**; **Table 1**):

To account for the influence of landscape context, we computed two landscape-level variables; edge length (density of forest edges) and landcover richness (total number of unique landcovers) within 500m radius of the focal field, using the Copernicus 100m resolution landcover dataset (Buchhorn et al., 2020).

Invertebrate Sampling and Crop Damage

At each field center and margin (2 m inside the field), we sampled invertebrates using three techniques - a combination of two Pitfall traps, a Sticky trap and three Pan Traps. Pitfall traps were installed with 1 m distance between them, sunk in the ground with the rim at the ground level, and filled with water with a drop of liquid soap to break the surface tension. The pan traps comprised a cluster of three pans (UV bright yellow, blue, and white) placed together half-filled with water and a drop of liquid soap. The yellow sticky traps were placed between the pitfall traps, approximately 100 cm above the ground. The traps operated for 72 h, after which the specimens

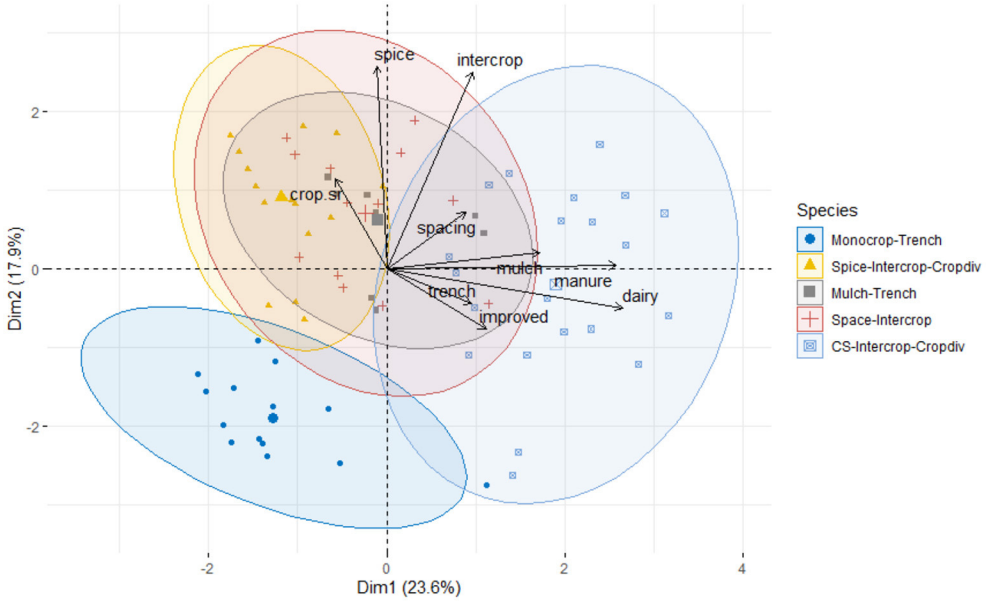

FIGURE 2 | PCA Biplot of Farm clusters, where five categories based on the dominant set of management activities emerged. First two axis indicates clear distinction between Monocrop-Trench and CS-Intercrop-Cropdiv. Third axis (not visible) distinguishes between the other three categories.

were collected and sorted into morphologically distinct groups (OTU, operational taxa units) by two field assistants (MSc. students from the Sokoine University of Agriculture, Tanzania), and two agricultural extension officers from Muheza District. The specimens were preserved in storage vials containing 90% ethanol to further identify orders, families, and genera. The vials containing the specimens were labeled with unique OTU codes corresponding to taxonomic id, sampling station, field number, and month. The OTUs were further classified into potential pests (predominantly crop herbivores) and potential natural enemies (insect predators and parasitoids). The total number of individuals and length and width (in centimeters) of 2–3 randomly selected individuals were recorded for each OTU. Further, for each sampling occasion (sampling station, technique, and month), we measured abundance (total number of individuals), invertebrate biovolume (volume here onwards, abundance × length × breadth) as a measure of biomass, and richness of OTU (number of unique OTUs), which were used as invertebrate response variables. The invertebrate volume is based on size i.e., length and breadth, as well as the number of individuals and is an indicator of body-size distribution in an invertebrate assemblage.

We also measured crop damage on two randomly selected plants of each crop species (for intercrop fields) at each sampling station by recording the approximate percentage of pest-induced damage observed on leaves, cobs or fruits, and stems. Mean damage observed in all plants and plant parts was used to derive a field-level measure of crop damage.

Annual Income and Crop Yields

We collected information about the annual income from the major crops in each field by asking farmers about the quantity they harvested for each crop in the field during our study in 2019–20 (details of each crop yields in supporting information, SI). We converted yields per annum to earnings per hectare per annum (in Tanzanian shillings) by asking the extension officers about the average market price a farmer would get after selling the harvested amount in the local market in Muheza during the period of study. Tanzanian shillings were converted to US dollars using the conversion rate of 1 USD = 2,319.05 TZS as of 30th April 2021. Hereafter, annual yield, or annual income indicates US dollars per hectare earnings during 2019–20.

Statistical Analyses

Management-Invertebrate Models

To investigate the effect of management, neighboring field, and landscape context on invertebrates, we used mixed-effects models with richness as a Generalized Poisson distribution (GLMM) and log-transformed values of abundance and volume as a General Normal distribution (GLM). We grouped the invertebrates into potential pests and natural enemies (hereafter, pests, and natural enemies), and modeled the groups and their richness, abundance, and volume separately.

Management-Crop Damage and Annual Yield Models

We further explored management effects on crop damage and yield by modeling crop damage and annual yields as a function of management, neighboring field and landscape context using GLMs.

Invertebrate-Crop Damage and Yield Models

We also tested the relationship between invertebrates and yields by using GLMs to model crop damage and annual yield as

TABLE 2 | Response and explanatory variables included in the mixed-effects models with the month as a random effect.

Response variables	Explanatory variables (Fixed effect)	Objectives
Invertebrate diversity – abundance, volume and richness of pest and natural enemies (6 models)	Field clusters, Management in neighboring field, altitude, and landscape context	Effect of field management categories on invertebrate diversity and prevalence
Crop damage and annual yield (2 models)	Field clusters, Management in neighboring field, altitude, and landscape context	Relationship between management, crop damage and crop yields
Crop damage and annual yield (4 models: 2 models for each group - pest and natural enemy)	Management clusters and Invertebrate diversity – abundance, volume, and richness of pests and natural enemies, modeled separately.	Effects of Invertebrate diversity – abundance, volume and richness of PS and NE on crop damage and crop yields

Each response variable represents a separate model.

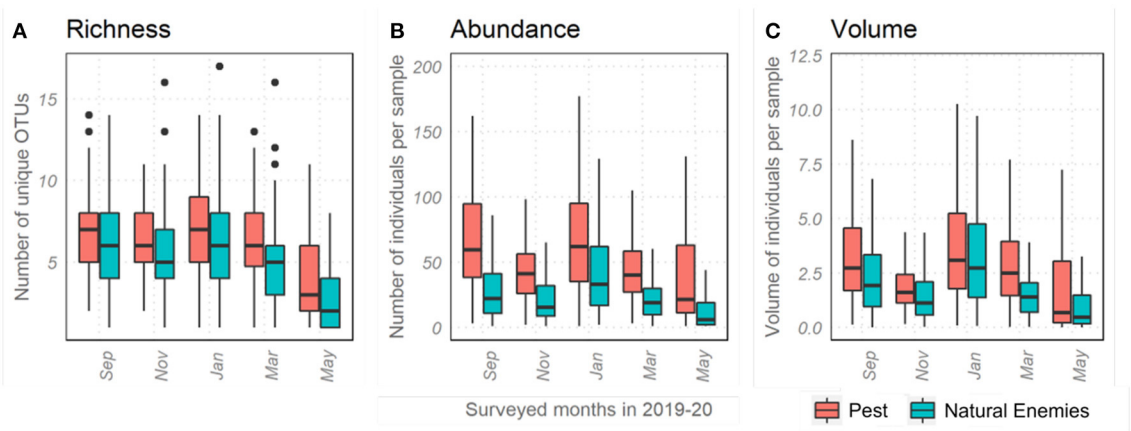

FIGURE 3 | Effect of sampling month on invertebrate richness **(A)** abundance **(B)** and volume **(C)**. November showed significantly reduced abundance and volume, which also correlated with flash floods in the study area.

response variables and richness, abundance and volume of pest and natural enemies as predictors.

To account for the effect of seasonality and repeated observations, we included sampling month as a random effect (**Table 2**). Models were specified using all possible combinations of the explanatory variables and subjected to backward model selection based on the lowest values of Akaike's information criterion (AIC). Estimates and unconditional 95% confidence intervals (CI) were derived from the best fit models (ΔAIC $<$ 2). The effect was considered significant when the 95% CI did not overlap zero. We also standardized all the continuous variables, tested for multicollinearity (with an aim to remove variables responsible for VIF$>$3) and checked for residual distribution against fitted values to verify model assumptions. All calculations and analyses were undertaken using the statistical software R version 3.4.2 (R Core Team, 2017).

RESULTS

Invertebrate Assemblage Sampling and Effect of Sampling Month

From September 2019 to May 2020, during the five sampling periods, we collected a total of 93,428 invertebrate individuals with a mean body size of 0.13 mm^2 (SD = 0.4 mm^2), ranging from 0.0002 to 27 mm^2. They were identified to 282 distinct morphospecies (OTUs) belonging to 33 orders, 122 families, and 164 genera (list of species and abundances in **Supplementary Tables 1, 2**).

The month of sampling had a significant effect explaining the majority of variance in abundance, richness and volume of pests and natural enemies (20–24% random effect; **Figure 3**). The abundance and volume of invertebrates dropped significantly in November 2019, coinciding with flash floods in the study area that destroyed fields and crops. Following the drop in November, abundance and volume recovered and increased significantly in January before gradually declining until the end of sampling in May.

Management Practices and Invertebrate Diversity

Farm management clusters showed a significant difference in richness, abundance and volume of pests and natural enemies (**Figures 4a–f**). Compared to the Monocrop-Trench farms, Mulch-Trench, Spacing-Intercrop and Spice-Intercrop-Cropdiv farms had lower pest diversities (**Figures 4a,b**). CS-Intercrop fields had a higher pest volume (**Figure 4c**) but

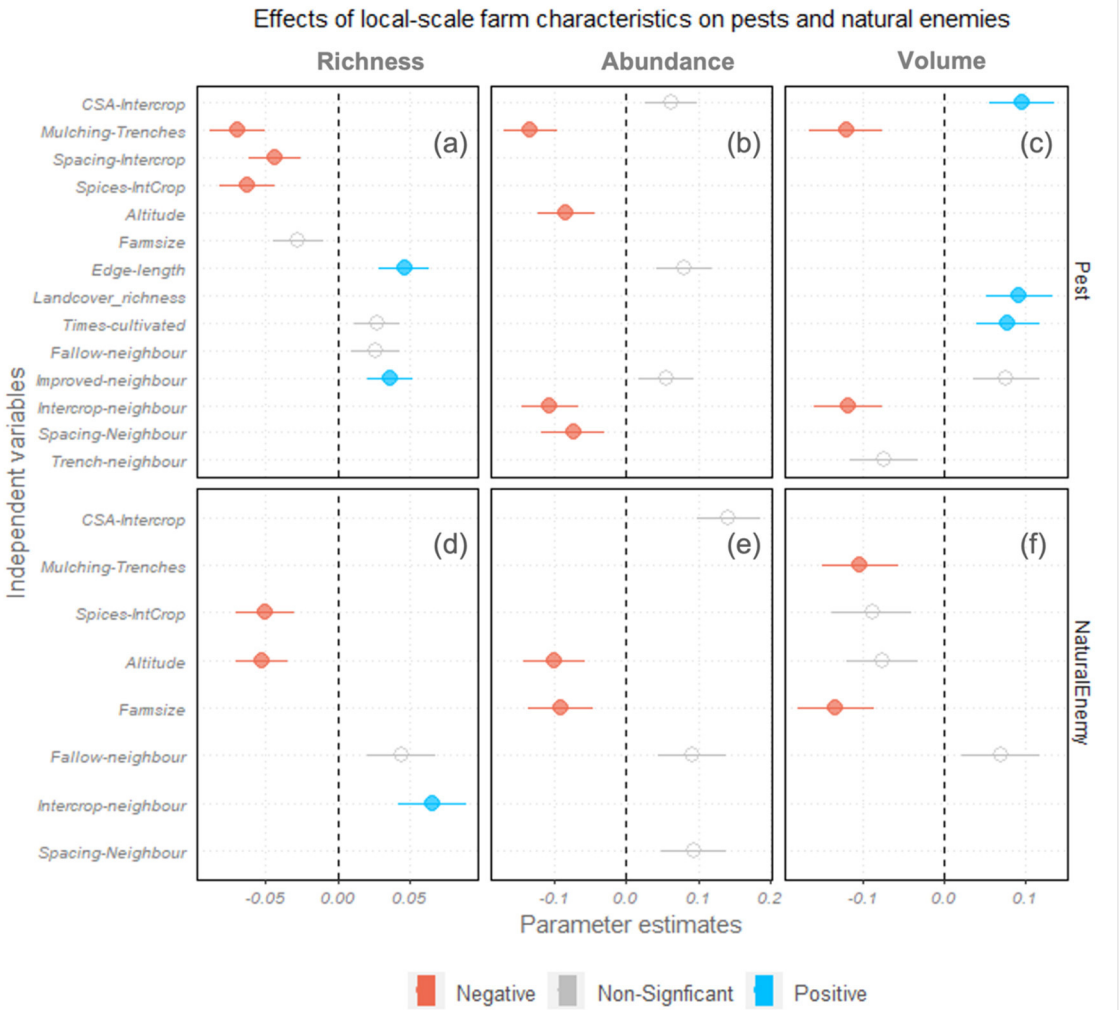

FIGURE 4 | The coefficient plot of richness **(a,d)**, abundance **(b,e)** and volume **(c,f)** of pests **(a–c)** and natural enemies **(d–f)** (3 × 2 models) in response to farm clusters based on management practices, neighbouring field characteristics, and landscape context. The independent variables selected in the best fit model (ΔAIC < 2) are shown. Each panel represents a different model. The positions of the circles represent β-coefficients, horizontal lines on the circles show SE, and colors signify the direction of the effect.

showed no significant difference in pest abundance and richness (**Figures 4a,b**) compared to monocrop-trench fields. Mulching was associated with lower natural enemy volume (**Figure 4f**) but did not significantly affect the richness and abundance of natural enemies (**Figures 4d,e**). Spice-Intercrop fields, however, had a lower richness of natural enemies (**Figure 4d**), in addition to lower pest richness (**Figure 4a**), suggesting that Spice-Intercrop fields are associated with reduced overall biodiversity.

Landscape fragmentation, indicated by edge-length, was associated with lower pest richness (**Figure 4a**), suggesting no evidence of spill-over of potential pests from non-crop forest habitats. In contrast, landcover diversity, measured by landcover richness, showed a positive effect on pest volume (**Figure 4c**), suggesting that landscapes with greater heterogeneity support a broader range of pest body sizes. The landscape context variables did not significantly affect natural enemies.

Characteristics of neighboring fields also influenced pest and natural enemy prevalence. Local variety monocrop focal fields, with neighbors practicing intercropping and wider crop row spacing, had fewer pests (**Figure 4b**) and more natural enemies (**Figure 4e**). In contrast, local variety focal fields had higher pest richness when the neighboring field had improved crop varieties (**Figure 4a**). Neighboring fallowed fields also led to a positive association with natural enemies in the focal field, albeit only marginally significant ($p = 0.06$). Also, at higher altitudes, there were a lower pest and natural enemy abundance (**Figures 4b,e**) and reduced natural enemy richness (**Figure 4d**).

In summary, farms with mulching, wider spacing between crop plants, and spice plantations had fewer pests, while management in the neighboring fields, mainly intercrop and fallow, had positive outcomes for natural enemies in the focal fields.

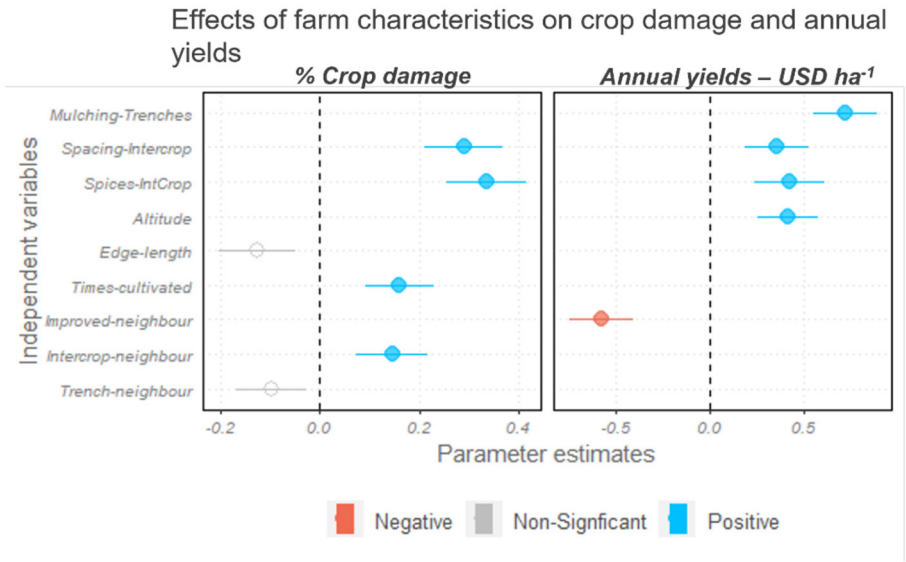

FIGURE 5 | The coefficient plot of crop damage (proportion of crop affected by pests) and crop yield earnings (Annual USD per hectare) in response to farm clusters based on management practices, neighboring field characteristics, and landscape context. The independent variables selected in the best fit model are shown. Each panel represent a different model. The positions of the circles represent β- coefficients, horizontal lines on the circles show SE, and colors signify the direction of the effect.

Management Practices, Crop Damage and Yields

Despite lower pest richness, crop damage in Spacing-Intercrop and Spice-Intercrop fields was significantly greater than CS-Intercrop and Monocrop-Trench fields (**Figure 5**), suggesting damage was caused by a small number of key crop pests. Crop damage was also positively associated with the number of times the field was cultivated and with neighboring intercrops. Edge length was negatively associated with crop damage, but this was only marginally significant ($p = 0.07$).

Annual yields were higher in mulching, spacing, and spice fields compared to Monocrop-trench and CS-intercrop fields. Also, fields at high altitudes had significantly higher earnings than lowland fields. Interestingly, local variety focal fields that had neighbors using improved variety crops showed lower yield earnings.

Invertebrate Diversity, Crop Damage and Yields

The models (presented in **Figure 6**), suggest that pest abundance had a significant positive effect on crop damage (0.12 ± 0.52) and a negative association with annual yields (−5.9 ± 2.7). Furthermore, pest abundance effects on crop damage were influenced by pest richness (-0.03 ± 0.01). At low pest richness (richness <4 OTUs), pest abundance had the strongest positive effect on crop damage and a severe negative relationship with annual yields, indicating that a small number of key pests caused the most damage. On the other hand, neither richness nor abundance of natural enemies showed any significant association with crop damage. Still, they had a significant positive effect on annual yields, which increased with natural enemy abundance (5.2 ± 2.06) and richness (4.3 ± 1.5). However, at very high natural enemy richness ($n > 8$), natural enemy abundance was negatively associated with annual yields.

DISCUSSION

Our study is the first to evaluate the ecological implications of CSA practices deployed in different combinations at field-scale. It helped identify potential synergies and trade-offs among the targeted objectives of CSA practices, annual agricultural yields and income, and outcomes for pest and natural enemy diversities and associated ecosystem service of biocontrol (**Table 3**). We showed that fields with mulches and *Fanya juu* trenches had the greatest synergy with the targeted objectives in terms of higher annual agricultural income and lower pest pressures. Surprisingly, the fields with maximum CSA practices did not have significantly different yields or invertebrate diversities, indicating that certain practices (mulches and *Fanya Juu* trenching) had a significant effect, but lots of practices combined ceased to produce any effect. This may simply be due to different practices having contrasting effects on biodiversity and yields – some positive and others negative, resulting in a no-net effect. Interventions such as greater spacing between crops and spice plantations had lower invertebrate diversities (pests as well as natural enemies), but higher annual returns. This indicates a possible trade-off between biodiversity and agricultural production. Further work in this area is needed to consider trade-offs in agricultural production over time, examining short term losses in the context of long-term goals.

We found that fields with trenches and mulching, primarily adopted to increase soil quality and moisture conservation in the

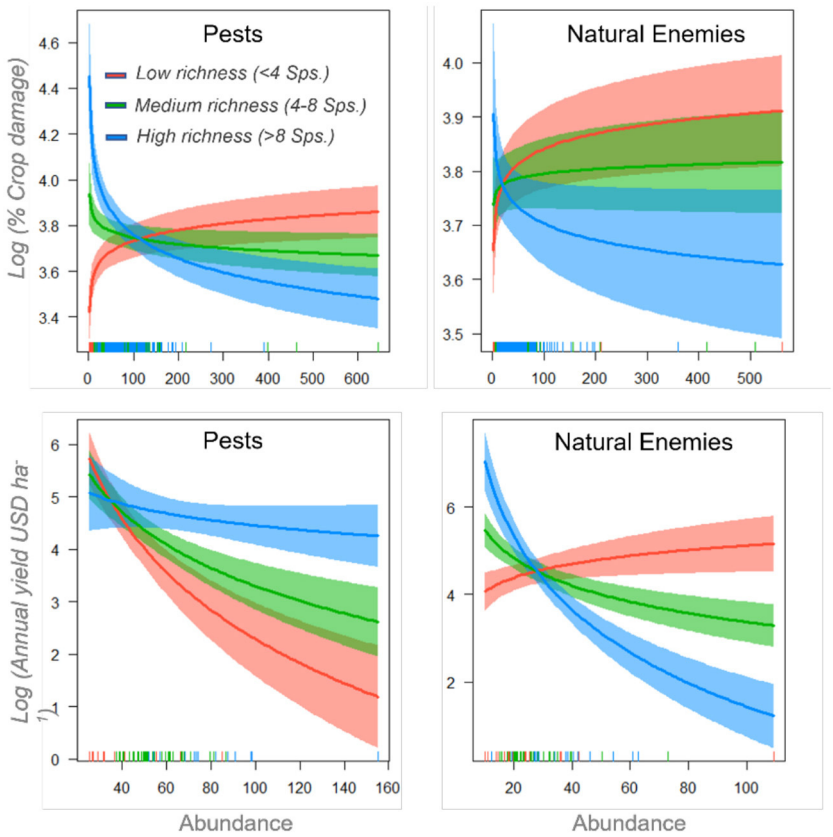

FIGURE 6 | Interactive effects of pest (left panels) and natural enemy (right panels) richness and abundance on percentage crop damage (top panels) and annual income from crop yield in USD (bottom panels). Colors represent the different levels of Species Richness – low (red), medium (green), and high (blue). Abundance was log-transformed in the model. The plots indicate back-transformed values for ease of interpretation.

TABLE 3 | Trade-off and synergies among the targeted objectives, biodiversity and annual income returned in the study area.

CSA practice	Targeted objective	Biodiversity impacts	Effects on annual agricultural income
Fanya juu trenches with live and compost mulches	Reduced runoff and soil erosion and fodder. Napier grasses as live mulches can also be used as "pull" crops in push-pull technology. However, farmers in the study area did not know about push-pull technology.	+ Higher pest suppression - Lower body-size diversity of invertebrates ~ No significant effect on non-pest or natural enemy diversity	+ Higher yields and income
Improved variety crops	Adaptability to climate shocks, increased soil biodiversity by decreased use of pesticides	~ No significant effect on biodiversity - Increased pest richness and abundance in the neighboring field	~ No significant change in crop damage, annual yields, and income - Lower yields and income in the neighboring field
Interrow spacing between crops	Higher grain yield and increase in above ground dry biomass	- Reduced pest species richness + Higher crop damage	+ Higher yields and income despite higher crop damage
Agroforestry with spice plantations	Greater income and reduced vulnerability and dependence on food crops, Increased carbon sequestration	- Reduced pest and natural enemy species richness, therefore greater trade-off with biodiversity + Higher crop damage	+ Higher yields and income despite higher crop damage due to spices being higher value crops

fields, generally also had improved pest suppression. This was indicated by lower abundance and volume of pests, and higher crop yields and annual agricultural earnings. These fields also had a lower volume of natural enemies, but no impact on natural enemy richness or abundance. The role of mulches in reducing pest densities and diversities have been observed in a number of other studies (Altieri et al., 1985; Hooks et al., 1998; Brown and Tworkoski, 2004; Massaccesi et al., 2020) and is generally attributed to the greater density and diversity of ground-dwelling predators (*Carabidae, Staphylinidae, and Arachnids)* in the fields with live or compost mulching (Altieri et al., 1985; Schmidt et al., 2004). Past studies have also indicated the positive effects

of mulching on predator populations and diversity (Schmidt et al., 2004). Natural enemy abundance and richness in the mulched fields in our study was not significantly different from other field management clusters. However, we observed that natural enemy volumes were significantly lower as most natural enemy individuals caught in the mulching fields were of smaller body sizes (mainly Parasitoids). This may be due to lower habitat diversity in and around the mulching fields, compared to the other fields which had agroforestry, spice plantations and intercropping and supported functionally diverse natural enemy communities comprising greater body-size distribution and diversity.

We did not find any other study evaluating the effect of *Fanya juu* trenches on invertebrates and our study is potentially the first to suggest that *Fanya juu* trenches and associated live mulching with grass strips offer significant benefits in terms of pest suppression in addition to the targeted objective of reduced run-off and soil erosion. Live mulches are generally associated with reduced pest infestations and crop damage (Altieri et al., 1985; Johnson and Gurr, 2016; Rehman et al., 2019), as also observed in our study. Our observations are comparable to the effects of push-pull technology where Napier grass has often been used as a "pull" crop, which attracts pests away from the crop and thereby reduces crop damage (Khan et al., 2011). Although it was not planted with the targeted objective of reducing crop pests, planting and live mulching with Napier grass demonstrates that there may be considerable synergies between CSA and conservation and pest management agricultural practices like push-pull. Thus, our study shows that the fields with mulching and trenching had the best outcomes in terms of pest suppression and productivity, and no significant reduction in non-pest or natural enemy diversity.

Among the other field clusters in this study, CS-Intercrop fields, where the maximum number of CSA technologies were deployed, were not significantly different from the monocrop traditional fields in terms of pest or natural enemy richness and abundance, crop damage or yields. Pest volumes, however, were the highest in CS-Intercrop fields. This may be because CSA fields containing improved crop varieties exhibited enhanced plant growth and higher foliar biomass, which attracted a larger functional or body-size diversity of insect herbivores (Real-Santillán et al., 2019). Furthermore, wider crop row spacing, and spice intercrops had lower richness of pest communities, higher crop damage, but greater yields than all other fields. This suggests that despite higher crop damage in food crops (maize and beans), the annual yields in Spice-Intercrop fields were not affected as spice plantations (clove and cardamom) and intercrops (cassava and bananas) mediated the net effect of pest damage.

Our study also showed that farm characteristics such as farm size, number of times it is cultivated, management practices in the neighboring fields and landscape context influenced the pests and natural enemies in the focal field as observed in other studies which are mainly from commercial farming landscapes (Rodriguez-Saona and Thaler, 2005; Madeira et al., 2016; Schulz-Kesting et al., 2021). Hence, this is one of the few studies from biodiverse smallholder farming landscapes in SSA that demonstrates such process are important in a wide range of farming systems. Particularly, farm size was associated with a reduction in abundance and volume of natural enemies. Increasing farm sizes is associated with fragmentation of natural landcover and landscape homogenisation, which may lead to a reduction in biocontrol as natural enemy communities with lower densities and a smaller range of body sizes are known to be less effective in pest control (Letourneau and Goldstein, 2001; Staton et al., 2021). Furthermore, neighbors practicing intercropping was associated with reduced pest abundance and an increase in natural enemy richness in local variety maize monocrops, mainly dominated by *Coccinellids*. Pest abundance was strongly related with an increase in crop damage and reduction in yields, while natural enemy richness was associated with a reduction in crop damage. This highlights the importance of local heterogeneity created by the difference in management practices between fields, which leads to spatial ecological interactions and flow of ecosystem services between neighboring fields where the characteristics of one field influences pest pressure and biocontrol in the other field (Landis et al., 2000; Sarthou et al., 2014).

Landscape heterogeneity, as indicated by forest edge length, had positive association with pest richness and negative relationship with crop damage. The effect of landscape configuration is typically context-dependent and has often been overlooked in the landscape-pest and biocontrol literature (Karp et al., 2018). An increase in landscape heterogeneity may lead to an increase in pest diversity resulting in aggravated pest pressures and crop damage (Martin et al., 2013; Zhang et al., 2020). In contrast, an increase in pest richness, diversity and evenness can also reduce pest-driven crop damage as some studies indicate (Crowder et al., 2010; Lundgren and Fausti, 2015). Diverse and more evenly distributed pest communities have higher inter-species competition, which reduces the dominance and impact of single and most impactful pest species. In our study, fields with species poor pest communities (2–3 species) and with greater mean abundances (mean 132 ± 74 individuals) were dominated by *Diptera, Orthoptera* and *Lepidoptera* groups, and had 4% higher crop damage and 28% lower annual earnings than fields with species-rich pest communities. This supports the possibility that lower pest richness with greater density and dominance of few and more specialized crop herbivores like locusts, fall armyworm, stalk borers and African cotton bollworm may lead to greater crop damage and yield losses. Our findings thereby suggest that diversity decreases herbivory potentially diluting the impact of dominant pests on crop production (Civitello et al., 2015). Therefore, scaling up of CSA must take in to account broader landscape-scale perspective and focus on maintaining heterogeneity in agricultural landscapes through mosaics of monocrop and intercrop fields intermixed with natural and semi-natural landscapes.

Use of improved crop varieties is widely promoted as a climate adaptation (Thierfelder et al., 2016). Our study showed that use of improved crop varieties for drought resistance and shorter growing season in a neighboring field was associated with increased pest richness and reduced yields in the focal fields with local varieties, mainly of maize. This could mean

that a shift to improved varieties among one group of farmers may lead to increased vulnerability of another group, thereby highlighting a form of maladaptation. Further studies are needed to explore the spatial flows and interactions of ecosystem services and disservices due to the adoption of new technologies.

We also found a strong effect of crop seasonality as months coinciding with maize plantation (January) and harvest (September), which are themselves timed with respect to expected rains, had the highest levels of pest and natural enemy diversity, abundance, and volume. The effect of sampling season has also been observed across the globe and shows that it is important to take in to account the temporal variability when evaluating ecological responses to agricultural interventions (Habel et al., 2018; Fanelli, 2020; Scheiner and Martin, 2020). Further, one of the sampling occasions, November 2019, coincided with flash floods in the study area during which the invertebrate communities significantly declined in richness, abundance, and volumes. This sudden decline was more likely due to the destructive effect of flash floods on invertebrate habitats as observed in other studies (Hickey and Salas, 1995; Moi et al., 2020). It also reveals the fragility of any farming system, whether they are CSA or not, in the face of increasing climate extremes.

Adoption of CSA may be necessary in the future to reduce agriculture's vulnerability to climate change and ensure food security for an estimated 9 billion people by 2050 (Taylor, 2018). CSA, presently, is focused primarily on technical fixes to increase agricultural productivity and adaptation (Dinesh et al., 2015). However, food production under climate change will also depend largely on sustainably increasing farmer's resilience to climate risks by developing adaptation strategies and managing trade-offs (risks and conflicts) between land use change, biodiversity, and food production (Chandra et al., 2018; Taylor, 2018). Our study highlights the need for agriculture industry to evaluate interactions, synergies, and trade-offs between the different outcomes relating agriculture change from a multi-dimensional perspective. Understanding of risks and challenges farmers face, adaptation strategies they use, and which strategies provide the best outcome in terms of productivity, food security net agricultural income, and environmental stability will be crucial for building more resilient and sustainable food systems of future (MacFall et al., 2015; Aggarwal et al., 2018).

The present study is an evaluation of management practices at local scales. Even though we sampled for multiple months in a year there may be variations and multi-year effects we could not account for. The CSA practices in the study areas were introduced only 3 years before the present study was implemented. Although the three-year time frame may be enough to effect the changes in some invertebrate communities - pests especially, there may still be time lags in responses of indirectly affected trophic groups (e.g., natural enemy communities) causing delayed biodiversity changes (Essl et al., 2015). Overlooking time lags may result in an underestimate of biodiversity impacts and associated trade-offs with food production. Hence, longer-term studies are needed to fully understand the ecological implications and biodiversity impacts of agricultural interventions. Our study, nevertheless, points toward possible trends.

CONCLUSION

Our study identifies mulching and *Fanya juu* trenches as CSA practices with potential for maximizing synergies among food production, biodiversity conservation and pest suppression via biocontrol. Furthermore, it also shows that that increasing inter-row spacing of Maize to 70–100 cm and integrating food crops like maize and beans with cash crops, such as spice plantations, improves grain yield and annual income. Broadly, our study highlights the importance of local management and landscape characteristics in maintaining biodiversity. Our study has also uncovered the real risk of negative impacts of CSA intervention and maladaptation on farmer livelihoods. In this study, increased pest richness and abundance, lower yields and income were evident in local-variety fields neighboring those where improved varieties are used, suggesting the use of improved varieties by farmers is creating increased vulnerability among neighboring farmers. The need for further research on assessing biodiversity impacts, and for holistic and long-term evaluation and monitoring of CSA across field and landscape scales is therefore very clear. CSA evaluations must look beyond productivity alone because the trade-offs and synergies among biodiversity, agricultural production and food security, livelihoods and health often interact and feedback on each other. Finally, more local-scale case and long-term studies and syntheses are needed to understand the combined and interactive effects of agriculture intervention and global change processes across different geographies and food production models.

DATA AVAILABILITY STATEMENT

The raw data supporting the conclusions of this article will be made available by the authors, without undue reservation.

AUTHOR CONTRIBUTIONS

HT conceived the idea, designed, and implemented this study with support from SSai, WK, SSal, SMau, and HS. All authors have contributed ideas that inform the structure and narrative of the paper, provided editorial support, agreed to the published version of the manuscript, and contributed to the article and approved the submitted version.

FUNDING

This work was funded by the Biotechnology and Biological Sciences Research Council through UK Research and Innovation, as part of the Global Challenges Research Fund: AFRICAP Programme, Grant Number BB/P027784/1. Research in Tanzania was conducted under COSTECH permit number: 2019-305-NA-2016-101. RD was supported by the University of Leeds MSc in Biodiversity and Conservation programme. Fieldwork in Tanzania was supported by the Economic and Social Research Foundation. The funders had no role in the design of the study, in the collection, analyses, or interpretation of data; in the

writing of the manuscript, or in the decision to publish the results.

ACKNOWLEDGMENTS

We are very grateful to the community members and village leaders who gave their valuable time and allowed us to conduct sampling in their fields. Special thanks to Elimeena Baraka, Suzan Donald, Majid Majidi, Mosha Florence, and Manzil Maburuki in Tanzania for their support with data collection.

SUPPLEMENTARY MATERIAL

The Supplementary Material for this article can be found online at: https://www.frontiersin.org/articles/10.3389/fsufs.2022.868870/full#supplementary-material

REFERENCES

Aggarwal, P. K., Jarvis, A., Campbell, B. M., Zougmoré, R. B., Khatri-Chhetri, A., Vermeulen, S. J., et al. (2018). The climate-smart village approach: Framework of an integrative strategy for scaling up adaptation options in agriculture. *Ecol. Soc.* 23, 14. doi: 10.5751/ES-09844-230114

Aguilera, G., Riggi, L., Miller, K., Roslin, T., and Bommarco, R. (2021). Organic fertilisation enhances generalist predators and suppresses aphid growth in the absence of specialist predators. *J. Appl. Ecol.* 58, 1455–1465. doi: 10.1111/1365-2664.13862

Altieri, M. A., Wilson, R. C., and Schmidt, L. L. (1985). The effects of living mulches and weed cover on the dynamics of foliage- and soil-arthropod communities in three crop systems. *Crop. Prot.* 4, 201–213. doi: 10.1016/0261-2194(85)90018-3

Beckmann, M., Gerstner, K., Akin-Fajiye, M., Ceauşu, S., Kambach, S., Kinlock, N. L., et al. (2019). Conventional land-use intensification reduces species richness and increases production: a global meta-analysis. *Glob. Chang Biol.* 25, 1941–1956. doi: 10.1111/gcb.14606

Bommarco, R., Vico, G., and Hallin, S. (2018). Exploiting ecosystem services in agriculture for increased food security. *Glob. Food Sec.* 17, 57–63. doi: 10.1016/j.gfs.2018.04.001

Brown, M. W., and Tworkoski, T. (2004). Pest management benefits of compost mulch in apple orchards. *Agric. Ecosyst. Environ.* 103, 465–472. doi: 10.1016/j.agee.2003.11.006

Buchhorn, M., Lesiv, M., Tsendbazar, N. -E., Herold, M., Bertels, L., and Smets, B. (2020). Copernicus global land cover layers-collection 2. *Remote Sens.* 12, 1044. doi: 10.3390/rs12061044

Chandra, A., McNamara, K. E., and Dargusch, P. (2018). Climate-smart agriculture: perspectives and framings. *Clim. Policy* 18, 526–541. doi: 10.1080/14693062.2017.1316968

Civitello, D. J., Cohen, J., Fatima, H., Halstead, N. T., Liriano, J., McMahon, T. A., et al. (2015). Biodiversity inhibits parasites: Broad evidence for the dilution effect. *Proc. Natl. Acad. Sci. U. S. A.* 112, 8667–8671. doi: 10.1073/pnas.1506279112

Crowder, D. W., Northfield, T. D., Strand, M. R., and Snyder, W. E. (2010). Organic agriculture promotes evenness and natural pest control. *Nature* 466, 109–112. doi: 10.1038/nature09183

Dainese, M., Martin, E. A., Aizen, M. A., Albrecht, M., Bartomeus, I., Bommarco, R., et al. (2019). A global synthesis reveals biodiversity-mediated benefits for crop production. *Sci. Adv.* 5, 1–14. doi: 10.1126/sciadv.aax0121

Dang, H. A. H., and Dabalen, A. L. (2017). Is Poverty in Africa Mostly Chronic Or Transient? Evidence from Synthetic Panel Data. *World Bank Gr.* 8033, 1–45. doi: 10.1596/1813-9450-8033

Dinesh, D., Frid-Nielsen, S., Norman, J., Mutamba, M., Rodriguez, A. M. L., and Campbell, B. (2015). Climate-smart agriculture effective? A review of selected cases. *CGIAR Res. Program Clim. Chang Agric. Food Secur. Work Pap.* 129, 89.

Duarte, G. T., Santos, P. M., Cornelissen, T. G., Ribeiro, M. C., and Paglia, A. P. (2018). The effects of landscape patterns on ecosystem services: meta-analyses of landscape services. *Landsc. Ecol.* 33, 1247–1257. doi: 10.1007/s10980-018-0673-5

Essl, F., Dullinger, S., Rabitsch, W., Hulme, P. E., Pyšek, P., Wilson, J. R. U., et al. (2015). Delayed biodiversity change: no time to waste. *Trends Ecol. Evol.* 30, 375–378. doi: 10.1016/j.tree.2015.05.002

Fanelli, R. M. (2020). The spatial and temporal variability of the effects of agricultural practices on the environment. *Environments* 7, 33. doi: 10.3390/environments7040033

Fankhauser, S., and McDermott, T. K. J. (2014). Understanding the adaptation deficit: Why are poor countries more vulnerable to climate events than rich countries? *Glob. Environ. Chang* 27, 9–18. doi: 10.1016/j.gloenvcha.2014.04.014

Habel, J. C., Seibold, S., Ulrich, W., and Schmitt, T. (2018). Seasonality overrides differences in butterfly species composition between natural and anthropogenic forest habitats. *Anim. Conserv.* 21, 405–413. doi: 10.1111/acv.12408

Hickey, J. T., and Salas, J. D. (1995). Environmental effects of extreme floods. *US-Italy Res Work Hydrometeorol Impacts Manag Extrem Floods* 2, 1–23.

Hooks, C. R. R., Valenzuela, H. R., and Defrank, J. (1998). Incidence of pests and arthropod natural enemies in zucchini grown with living mulches. *Agric. Ecosyst. Environ.* 69, 217–231. doi: 10.1016/S0167-8809(98)00110-8

Johnson, A. C., and Gurr, G. M. (2016). Invertebrate pests and diseases of sweetpotato (Ipomoea batatas): A review and identification of research priorities for smallholder production. *Ann. Appl. Biol.* 168, 291–320. doi: 10.1111/aab.12265

Karp, D. S., Chaplin-Kramer, R., Meehan, T. D., Martin, E. A., DeClerck, F., Grab, H., et al. (2018). Crop pests and predators exhibit inconsistent responses to surrounding landscape composition. *Proc. Natl. Acad. Sci.* 115, E7863–E7870. doi: 10.1073/pnas.1800042115

Khan, Z., Midega, C., Pittchar, J., Pickett, J., and Bruce, T. (2011). Push-pull technology: a conservation agriculture approach for integrated management of insect pests, weeds and soil health in Africa. *Int. J. Agric. Sustain.* 9, 162–170. doi: 10.3763/ijas.2010.0558

Landis, D. A., Wratten, S. D., and Gurr, G. M. (2000). Habitat management to conserve natural enemies of arthropod pests in agriculture. *Annu. Rev. Entomol.* 45, 175–201. doi: 10.1146/annurev.ento.45.1.175

Letourneau, D. K., and Goldstein, B. (2001). Pest damage and arthropod community structure in organic vs. conventional tomato production in California. *J. Appl. Ecol.* 38, 557–570. doi: 10.1046/j.1365-2664.2001.00611.x

Lipper, L., McCarthy, N., Zilberman, D., Asfaw, S., and Branca, G. (2018). Climate smart agriculture building resilience to climate change. *Springer Nat.* 1, 629. doi: 10.1007/978-3-319-61194-5

Lobell, D. B., Schlenker, W., and Costa-Roberts, J. (2011). Climate trends and global crop production since 1980. *Science* 333, 616–620. doi: 10.1126/science.1204531

Lundgren, J. G., and Fausti, S. W. (2015). Trading biodiversity for pest problems. *Sci. Adv.* 1, e1500558. doi: 10.1126/sciadv.1500558

MacFall, J., Lelekacs, J. M., LeVasseur, T., Moore, S., and Walker, J. (2015). Toward resilient food systems through increased agricultural diversity and local sourcing in the Carolinas. *J. Environ. Stud. Sci.* 5, 608–622. doi: 10.1007/s13412-015-0321-1

Madeira, F., Tscharntke, T., Elek, Z., Kormann, U. G., Pons, X., Rösch, V., et al. (2016). Spillover of arthropods from cropland to protected calcareous grassland – the neighbouring habitat matters. *Agric. Ecosyst. Environ.* 235, 127–133. doi: 10.1016/j.agee.2016.10.012

Martin, E. A., Reineking, B., Seo, B., and Steffan-Dewenter, I. (2013). Natural enemy interactions constrain pest control in complex agricultural landscapes. *Proc. Natl. Acad. Sci. U. S. A.* 110, 5534–5539. doi: 10.1073/pnas.1215725110

Massaccesi, L., Rondoni, G., Tosti, G., Conti, E., Guiducci, M., and Agnelli, A. (2020). Soil functions are affected by transition from conventional to organic mulch-based cropping system. *Appl. Soil Ecol.* 153, 1:12. doi: 10.1016/j.apsoil.2020.103639

Mkenda, P. A., Ndakidemi, P. A., Mbega, E., Stevenson, P. C., Arnold, S. E. J., Gurr, G. M., et al. (2019). Multiple ecosystem services from field margin vegetation

for ecological sustainability in agriculture: Scientific evidence and knowledge gaps. *PeerJ*. 2019, 17:49. doi: 10.7717/peerj.8091

Moi, D. A., Ernandes-Silva, J., Baumgartner, M. T., and Mormul, R. P. (2020). The effects of river-level oscillations on the macroinvertebrate community in a river–floodplain system. *Limnology* 21, 219–232. doi: 10.1007/s10201-019-00605-y

Neufeldt, H., Jahn, M., Campbell, B. M., Beddington, J. R., DeClerck, F., De Pinto, A., et al. (2013). Beyond climate-smart agriculture: toward safe operating spaces for global food systems. *Agric. Food Secur.* 2, 2:12. doi: 10.1186/2048-7010-2-12

Newbold, T. (2018). Future effects of climate and land-use change on terrestrial vertebrate community diversity under different scenarios. *Proc. R.Soc.B Biol. Sci.* 285, 20180792. doi: 10.1098/rspb.2018.0792

Nunez, S., Arets, E., Alkemade, R., Verwer, C., and Leemans, R. (2019). Assessing the impacts of climate change on biodiversity: is below 2 C enough? *Clim. Change* 154, 351–365. doi: 10.1007/s10584-019-02420-x

Ongawa (2019). The integrated approaches for climate change adaptation in the East Usambara Mountains. *Glob. Clim. Chang Alliance* 1, 50.

Pecl, G. T., Araújo, M. B., Bell, J. D., Blanchard, J., Bonebrake, T. C., Chen, I. C., et al. (2017). Biodiversity redistribution under climate change: Impacts on ecosystems and human well-being. *Science 355,* 1389:1399. doi: 10.1126/science.aai9214

Porter, J. R., Xie, L., Challinor, A. J., Cochrane, K., Howden, S. M., Iqbal, M. M., et al. (2015). Food security and food production systems. *Clim Chang 2014 Impacts, Adapt Vulnerability Part A Glob Sect Asp AR5,* 485–534.

Qi, J., Yu, Y., Wang, L., Liu, J., and Wang, Y. (2017). An effective and efficient hierarchical K-means clustering algorithm. *Int. J. Distrib. Sens. Netw.* 13, 1–17. doi: 10.1177/1550147717728627

R Core Team (2017). R: A Language and Environment for Statistical Computing. *R. Found Stat. Comput.* 55, 275–286.

Ray, D. K., West, P. C., Clark, M., Gerber, J. S., Prishchepov, A. V., and Chatterjee, S. (2019). Climate change has likely already affected global food production. *PLoS ONE* 14, 1–18. doi: 10.1371/journal.pone.0217148

Real-Santillán, R. O., del-Val, E., Cruz-Ortega, R., Contreras-Cornejo, H. Á., González-Esquivel, C. E., and Larsen, J. (2019). Increased maize growth and P uptake promoted by arbuscular mycorrhizal fungi coincide with higher foliar herbivory and larval biomass of the Fall Armyworm Spodoptera frugiperda. *Mycorrhiza* 29, 615–622. doi: 10.1007/s00572-019-00920-3

Redlich, S., Martin, E. A., and Steffan-Dewenter, I. (2018). Landscape-level crop diversity benefits biological pest control. *J. Appl. Ecol.* 55, 2419–2428. doi: 10.1111/1365-2664.13126

Rehman, M., Liu, J., Johnson, A. C., Dada, T. E., and Gurr, G. M. (2019). Organic mulches reduce crop attack by sweetpotato weevil (Cylas formicarius). *Sci. Rep.* 9, 1:12. doi: 10.1038/s41598-019-50521-5

Rodriguez-Saona, C., and Thaler, J. S. (2005). Herbivore-induced responses and patch heterogeneity affect abundance of arthropods on plants. *Ecol. Entomol.* 30, 156–163. doi: 10.1111/j.0307-6946.2005.00682.x

Rosenstock, T. S., Nowak, A., and Girvetz, E. (2019). The climate-smart agriculture papers - investigating the business of a productive, resilient and low emission future. *Springer Nat.* 1, 197. doi: 10.1007/978-3-319-92798-5

Rusch, A., Chaplin-Kramer, R., Gardiner, M. M., Hawro, V., Holland, J., Landis, D., et al. (2016). Agricultural landscape simplification reduces natural pest control: a quantitative synthesis. *Agric. Ecosyst. Environ.* 221, 198–204. doi: 10.1016/j.agee.2016.01.039

Sarthou, J. P., Badoz, A., Vaissière, B., Chevallier, A., and Rusch, A. (2014). Local more than landscape parameters structure natural enemy communities during their overwintering in semi-natural habitats. *Agric. Ecosyst. Environ.* 194, 17–28. doi: 10.1016/j.agee.2014.04.018

Scheiner, C., and Martin, E. A. (2020). Spatiotemporal changes in landscape crop composition differently affect density and seasonal variability of pests, parasitoids and biological pest control in cabbage. *Agric. Ecosyst. Environ.* 301, 107051. doi: 10.1016/j.agee.2020.107051

Schmidt, M. H., Thewes, U., Thies, C., and Tscharntke, T. (2004). Aphid suppression by natural enemies in mulched cereals. *Entomol. Exp. Appl.* 113, 87–93. doi: 10.1111/j.0013-8703.2004.00205.x

Schulz-Kesting, K., Thiele, J., Everwand, G., and Dauber, J. (2021). Neighbourhood effect of faba bean (Vicia faba L.) on density of vegetation-dwelling natural biocontrol agents in winter wheat. *Biol. Control* 160, 104673. doi: 10.1016/j.biocontrol.2021.104673

Staton, T., Walters, R. J., Smith, J., Breeze, T. D., and Girling, R. D. (2021). Evaluating a trait-based approach to compare natural enemy and pest communities in agroforestry vs. arable systems. *Ecol. Appl.* 31, e02294. doi: 10.1002/eap.2294

Taylor, M. (2018). Climate-smart agriculture: what is it good for? *J. Peasant Stud.* 45, 89–107. doi: 10.1080/03066150.2017.1312355

Thierfelder, C., Rusinamhodzi, L., Setimela, P., Walker, F., and Eash, N. S. (2016). Conservation agriculture and drought-tolerant germplasm: Reaping the benefits of climate-smart agriculture technologies in central Mozambique. *Renew. Agric. Food Syst.* 31, 414–428. doi: 10.1017/S1742170515000332

Thornton, P. K., Whitbread, A., Baedeker, T., Cairns, J., Claessens, L., Baethgen, W., et al. (2018). A framework for priority-setting in climate smart agriculture research. *Agric. Syst.* 167, 161–175. doi: 10.1016/j.agsy.2018.09.009

van Wijk, M. T., Merbold, L., Hammond, J., and Butterbach-Bahl, K. (2020). Improving assessments of the three pillars of climate smart agriculture: current achievements and ideas for the future. *Front. Sustain. Food Syst.* 4, 558483. doi: 10.3389/fsufs.2020.558483

Venkatramanan, V., and Shah, S. (2019). Climate-smart agriculture technologies for environmental management: The intersection of sustainability, resilience, wellbeing and development. *Sustain. Green Technol. Environ. Manag.* 1, 29–51. doi: 10.1007/978-981-13-2772-8_2

Woodcock, B. A., Bullock, J. M., McCracken, M., Chapman, R. E., Ball, S. L., Edwards, M. E., et al. (2016). Spill-over of pest control and pollination services into arable crops. *Agric. Ecosyst. Environ.* 231, 15–23. doi: 10.1016/j.agee.2016.06.023

Zhang, Y., Haan, N. L., and Landis, D. A. (2020). Landscape composition and configuration have scale-dependent effects on agricultural pest suppression. *Agric. Ecosyst. Environ.* 302, 107085. doi: 10.1016/j.agee.2020.107085

Conflict of Interest: The authors declare that the research was conducted in the absence of any commercial or financial relationships that could be construed as a potential conflict of interest.

Publisher's Note: All claims expressed in this article are solely those of the authors and do not necessarily represent those of their affiliated organizations, or those of the publisher, the editors and the reviewers. Any product that may be evaluated in this article, or claim that may be made by its manufacturer, is not guaranteed or endorsed by the publisher.

Advantages of publishing in Frontiers

OPEN ACCESS
Articles are free to read for greatest visibility and readership

FAST PUBLICATION
Around 90 days from submission to decision

HIGH QUALITY PEER-REVIEW
Rigorous, collaborative, and constructive peer-review

TRANSPARENT PEER-REVIEW
Editors and reviewers acknowledged by name on published articles

Frontiers
Avenue du Tribunal-Fédéral 34
1005 Lausanne | Switzerland

Visit us: www.frontiersin.org
Contact us: frontiersin.org/about/contact

REPRODUCIBILITY OF RESEARCH
Support open data and methods to enhance research reproducibility

DIGITAL PUBLISHING
Articles designed for optimal readership across devices

FOLLOW US
@frontiersin

IMPACT METRICS
Advanced article metrics track visibility across digital media

EXTENSIVE PROMOTION
Marketing and promotion of impactful research

LOOP RESEARCH NETWORK
Our network increases your article's readership